Inverse solution techniques for determining aquifer parameters from pump test data

Jonathan Peter Reed

Inverse Solution Techniques For Determining Aquifer Parameters From Pump Test Data

Jonathan Peter Reed

Abstract

The estimation of aquifer parameters is often difficult, inaccurate and time consuming. A method of analysing pumping test data is presented which automatically estimates aquifer parameters. The inverse solution technique of least squares is used to obtain the parameters which give the best fit between the observed and theoretical values of drawdown. Three different solution methods are presented. Data from a confined aquifer is analysed using the Theis solution. For leaky aquifer data, either the Walton or Hantush solution may be used.

The least squares algorithms for the leaky condition were combined with an Hermitian interpolation algorithm to reduce the running time. In each case the algorithm converged from a range of values to the correct solution. The algorithms were validated by comparing the results of well documented pumping tests with the results of other authors. A programme of fieldwork was conducted which was analysed using the algorithms. The results of this analysis were further validated by numerical modelling. The pumping test was simulated using the calculated values of aquifer parameters. The theoretical drawdown curve matches very closely to the field values observed during the pumping tests.

Inverse Solution Techniques For Determining Aquifer Parameters From Pump Test Data

Jonathan Peter Reed

BSc (Hons) Dunelm

Submitted for the degree of

Master of Science

University of Durham

School of Engineering

September 1995

Table of Contents

Appendices

Table of Tables

Table of Figures

Acknowledgements

This past year has given me a multitude of opportunities to learn, meet, support and be supported. I have benefited from the help of so many people, that it is difficult for me to thank and recognise them all.

I would like to start by thanking my supervisor, Dr. Stephen Thomas, for his ideas and his support of this project. Also Dr. Alan Selby for his guidance at essential times. The staff and technicians at the School of Engineering have always been friendly and keen to help, which has made this project far more enjoyable.

I am also grateful to Oxford Geotechnica Limited (OGL), for sponsoring the project and providing the opportunity to work in this field. I am particularly grateful to Sue Pickering of OGL for her patience, support and sense of humour, which have all been highly valued.

I would also most sincerely like to thank Rachel Carrington for being a wonderful colleague and an even better friend. Also Iwan Jones, for his ideas and ability to bring me back down to ground with geological zest. Martin Bradley has given many a wise counsel in addition to lifts in on wet mornings! All the postgrads at the School of Engineering made coffee times fun and interesting - may Friday afternoon football and 'A4 Day' carry on to ever greater heights!

Everyone who has been involved with SCA, DUCK or SPARK has contributed much to this year. I am very grateful to all those involved with these organisations, particularly Louise Smith, Helen Swift and Glenn Rees.

Vanessa Humphreys and Anthea Tyndale-Biscoe were wonderful housemates, providing many 'displacement activities', crossword blunders and happy memories. I would also like to thank my parents, brothers and family for all their support and kindness over many years. Finally, I cannot thank Fiona Gooch enough, for her kindness, support and for just being her.

Nomenclature

Symbol	Dimensions	Meaning
c	T	Hydraulic resistance of aquitard
d	L	Aquifer thickness
d'	L	Aquitard thickness
erfc(x)	-	Complementary error function
f(u)	-	Rai well function
F(u)	-	Chow well function
K	LT^{-1}	Aquifer permeability
K'	LT^{-1}	Aquitard permeability
L	L	Leakage factor
Q	L^3T^{-1}	Discharge
r	L	Radius
s	L	Drawdown
s'	L	Residual drawdown
S	-	Aquifer storativity
S'	-	Aquitard storativity
S_s	L^{-1}	Specific storage
S_y	L^{-1}	Specific yield
t	T	Time
T	L^2T^{-1}	Transmissivity
W(u)	-	Theis well function
W(u,r/L)	-	Walton well function
W(u,β)	-	Hantush well function
β	-	Hantush leakage coefficient
χ	L^2	Magnitude of the difference between theoretical and observed drawdown values.
γ	T^{-1}	Hantush leakage function

Chapter 1

Introduction

Knowledge of the effect of groundwater is necessary when either considering water supply or a range of other civil engineering applications. In some regions of the world groundwater is an essential part of water supply. In the UK, approximately 35% of freshwater is obtained from groundwater sources. Other examples where groundwater is significant include the analysis of contaminant transport and the effect of groundwater on the engineering properties of soil, particularly where construction dewatering is considered.

Accurate methods of calculating the parameters which control the flow of groundwater is thus important. The method of pumping tests is commonly used to evaluate aquifer parameters. The analysis of the drawdown of the piezometric surface in response to pumping is used to estimate the aquifer parameters.

This research is aimed at improving the accuracy and speed of the determination of aquifer parameters. An accurate and fast method of analysis is presented, which calculates aquifer parameters using either the Theis, Walton or Hantush solutions. The analysis by hand of pump test results from a complex geological system may be difficult. Instead, a simpler method of analyis may be used, which would lead to innacurate parameters. The least squares algorithms developed during this research reduce the time and difficulty involved with the more complex methods of analysis. Thus a method may be used that is more appropriate to the geological conceptual model. These methods allow the hydrogeolgist to apply the results of more complex analysis with confidence.

Aquifer parameters may be determined from pumping test data by several methods. This research uses the method of least squares curve matching. The inverse solution technique of least squares evaluates the parameters which minimise the difference between the

observed and theoretical values of drawdown. The accuracy of the results may be observed by comparing the average error between the observed and theoretical drawdown values.

A significant part of the research consisted of conducting field pump tests in order to determine aquifer parameters. If pump tests use high capacity pumps over long periods of time, the resulting drawdown in an aquifer can be great. If this occurs, the flow regime within the aquifer is significantly different to the normal condition. If an investigation into well yield is being performed, this is an appropriate approach to take. However, if the aquifer is being investigated to analyse its characteristics in its normal condition, the results of a pumping test of this type may give misleading results. It is important to design the method of testing to reflect how the results will be applied.

This fieldwork investigated the characteristics of the aquifer under normal conditions to determine aquifer parameters for use in a model as part of a hydrological investigation. The pumping tests used a low capacity pump and very accurate measuring equipment. This ensured drawdown was small compared with the saturated thickness of the aquifer. Thus accurate results were obtained, but the impact on the aquifer as a whole was minimised.

The results of this fieldwork and other published pump test data were analysed using the least squares algorithms. The analysis of the published pump test data gave results close to those obtained by other authors. The average results from the analysis of the fieldwork were used to set the parameters in a two dimensional finite element model. Simulations of the pumping tests led to drawdown curves which matched the observed results well. This further validates the accuracy of the least squares programmes.

Accurate analysis of pumping test data is very difficult due to the complexities of most realistic geological systems. However, the reduction in the number of assumptions made by the method of analysis allows results to be treated with greater confidence. The leaky aquifer programmes increase accuracy. However, any results should be treated with

caution. Experience and common sense should be used by the hydrogeologist to evaluate the accuracy and applicability of all results.

Chapter 2

Background and Literature Review

There is a wide variety of terms which describe the hydrological and physical properties of aquifers. These terms are used in the analysis of pumping test data. The first section of this chapter describes these terms and some hydrological concepts.

Successive sections consist of a literature review which focuses on pumping tests. The theories of flow within some types of aquifers and the solution of these equations for the case of radial flow to a pumped well are examined. Some methods of applying these solutions to estimate aquifer parameters using pumping test data are described. The last section describes the subsequent methods of calculating aquifer parameters using computer techniques.

2.1. Definitions

Kruseman and de Ridder (1990) define a number of properties that are used in the analysis of pumping tests. Some are included in this section.

2.1.1. Basic concepts

Three types of geological strata will be defined that characterise aquifers and groundwater flow. The first is an aquifer, which is generally defined as a saturated permeable geological unit which may be used to provide a water supply. It is able to carry and transmit water. Sands and gravels are a common type of aquifer. An aquitard is again permeable enough to transmit water in significant quantities, but only over a large area. The permeability is too low to support a production well of any significant capacity. Clays and shales are examples of this feature. The third type is an aquiclude. This is considered impermeable. Some unfractured igneous or metamorphic rocks are regarded as aquicludes.

2.1.2. Different types of aquifers

Aquifers are characterised by the nature of the strata that over or underlie them. A confined aquifer is bounded above and below by an aquiclude. The water is under pressure and so the piezometric surface is above the top of the aquifer. An unconfined aquifer is bounded below by an aquiclude, but not restricted on the upper surface. The piezometric surface is coincident with the water table. A leaky aquifer is bounded by an aquitard on one or both sides. The aquitard allows a quantity of water, known as leakage, to re-supply the aquifer if the piezometric surface of the aquifer is reduced. When pumping occurs in a leaky aquifer, the head is reduced and some of the discharge will be derived from leakage through the aquitards. These different types of aquifers are shown diagramtically in Figures 2.1, 2.2 and 2.3.

2.1.3. Physical properties of aquifers and aquitards

Hydraulic conductivity (K) [LT^{-1}] is the rate at which water flows through a material of unit area in unit time under a unit hydraulic gradient. It is commonly replaced by transmissivity (T) [L^2T^{-1}], which represents the rate of flow over the whole of the saturated thickness of the aquifer.

Specific storage (S_s) [L^{-1}] is a property of confined aquifers. It represents the volume of water that a unit volume of aquifer releases from storage under a unit decline in head. The release of water comes from both the compaction of the aquifer and expansion of the water. The storativity (S) [-] is the specific storage multiplied by the aquifer thickness, or the volume of water released from the aquifer when the peizometric surface drops over a unit distance.

The hydraulic resistance of an aquitard (c) [T] represents the resistance of an aquitard to vertical flow. It is defined as the thickness of the aquitard, (d') [L], divided by the hydraulic conductivity of the aquitard for vertical flow, (K') [LT^{-1}]. The leakage factor, (L), is a

measure of the spatial distribution of the leakage through an aquitard. It is defined as $L = \sqrt{Tc}$, and has units of [L]. A large value of L represents a low leakage rate through the aquitard, and a small value of L a greater leakage rate.

2.1.4. The pump test procedure

A pumping test is a method used in order to determine some of the properties that are described above. During a pumping test, water is pumped from a borehole and this pumping rate recorded. The changing drawdown in the pumped well, and also in nearby observation wells, is recorded as the pumping test progresses. A plan view showing a pumping well and three observation wells is shown in Figure 2.4. The drawdown profile at a particular time is shown as a cross-section through this pumping site in Figure 2.5. This drawdown is in the form of a cone of depression, the radius of which expands as the quantity of water removed from the aquifer increases.. At the end of the pumping test, the pump is stopped and the recovery of the water in the wells also recorded. Different methods of analysis have been proposed, which are discussed later, in order to calculate the aquifer parameters from this drawdown data.

2.2. Theories of flow in aquifers and the analysis of pumping test data

Two aquifer types are considered in this section, the first a confined and the second a leaky aquifer. The previous work examined describes the theoretical behaviour of flow within these aquifers, and the solution of these equations when considering radial flow to a well. Methods of calculating the aquifer parameters by analysing pumping test data are then discussed.

2.2.1. Confined Aquifers

2.2.1.1. Solutions to flow in confined aquifers

Theis (1935) analysed the flow of water in a confined aquifer by using an analogy to heat flow. This solution is based on a number of restrictive assumptions. These are:-

1. The aquifer is confined.
2. The aquifer has a seemingly infinite areal extent.
3. The aquifer is homogeneous, isotropic and of uniform thickness over the area influenced by the test.
4. Prior to pumping, the piezometric surface is horizontal (or nearly so) over the area that will be influenced by the test.
5. The aquifer is pumped at a constant discharge rate.
6. The well penetrates the entire thickness of the aquifer and thus receives water by horizontal flow.

The solution derived by Theis to determine the drawdown, s, was reported as:

$$s = \frac{Q}{4\pi T} \cdot W(u) \tag{2.1}$$

where the Theis well function, $W(u)$ is defined as:

$$W(u) = \int_{u}^{\infty} \frac{\exp(-y)}{y} dy \tag{2.2}$$

and $$u = \frac{r^2 S}{4Tt} \tag{2.3}$$

where t is the time since pumping started.

Theis also included the analysis of the recovery of groundwater after pumping has ended. The residual drawdown can be evaluated by introducing an imaginary recharge well, of identical but opposite flow, at the time pumping stopped. The pumping is considered as continuous and equation 2.1 adapted to calculate the residual drawdown, s', as:

$$s' = \frac{Q}{4\pi T} \cdot \{W(u) - W(u')\} \tag{2.4}$$

where $u' = \frac{r^2 S'}{4Tt'}$ (2.5)

Jacob (1940) derived the fundamental differential equation governing the flow of water in an elastic artesian aquifer. For radial conditions this equation is written:

$$\frac{1}{r} \cdot \frac{\partial}{\partial r}\left(rT \cdot \frac{\partial h}{\partial r}\right) = S \cdot \frac{\partial h}{\partial t} \quad (2.6)$$

Jacob solved this for the case of radial flow and determined the same solution as Theis obtained (equation 2.1) by using the heat flow analogy.

2.2.1.2. Use of the Theis equation to determine aquifer parameters

The aquifer parameters of transmissivity and storativity may be determined using the Theis equation and data from pumping tests. Due to the complex nature of the equation, these values may not be calculated analytically, and an alternative solution method must be used. Three methods have been put forward to solve the equation and so determine these aquifer parameters. The first is the curve matching or log-log method, the second the straight line or semi-log method and the third the slope matching method.

Jacob (1940) described the log-log or curve matching method, devised by Theis. This method determines transmissivity and storativity by a method called type curve matching. A Theis curve is shown in Figure 2.6, and the curve matching procedure is shown graphically in Figure 2.7. The method of curve fitting by hand is summarised below:-

1. Prepare a type curve of the Theis well function using log-log paper, with *W(u)* plotted on the *y* axis against *1/u* on the *x* axis.
2. Plot the observed data on log-log paper, with drawdown '*s*' on the *y* axis and 't/r^2' on the *x* axis. It is important that the graph paper used for each curve is to the same scale.
3. Superimpose the observed data curve on the theoretical curve. Keep the axes parallel and adjust the data curve to obtain a 'best match' with the theoretical type curve.

4. Select a 'match point', and read from this point the values of '*W(u)*', '*1/u*', and the corresponding values of '*s*' and 't/r^2'. Choosing simple values of *W(u)* and *1/u* (e.g. 1.0 and 10.0) simplifies the calculations.
5. Calculate the value of *T* by substituting the values of *W(u)*, *s* and *Q* in equation 2.1. The value of *S* can then be calculated using equation 2.3.

In order to perform this curve matching technique it is necessary to evaluate the well function, *W(u)*. Jacob gave a series approximation to evaluate the well function, which is defined as follows:

$$W(u) = -0.5772 - \ln(u) + u - \frac{u^2}{2.2!} + \frac{u^3}{3.3!} - \ldots + \frac{(-1)^{n+1}(u)^n}{n.n!} \qquad (2.7)$$

Cooper and Jacob (1946) observed that if an interval of time has passed since a well has begun discharging, then the drawdown increases approximately in proportion to the logarithm of the time since pumping started, and decreases in proportion to the logarithm of the distance from the pumped well. They also established that for small values of *u* the series approximation for the value of *W(u)* could be simplified to:

$$W(u) = \ln\left(\frac{1}{u}\right) - 0.5772 \qquad (2.8)$$

They determined that this approximation is acceptable for values of $u < 0.02$.

The semi-log approach was then devised in order to determine aquifer parameters. Three equations were developed which contained only three variables, the drawdown *s*, radial distance *r* and the time *t* since pumping started. These equations are:

$$s = \left(\frac{-2.3Q}{2\pi T}\right)\left[\log_{10} r - 0.5\log_{10}\left(\frac{2.25Tt}{S}\right)\right] \qquad (2.9)$$

$$s = \left(\frac{2.3Q}{4\pi T}\right)\left[\log_{10} t - \log_{10}\left(\frac{r^2 S}{2.25T}\right)\right] \qquad (2.10)$$

$$s = \left(\frac{-2.3Q}{4\pi T}\right)\left[\log_{10}\left(\frac{r^2}{t}\right) - \log_{10}\left(\frac{2.25T}{S}\right)\right] \qquad (2.11)$$

Equation 2.9 can be used when the drawdown at several wells at the same time are known by plotting drawdown against $\log_{10} r$. This is shown in Figure 2.8. Equation 2.10 may be used when the drawdown in one well is observed over time, by plotting the drawdown against $\log_{10} t$. Figure 2.9 shows this procedure for observation wells at 30, 90 and 215 metres from the pumped well. The drawdown from many wells can be used in equation 2.11 by combining the radius r and time t into one variable, r^2/t. This variable is plotted on the log scale against drawdown. The drawdown data from all three observation wells should lie on the same straight line. A graph showing this method is presented in Figure 2.10.

To calculate the values of transmissivity and storativity, the slope and the intercept of the graph are measured. The slope of the graph corresponds to the term outside the square brackets, and so the appropriate equation can be used to calculate the value of transmissivity. The terms inside the square brackets correspond to the intercept, and so the storativity can be evaluated.

These methods were then extended to a more generalised form. This allows the interpretation of pumping test data from observing drawdowns in an area where several wells are pumping simultaneously.

Butler (1990) considered the two methods described above, (log-log and semi-log), and evaluated the difference in the values of transmissivity and storativity that would be obtained if the method were used in an aquifer where the flow properties were not uniform. These methods were considered for three different situations. The first is observing the drawdown in a pumped well and the second for an observation well. The third consideration

involved examining which method to use when considering the objective of conducting the pumping test.

The material close to a pumped well may be of anomalous properties due to the heterogeneity of the aquifer material and/or the effect of the well being drilled. If the semi-log method is considered, transmissivity is calculated from the gradient of the drawdown with respect to time. The change in drawdown is a function of the value of transmissivity at the front of the cone of depression. As pumping progresses, the front of the cone of depression moves away from the pumped well. Theis (1940) stated that after a significant time, the material close to the well does not contribute to the discharge to the well, but serves as a conduit to transport water from a distance. Thus the semi-log method measures the transmissivity at the edge of the cone of depression, which is independent of the material between this point and the pumping well, which may be of anomalous properties. However, the value of storativity is calculated from the 'x' intercept of the graph. Thus the value of storativity calculated is dependent on the values of transmissivity between the pumping well and the front of the cone of depression.

When using the log-log method, the total drawdown, not the change in drawdown, is measured. Thus many errors, such as head losses, may be included in the determination of the aquifer properties. Also, when curve matching, the part of the curve which is of greatest curvature is heavily emphasised. These are the results which reflect the material near the pumping well. Thus when analysing data from a pumping well, Butler suggests that the semi-log method will be more accurate.

As the pumping test continues, the value of transmissivity may change. These changes may be calculated using the log-log method as the heavy weighting of the near well material becomes less important. When using the semi-log method, the value of transmissivity calculated will change as the front of the cone of depression moves into material of differing properties, and the slope of the line will change.

When considering the results of calculating transmissivity and drawdown from observation wells, the differences between the semi-log and log-log methods are minimised. As the distance from the pumped well increases, the volume of the aquifer controlling the drawdown is significant. Thus the errors introduced by the anomalous properties of the material near the well are negligible. The case of the observation well being situated within anomalous properties is also considered. This case was found to minimally impact drawdown, and thus the values of transmissivity and storage calculated using either the semi-log or log-log method will be an accurate representation of the material between the pumped and observation well. The log-log method is likely to give a better average value of aquifer properties.

When conducting a pumping test, the information required should point to the best method of analysis. If the potential well yield is being investigated, the semi-log method would be the best approach. The log-log method could also be used, if data from an observation borehole were available. However, if the total drawdown after a certain period of pumping was required, the value of transmissivity from a log-log method would be more appropriate.

Chow (1952) developed a slope matching method to determine the values of transmissivity and storativity. This method enables these values to be calculated from the gradient of the drawdown curve. Values of transmissivity and storativity can thus be calculated at different times during the pumping test, and any variance in the values observed. One reason for a change in the values is the compaction of the aquifer as a result of pumping.

Chow defines another well function *F(u)*, as

$$F(u) = \frac{s}{ds/d\log_{10} t} \qquad (2.12)$$

After differentiating equation 2.1 and further manipulation, Chow established a relationship between *F(u)* and *W(u)* as:

$$F(u) = W(u) \cdot e^u / 2.3 \qquad (2.13)$$

and when u is very small, $e^u \rightarrow 1.0$ and equation (2.13) becomes:

$$F(u) = W(u) / 2.3 \qquad (2.14)$$

Chow assumed this to be true for $u < 0.01$. A graph may be plotted to determine the relationship between the values of *W(u)*, *F(u)* and u. The value of *F(u)* can be calculated by drawing a tangent to the drawdown curve, and measuring the gradient. *W(u)* and u can then be derived from the graph of *F(u)* and *W(u)*. Once *W(u)* and u are known, the values of transmissivity and storativity are calculated from equations 2.1 and 2.3.

Thus Chow presented a method to calculate the values of transmissivity and storativity using the slope of the drawdown curve. The method can observe the changing values of transmissivity and storativity as the pumping test progresses, and removes the element of human error from the curve matching procedure. However, when using Chow's method by hand, the accuracy will be reduced as the act of drawing a tangent to the drawdown curve is also likely to be affected by human error.

Rai (1985) presented a method which followed the analytical development of Chow (1952). It uses a finite difference method to calculate the values of transmissivity and storativity from the Theis equation. Rai defines the function, *f(u)*, as

$$f(u) = W(u) \cdot e^u = \frac{s/t}{ds/dt} \qquad (2.15)$$

To evaluate the aquifer constants the right hand side of equation 2.15 is written in finite difference form. The drawdowns, s_1 and s_2 are evaluated at times t_1 and t_2 respectively. Thus *f(u)* can be written as

$$f(u)=\left(\frac{s_2+s_1}{t_2-t_1}\right)\Big/\left(\frac{s_2-s_1}{t_2+t_1}\right)$$

and thus the values of T and S calculated from equations 2.1 and 2.3 respectively as:

$$T=\frac{Q}{2\pi(s_2+s_1)}\cdot W(u) \tag{2.16}$$

and

$$S=\frac{2u(t_2+t_1)T}{r^2} \tag{2.17}$$

Rai also expanded this method to use three sets of pumping test data measured at equal time intervals. This improves the accuracy of the calculation of *f(u)*. This method allows the aquifer parameters, transmissivity and storativity, to be evaluated at different times during the pumping test. Thus a number of points can be chosen to evaluate these parameters.

2.2.2. Leaky aquifers

2.2.2.1. Analysis of leaky aquifers including the permeability of the aquitard

The analysis of flow in leaky aquifers introduces more complexity, due to the leakage through the aquitard to the aquifer. Jacob (1946) evaluated the condition of an artesian bed which is overlain by a semi-pervious confining bed. The assumptions made in this analysis are:-

1. The head in the layer supplying the leakage is constant.
2. The permeability contrast between the semipervious layers and the artesian sand is very great, so that the flow is vertical in the semiconfining beds and horizontal in the artesian sand.
3. Storage in the impervious layers is neglected.

Jacob developed an equation which describes the radial flow of water in a leaky artesian aquifer. This governing equation is written:

$$\frac{\partial^2 s}{\partial r^2}+\frac{1}{r}\cdot\frac{\partial s}{\partial r}=\frac{1}{a^2}\cdot\frac{\partial s}{\partial t}+s\cdot\frac{b^2}{a^2} \qquad (2.18)$$

where $a = \sqrt{(Kd/S)}$

$b = \sqrt{(K'/d'S)}$

The solution for this equation was then evaluated for radial flow for both transient and steady state conditions, with a boundary at a distance that is maintained at a constant head. These solutions are complex. The problem was investigated further by Hantush and Jacob (1955). In this case the problem was solved for the case of the outer boundary removed to infinity. The solution presented is again complex, but a simplification for the transient solution at early time was given as:

$$s=\frac{Q}{4\pi T}\cdot W\left(u, r/L\right) \qquad (2.19)$$

where the Walton well function is defined as:

$$W\left(u, r/L\right)=\int_u^\infty \frac{1}{y}\exp\left(-y-r^2/4L^2y\right)dy \qquad (2.20)$$

and $L^2=\dfrac{T}{K'/d'}$

It is clear that as the leakage factor, $L \rightarrow \infty$, equation 2.20 reduces further to

$$s=\frac{Q}{4\pi T}\int_u^\infty \frac{\exp(-y)}{y}dy$$ which is the Theis solution (equation 2.1)

Hantush (1956) expanded this work on the theory of flow in leaky aquifers by presenting two methods to calculate the coefficients of transmissivity, storage and leakage, one for steady state and the second for transient conditions. The maximum, or steady state drawdown was first calculated by letting *t* approach infinity. The solution for drawdown under these conditions is:

$$s_m = \left(\frac{Q}{2\pi T}\right) K_0\left(r/L\right) \tag{2.21}$$

where s_m is the steady state drawdown and $K_0(x)$ is a modified Bessel function of the second kind and of zero order.

The method of steady distribution of drawdown may be used when the value of r/L is small (< 0.05). In this case, equation 2.21 may be approximated as:

$$s_m = \left(\frac{2.3Q}{2\pi T}\right) \log_{10}\left(0.89r/L\right) \tag{2.22}$$

Thus if the steady state drawdown at a series of wells at different radii from the pumped well is recorded, a plot of s_m against r on semi-log paper will exhibit a straight line. Where r/L is large, the points will form a curve. The slope of the straight line is equal to $(2.3Q/2\pi T)$ from which T may be calculated. The value of L may also be evaluated by measuring the intercept on the log axis, r_0. L may then be calculated from $L = 0.89r_0$. A value of the storage coefficient may not be calculated using this method as it uses steady state data.

The second method, for a non-steady distribution of drawdown, uses a semi-log plot of the time drawdown curve. This method calculates the leakage, transmissivity and storativity using the inflection point from the time vs. drawdown curve. This method is complicated and would be very susceptible to human error.

Walton (1970) described a curve matching method to calculate the values of transmissivity, storativity and the leakage factor. The method is similar to that of the Theis curve matching method, except in this case there is a series of curves, for different values of r/L, as shown in Figure 2.11. Once the value of r/L has been determined, it is then possible to calculate the value of K', the vertical permeability of the aquitard.

2.2.2.2. Analysis of leaky aquifers including the permeability and storativity of the aquitard

All of the above theories were developed subject to the three assumptions made at the beginning of section 2.2.2. However, often the confining bed yields significant amounts of water from storage, which is ignored by the methods above. Hantush (1960) developed a solution to the drawdown in a leaky artesian aquifer, which takes both the vertical permeability and storativity of the aquitard into account.

Hantush developed the following equation for drawdown in a leaky aquifer for early time, when $t < (d'S'/10K')$:

$$s = \frac{Q}{4\pi T} W(u,\beta) \tag{2.23}$$

where

$$W(u,\beta) = \int_u^\infty \left\{ \frac{\exp(-y)}{y} \cdot erfc\left(\frac{\beta\sqrt{u}}{\sqrt{y(y-u)}} \right) \right\} dy \tag{2.24}$$

and

$$\beta = \frac{r}{4}\sqrt{\frac{K'/d'}{T} \cdot \frac{S'}{S}} \tag{2.25}$$

Solutions for longer time were also given, for three different cases of geological formations. When the ratio of S'/S is small, then the contribution to leakage from the storage is negligible, and equation 2.19 may be used to calculate drawdown in the aquifer.

Walton (1970) used this method to calculate aquifer parameters. The method is described and values of the Hantush well function, equation 2.24, are also given. The Hantush curves are shown in Figure 2.12.

2.2.2.3. Analysis of leaky aquifers including the aquitard parameters and drawdown in the unpumped aquifer

Neuman and Witherspoon (1969a) recognised that the assumption made by Jacob and Hantush that there would be no drawdown in the unpumped aquifer which overlies the

aquitard would only be true at small values of time. Thus they proposed a method to analyse the transient flow in a leaky two aquifer system. The only assumption made is that the flow is vertical in the aquitard and horizontal in the aquifers. They have thus expanded the Hantush solution that includes leakage (1960) to include the drawdown in the unpumped aquifer.

A solution to this general problem was put forward which gave drawdown in the pumped and unpumped aquifers as well as the aquitard. The solution was then modified for the case of no drawdown in the unpumped aquifer, which was shown to agree with the Hantush solution (equation 2.23). By reducing the permeability of the aquitard to zero, the aquifer is in effect confined, and the solution again reduces to the Theis solution (equation 2.1).

Following the publication of the theory of flow in leaky aquifers that took drawdown in the unpumped aquifer into account, Neuman and Witherspoon (1969b) examined the theories of flow proposed by Hantush and Jacob (1955) and Hantush (1960). The validity of the assumptions made to develop these theories are discussed, and the accuracy of the methods examined.

When considering the assumption that the storage of the aquitard may be neglected (equation 2.19, the '*r/L* solution'), the family of type curves is similar to the Neuman and Witherspoon solution for small β. The only difference is that as time increases, the Neuman and Witherspoon solution slowly diverges from the Theis solution, and the *r/L* solution converges to it. Thus it can be seen that only a small error will be introduced if the *r/L* solution is used to analyse the pump test results, if the values of *r/L* and β are small (<0.01).

At early time for a system where the aquitard storage is significant, the effect of pumping water from the lower aquifer has not significantly affected the unpumped aquifer. Thus most of the leakage at early time is from the aquitard. The quantity of water that recharges the aquifer from the aquitard is highly dependent on the value of storage. Thus the *r/L*

solution effectively disregards the leakage at early time, and thus cannot form an accurate representation of the aquifer drawdown. Considering this argument as time increases towards steady state, it can be seen that the portion of recharge from storage will be negligible. Thus the *r/L* solution can be applied as steady state is approached. It can be considered as accurate when time,

$$t \geq \frac{80\beta^2}{\left(r/L\right)^4} \tag{2.26}$$

The solution of no drawdown in the unpumped aquifer was also considered, for equation 2.23 (the 'β solution'). As was discussed earlier, at early time the drawdown in the unpumped aquifer will be negligible and so the β solution can be applied when the time,

$$t \leq \frac{1.6\beta^2}{\left(r/L\right)^4} \tag{2.27}$$

However, this is only true for the drawdown in the pumped aquifer and aquitard, not the unpumped aquifer itself. At early time the Neuman and Witherspoon solution is a single type curve, so the range of values for the unpumped aquifer has no effect. But as time increases, the single type curve becomes a family of curves, and so the drawdown in the unpumped aquifer can have a significant effect on the aquifer system.

The magnitude of the errors introduced by ignoring the drawdown in the unpumped aquifer is dependent on the coefficients of the pumped aquifer and aquitard. As the ratio between the characteristics of the pumped aquifer and the aquitard increases, the errors introduced are reduced, also depending on the ratio of the transmissivity and storage coefficients of the pumped and unpumped aquifers.

From this evaluation of the techniques for estimating the properties of leaky aquifers, it can be seen that the β solution is a more accurate representation of the drawdown in aquifers

than the *r/L* solution. Neuman and Witherspoon also examined the typical errors that could occur due to the analysis of field data using the *r/L* solution, and found that these errors could be substantial.

Walton (1979) reviewed the methods available to calculate the aquifer characteristics of leaky aquifers. Solutions were given for a range of practical situations, using the theory from Hantush and Jacob (1955) and Hantush (1960) as described above. Solutions were given for varying discharge rates, storage capacity of the pumped well and partial penetration of pumped and observation wells.

The analysis of pumping tests in leaky aquifers to determine aquifer parameters is highly complex. However, if the aquifer system is over simplified the results will lead to errors. Thus a 'trade off' needs to be made between accuracy and practicality. It must be possible to calculate aquifer parameters using an efficient method, without a loss of accuracy. The hydrogeologist can then have confidence in the results of the analysis and may pursue the objectives of the project.

2.3. Computer methods to calculate aquifer parameters from pumping test data

The use of computer methods are able to greatly increase the speed of analysis, thus enabling a more complex and accurate approach to be taken than a manual method in the same, or less time. It is important, however, that the method used is appropriate to the conceptual model. The geology must be quantified and the flow regime understood, in order that the correct approach is taken.

Many different computer methods have been proposed which may be used to determine aquifer parameters from pumping test data. First the techniques that match observed and theoretical values of drawdowns will be discussed. The next section examines the slope matching methods, which match the derivative of the observed drawdowns with time against

theoretical values. The last section examines other methods which use, for example, finite element techniques. A number of methods in all of these sections use the theory of least squares. This theory minimises the difference between the observed and theoretical values. The theory of least squares is examined in detail in section 4.2.4.

2.3.1. Curve matching methods

Saleem (1970) produced a computer programme which used non-linear programming to determine parameters. This programme was used to calculate the values of transmissivity, storativity and leakage coefficients for either a confined or a leaky confined aquifer system.

McElwee (1980) used non-linear least squares and sensitivity analysis to determine confined aquifer parameters. In this approach, the sensitivity coefficients, $\partial s/\partial S$ and $\partial s/\partial T$ are determined by differentiating the Theis equation for drawdown in a confined aquifer (equation 2.1). These functions can then be used to evaluate the impact on drawdown of changing the values of transmissivity and storage. This approach is then used as part of a least squares analysis to estimate the parameters of a confined aquifer.

This work was extended further by McElwee and Paschetto (1982) when the programme was altered so that it could be run using a hand-held calculator. Up to 44 drawdown-time pairs could be input simultaneously. The programme used sensitivity analysis and non-linear least squares, as before. An indication of the accuracy of the results was given by the inclusion of the root mean square error between the observed and calculated values of drawdown, using the final values of transmissivity and storativity.

A method was also proposed by Rayner (1980), which calculated the values of transmissivity and specific storativity using a hand-held calculator. This also uses the method of least squares, and the equation minimised is the Cooper Jacob equation (2.10). This programme had a restriction that the value of u should be less than 0.02. Drawdown

data which lead to values of u which are greater than 0.02 will be early time data which may be erroneous due to the nature of data from a pumping test.

Chander, Goyal and Kapoor (1981) proposed a method which used the Marquardt algorithm and non-linear least squares to determine confined and leaky aquifer parameters, using the Theis (2.1) and Hantush/Jacob (2.19) equations. The Marquardt algorithm determines the final values of aquifer parameters by calculating increments in the parameters that will minimise the error between calculated and observed values of drawdown. It is similar in method to that of McElwee (1980).

Butt, Cobb and McElwee (1982) further extended the work by McElwee (1980) by expanding the sensitivity analysis to evaluate the parameters of leaky aquifers using the Hantush/Jacob equation (2.18). This work was very similar to that of Chander, Goyal and Kapoor (1981), but more mathematical detail was given. The leaky equation was first evaluated using the Laguerre Quadrature formula. However, it was found to be inaccurate at small values of u. Thus further methods were used in order to evaluate the leaky well function $W(u,R/L)$ for all necessary values of u and r/L.

The sensitivity coefficients, $\partial s/\partial S$ and $\partial s/\partial T$ were evaluated analytically by applying Leibnitz's rule. The value of $\partial s/\partial L$ was evaluated using numerical techniques due to the complicated nature of the function.

The values of these sensitivity coefficients were then examined. Graphs were plotted which showed how the value of the coefficients changed with increasing distance from the well, and as time increased at a particular radius from the well. These graphs can then be interrogated and compared to the changes observed in practise in a leaky aquifer when a pumping test is performed. These coefficients are more fully discussed in chapter 7.

The sensitivity coefficients were then used to compute the 'best fit' aquifer parameters in a least squares sense. This best fit can be assessed by examining the value of the root mean square (rms) error between observed and calculated drawdowns. This algorithm was capable of calculating the aquifer parameters for a leaky confined system quickly and easily.

Das Gupta and Joshi (1984) presented a method based on minimising the integral square error to determine aquifer parameters for a confined system. The method follows the method of curve matching and is able to identify and eliminate data which is erroneous in order to select the group of observations which most closely follows the theoretical curve, and needs no initial approximation of the aquifer parameters.

The method takes a 'curve shifting' approach. If the type curve $W(u)$ versus u were plotted on a graph with the data from a pump test of s versus r^2/t, the data would be offset horizontally by $\ln(4T/S)$ and vertically by $\ln(Q/4\pi T)$. A procedure is set up which moves the theoretical curve first horizontally and then vertically by changing the value of the aquifer parameters. This process is repeated and the percentage deviation of each point from the theoretical curve is calculated. The segment of data with the minimum variation is then used to match the two curves, and thus a certain portion of the data is eliminated from the procedure. This is then repeated until a preassigned minimum number of points are left which best fit the type curve such that the integral square error is a minimum.

Some problems may be incurred with this point elimination approach, as the aquifer is likely not to conform to the stringent assumptions made by the Theis formula. Contribution from leakage is possible and would reduce drawdowns towards late time. This algorithm would disregard these points as they would not be a good fit to the classical solution, but this would give a false indication of the real aquifer parameters.

Mukhopadhyay (1985) also used a curve shifting method to obtain values of the aquifer parameters for a confined system. It uses the assumption made by Cooper and Jacob to approximate *W(u)* for values of $u < 0.05$ and so only uses data that conforms with this assumption. The aquifer parameters that are calculated are the best in the least squares sense. The method was tested and found to calculate parameters that were close to those of other methods.

Yeh (1987a) developed a method to determine aquifer parameters for a confined system. Newton's finite-difference method was used to solve the system of non-linear equations. The non-linear equations were the first partial derivatives of the error between the observed and theoretical data, with respect to transmissivity and storativity.

The values of the parameters *S* and *T* can then be determined by using Newton's finite difference method. These values were then used in a non-linear least-squares algorithm to determine the aquifer parameters. The programme uses all of the data from the pumping test, converged quickly and accurately.

Bardsley (1991) used a point fitting method in order to determine aquifer parameters for a confined system. Two methods are described. The first uses two drawdown/time pairs. This pair of values is then used to compute values of transmissivity and storativity that will enable a theoretical drawdown curve to pass through the prescribed points. These values are calculated by locating the zero of a simple function.

The second method uses three drawdown/time pairs of data, and incorporates the presence of a single linear aquifer boundary of zero drawdown or constant head. This process uses image well theory in order to determine the aquifer parameters. These point fitting methods are subjective. If the chosen points are not reflective of the pumping test, inaccurate values would result. A number of different points should thus be chosen, in order to observe any

large variations in the calculation of the parameters. However, if a variation in the parameters occurs, there is no process by which inaccurate values may be disregarded.

Alvarez and Kohlbeck (1991) used a least squares method to determine aquifer parameters for a leaky aquifer. The Hantush and Jacob (1955) leaky equation was evaluated and a number of non-linear optimisation methods used to search for a solution which gives the minimum error in a least squares sense. The programme was tested against pump test data from other publications, and also two pump tests in Colombia.

2.3.2. Slope matching methods

Slope matching methods determine the values of the parameters by evaluating the slope of the drawdown equation with respect to time. This provides a different method of solution to the curve matching methods described above.

Grimestead (1981) used Newton's iterative method to solve the Theis equation using two drawdown/time pairs. The Theis equation was manipulated, differentiated and the value of (S/T) determined by Newton's iterative method using the equation:

$$\frac{\left(S/T\right)_{n+1}}{\left(S/T\right)_{n}} = 1 + \frac{W_2 \ln\left(\Delta h_1 Q_2 W_2 \,/\, \Delta h_2 Q_1 W_1\right)}{\exp\left(-u_2\right) - \left(W_2 \,/\, W_1\right)\exp\left(-u_1\right)} \qquad (2.28)$$

Once the optimum value of (S/T) had been calculated, the value of T and hence S could be determined. The programme requires an estimate of the value of (S/T).

Rai introduced a slope matching method which used finite difference calculations to determine aquifer parameters, based on the method devised by Chow. This method is discussed in section 2.1.1.2.

Sen (1986) also investigated the calculation of the parameters by a slope matching method. Curve matching methods match observed and theoretical values of drawdown. As these

curves overlap, the derivatives of the curves should also be identical at the match points. The slope matching method matches these slopes, rather than the values of drawdown. The slope of a log-log type curve can be defined as:

$$\alpha = u \cdot \frac{d\ln\left[W(u)\right]}{du} = u \cdot \frac{W'(u)}{W(u)} \tag{2.29}$$

The values of *W(u)* and *W'(u)* can be evaluated from the series approximation (equation 2.7). Thus the slope, α, at any point can be defined as:

$$\alpha = -\frac{e^{-u}}{W(u)} \tag{2.30}$$

Thus two time vs. drawdown pairs can be used to calculate the values of *u* and *W(u)*. The value of α can be calculated from:

$$\alpha = \frac{\ln\left(s_i / s_{i-1}\right)}{\ln\left(t_{i-1} / t_i\right)} \tag{2.30}$$

This value of α may then be used to find *u* from a table of values. The value of *W(u)* is then calculated using equation 2.30. Equations 2.1 and 2.3 are then used to determine the values of *T* and *S*. This process can be repeated for a number of different time vs. drawdown pairs and a sequence of parameter estimations recorded.

The different slope matching methods are examined by Guzman-Guzman and Srivastava (1994). These methods determine the value of the slope, or the time derivative of the drawdown equation in order to calculate the aquifer parameters.

First the Theis equation is written in a form which is dependent on time, *t*.

$$s = \alpha \cdot W\left(\frac{\beta}{t}\right) \tag{2.31}$$

where $\alpha = \frac{Q}{4\pi T}$ and $\beta = \frac{r^2 S}{4T}$

This equation can then be differentiated to give the value of the slope as:

$$t \cdot \frac{\partial s}{\partial t} = \alpha \cdot \exp\left(-\beta / t\right) \tag{2.32}$$

Different methods are discussed which determine the value of $\partial s/\partial t$. The values of α and β can then be determined using two solution methods. The first uses two successive points to determine the value of slope, and so can show how the values of the aquifer parameters change with time The second method uses a straight line method to calculate an average value of parameters, and uses the least-squares method to obtain the best fit.

Four methods of calculating $\partial s/\partial t$ are examined below.

a) This method uses a central difference scheme, similar to that devised by Rai. This is:

$$t_2 \frac{s_3 - s_1}{t_3 - t_1} = \alpha \cdot \exp\left(-\beta / t_2\right) \text{and } t_3 \frac{s_4 - s_2}{t_4 - t_2} = \alpha \cdot \exp\left(-\beta / t_3\right) \tag{2.33}$$

Thus the values of α and β can be determined at the average time value $(t_2 + t_3)/2$, given two drawdown/time values.

b) Yeh (1987b) suggested adapting Rai's method. This method replaces $t \cdot \frac{\partial s}{\partial t}$ by $\frac{\partial s}{\partial \ln(t)}$. The finite difference form can then be written as:

$$\frac{s_{i+1} - s_i}{\ln\left(t_{i+1} / t_i\right)} = \alpha \cdot \exp\left(-\beta / \bar{t}_{i,i+1}\right) \tag{2.34}$$

c) Sen took a double logarithmic approach to solving the equation, which can be written as:

$$\frac{\partial(\ln s)}{\partial(\ln t)} = \frac{\alpha}{s} \cdot \exp\left(-\beta / t\right) \tag{2.35}$$

This is then written in finite difference form as:

$$\bar{s}_{i,i+1} \cdot \frac{\ln\left(s_{i+1}/s_i\right)}{\ln\left(t_{i+1}/t_i\right)} = \alpha \cdot \exp\left(\frac{-\beta}{\bar{t}_{i,i+1}}\right) \tag{2.36}$$

d) A different approach was proposed in the paper which included a derivative of the well function. This was written as:

$$\frac{\partial s}{\partial W\left(\beta_g/t\right)} = \alpha \cdot \exp\left(\frac{\left(\beta_g - \beta\right)}{t}\right) \tag{2.37}$$

which can be written in finite difference form as:

$$\frac{s_{i+1} - s_i}{W\left(\beta_g/t_{i+1}\right) - W\left(\beta_g/t_i\right)} = \alpha \cdot \exp\left(\frac{\beta_g - \beta}{\bar{t}_{i,i+1}}\right) \tag{2.38}$$

where β_g is an initial guess for the value of β.

These methods were used to evaluate both synthetic and field data. The method devised by Yeh, which used the slope of the drawdown with respect to the logarithm of time, and method (d), which involved the derivative of the drawdown with respect to the well function were found to give the best results.

2.3.3. Further methods

Rushton and Chan (1976) developed a discrete space/discrete time model which simulated the flow of groundwater towards a well. The method is a finite element method in which all the different components of the flow system may be incorporated. The method was tested for both a confined and leaky aquifer, and was found to agree with the classical solutions. It is also possible to use this model to investigate localised changes in parameters.

Holzschuh (1976) developed a computer method to analyse pumping test data using the Hantush inflection point method. An example is given from which aquifer parameters are calculated which closely match previously calculated values from type curve analysis.

Motz (1990) developed a model which determined transmissivity and leakage by considering the steady state drawdowns at different distances from a line sink (canal). A drain function was developed and a type curve plotted. The steady state drawdowns can then be compared against this type curve and the transmissivity and leakage determined.

Doherty (1990) evaluated aquifer parameters using data from a pump test in the workings of a disused underground mine. The object of the test was to determine the long term inflow of water to the mine. Water was extracted from the aquifer through the network of mine workings. This complicated pumping test meant that standard methods could not be used to determine the aquifer parameters. A mathematical model was set up which incorporated linear flow, sink storage and a connection to the regional groundwater regime. Numerical inverse Laplace transformations are then used to solve the problem and the aquifer parameters estimated using non-linear least squares analysis.

This literature review has discussed a large number of methods available for the determination of aquifer parameters by analysing pump test data. These have included both hand and computer methods. It has also discussed the assumptions made by some of these methods, and so those that are more accurate and relevant to the field situation encountered may be used to develop a method of pump test analysis.

2.4. Conclusions

The aim of this research is to produce a tool to estimate aquifer parameters using pumping test data. Thus it should be accurate and able to work in a variety of situations. Some of the most accurate methods of pump test analysis were discussed in the section above. They are site specific, and so take into account all of the known geological data. To perform such analysis for every pump test would be time consuming and expensive. However, such analysis would be warranted in certain situations where extensive knowledge of the aquifer parameters was required.

The method chosen is that of curve matching using a least squares algorithm, for confined and leaky aquifers. This will estimate the parameters that minimise the difference between the observed and theoretical drawdown. The research aims to calculate aquifer parameters using the Hantush solution to drawdown in a leaky aquifer. This represents a more complex solution than Walton, as it takes the storage of the aquitard into account. This will thus present the most accurate and realistic results of leaky aquifer pump test analysis.

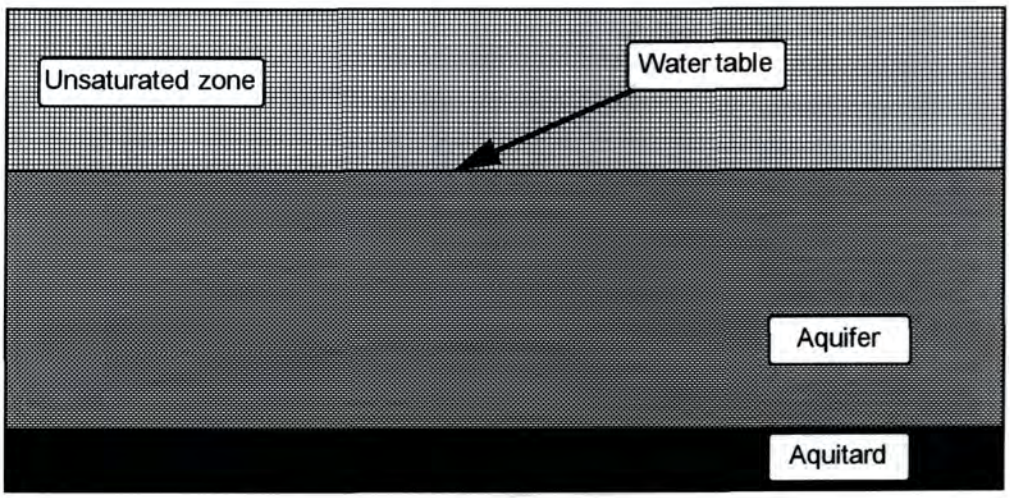

Figure 2.1: An unconfined aquifer

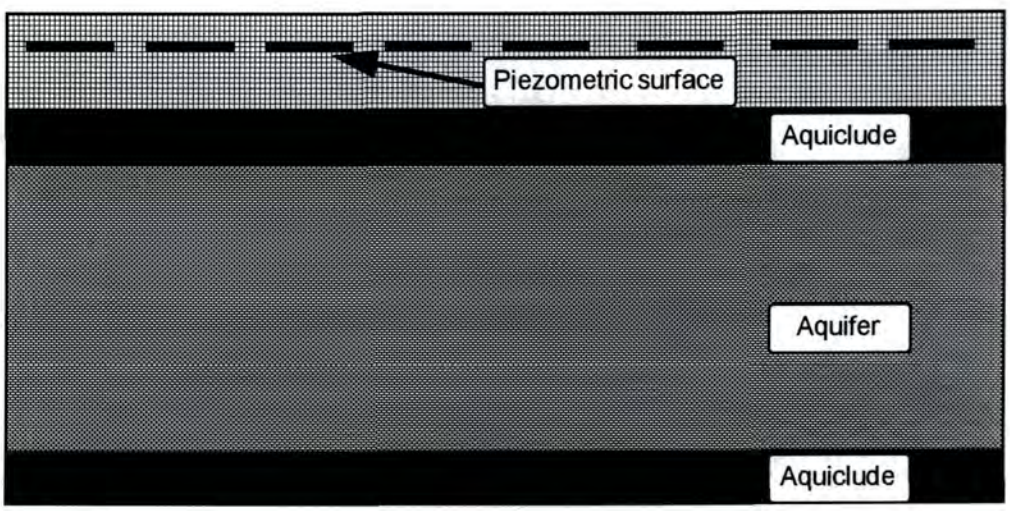

Figure 2.2: A confined aquifer

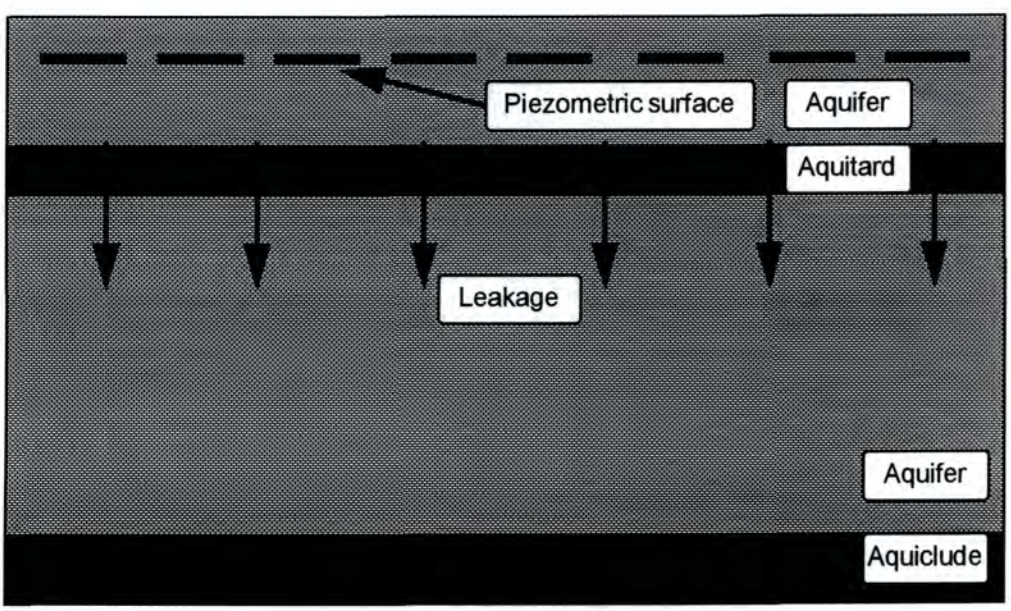

Figure 2.3: A leaky aquifer

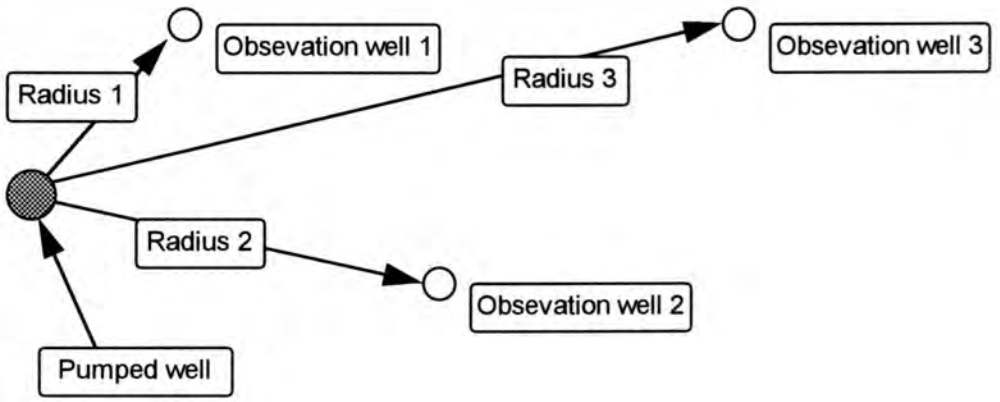

Figure 2.4: Plan view of a pumping site showing pumping and observation wells

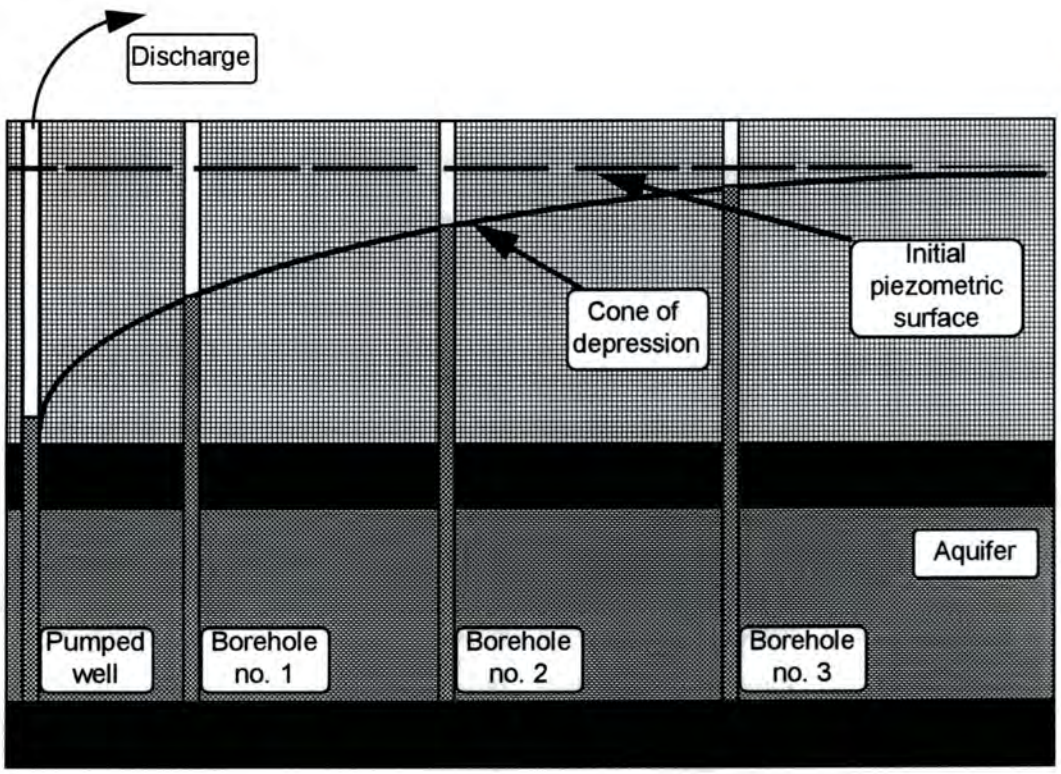

Figure 2.5: Cross-section through the pumping site showing the cone of depression

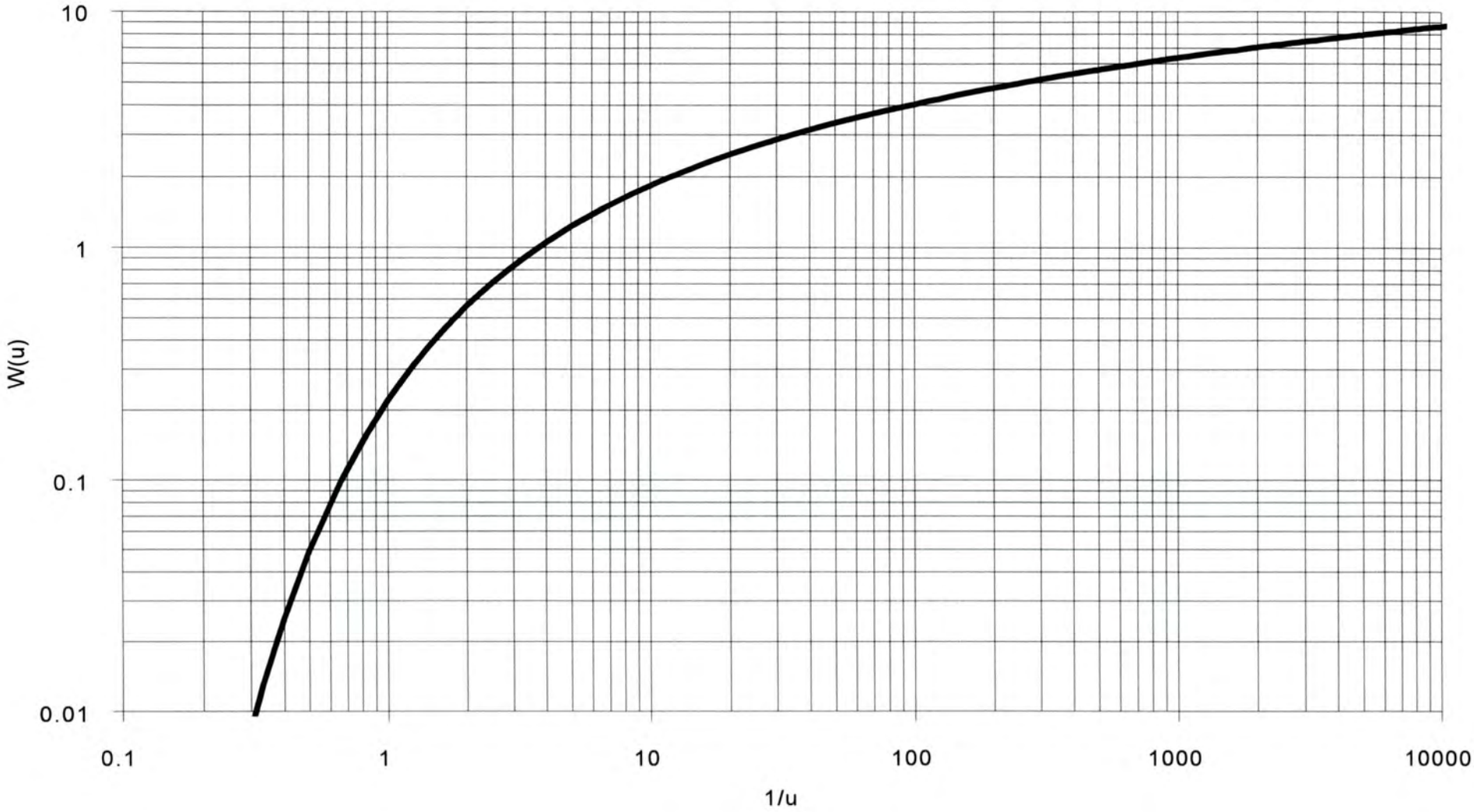

Figure 2.6: The Theis curve

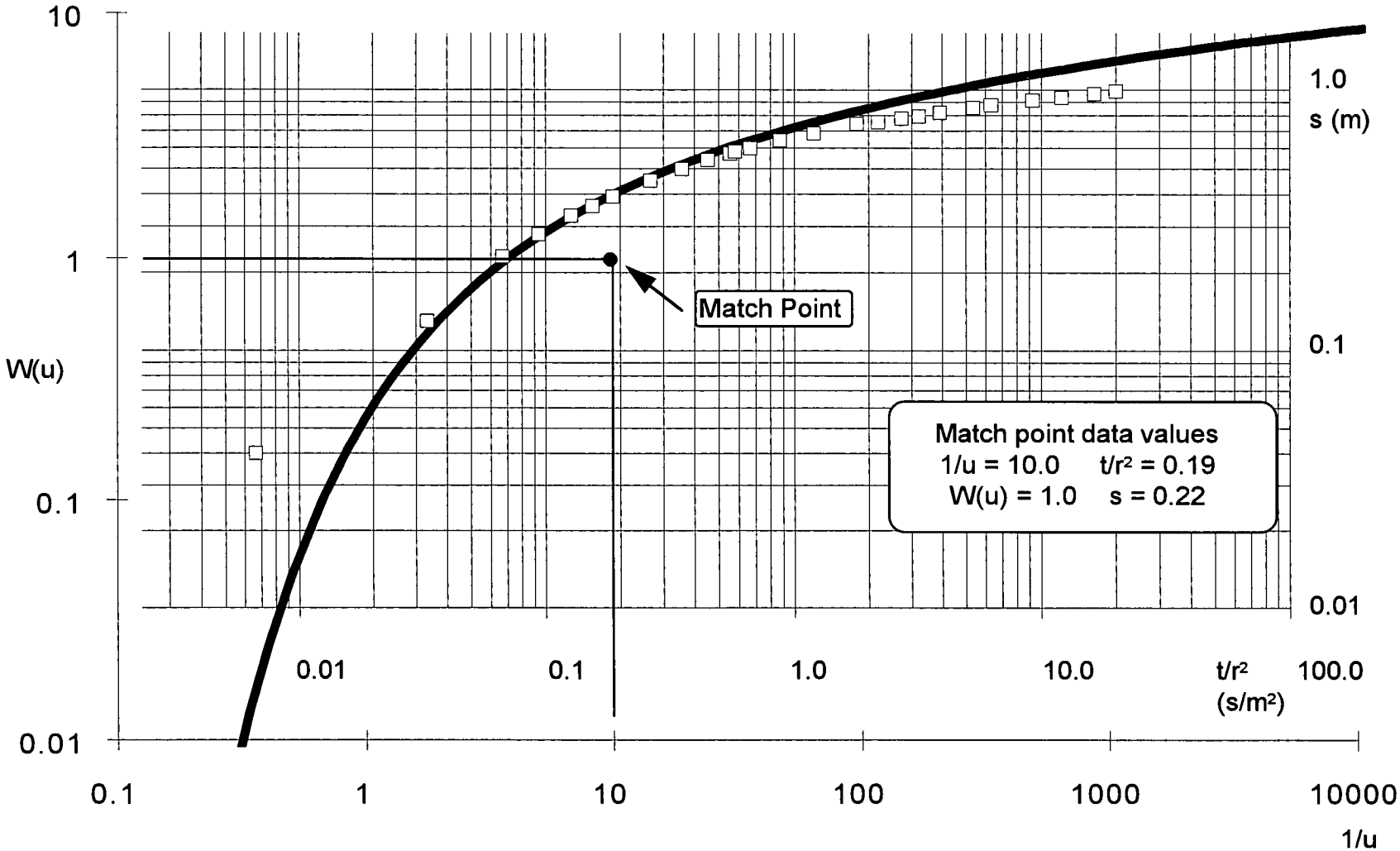

Figure 2.7: The curve matching procedure

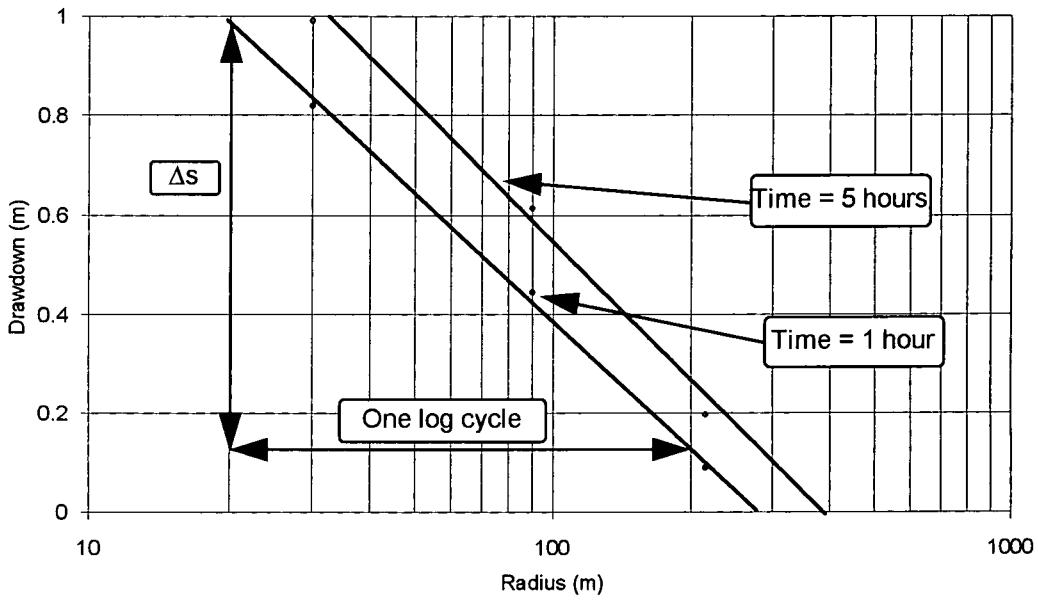

Figure 2.8: The constant time method of evaluating aquifer parameters. From Cooper/Jacob, equation 2.9.

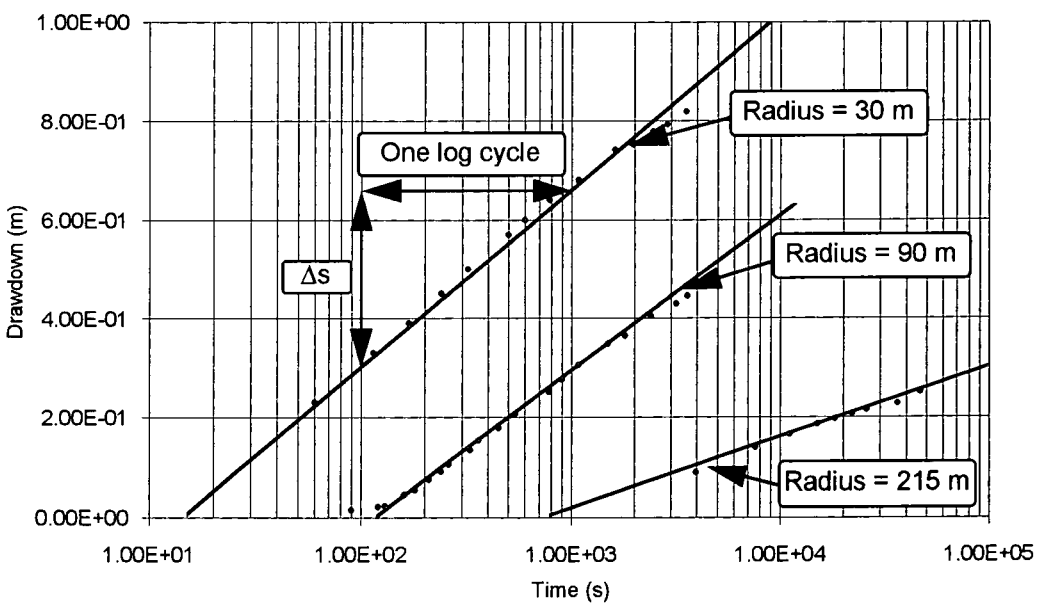

Figure 2.9: The constant radius method of evaluating aquifer parameters. From Cooper/Jacob, equation 2.10.

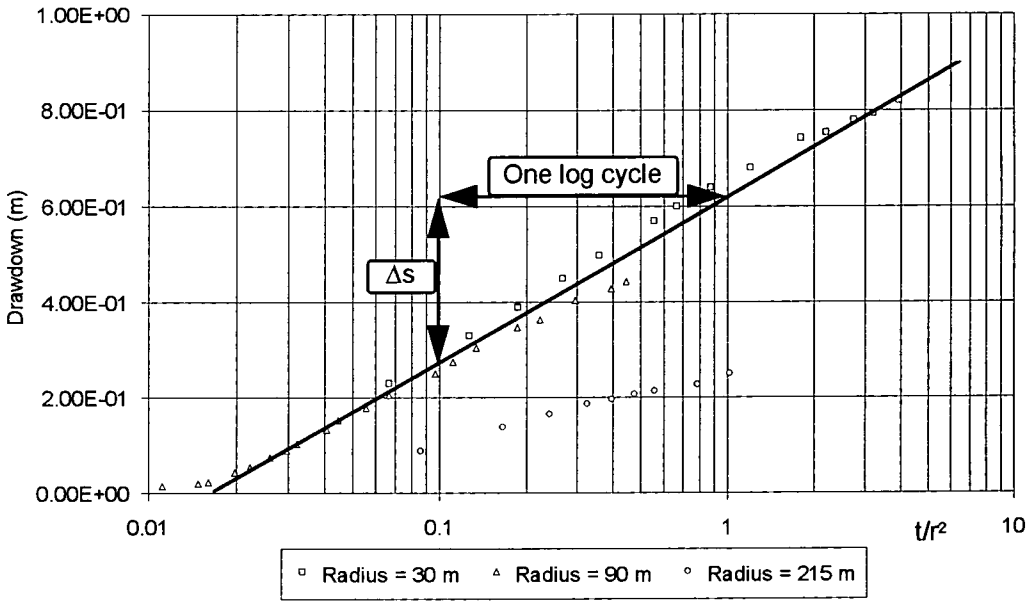

Figure 2.10: The constant t/r^2 method of evaluating aquifer parameters. From Cooper/Jacob, equation 2.11.

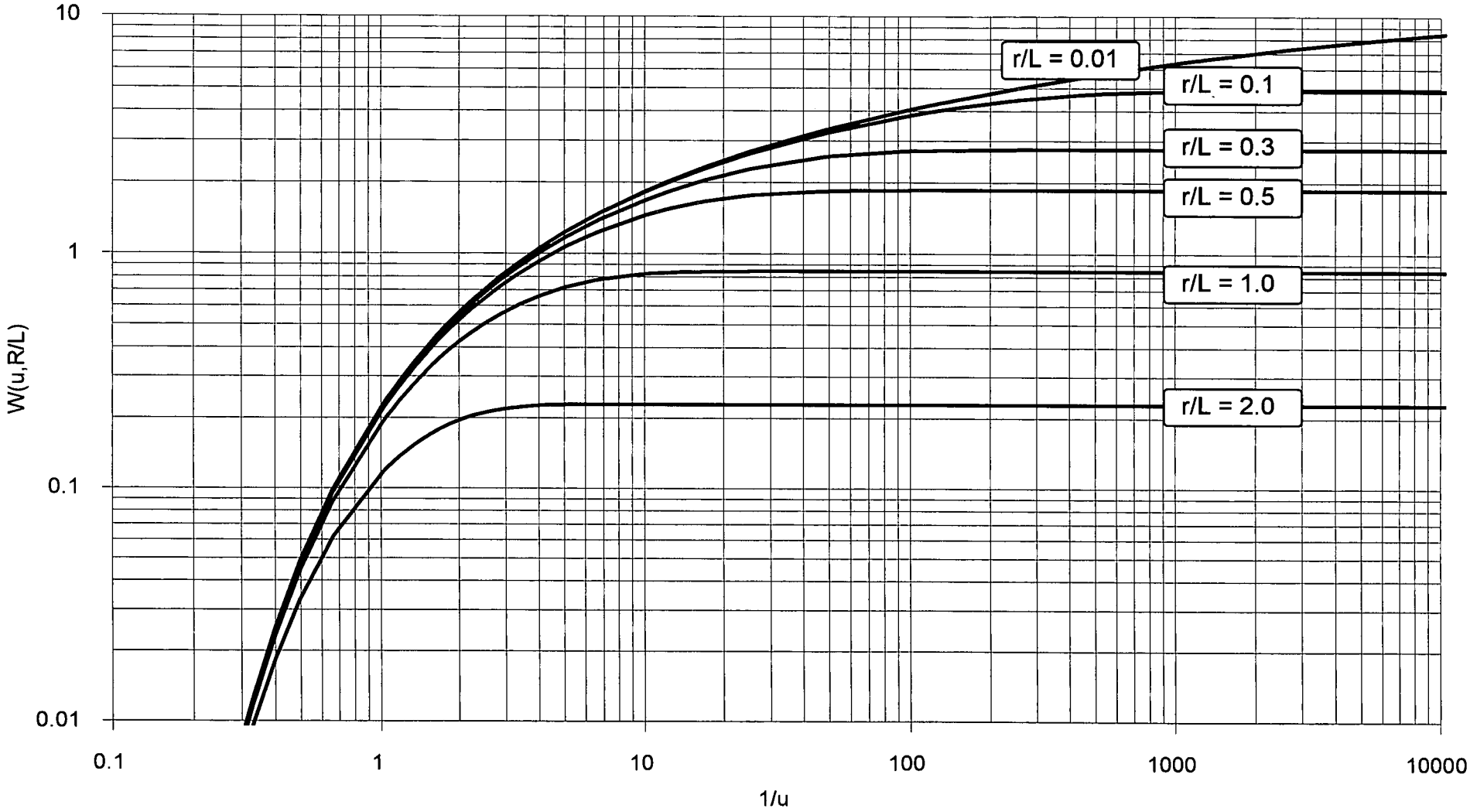

Figure 2.11: The Walton type curve

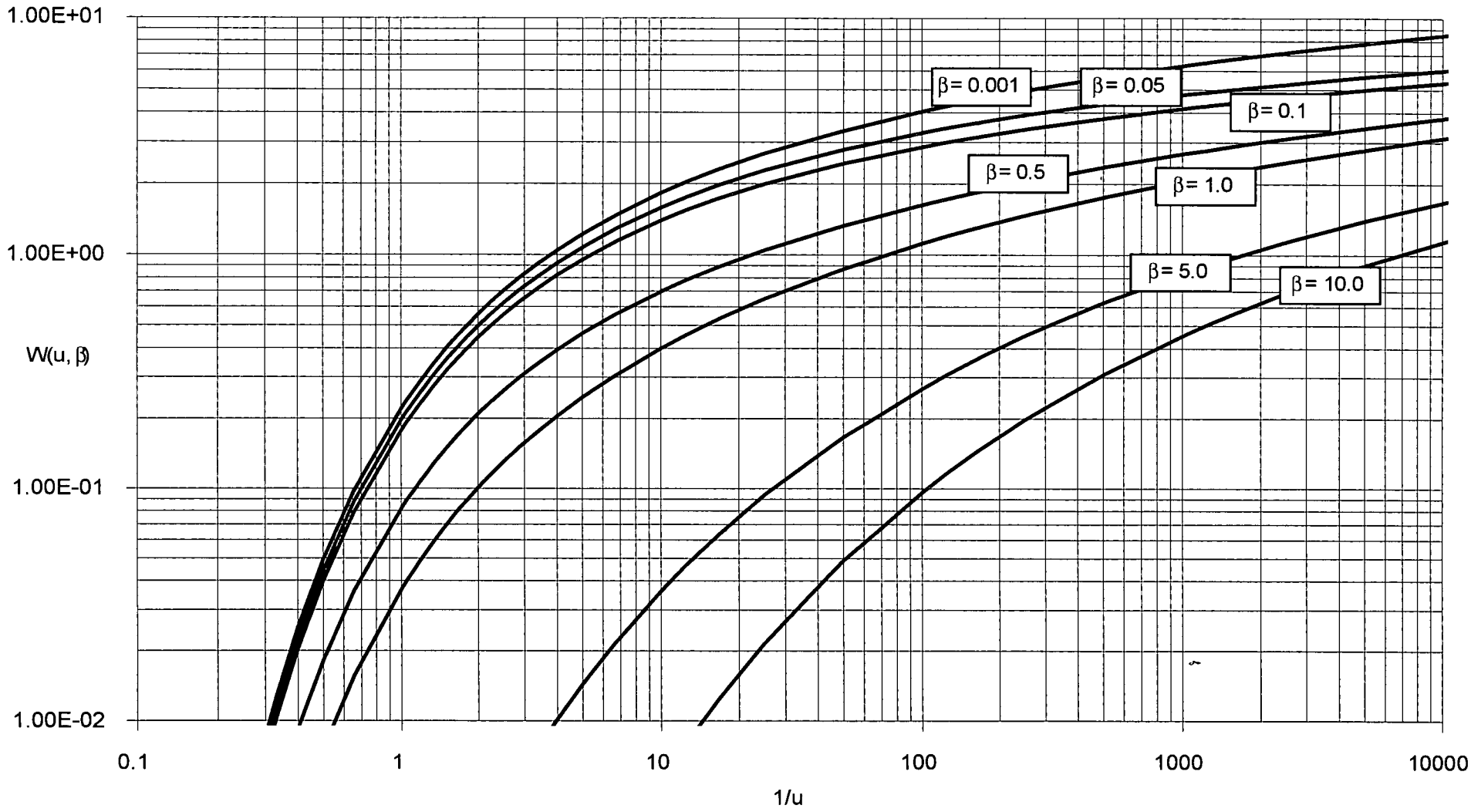

Figure 2.12: The Hantush type curve

Chapter 3

Fieldwork

3.1. Introduction

This fieldwork was carried out in conjunction with Oxford Geotechnica Limited (OGL). OGL had been instructed to develop a mathematical model to study the groundwater behaviour at a proposed mineral extraction site. The fieldwork was conducted so that the parameters necessary for the development of this groundwater flow model could be provided.

3.2. Site description

3.2.1. Geographical features

The proposed extraction site covers an area of 63.3 Hectares (Ha) and is currently agricultural land. It is essentially a ridge of ground which slopes East towards the coast and West towards a local stream network. To the South-West of the site at a distance of approximately 600 metres there is a Site of Special Scientific Interest (SSSI). The model was developed in order to evaluate the impact of the mineral extraction on the flow of water to this SSSI.

3.2.2. Geological features

The surface geology is made up of a sandy gravel which varies in thickness across the site. This is an alluvial terrace deposit. The gravel reaches a maximum thickness of approximately 6 metres, reducing to less than 3 metres at the Western boundary and 1 metre at the Eastern boundary of the site.

Beneath the sand and gravel lies a formation which may be divided into three sections. The uppermost formation (underlying the sandy gravel) is the upper sand layer. Where this is

weathered this is a yellow to pale grey, well sorted, fine to very fine sand, occasionally with beds of clayey fine sand and very sandy clay. Where it is unweathered, it is a greenish grey colour.

Below the sand layer lies a silty sand formation. The boundary between the two formations is difficult to define as it is gradational. The two formations are distinguished by their relative plasticity values, the silty sand being more clayey. A clay layer forms the lowest formation of the group. It is expected that the thickness of this formation is in excess of 50 metres.

The fieldwork only investigates the characteristics of the upper two formations, the sandy gravel deposits and the upper sand.

3.3. Pump test equipment

A variety of pump tests were performed which produced the data analysed in this research. The pump tests were conducted by using a Grundfos MP-1 2" electric pump. The water was pumped from a standpipe, and the resulting drawdown due to the pumping recorded in observation boreholes. The drawdown was measured using high quality pressure transducers and logging equipment. The pressure transducers were secured to the bottom of the boreholes, and the head of water above them measured every 10 seconds.

A full description of the pumping test equipment used for the fieldwork is included in Appendix C1.

3.4. Pump test design

A total of 12 boreholes were available for pump tests. Standpipes or piezometers were located within the boreholes. These could be used to record the water level in either the sandy gravel (surface formation) or the underlying sand. An approximate schematic plan showing the borehole locations is shown in Figure 3.1.

Some of these boreholes contained two 50 mm standpipes, one in the gravel and one in the sand formation. Some contained only one standpipe, and one piezometer tube. The Grundfos MP1 electric pump could be used to pump water from the 50 mm standpipes. The Waterra hand pump was used to pump water from the piezometer tubes.

The accuracy of pumping tests is greatly enhanced by recording the drawdown in an observation well at a distance from the pumped well as the pumping test progresses. This was only possible in one region, where boreholes 16, 17 and 18 are situated. A diagram showing the construction of these boreholes is shown in Figure 3.2. The positions of these boreholes relative to each other was designed in order to maximise the results from the pumping tests. This was achieved by first obtaining an estimate of the aquifer parameters. These parameters were then used in a simulation of a pumping test of typical duration and flowrate using the one dimensional finite element model, CVM[1]. An estimate of the drawdown at different radii was thus produced for a typical pumping test. This information was used to specify the distances these boreholes should be drilled relative to each other.

3.5. Method of pump testing

The pump tests were conducted in the following manner:-

1. The borehole from which pumping was planned was purged using the Waterra hand pump. This removed silt that was left in the well from the drilling. This operation was carried out the day before pumping was planned. This allowed groundwater levels to recover before pumping began.
2. The data collection equipment was installed in the observation boreholes. First the level of water below ground level was measured using a dipmeter and the level recorded. The pressure transducer was then lowered to the lower part of the borehole. It was secured to the borehole using plastic ties so it could not be accidentally moved.

---

[1]CVM - Curved Valley Model, Oxford Geotechnica Limited, 1994.

The pressure transducer was then plugged into the logging recorder. The logger was initialised, and the time and initial measurement noted. This process was repeated in all of the observation wells.

3. A pressure transducer was secured to the riser of the Grundfos MP1 pump in a position that would be below the water level. The Grundfos MP1 pump was then lowered into the pumping borehole, and secured. It was necessary to ensure that the head of the pump was above the bottom of the borehole.
4. The logger in the pumped borehole was initialised. Once the water levels had reached steady state, the value of the flow gauge was recorded and the pump started, noting the start time.
5. At the end of the pumping test, the pump was stopped and the time noted. The water in the riser was prevented from flowing back into the borehole by sealing the outlet pipe, forming a simple non return system. The pump was not removed until the recording of the recovery of the groundwater within the boreholes was complete.
6. The average discharge during the test was determined by calculating the difference between the start and finish values of the flow gauge, and dividing this value by the total pumping time.

Table 1 shows a summary of the pump tests carried out using the Grundfos electric pump.

3.6. Analysis of the fieldwork

The fieldwork was analysed by hand using the straight line (semi-log) method, of drawdown versus time during pumping and during recovery. The analysis was restricted to that of a confined system, and so the values of transmissivity (m^2/s) and storativity were calculated using the drawdown analysis, and transmissivity only calculated from the analysis of the recovery data. The results of this analysis are included in chapter 6.

Borehole pumped	Material	Date	Pump rate (m^3/hr)	Pump time (hours)	Observations	Notes
6	Sand	13/10 1994	0.305	1.5	BH 06 Gravel	Re-inject to BH 06 gravel layer.
6	Sand	13/10 1994	0.338	2.0	BH 06 Gravel	Discharge at a distance from the pumped well
7	Sand	14/10 1994	0	0	BH 07 Gravel	Yield of well too low for the MP 1 pump.
7	Gravel	14/10 1994	1.05	2.0	BH 07 Sand	Discharge at a distance from the pumped well
8	Sand	15/10 1994	0	0	BH 08 Gravel	Yield of well too low for the MP 1 pump.
8	Gravel	15/10 1994	0	0	BH 08 Sand	Yield of well too low for the MP 1 pump.
16	Gravel	18/10 1994	1.32	5.0	BH 16 Sand BH 17 Gravel BH 18 Gravel BH 18 Sand(3)	Discharge at a distance from the pumped well
17	Gravel	20/10 1994	1.34	4.0	BH 16 Sand BH 16 Gravel BH 18 Gravel BH 18 Sand(3)	Discharge at a distance from the pumped well
18	Gravel	24/10 1994	1.33	6.5	BH 16 Sand BH 16 Gravel BH 17 Gravel BH 18 Sand(3)	Discharge at a distance from the pumped well
16	Sand	25/10 1994	0.511	4.0	BH 16 Gravel BH 17 Gravel BH 18 Gravel BH 18 Sand(3)	Discharge at a distance from the pumped well

Borehole pumped	Material	Date	Pump rate (m^3/hr)	Pump time (hours)	Observations	Notes
16	Sand	25/10 1994	0.45	1.5	BH 16 Gravel BH 17 Gravel BH 18 Gravel BH 18 Sand(3)	Re-inject to BH 16 gravel layer.
18	Gravel	26/10 1994	1.49	1.0	BH 16 Gravel BH 17 Gravel	Re-inject to BH 17 gravel layer
18	Gravel	26/10 1994	1.35	1.0	BH 16 Gravel BH 17 Gravel	Re-inject to BH 16 gravel layer
17	Gravel	26/10 1994	0.39	1.0	BH 16 Gravel BH 18 Gravel	Re-inject to BH 16 gravel layer
17	Gravel	26/10 1994	0.83	1.0	BH 16 Gravel BH 18 Gravel	Re-inject to BH 18 gravel layer
16	Gravel	27/10 1994	0.87	1.0	BH 17 Gravel BH 18 Gravel	Re-inject to BH 17 gravel layer
16	Gravel	27/10 1994	0.87	1.0	BH 17 Gravel BH 18 Gravel	Re-inject to BH 18 gravel layer.

Table 3.1: Summary of the pump tests using the Grundfos pump

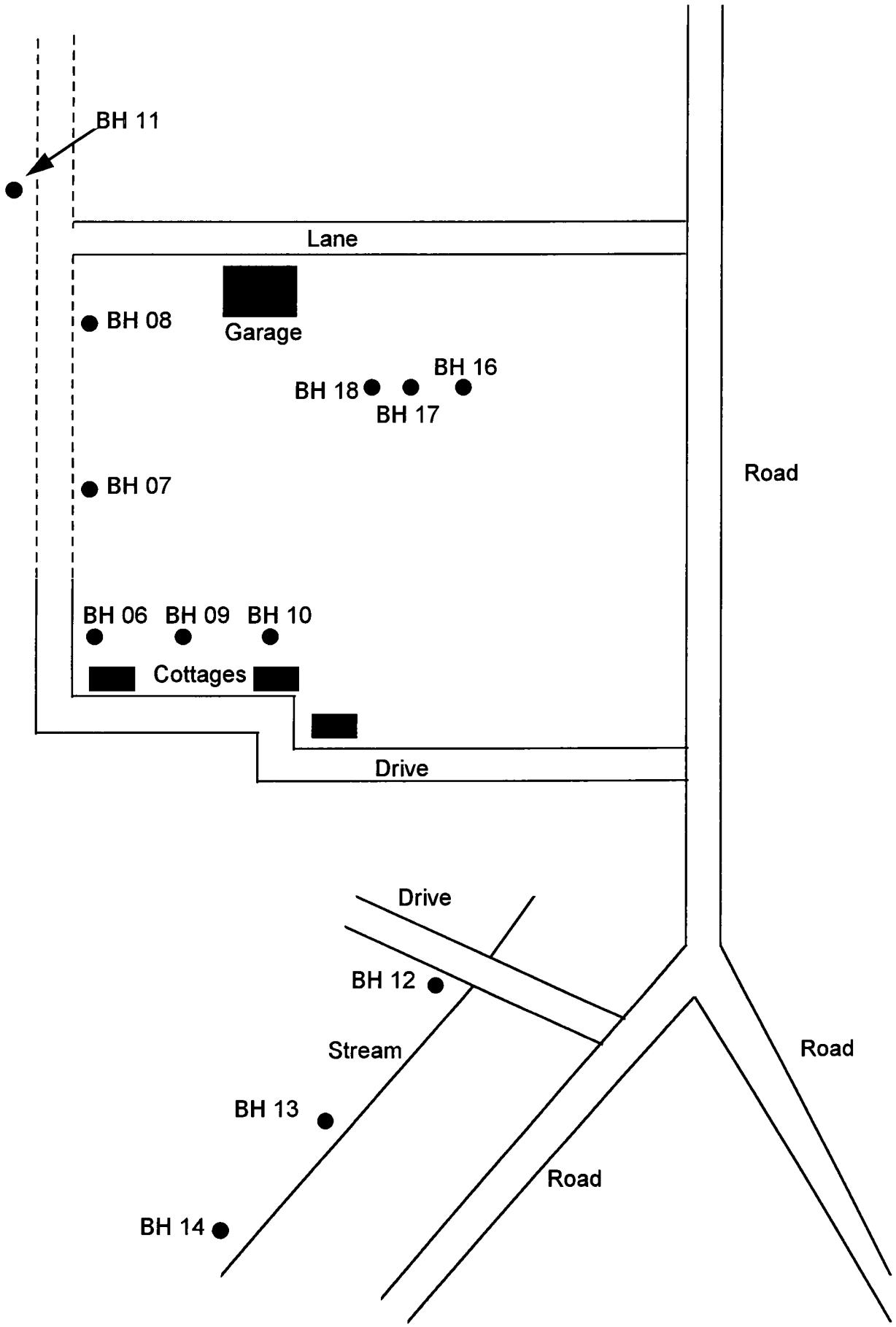

Figure 3.1: A schematic plan of the site, showing the borehole locations. (Not to scale).

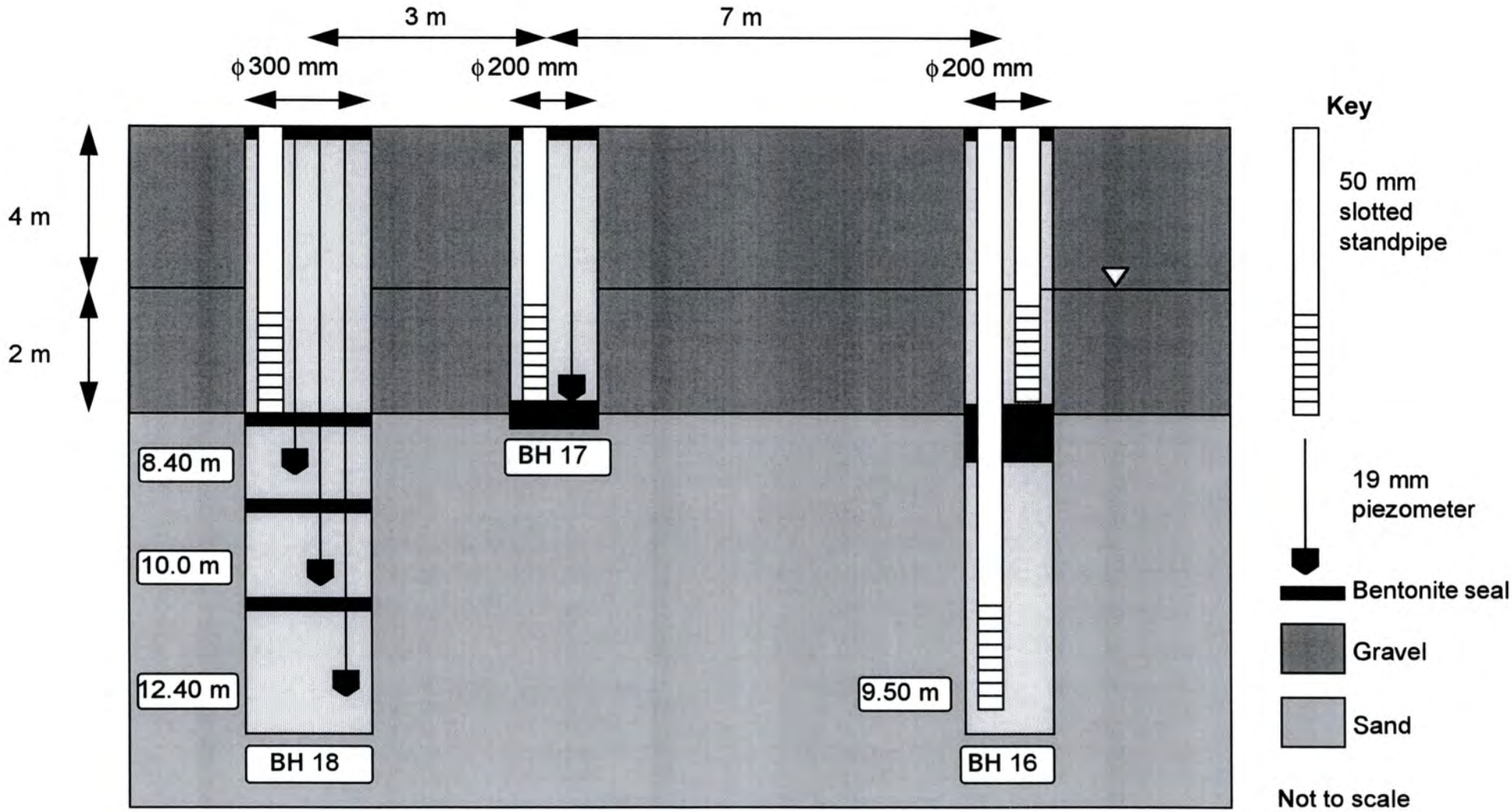

Figure 3.2: Cross section showing the positions of boreholes 16, 17 and 18.

Chapter 4

Computer methods to calculate aquifer parameters from pumping test data

4.1. Introduction

During the fieldwork a series of pump tests was completed, the data from which were analysed to determine the aquifer parameters using the Cooper and Jacob (1946) semi-log method. This technique is simple, but only transmissivity and storativity are determined as it is the solution to the governing equation of flow in a confined aquifer (equation 2.6).

Computer methods were developed to calculate aquifer parameters from pumping tests in both confined and leaky aquifer systems. The method used is a least squares curve fitting algorithm, where parameters are calculated that give the smallest error between the observed and calculated values of drawdown.

The simplest case was solved first, which analyses the results of a pumping test in a confined aquifer using the solution developed by Theis (equation 2.1). The Walton formula (equation 2.19) for drawdown in a leaky aquifer was used, thus introducing the vertical permeability of the aquitard. The final solution examined is that of Hantush (equation 2.23). This solution includes the storativity of the aquitard, and was considered by Neuman and Witherspoon (1969b) as being the most accurate method of determining aquifer parameters from pumping test data, without including drawdown in the aquifer overlying the aquitard. These methods calculate results quickly, accurately, and are in a form which may be easily included in a technical report.

4.2. Confined aquifers

4.2.1. The Theis equation

Theis determined a solution to radial transient flow in a confined aquifer. Recalling this equation from chapter 2, the drawdown *s* can be written as follows:

$$s = \frac{Q}{4\pi T} \cdot W(u) \tag{4.1}$$

For confined conditions the well function *W(u)* is defined as:

$$W(u) = \int_u^{\infty} \frac{e^{-y}}{y} dy \tag{4.2}$$

where

$$u = \frac{r^2 S}{4Tt} \tag{4.3}$$

4.2.2. Evaluation of the Theis equation

The well function *W(u)* has a solution in the form of a series approximation. Recalling the series approximation from chapter 2:

$$W(u) = -0.5772 - \ln(u) + u - \frac{u^2}{2.2!} + \frac{u^3}{3.3!} - ... + \frac{(-1)^{n+1}(u)^n}{n.n!} \tag{4.4}$$

For simplicity a table of values of *W(u)* is presented in Appendix D1.

Two approximations can be made to evaluate the function *W(u)* for high and low values of *u*. The first was derived by Cooper and Jacob (1946) for small values of *u*, and was presented in section 2.2.1. This approximation is:

$$W(u) = \ln\left(\frac{1}{u}\right) - 0.5772 \tag{4.5}$$

and can be used for values of $u < 1.0 \times 10^{-2}$. The second approximation, for values of $u > 1.0$, is written:

$$W(u) = u \cdot e^{u} \cdot \left(\frac{u^2 + a_1 \cdot u + a_2}{u^2 + b_1 \cdot u + b_2} \right) \qquad (4.6)$$

where $a_1 = 2.334733$ $a_2 = 0.250621$

$b_1 = 3.330657$ $b_2 = 1.681534$

which is an approximation of the exponential integral.

Thus three methods are used to evaluate the Theis well function, *W(u)*.

$u < 1.0 \times 10^{-2}$	Cooper/Jacob approximation
$1.0 \times 10^{-2} < u < 1.0$	Series approximation
$u > 1.0$	Exponential integral approximation

4.2.3. Least squares algorithm for the Theis equation

The computer curve fitting method is effectively a more rigorous approach of the log-log curve matching method devised by Theis, and reported by Walton (1940). If the Theis solution is examined, the drawdown during a pumping test, *s*, is a function of 5 parameters as follows:-

$$s = f(r,t,Q,T,S) \qquad (4.7)$$

If a pumping test is performed, the radius *r*, flowrate *Q* and the time *t* at which drawdown measurements are taken are all known. This leaves two unknowns, transmissivity *T* and storativity *S*. This technique estimates these parameters by determining the values of transmissivity and storativity which give the minimum difference between the theoretical and observed values of drawdown for all the points recorded during the pumping test.

4.2.4. Theory of least squares curve matching for two variables

The theoretical drawdown at any time, s_i is a function of transmissivity and storativity. Thus if these values are changed by small amounts, ΔT and ΔS, there will be a small change in drawdown, Δs. This is written as:

$$(s + \Delta s)_i = s_i + \frac{\partial s}{\partial T} \cdot \Delta T + \frac{\partial s}{\partial S} \cdot \Delta S \qquad (4.8)$$

$$\text{i.e.} \quad \Delta s = \frac{\partial s}{\partial T} \cdot \Delta T + \frac{\partial s}{\partial S} \cdot \Delta S \tag{4.9}$$

To determine values of transmissivity and storativity that give the 'best fit' between the observed and theoretical values of drawdown, the square of the difference between these values, χ, should be minimised (Kreyszig, 1988).

$$\chi = \sum_{i=1}^{n} \left(\hat{s}_i - s_i \right)^2 \tag{4.10}$$

where n is the number of time vs. drawdown observation pairs, i a particular observation at time t and $\hat{s}_i$ the measured value of drawdown, s, at observation point i.

The minimum value of χ will be when

$$\frac{\partial \chi}{\partial T} \text{ and } \frac{\partial \chi}{\partial S} = 0 \tag{4.11}$$

This is shown diagramatically by Figures 4.1 and 4.2. Figure 4.1 shows the value of χ for a hypothetical pumping test in a confined aquifer. The variables radius, flowrate, time and storativity are known. The only unknown is transmissivity. Using the Theis solution, a range of theoretical drawdown values is calculated over a number of values of transmissivity. As the observed drawdown is known, the value of χ may be calculated. This is plotted against the range of transmissivity values. The point of least error, where χ is a minimum, is at the minimum of the graph. This is where $\partial \chi / \partial T = 0$. Thus the point where $\partial \chi / \partial T = 0$ will lead to the 'best fit' values of aquifer parameters. Similarly, Figure 4.2 shows the value of χ where the unknown is storativity.

Differentating equation 4.11 with respect to T and S gives:-

$$\frac{\partial \chi}{\partial T} = -2 \frac{\partial s}{\partial T} \left(\hat{s}_i - s_i^{k+1} \right) \tag{4.12}$$

and

$$\frac{\partial \chi}{\partial S} = -2 \frac{\partial s}{\partial S} \left(\hat{s}_i - s_i^{k+1} \right) \tag{4.13}$$

where k is the iteration number. We know

$$s_i^{k+1} = s_i^k + \Delta s \tag{4.14}$$

and substituting for Δs from equation 4.9

$$s_i^{k+1} = s_i^k + \frac{\partial s}{\partial T}\cdot \Delta T + \frac{\partial s}{\partial S}\cdot \Delta S \tag{4.15}$$

Substituting for s_i^{k+1} from (4.15) into (4.12) and (4.13)

$$\frac{\partial \chi}{\partial T} = -2\frac{\partial s}{\partial T}\left(\hat{s}_i - \left[s_i^k + \frac{\partial s}{\partial T}\cdot \Delta T + \frac{\partial s}{\partial S}\cdot \Delta S\right]\right) \tag{4.16}$$

and

$$\frac{\partial \chi}{\partial S} = -2\frac{\partial s}{\partial S}\left(\hat{s}_i - \left[s_i^k + \frac{\partial s}{\partial T}\cdot \Delta T + \frac{\partial s}{\partial S}\cdot \Delta S\right]\right) \tag{4.17}$$

Substituting these values into equation 4.11 and rearranging gives the same solution:-

$$\frac{\partial s}{\partial T}\cdot \Delta T + \frac{\partial s}{\partial S}\cdot \Delta S = \left(\hat{s}_i - s_i^k\right) \tag{4.18}$$

This can be written in matrix form as

$$[J^T][J\ ]\{\Delta T, \Delta S\}_k^T = [J^T]\{\hat{s} - s\}_k \tag{4.19}$$

where

$$[J] = \begin{bmatrix} \frac{\partial s_1}{\partial T} & \frac{\partial s_1}{\partial S} \\ \frac{\partial s_2}{\partial T} & \frac{\partial s_2}{\partial S} \\ \vdots & \vdots \\ \frac{\partial s_n}{\partial T} & \frac{\partial s_n}{\partial S} \end{bmatrix} \tag{4.20}$$

Equation (4.21) can then be used to solve for ΔT and ΔS

$$\{\Delta T, \Delta S\}_k^T = \left([J]^T[J]\right)^{-1}[J]^T\{\hat{s}_l - s_k\} \tag{4.21}$$

For the next iteration, we estimate $\{T,S\}_{k+1}$ from

$$\{T,S\}_{k+1} = \{T,S\}_k + \{\Delta T, \Delta S\}_k \tag{4.22}$$

This process is repeated until the successive changes in T and S have become sufficiently small.

4.2.5. Application of least squares curve matching to the Theis equation

In order to use this algorithm successfully, the partial derivatives of the theroetical drawdown (for Theis), with respect to transmissivity and storativity must be evaluated. To determine these values, it is required to differentiate the Theis well function, *W(u)*, with respect to u. Noting that the well function, *W(u)*, may be determined from evaluating the exponential integral, which may be approximated as:

$$W(u)=\int_u^{\infty}\frac{e^{-u}}{u}\,du \cong e^{-u}\left(\frac{1}{u}-\frac{1}{u^2}+\frac{2!}{u^3}-\frac{3!}{u^4}+\cdots\frac{(-1)^n\cdot n!}{u^{n+1}}\right) \qquad (4.23)$$

Differentiating equation (4.23) with respect to u:

$$\begin{aligned}\frac{d}{du}\{W(u)\} &= -e^{-u}\cdot\left(\frac{1}{u}-\frac{1}{u^2}+\frac{2!}{u^3}-\frac{3!}{u^4}+\cdots\frac{(-1)^n\cdot n!}{u^{n+1}}\right)\\ &\quad + e^{-u}\cdot\left(-\frac{1}{u^2}+\frac{2!}{u^3}-\frac{3!}{u^4}+\cdots\frac{(-1)^{n+1}\cdot(n+1)!}{u^{n+2}}\right) \qquad (4.24)\\ &= -\frac{e^{-u}}{u}\end{aligned}$$

Values of $\frac{\partial s}{\partial T}$ and $\frac{\partial s}{\partial S}$ can then be determined by differentiating the Theis equation (2.1).

$$\begin{aligned}\frac{\partial s}{\partial T} &= \frac{d}{dT}\left(\frac{Q}{4\pi T}\right)W(u)+\frac{Q}{4\pi T}\cdot\frac{d}{dT}(W(u))\\ &= \frac{-Q}{4\pi T^2}\cdot W(u)+\frac{Q}{4\pi T}\cdot\frac{dW(u)}{du}\cdot\frac{du}{dT}\\ &= \frac{-Q}{4\pi T^2}\cdot W(u)+\frac{Q}{4\pi T}\cdot\left(-\frac{e^{-u}}{u}\right)\left(-\frac{r^2S}{4T^2t}\right)\\ &= \frac{Q}{4\pi T^2}\left(e^{-u}-W(u)\right) \qquad (4.25)\end{aligned}$$

Similarly,

$$\frac{\partial s}{\partial S} = \frac{Q}{4\pi T} \cdot \frac{\partial}{\partial S}(W(u))$$
$$= \frac{Q}{4\pi T} \cdot \frac{d(W(u))}{du} \cdot \frac{du}{ds}$$
$$= \frac{Q}{4\pi T} \cdot \left(-\frac{e^{-u}}{u}\right) \cdot \frac{r^2}{4Tt}$$
$$= -\frac{Q}{4\pi T} \cdot \frac{4Tte^{-u}}{r^2 S} \cdot \frac{r^2}{4Tt}$$
$$= -\frac{Q}{4\pi TS} \cdot e^{-u} \qquad (4.26)$$

4.2.6. Computer programme CONPUTS (CONfined PUmp Test Solutions)

The least squares method described above requires a large number of calculations before the parameters that give the best fit between the observed and theoretical values of drawdown are determined. A computer programme was produced to complete these calculations quickly and accurately, and so estimate the confined aquifer parameters. The programme was written in FORTRAN77 and compiled with a Microsoft FORTRAN 4.1 compiler. A complete listing of the programme is included on the floppy disc in Appendix D17. The main features of the programme, and the user information, are described below.

Figure 4.3 shows a flowchart of the main programme. The programme first calculates the values of drawdown at each time value using the current transmissivity and storativity parameters. The difference between the observed and calculated values is then evaluated. The least squares algorithm is then used to calculate increments of transmissivity and storativity to reduce the difference between the observed and theoretical values. The programme iterates until the difference between the errors of successive iterations has become sufficiently small. Figures 4.4 and 4.5 show the flowcharts for the two subroutines.

Subroutine DELTA calculates the value of *W(u)*, using the appropriate method from section 4.2.2. It is essential that these methods are accurate. In order to assess this accuracy, the subroutine was tested and the results compared with the standard values of *W(u)*, shown in

Appendix D1. The results of these tests are tabulated in Appendix D2. This table shows that these methods accurately determine *W(u)*.

4.2.7. User information

The input data must be stored in the form of a datafile called THEISIN.DAT. This file gives data about the pumping rates, observed drawdowns and an initial guess of transmissivity and storage. It is important that the values are in the correct columns, otherwise the programme will be unable to read the values correctly.

Row 1 (2 I10)

Columns 1 - 10	Number of observations
Columns 10 - 20	Maximum number of iterations

Row 2 (E10.7)

Columns 1 - 10	Convergence factor (m)

Row 3 (2 F10.4)

Columns 1 - 10	Radius (m)
Columns 10 - 20	Flowrate (m^3/s)

Row 4 (2 F10.4)

Columns 1 - 10	Transmissivity guess (m^2/s)
Columns 10 - 20	Storativity guess

Rows 5 to end (2 F10.4) (Repeat for each time value)

Columns 1 - 10	Time (s)
Columns 10 - 20	Drawdown (m)

The number of time vs. drawdown pairs should not exceed 100. It is important that the data should be input using the correct units and formats. An example of an input file is presented in Appendix D3.

To run the programme, first ensure that the input file is in the same directory as the Theis least squares programme, CONPUTS. Then type the name of the programme, CONPUTS, followed by a carriage return. When the programme has finished running a message will appear saying 'STOP - Programme terminated'. The results can then be examined in the output file, THEISOUT.DAT.

If the programme crashes during a run, it is usually because the input guesses of transmissivity and storativity were not close enough to the solution, or some of the input data was wrong. Check the input data, and change the values of the guesses of transmissivity and storativity.

The output file, THEISOUT.DAT, first presents the input data. After each iteration, the computer writes the average error, $\sqrt{\chi}$, from equation 4.10 and the new values of transmissivity and storativity to the datafile. When the difference between the errors is less than the convergence factor, or the maximum number of iterations have been completed, the programme stops iterating. The values of transmissivity, storativity and final root mean square error are output to this datafile . A table of time, observed and theoretical head values is produced, using the 'best fit' values of transmissivity and storativity. An output file, using the data in Appendix D3, is presented in Appendix D4. The log values of time and drawdown are also given. These values may be imported to a spreadsheet and the results plotted to observe the accuracy of the results.

4.2.8. Testing the CONPUTS programme

A hypothetical pumping test of six hours duration in a confined aquifer was used to test the programme. Data was produced which simulates the drawdown in an observation well 20 metres from the pumped well during the pumping test. This data is shown in the input file in Appendix D3. The programme was then run, with input 'guess' values of T = 250 m^2/day and $S = 5.0 \times 10^{-4}$. The output file is shown in Appendix D4. The programme took 7

iterations, with a convergence factor of 1.0×10^{-10}. The best fit values of transmissivity and storativity are:

Transmissivity = 510.93 m^2/day

Storativity = 9.683E-04

Root mean square error = 2.05 mm

A graph showing the hypothetical drawdown, the input and 'best fit' values of drawdown are shown in Figure 4.6.

This data were also used to test if the programme converged with wide ranging input values of transmissivity and storativity. It is important that the programme converges. The accuracy of the result is shown by the magnitude of the root mean square error. A number of different starting values were used. The input 'guess' values of transmissivity and storativity ranged between 5 and 2500 m^2/day and 1.0×10^{-1} and 1.0×10^{-5} respectively. The greater the difference between the input values and the results, the more iterations were required to achieve convergence. In only one case convergence was not achieved, when the input values were T = 5 m^2/day and S = 0.1. The results of these tests are shown in Appendix D5. In every case where convergence was possible, the programme converged to the parameters determined in the first test.

4.2.9. Conclusion

An algorithm has been produced which calculates the values of confined aquifer parameters accurately and efficiently. The programme converges well, even if the parameter guesses are inaccurate by up to two orders of magnitude. However, the validity of the assumptions made by Theis must be questioned. It is extremely unlikely that an aquifer will be completely confined. In practice, it is more likely for the aquifer to show leaky characteristics. In this case, as pumping continues, leakage of water through the overlying or underlying aquitard will contribute to the discharge. This will result in reduced drawdown, particularly at late time. The leaky condition will next be investigated, to devise an algorithm that reflects this situation.

4.3. Leaky aquifers - the Walton case

As the time since the start of the pumping test increases, the contribution to discharge from leakage through the aquitard will be more significant. Eventually leakage will dominate, and all of the water that is discharged from the well will be derived from leakage. Thus if a leaky aquifer is analysed as a confined aquifer, the parameters determined will be inaccurate, because of the different methods of flow within each aquifer.

4.3.1. The Walton equation

Walton described the '*r/L*' method of leaky aquifer pump test analysis. The theory behind this method is the solution to drawdown in a leaky aquifer devised by Hantush and Jacob (1955). This incorporates the vertical permeability of the aquitard. Recalling this equation from chapter 2:

$$s = \frac{Q}{4\pi T} \cdot W\left(u, r/L\right) \tag{4.27}$$

where the Walton well function is defined as:

$$W\left(u, r/L\right) = \int_u^\infty \frac{1}{y} \exp\left(-y - r^2/4L^2 y\right) dy \tag{4.28}$$

The method of curve matching by hand is identical to the Theis method described in section 2.2.1. However, instead of matching against a single curve, the Walton solution is presented as a series of curves. The position of these curves is dependent on the value of leakage, *L*. The individual curves are labelled by the dimensionless quantity '*r/L*', thus this method is known as the '*r/L*' method. The least squares theory used to solve this problem will incorporate three variables, transmissivity *T*, storativity *S* and the leakage factor *L*.

From the graph of the Walton equation, (Figure 2.11) it can be seen that the value of *W(u,r/L)* tends to a steady state value as the value of *u* decreases. This is explained by considering the response of a leaky aquifer system during a pumping test. When the time is reached where all the discharge from the well is derived from leakage through the aquitard,

the drawdown within the pumped aquifer will reach steady state. This drawdown corresponds to the drawdown when time reaches infinity, which would lead to a value of $u = 0$. This in turn leads to a simpler solution to the Walton well function, of *W(0,r/L)*.

As the value of *L* increases, the quantity of leakage is reduced. Thus when '*r/L*' is small, the aquifer will show non-leaky characteristics, and so the problem may be solved using the confined aquifer theory. In this case, the value of *W(u,r/L)* will be calculated from *W(u,0)*. A table of values of *W(u,r/L)* is shown in Appendix D6.

The Walton well function, *W(u,r/L)*, cannot be approximated by a simple power series, as in the case of the Theis function. Instead, a numerical method was used.

4.3.2. Evaluation of *W(u,r/L)*

This method was developed to calculate the value of W(u,r/L) for the normal case, where no approximations can be made. In order to increase accuracy of the numerical method, the function *W(u,r/L)* was calculated as a function of *ln(u)*. Thus *W(v,r/L)* was determined, where $v = ln(u)$. The Walton well function thus becomes:

$$W\left(u, {}^{r}/_{L}\right) = W\left(v, {}^{r}/_{L}\right) = \int_{v}^{\infty} \exp(-y) \cdot \exp\left(-\exp(y) - \frac{\left({}^{r}/_{L}\right)^{2}}{4\exp(y)}\right) dy \qquad (4.29)$$

The function *W(v,r/L)* is determined using the trapezoidal rule at different values of *y*. The first value is where $y = v$, and then the value of *y* is increased until the value of *W(v,r/L)* tends to zero. The trapezoidal rule sums the individual values of *W(v,r/L)*, and hence evaluates the integral.

A graph of the function *W(v,r/L)* is shown in Figure 4.7. The value of the function is high for small values of *u*. Then as the value of *y* increases, *W(v,r/L)* decreases. As the scale is

logarithmic, the increments in y become slightly greater with each iteration. This process continues until the value of $W(v,r/L) < 1.0 \times 10^{-5}$.

4.3.3. Evaluation of *W(0,r/L)*

For this case, where $u = 0$, a second method of determining $W(v,r/L)$ is used. A graph of this function is shown in Figure 4.8. The graph shows the function has a low initial value which then increases to a peak and subsequently reduces to zero. The function is evaluated using the trapezoidal rule. The difference between the case of $W(v,r/L)$ and $W(0,r/L)$ is that for this case an initial value of 'y' was determined from which point the iterations would begin. If the Walton well function is examined (equation 4.28), it can be seen that a value of $u = 0$ would lead to two infinite terms.

A simple method of calculating a starting value was devised. The parameter 'v' was assigned an initial value of -17.0, corresponding to $u = 4.0 \times 10^{-8}$. From the calculations of the well function, there is negligible difference between this starting position and $u = 0$. The exponential equation was then evaluated, and 'y' increased until the magnitude of this expression was greater than a certain minimum value. This value of 'y' is then used as the starting value. The trapezoidal rule is used to evaluate the integral. However, instead of continuing until the magnitude of the well function is less than a minimum value, the integration takes place over a range of values of y.

In addition, the evaluation of the function $W(v,r/L)$ at the initial value of 'y' may yield a small value. In this case, the same procedure as the calculation of $W(0,r/L)$ is used. However, instead of assigning an initial value of $v = -17.0$, the first value of v is calculated from $v = ln(u)$. The evaluation of the well function is then carried out in exactly the same manner.

4.3.4. Evaluation of *W(u,0)*

The third case, of the Theis condition, was solved using the power series developed in the algorithm for the CONPUTS programme.

4.3.5. Defining the regions where the approximate methods are used to evaluate *W(u,r/L)*

Appendix D6 gives values of the Walton well function, *W(u,r/L)*. This table also shows where the approximations of *W(u,r/L)* may be made. To use these approximations, which would reduce computer calculation time and increase accuracy, these regions, with respect to '*u*' and '*r/L*', must be defined. Using the data from the table of values of *W(u,r/L)* (Appendix D6), the values where the approximations began were plotted on a log-log graph of '*u*' against '*r/L*'. This graph is presented in Figure 4.11, and shows that these points lie on a straight line. From this, it is possible to define the regions where the approximations to *W(u,r/L)* may be made.

The first approximation is for the case of W(0,r/L). The line that defined this area is:

$$\alpha = 0.55\ ln(u) + 2.56$$

$$= 0.55\ v + 2.56 \qquad (4.30)$$

Thus if a value of α is calculated, and is found to be < *ln(r/L)*, the point where *W(v,r/L)* is required must lie above the 'α' line shown in Figure 4.11. Thus the approximation of *W(u,r/L)* = *W(0,r/L)* should be used.

In a similar manner an approximation to the Theis condition was defined over the range of:

$$2.5 \times 10^{-3} < u < 1.0$$

The line that defined this area was:

$$\beta = 0.5\ ln(u) - 2.5$$

$$= 0.5\ v - 2.5 \qquad (4.31)$$

Thus if a value of β is calculated, and found to be greater than the value of *ln(r/L)* and within the defined range of *u*, the approximation to Theis should be used.

Appendix D7 shows comparisons of *W(u,r/L)* calculated using these methods, and the corresponding values obtained from the table in Appendix D6. It can be clearly seen from

this table that the values of $W(u,r/L)$ may be calculated accurately for a range of values of both u and r/L.

4.3.6. Least squares algorithm for the Walton solution

The theory of least squares was developed in section 4.2.4. It is simple to expand this from two to three variables. The variables used in this least squares algorithm are those of transmissivity T, storativity S and the non-dimensional leakage coefficient, r/L. The value of L, and hence the aquitard vertical permeability, may be easily determined as the radius is known. To simplify the mathematics, the value of r/L is represented by λ.

4.3.7. Theory of least squares curve matching for three variables

The drawdown during a pumping test in a confined leaky aquifer, s, is dependent on the following paramerers:-

$$s = f(r,t,Q,T,S,L) \tag{4.32}$$

During a pumping test, the radius, time and flowrate may all be measured. The unknowns that effect the drawdown at any point in time, s_i are the transmissivity, storativity and leakage. Changing these values by small amounts ΔT, ΔS and $\Delta\lambda$, will result in a small change in drawdown, Δs. This is written as:

$$(s+\Delta s)_i = s_i + \frac{\partial s}{\partial T}\cdot\Delta T + \frac{\partial s}{\partial S}\cdot\Delta S + \frac{\partial s}{\partial \lambda}\cdot\Delta\lambda \tag{4.33}$$

$$\text{i.e.} \quad \Delta s = \frac{\partial s}{\partial T}\cdot\Delta T + \frac{\partial s}{\partial S}\cdot\Delta S + \frac{\partial s}{\partial \lambda}\cdot\Delta\lambda \tag{4.34}$$

The object is again to minimise the difference, χ, between the observed and theoretical values of drawdown.

$$\chi = \sum_{i=1}^{n}\left(\hat{s}_i - s_i\right)^2 \tag{4.35}$$

where n is the number of observation points, i a particular observation point in time and $\hat{s}_i$ the measured value of drawdown, s, at observation point i.

The minimum value of χ will be when

$$\frac{\partial \chi}{\partial T}, \frac{\partial \chi}{\partial S} \text{ and } \frac{\partial \chi}{\partial \lambda} = 0 \tag{4.36}$$

Continuing with this theory as before, the drawdown at the next iteration can be calculated from:

$$s_i^{k+1} = s_i^k + \frac{\partial s}{\partial T} \cdot \Delta T + \frac{\partial s}{\partial S} \cdot \Delta S + \frac{\partial s}{\partial \lambda} \cdot \Delta \lambda \tag{4.37}$$

Substituting for s_i^{k+1} and setting $\frac{\partial \chi}{\partial T}, \frac{\partial \chi}{\partial S}$ and $\frac{\partial \chi}{\partial \lambda} = 0$ gives three similar equations:

$$\frac{\partial s}{\partial T} \cdot \Delta T + \frac{\partial s}{\partial S} \cdot \Delta S + \frac{\partial s}{\partial \lambda} \cdot \Delta \lambda = \left(\hat{s}_i - s_i^k\right) \tag{4.38}$$

This can be written in matrix form as:-

$$[J^T][J\ ]\{\Delta T, \Delta S, \Delta \lambda\}_k^T = [J^T]\{\hat{s} - s\}_k \tag{4.39}$$

where

$$[J] = \begin{bmatrix} \frac{\partial s_1}{\partial T} & \frac{\partial s_1}{\partial S} & \frac{\partial s_1}{\partial \lambda} \\ \frac{\partial s_2}{\partial T} & \frac{\partial s_2}{\partial S} & \frac{\partial s_2}{\partial \lambda} \\ \vdots & \vdots & \vdots \\ \frac{\partial s_n}{\partial T} & \frac{\partial s_n}{\partial S} & \frac{\partial s_n}{\partial \lambda} \end{bmatrix} \tag{4.40}$$

Equation (4.41) can then be used to solve for ΔT, ΔS and $\Delta \lambda$:

$$\{\Delta T, \Delta S, \Delta \lambda\}_k^T = \left([J]^T [J]\right)^{-1} [J]^T \{\hat{s}_i - s_k\} \tag{4.41}$$

For the next iteration, $\{T, S, \lambda\}_{k+1}$ are estimated from:

$$\{T, S, \lambda\}_{k+1} = \{T, S, \lambda\}_k + \{\Delta T, \Delta S, \Delta \lambda\}_k \tag{4.42}$$

This process is repeated until the successive changes in T, S and λ have become sufficiently small.

4.3.8. Application of least squares curve matching to the Walton equation

The values of $\partial s/\partial T$, $\partial s/\partial S$ and $\partial s/\partial \lambda$ must be determined in order to use the least squares algorithm. The Walton equation is more complex than the Theis case. Some numerical approximations need to be made in order to evaluate these functions.

Recalling the Walton solution to drawdown in a leaky aquifer (equation 4.27):

$$s = \frac{Q}{4\pi T} \cdot W(u,\lambda)$$

Differentiating with respect to T:

$$\frac{\partial s}{\partial T} = -\frac{Q}{4\pi T^2} \cdot W(u,\lambda) + \frac{Q}{4\pi T} \cdot \frac{\partial}{\partial T} W(u,\lambda)$$

$$= -\frac{Q}{4\pi T^2} \cdot W(u,\lambda) + \frac{Q}{4\pi T} \cdot \left(\frac{\partial W(u,\lambda)}{\partial u} \cdot \frac{du}{dT} + \frac{\partial W(u,\lambda)}{\partial \lambda} \cdot \frac{d\lambda}{dT} \right)$$

$$\frac{du}{dT} = \frac{-r^2 S}{4T^2 t}$$

$$= -\frac{u}{T}$$

and

$$\lambda = \frac{r}{\sqrt{Tc}} \qquad \text{so} \qquad \frac{d\lambda}{dT} = -\frac{r}{2\sqrt{c}} \cdot T^{-3/2}$$

$$= -\frac{\lambda}{2T}$$

Substituting for $\frac{du}{dT}$ and $\frac{d\lambda}{dT}$

$$\frac{\partial s}{\partial T} = -\frac{Q}{4\pi T^2} \cdot \left\{ W(u,\lambda) + \frac{\partial W(u,\lambda)}{\partial u} \cdot u + \frac{\partial W(u,\lambda)}{\partial \lambda} \cdot \frac{\lambda}{2} \right\} \qquad (4.43)$$

The values of $\frac{\partial W(u,\lambda)}{\partial u}$ and $\frac{\partial W(u,\lambda)}{\partial \lambda}$ must be evaluated numerically.

Similarly,

$$\frac{\partial s}{\partial S} = \frac{Q}{4\pi T} \cdot \frac{\partial}{\partial T} W(u,\lambda)$$
$$= \frac{Q}{4\pi T} \cdot \left(\frac{\partial W(u,\lambda)}{\partial u} \cdot \frac{du}{dS} + \frac{\partial W(u,\lambda)}{\partial \lambda} \cdot \frac{d\lambda}{dS} \right)$$

Now

$$\frac{du}{dS} = \frac{r^2}{4Tt} \qquad \text{and} \qquad \frac{\partial \lambda}{\partial S} = 0$$

Substituting for the values of $\frac{du}{dS}$ and $\frac{d\lambda}{dS}$ gives

$$\frac{\partial s}{\partial S} = \frac{Qr^2}{16\pi T^2 t} \cdot \left(\frac{\partial W(u,\lambda)}{\partial u} \right) \tag{4.44}$$

Finally

$$\frac{\partial s}{\partial \lambda} = \frac{Q}{4\pi T} \cdot \left(\frac{\partial W(u,\lambda)}{\partial \lambda} \right) \tag{4.45}$$

In order to evaluate these equations it is first necessary to calculate $\partial W(u,\lambda)/\partial \lambda$ and $\partial W(u,\lambda)/\partial u$. These are determined numerically. The value of $\partial W(u,\lambda)/\partial \lambda$ is calculated from:-

$$\frac{\partial W(u,\lambda)}{\partial \lambda} = \frac{W(u,\lambda+\delta\lambda) - W(u,\lambda-\delta\lambda)}{2 \cdot \delta\lambda} \tag{4.46}$$

In section 4.3.2, the calculation of the function W(u,λ) as W(v,λ), where v = ln(u), was discussed. A graph of W(v,λ) against v is straighter than that of W(u,λ) against u. Thus it is more accurate to determine $\partial W(v,\lambda)/\partial v$ than $\partial W(u,\lambda)/\partial u$, when a numerical method such as the above is being used. The function $\partial W(v,\lambda)/\partial v$ is determined from:-

$$\frac{\partial W(v,\lambda)}{\partial v} = \frac{W(v+\delta v,\lambda) - W(v-\delta v,\lambda)}{2 \cdot \delta v} \tag{4.47}$$

The function $\frac{\partial W(u,\lambda)}{\partial u}$ may then be evaluated from:-

$$\frac{\partial W(u,\lambda)}{\partial u} = \frac{1}{u} \cdot \frac{\partial W(v,\lambda)}{\partial v} \tag{4.48}$$

4.3.9. Computer programme WALPUTS (WALton PUmp Test Solutions)

A computer programme was written using FORTRAN77 to evaluate the least squares algorithm for a leaky aquifer using the Walton theory. It is more complex than the CONPUTS programme, as the number of variables solved has increased from two to three, and the determination of the Walton well function *W(u,r/L)* involves more numerical methods.

A listing of the computer programme WALPUTS is included on the floppy disc in Appendix D17. The main functions of the programme are described below.

The flowchart in Figure 4.9 shows the main programme. After the data has been read in and stored, the theoretical values of drawdown, $\partial s/\partial T$, $\partial s/\partial S$ and $\partial s/\partial \lambda$ are calculated using subroutine DELTA. A flowchart of subroutine DELTA is shown in Figure 4.10. Equation 4.41 is then used to calculate the increments in T, S and λ in order to reduce the error between the observed and calculated values of drawdown.

To help the user achieve convergence, this programme incorporates an approach called relaxation. This process may be used to enhance convergence. If the iterative process is considered, where the value of transmissivity 'T' is calculated, each iteration may give values of T that oscillate above and below the 'best fit' value. The magnitude of the difference between the calculated and 'best fit' T decreases as the number of iterations increases until the difference is negligible and the algorithm converges. This process is shown in Figure 4.12.

The relaxation approach reduces or increases the new value of T, using the formula:

$$T_{i+1} = T_{i+1} \cdot \theta + T_i(1-\theta) \qquad (4.49)$$

where θ is the relaxation factor.

Thus a value of θ = 1.0 represents no relaxation. If θ < 1.0, the algorithm will be under relaxed, i.e. the new value of T will not be as great as calculated within the algorithm. A value of θ > 1.0 will represent over relaxation, and the new value of T will be greater than that calculated within the algorithm. This process is shown in Figure 4.13. The value of θ should be chosen such that:

$$0.0 < \theta < 2.0$$

Obviously, for some cases under, and others over relaxation will be required. This gives the user a tool to help the programme converge.

Subroutine INVERT is used to invert a 3 x 3 matrix. This uses the standard method, of calculating a matrix of cofactors from which the determinant is evaluated. The cofactors are then used to determine the terms within the inverted matrix.

Subroutine DELTA is used to calculate all the values required from the Walton solution. A flowchart which describes this subroutine is shown in Figure 4.10. It uses the approximations which were discussed previously. Numerical methods are used to calculate these values.

4.3.10. User information

The data for the WALPUTS programme is stored in a datafile, called WALTIN.DAT. Information is required in the following format:-

Row 1 (2 I10)

Columns 1 - 10	Number of observations
Columns 10 - 20	Maximum number of iterations

Row 2 (2 F10.4)

Columns 1 - 10	Convergence factor (m)
Columns 10 - 20	Relaxation factor

Row 3 (F10.4)

Columns 1 - 10	Radius (m)

Row 4 (F10.4)

Columns 1 - 10 Flowrate (m^3/s)

Row 5 (F10.4)

Columns 1 - 10 Transmissivity guess (m^2/s)

Row 6 (F10.4)

Columns 1 - 10 Storage guess

Row 7 (F10.4)

Columns 1 - 10 Leakage guess (m)

Rows 8 to end (2 F10.4)

Columns 1 - 10 Time (s)

Columns 10 - 20 Drawdown (m)

The programme is run by typing the name, WALPUTS, followed by a carriage return. The relaxation factor should be input as 1.0 if no relaxation is required. A sample input file is shown in Appendix D8. If the programme does not converge, the input guesses of *T*, *S* and *L*, convergence and relaxation factors should be changed. When convergence has occurred, the final values of aquifer parameters are presented in WALTOUT.DAT. An example of this output file is shown in Appendix D9.

4.3.11. Testing the WALPUTS programme

A hypothetical pumping test of 6 hours duration in a leaky aquifer was used to test and validate the programme. Data was produced which simulates the drawdown in an observation well 20 m from the pumped well. This data is presented as part of the input file shown in Appendix D8. The WALPUTS programme was used to estimate the aquifer parameters that match the best fit values of drawdown to those observed, with initial guesses of T = 250 m^2/day, S = 5.0 x 10^{-4} and a leakage factor of 500 m. The programme took ten iterations with a convergence factor of 1.0 x 10^{-10} and gave the following best fit parameters:

Transmissivity = 473 m^2/day

Storativity	= 1.09×10^{-3}
Leakage factor	= 214.0 m
Root mean square error	= 9.59 mm

The results of this test show that the programme is able to rapidly converge to the solution, minimising the difference between the observed and calculated values of drawdown. A graph of the observed and theoretical drawdown values is presented in Figure 4.14.

Again this data can be used to test the convergence of the programme over a range of input values of T, S and L. This was tested with starting values of:

T = 5, 250, 750, and 1000 m^2/day

S = 1.0×10^{-2}, 1.0×10^{-3} and 1.0×10^{-4}

L = 100, 400 and 800 m

The results of these tests are shown in Appendix D10. For a number of the tests the programme did not converge correctly. In some cases the programme converged to the Theis solution, where the value of r/L is small. In others the solution diverges from the correct values. In this case the programme terminates when it reaches the maximum number of iterations.

The WALPUTS programme is more susceptible to the problems of non convergence, due to the increased number of parameters and the more complicated nature of the function. The input parameters should be chosen with care and changed if the solution diverges. Once the solution has converged, a second set of input guesses of parameters should be used to converge to the same solution. If the same solution is not obtained, then for one case the programme is converging to a local, and not the global, minimum. To aid convergence, the convergence factor can be reduced and the relaxation technique incorporated with the algorithm.

4.3.12. Conclusion

An accurate method has been produced which is capable of calculating the values of transmissivity, storativity, and leakage factor from pumping test data. It converges from a wide range of input values.

If the assumptions behind the '*r/L*' theory are examined, there are two significant assumptions that could lead to incorrect values being calculated. The first is that of disregarding the contribution to discharge from storage within the aquitard. The second is the assumption of a constant head of water in the aquifer overlying the aquitard.

Hantush examined the first assumption, and included the aquitard storativity in his solution to drawdown during a pumping test in a leaky aquifer, equation 2.23. The final programme uses this solution to calculate the drawdown in leaky aquifers. This programme is more realistic as it minimises the number of assumptions that are made.

4.4. Leaky aquifers - the Hantush case

The Hantush solution to drawdown in a leaky aquifer during a pumping test is based on less assumptions than the Walton solution, as the storativity of the aquitard is included. This could have a significant effect, as reported by Neuman and Witherspoon (1969b). Considering the recharge to the aquifer from the aquitard at early time, a large proportion is from storage. As the pumping test continues towards late time, the proportion of recharge from storage is reduced. The Walton solution thus becomes more accurate as steady state approaches.

4.4.1. The Hantush equation

Recalling the Hantush solution to drawdown in a leaky aquifer from chapter 2:

$$s = \frac{Q}{4\pi T} W(u,\beta) \qquad (4.50)$$

where the Hantush well function is defined as:

$$W(u,\beta)=\int_{u}^{\infty}\left\{\frac{\exp(-y)}{y}\cdot erfc\left(\frac{\beta\sqrt{u}}{\sqrt{y(y-u)}}\right)\right\}dy \tag{4.51}$$

and

$$\beta=\frac{r}{4}\sqrt{\frac{K'/d'}{T}\cdot\frac{S'}{S}} \tag{4.52}$$

for time, $t < (d'S'/10K')$. It is clear that the solution contains 4 unknowns, the transmissivity T and storativity S of the aquifer, and vertical permeability K' and storativity S' of the aquitard. A table of the Hantush well function is presented in Appendix D11.

The term, $erfc\left(\frac{\beta\sqrt{u}}{\sqrt{y(y-u)}}\right)$, is the complementary error function, which is defined as:

$$\begin{aligned} erfc(x) &= 1-erf(x) \\ &= 1-\frac{2}{\sqrt{\pi}}\int_{x}^{\infty}\exp(-t^2)\,dt \end{aligned} \tag{4.53}$$

To determine the theoretical drawdown during a pumping test these equations must be evaluated.

4.4.2. Evaluation of the Hantush well function

The evaluation of the Hantush well function consists of two separate parts. The first is the determination of the complementary error function, the second the evaluation of the integral using the trapezoidal rule.

If the complementary error function, *erfc(x)* is considered, the solution has a value of between 0.0 and 1.0. When x is small, the value of *erfc(x)* tends to 1.0. When x is large, the value of *erfc(x)* tends to 0.0. If $x > 4.0$, the *erfc(x)* will be 0.0. A table of values of the *erfc(x)* is presented in Appendix D12.

The complementary error function may be determined from the power series approximation:-

$$erfc(x) = 1 - \frac{2}{\sqrt{\pi}}\left(x - \frac{x^3}{1!3} + \frac{x^5}{2!5} - \frac{x^7}{3!7} + - \cdots\right) \qquad (4.54)$$

A computer programme was written to evaluate this function. The results are shown in Appendix D12, compared with the values from a table. This shows that the complementary error function may be evaluated accurately for all input values.

The well function is evaluated using the trapezoidal rule in the same way as before. A graph of this function is shown in Figure 4.15. The function is evaluated on a logarithmic scale '*y*', where the initial value is equal to *ln (u)*. The value of *y* is then increased in small amounts. The advantage of using a logarithmic scale is that when the value of *u* is small, the function $W(u,\beta)$ is large. As *u* increases, $W(u,\beta)$ tends to zero. A logarithmic scale thus has small steps where the function changes rapidly, and so increases the accuracy of this calculation.

If the complementary error function in equation 4.51 is examined, the initial value, where $y = u$, will result in an infinite term. A starting value of '*y*' should be determined to avoid this infinite term. A suitable point is where the *erfc(x)* equals zero, which is where '*x*' = 4.0. Thus when the values of *u* and β are known, a starting value of '*y*' is calculated, where the complementary error function is 0.0, from:

$$y = \frac{u}{2} + \frac{\sqrt{u}}{2} \cdot \sqrt{u + \left(\frac{\beta}{2}\right)^2} \qquad (4.55)$$

The value of '*y*' is then increased in small increments, the individual values of the function calculated and the integral evaluated using the trapezoidal rule.

A programme was written, incorporating the routine which evaluates the complementary error function, to calculate the Hantush well function. The programme was validated by

evaluating $W(u,\beta)$ for different u and β, and comparing the results against those from tables. The results are presented in Appendix D13. From this table it can be seen that $W(u,\beta)$ was calculated accurately for a wide range of u and β.

To improve the accuracy of the calculation of $\partial W(u,\beta)/\partial u$, the function W(u,β) is calculated at different values of v, where $v = ln(u)$. In this way, $\partial W(u,\beta)/\partial v$ is calculated by the gradient method. The graph of $W(u,\beta)$ against $ln\ (u)$ is straighter than $W(u,\beta)$ against u. Thus to calculate $\partial W(u,\beta)/\partial v$ using a gradient method is more accurate. The value of $\partial W(u,\beta)/\partial u$ is determined by dividing $\partial W(u,\beta)/\partial v$ by u.

4.4.3. Computer programme HANPUTS (HANtush PUmp Test Solutions)

The least squares algorithm could now be applied to the Hantush solution and a computer programme developed to solve for aquifer parameters using this theory. The parameters which are solved by this programme are the transmissivity T, storativity S and the leakage factor γ.

The leakage factor represents the parameters relating to the aquitard, which is part of the variable β. Thus:

$$\gamma = \frac{K'S'}{d'} \tag{4.56}$$

and

$$\beta = \frac{r}{4}\sqrt{\frac{\gamma}{TS}} \tag{4.57}$$

Recalling the least squares algorithm for three variables from section 4.3.6, the HANPUTS programme solves the equation:

$$\{\Delta T, \Delta S, \Delta\gamma\}_k^T = \left([J]^T[J]\right)^{-1}[J]^T\{\hat{s}_l - s_k\} \tag{4.58}$$

where

$$[J]=\begin{bmatrix} \frac{\partial s_1}{\partial T} & \frac{\partial s_1}{\partial S} & \frac{\partial s_1}{\partial \gamma} \\ \frac{\partial s_2}{\partial T} & \frac{\partial s_2}{\partial S} & \frac{\partial s_2}{\partial \gamma} \\ \vdots & \vdots & \vdots \\ \frac{\partial s_n}{\partial T} & \frac{\partial s_n}{\partial S} & \frac{\partial s_n}{\partial \gamma} \end{bmatrix} \qquad (4.59)$$

The partial derivatives of the theoretical drawdown with respect to T, S and γ are required in order that this equation may be evaluated. We know:-

$$s=\frac{Q}{4\pi T}W(u,\beta)$$

Differentiating with respect to T:

$$\frac{\partial s}{\partial T}=-\frac{Q}{4\pi T^2}\cdot W(u,\beta)+\frac{Q}{4\pi T}\cdot\left\{\frac{\partial W(u,\beta)}{\partial u}\cdot\frac{du}{dT}+\frac{\partial W(u,\beta)}{\partial \beta}\cdot\frac{d\beta}{dT}\right\}$$

$$\frac{du}{dT}=-\frac{r^2S}{4T^2t}=-\frac{u}{T} \qquad \text{and} \qquad \frac{d\beta}{dT}=-\frac{r}{8}\cdot\frac{1}{\sqrt{T^3}}\cdot\sqrt{\frac{\gamma}{S}}=-\frac{\beta}{2T}$$

Substituting for $\frac{du}{dT}$ and $\frac{d\beta}{dT}$ and rearranging gives:

$$\frac{\partial s}{\partial T}=-\frac{Q}{4\pi T^2}\left\{W(u,\beta)+\frac{\partial W(u,\beta)}{\partial u}\cdot u+\frac{\partial W(u,\beta)}{\partial \beta}\cdot\frac{\beta}{2}\right\} \qquad (4.60)$$

Similarly

$$\frac{\partial s}{\partial S}=\frac{Q}{4\pi T}\left\{\frac{\partial W(u,\beta)}{\partial u}\cdot\frac{du}{dS}+\frac{\partial W(u,\beta)}{\partial \beta}\cdot\frac{d\beta}{dS}\right\}$$

$$\frac{du}{dS}=\frac{r^2}{4Tt}=\frac{u}{S} \qquad \text{and} \qquad \frac{d\beta}{dS}=-\frac{r}{8}\cdot\frac{1}{\sqrt{S^3}}\cdot\sqrt{\frac{\gamma}{T}}=-\frac{\beta}{2S}$$

Substituting for $\frac{du}{dS}$ and $\frac{d\beta}{dS}$ and rearranging gives:

$$\frac{\partial s}{\partial S} = \frac{Q}{4\pi T}\left\{\frac{\partial W(u,\beta)}{\partial u}\cdot\frac{u}{S} - \frac{\partial W(u,\beta)}{\partial \beta}\cdot\left(\frac{\beta}{2S}\right)\right\} \qquad (4.61)$$

Finally

$$\frac{\partial s}{\partial \gamma} = \frac{Q}{4\pi T}\cdot\left\{\frac{\partial W(u,\beta)}{\partial u}\cdot\frac{du}{d\gamma} + \frac{\partial W(u,\beta)}{\partial \beta}\cdot\frac{d\beta}{d\gamma}\right\}$$

$$\frac{du}{d\gamma} = 0 \qquad \text{and} \qquad \frac{d\beta}{d\gamma} = \frac{r}{8}\cdot\frac{1}{\sqrt{TS\gamma}} = \frac{\beta}{2\gamma}$$

Substituting for $\frac{du}{d\gamma}$ and $\frac{d\beta}{d\gamma}$ and rearranging gives:

$$\frac{\partial s}{\partial \gamma} = \frac{Q}{4\pi T}\cdot\frac{\partial W(u,\beta)}{\partial \beta}\cdot\frac{\beta}{2\gamma} \qquad (4.62)$$

The mechanics of this programme are identical to the Walton programme. It is simpler, due to the fact that only one method of caluclating the Hantush well function is used. However, the calculation of this function is more complex. A listing of the programme is included on the floppy disc in Appendix D17.

4.4.4. User information

The data for the HANPUTS programme is input using a datafile, called 'HANTIN.DAT', in the same manner as the previous two programmes. The structure of the datafile is as follows:-

Row 1 (2 I10)

Columns 1 - 10	Number of observations
Columns 10 - 20	Maximum number of iterations

Row 2 (2 F10.4)

Columns 1 - 10	Convergence factor
Columns 10 - 20	Relaxation factor

Row 3 (2 F10.4)

Columns 1 - 10	Radius (m)
Columns 10 - 20	Flowrate (m^3/s)

Row 4 (2 F10.4)

Columns 1 - 10	Transmissivity guess (m^2/s)
Columns 10 - 20	Aquifer storativity guess

Row 5 (2 F10.4)

Columns 1 - 10	Leakage factor guess (1/s)
Columns 10 - 20	Aquitard storativity guess

Rows 6 to end (2 F10.4)

Columns 1 - 10	Time (s)
Columns 10 - 20	Drawdown (m)

It is important that the data is in the correct columns. A sample input file is shown in Appendix D14. The programme is run by typing the name of the programme, HANPUTS, followed by a carriage return. The results may be examined in the output file, HANTOUT.DAT. An example of this file is shown in Appendix D15. If the programme does not converge, different values of initial parameter estimations should be used. The method of relaxation is included, and may be used to speed up convergence as before.

4.4.5. Testing the HANPUTS programme

The programme was tested using data from a hypothetical pumping test. After running the programme, the 'best fit' parameters generated by the HANPUTS programme were used to calculate the drawdown values, which are shown compared with the input values in Figure 4.16. The algorithm took 8 iterations with a convergence factor of 1.0×10^{-10}. The average error between the observed and input values is 6.7 mm. The programme estimated parameters of:

Transmissivity = 588 m^2/day

Storativity = 9.80×10^{-4} (-)

Beta = 0.0164 (-)

An important consideration is to check that the algorithm converges. The convergence properties were tested by using the same input values of drawdown, and a range of initial estimations of the aquifer parameters. These values were:

Transmissivity: 50, 250, 750 and 1000 m^2/day

Storativity: 5.0×10^{-2}, 5.0×10^{-3} and 5.0×10^{-4}

Beta: 2.0×10^{-3}, 2.0×10^{-2} and 1.0×10^{-1}.

The results of these tests are shown in Appendix D16. This shows that the programme converged for a wide range of input parameter estimations. For some values the algorithm diverged, which was the case for all input values of $S = 5.0 \times 10^{-2}$. However, it is easy to see when the programme has diverged, as the average error between the input and 'best fit' values is very large. In each case where converged was achieved the final parameters were the same as those shown above.

4.4.6. Conclusions

Thus a method has been devised and evaluated to estimate the parameters of a leaky aquifer system using the results of a pumping test. It uses the Hantush theory, which makes fewer assumptions about the aquifer system than the Walton solution.

Three least squares algorithms have been devised successfully that converge well. They were tested using data from hypothetical pumping tests. However, the leaky programmes, WALPUTS and HANPUTS, are slow in achieving convergence. The numerical methods used to evaluate the well function and the derivatives of the well function require a large number of calculations, which must be repeated many times. A method to increase the speed of these calculations would greatly enhance the the programmes by reducing user time.

To achieve this, a numerical method was used to evaluate the well function and the derivative terms. This technique is known as Hermitian interpolation. The theory of

Hermitian interpolation, and how this is applied to determing the value of the well function, is discussed in the next chapter.

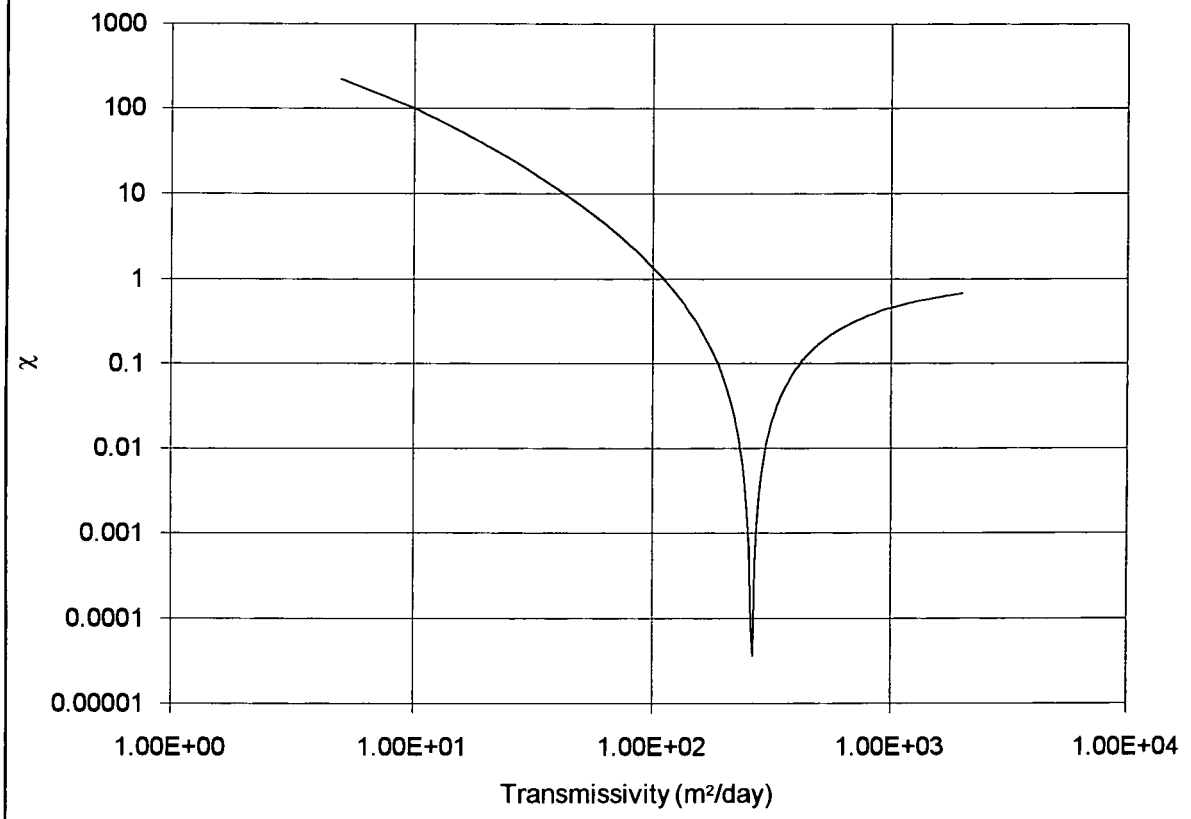

Figure 4.1: Variation of χ with transmissivity

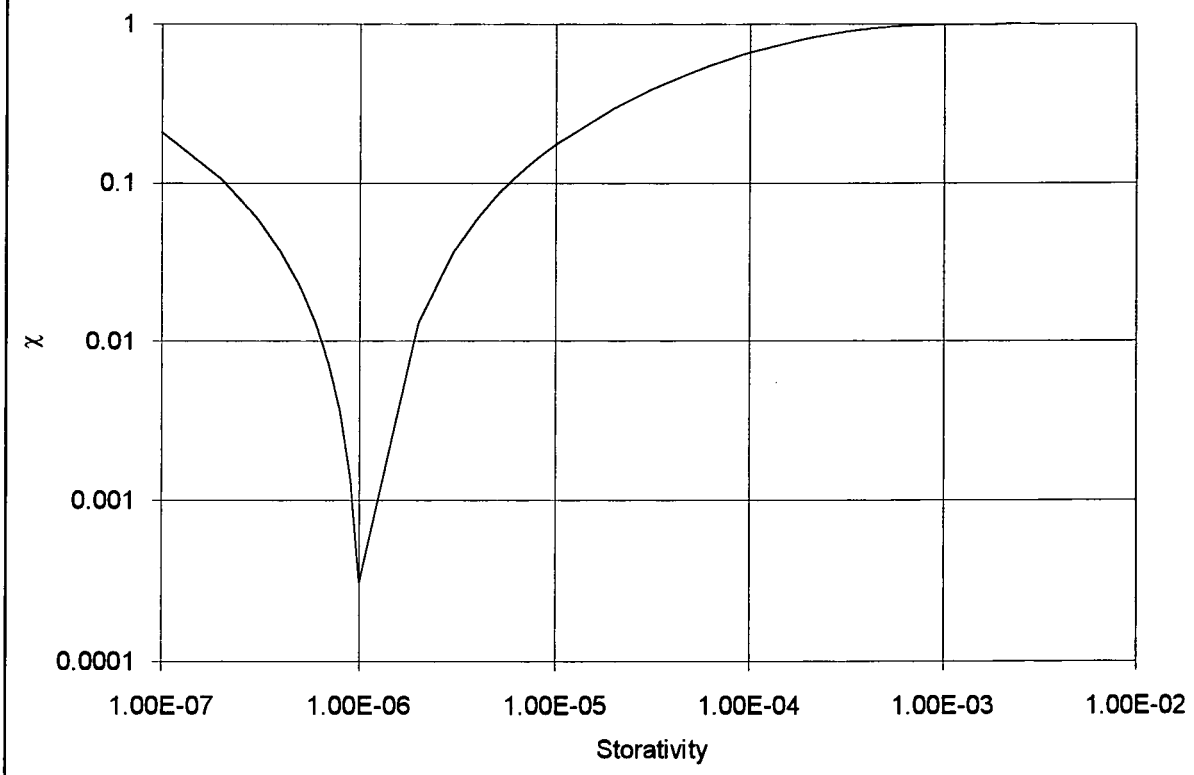

Figure 4.2: Variation of χ with storativity

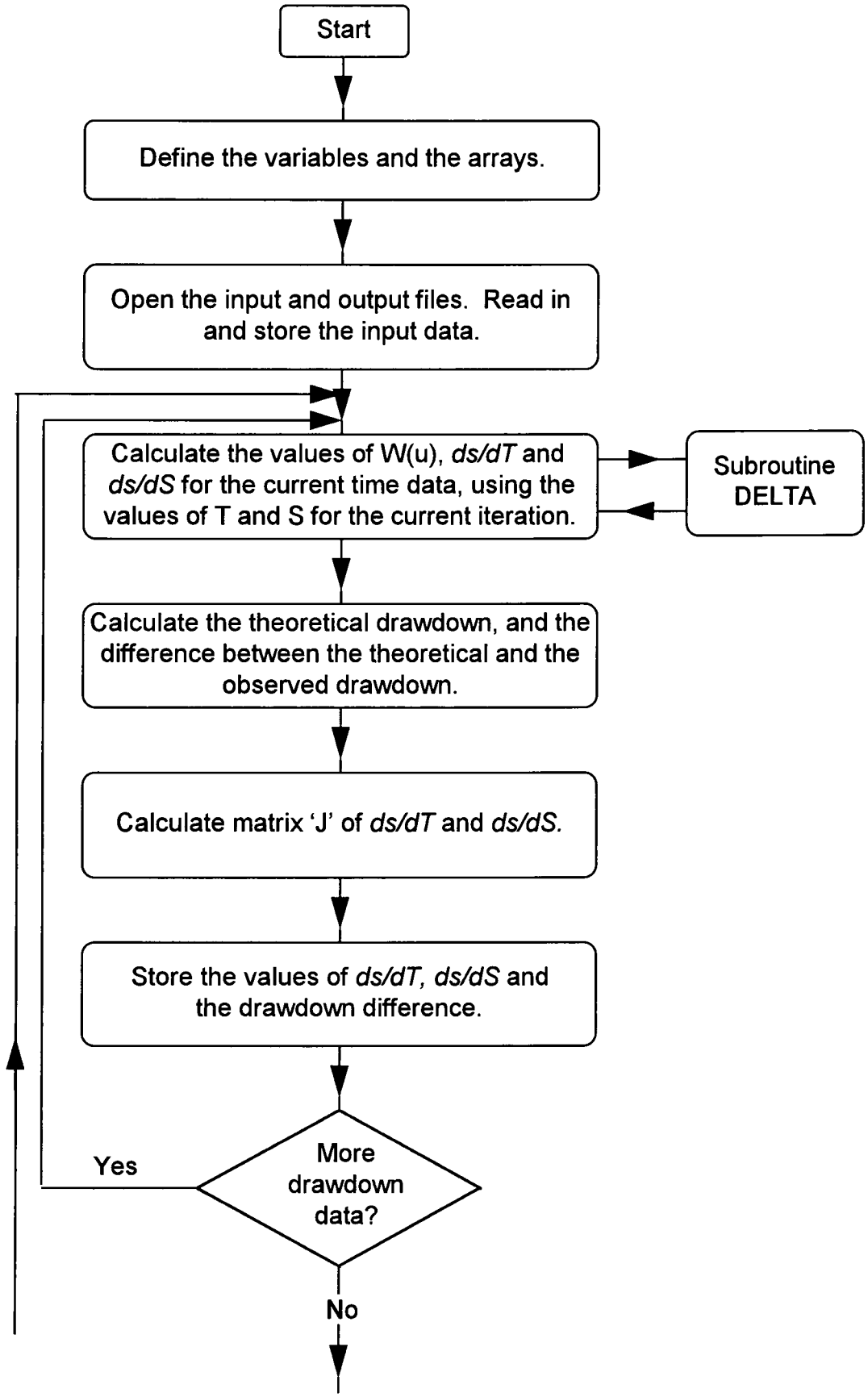

Figure 4.3: Flowchart showing the CONPUTS main programme

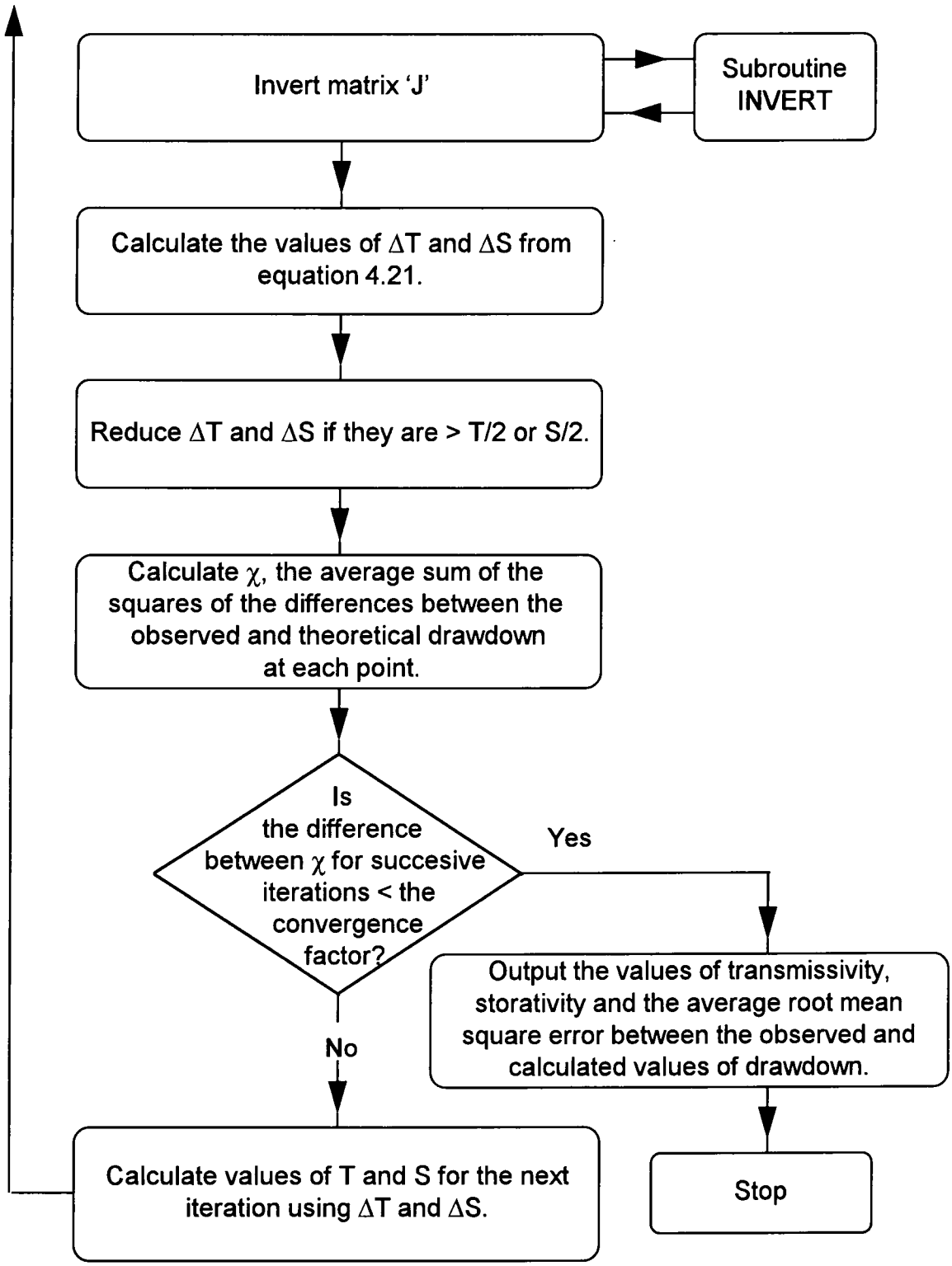

Figure 4.3: Flowchart showing the CONPUTS main programme (continued)

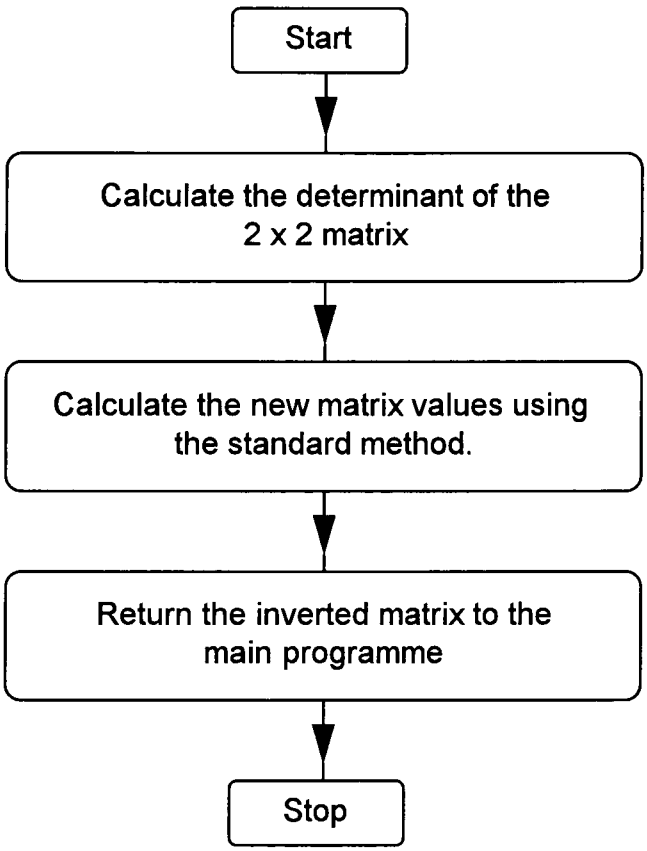

Figure 4.4: Flowchart showing subroutine INVERT from the CONPUTS programme.

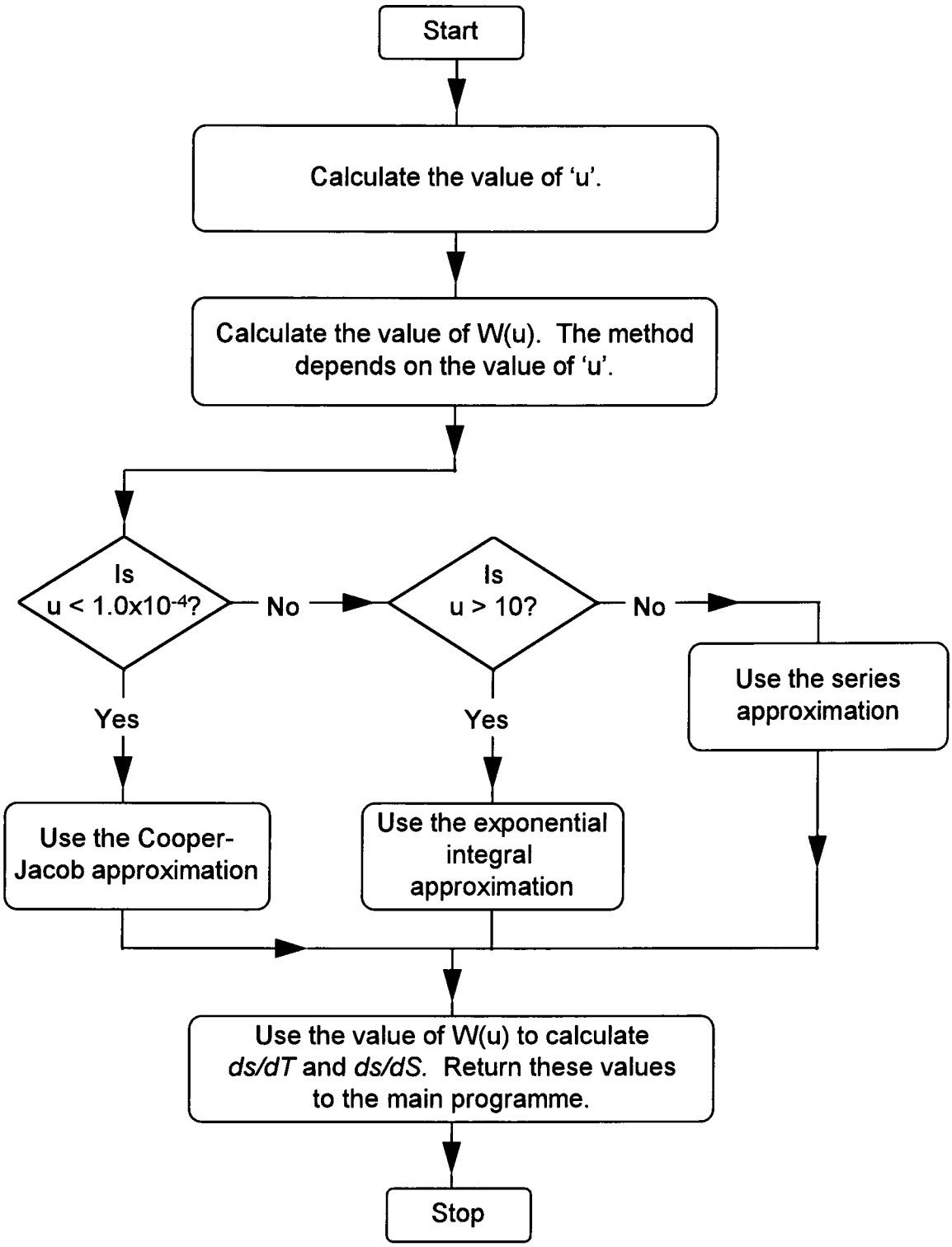

Figure 4.5: Flowchart showing subroutine DELTA from the CONPUTS programme.

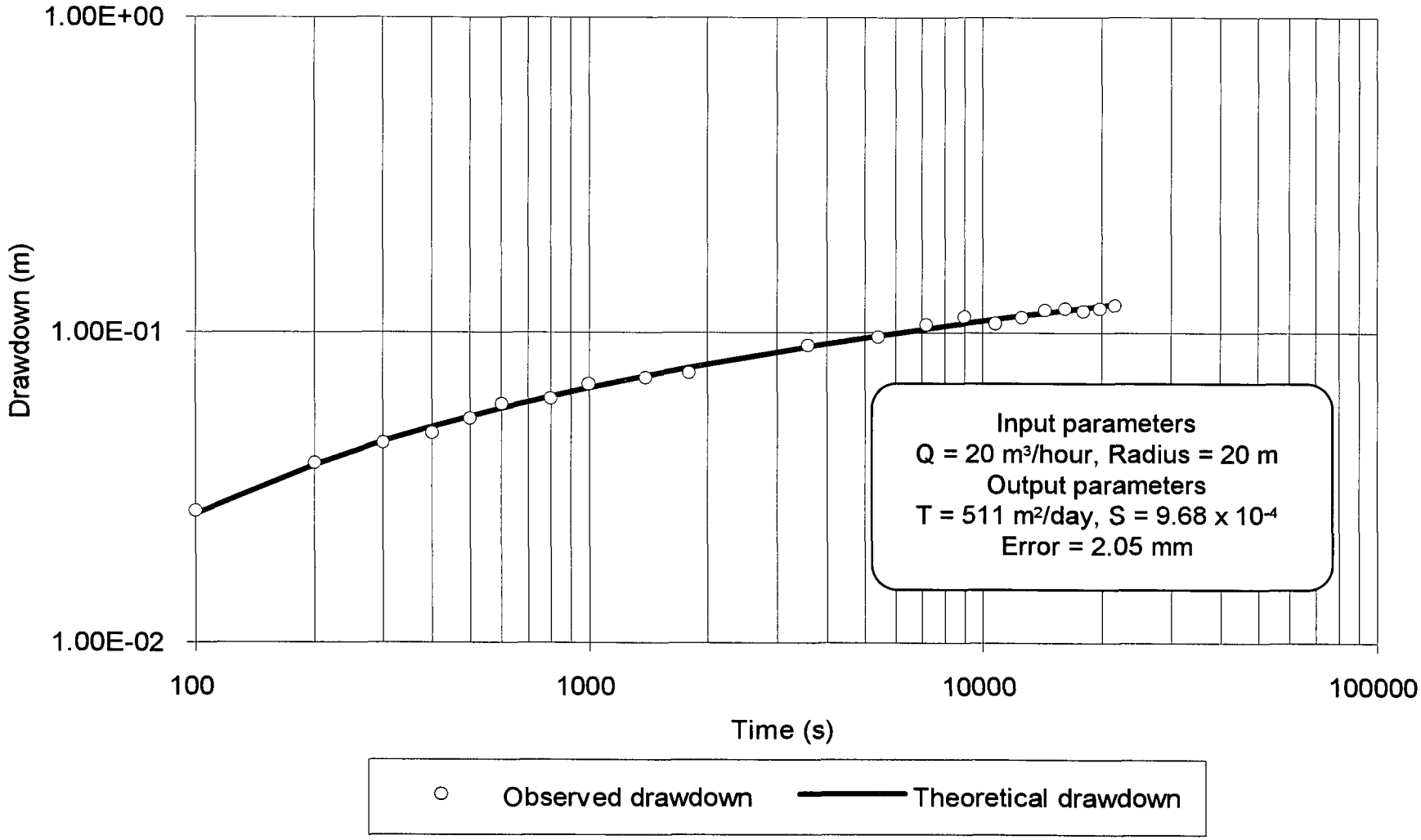

Figure 4.6: Results of a hypothetical pumping test using the CONPUTS programme

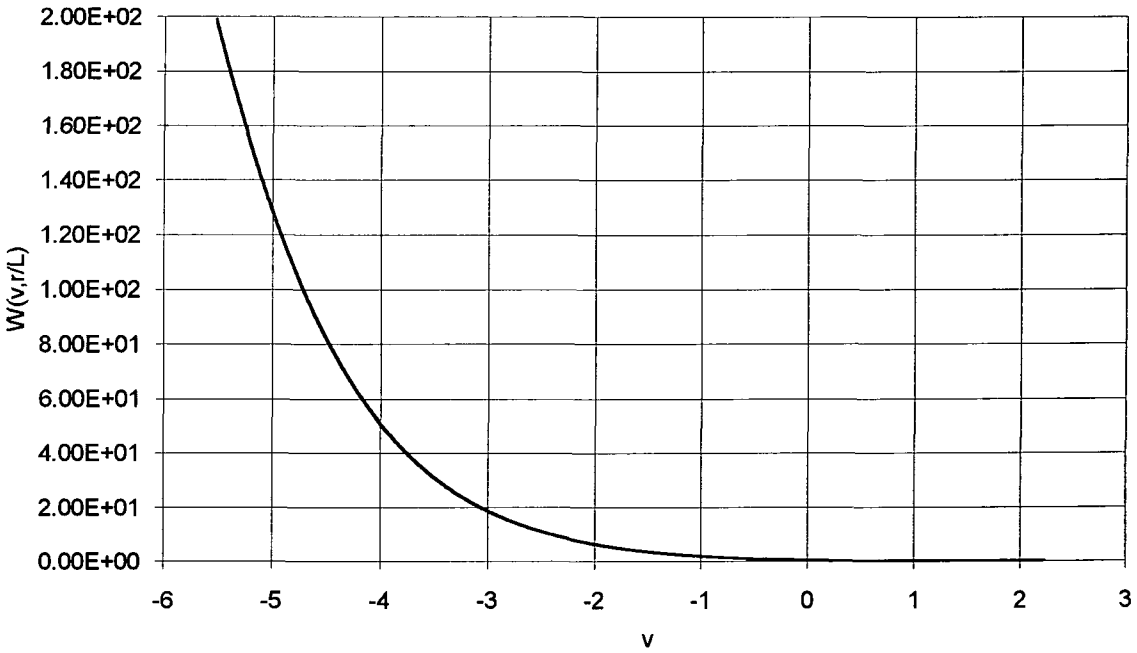

Figure 4.7: Graph of the function W(v,r/L)

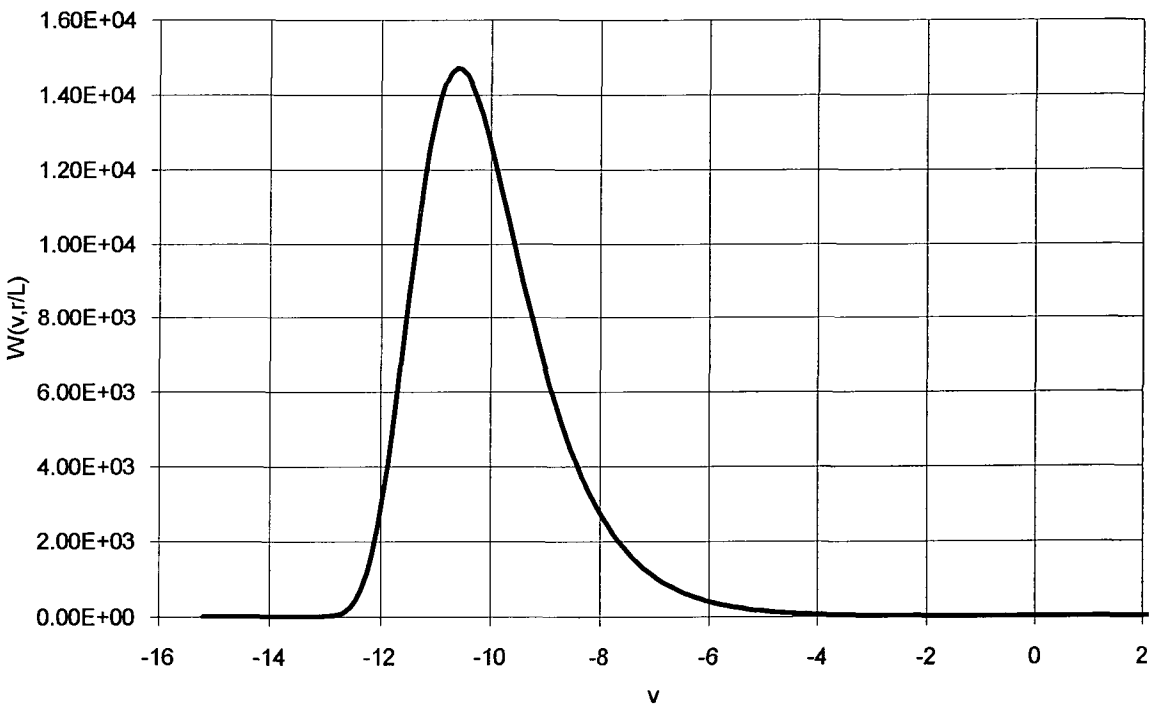

Figure 4.8: Graph of the function W(0,r/L)

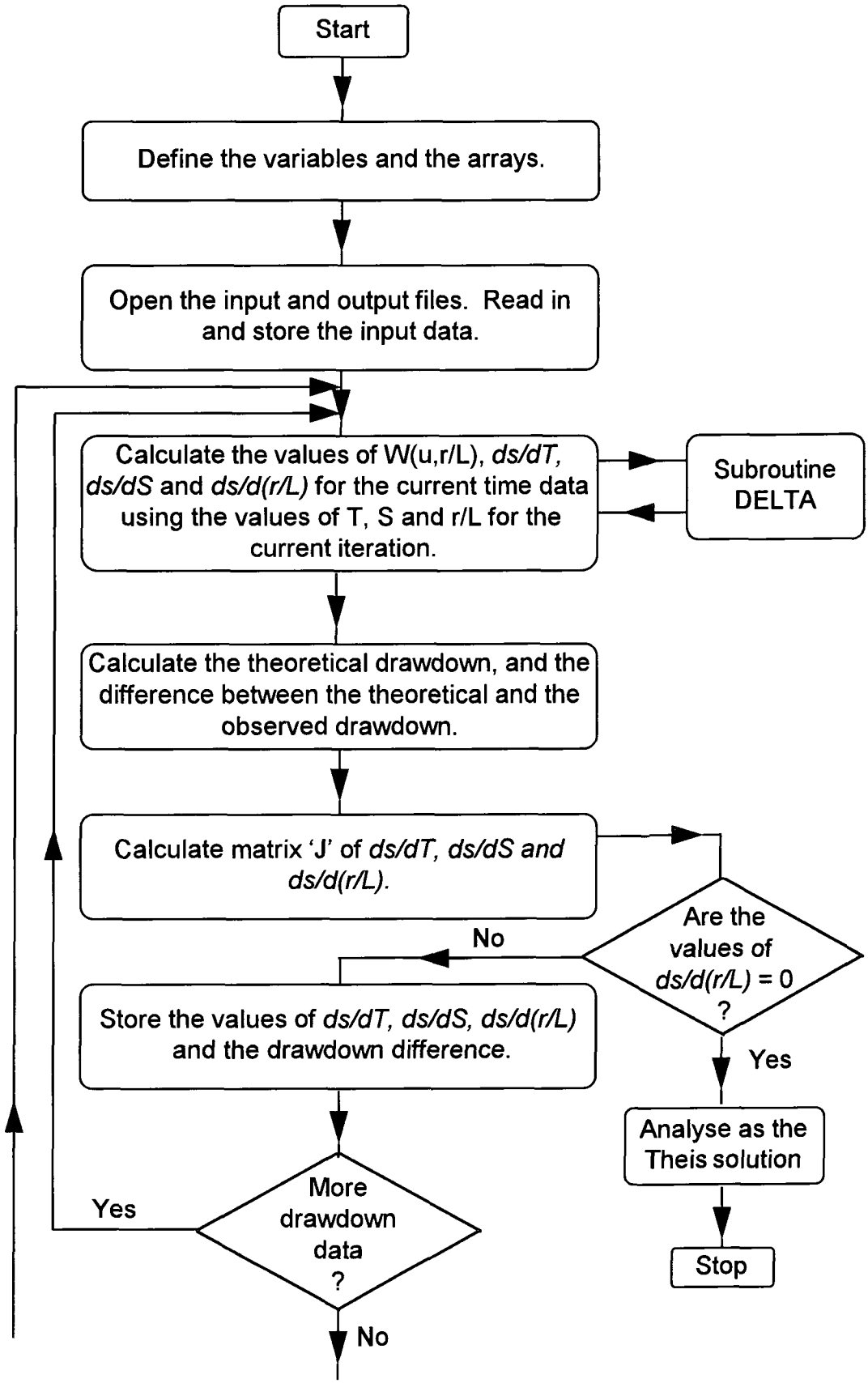

Figure 4.9: Flowchart showing the WALPUTS main programme

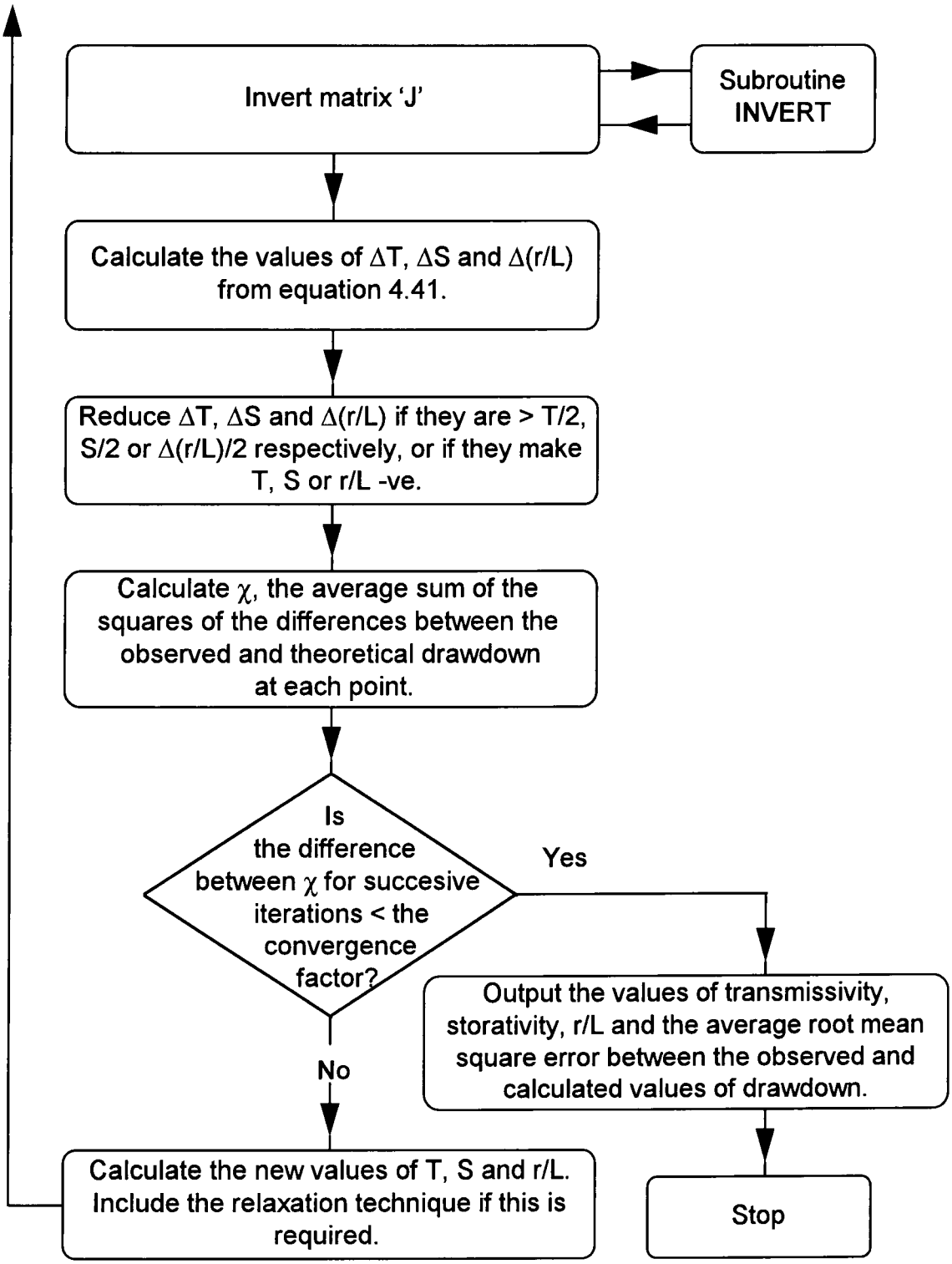

Figure 4.9: Flowchart showing the WALPUTS main programme (continued)

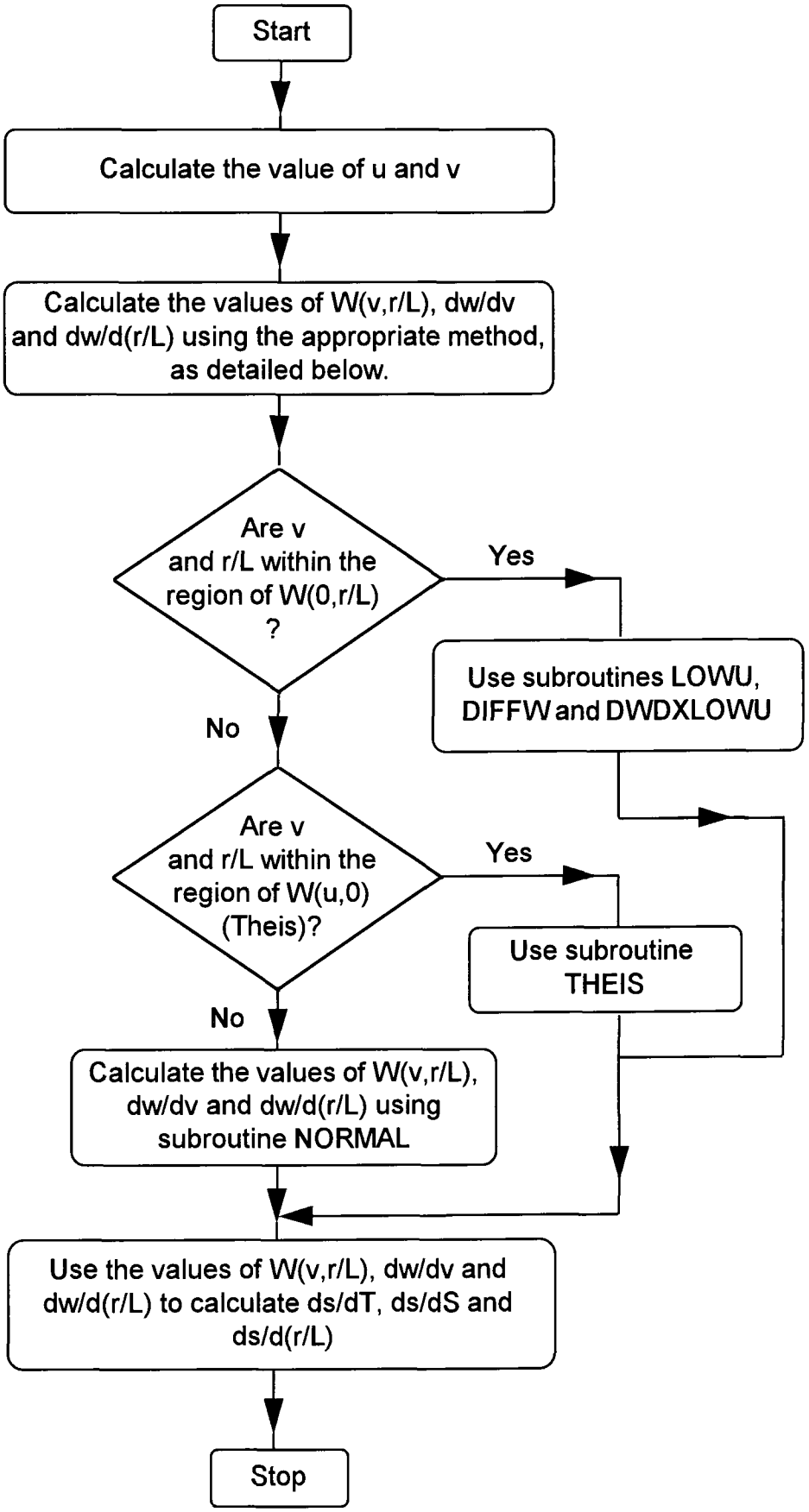

Figure 4.10: Flowchart showing subroutine DELTA from the WALPUTS programme

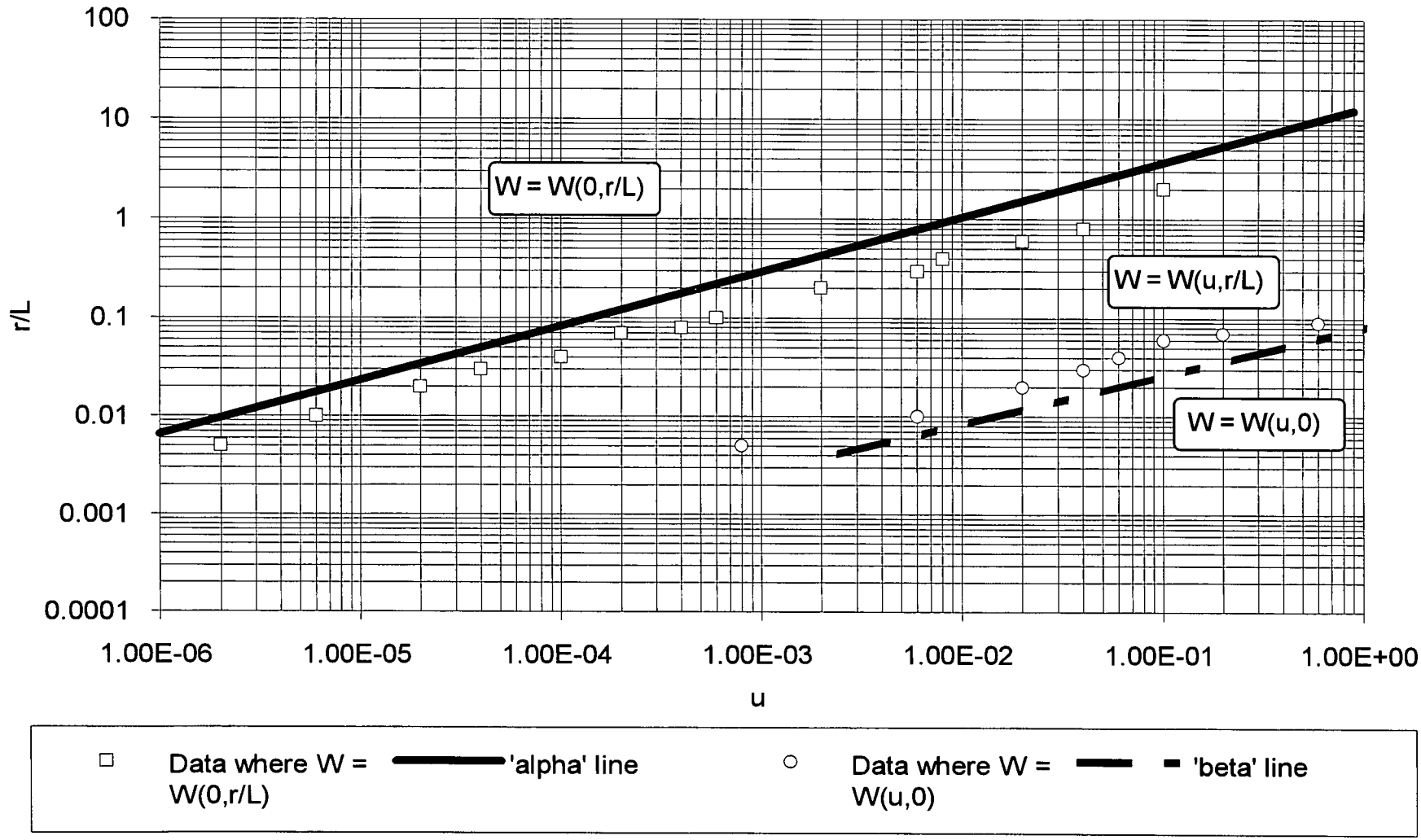

Figure 4.11: Graph showing the regions where W(u,r/L) is approximated

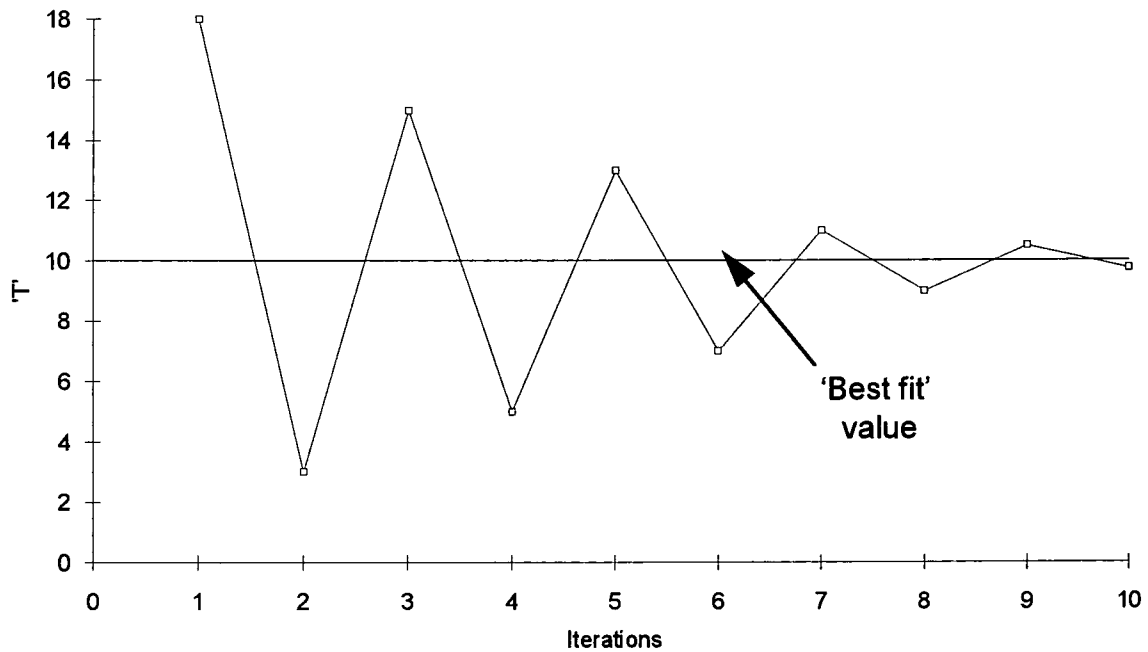

Figure 4.12: Convergence of an algorithm

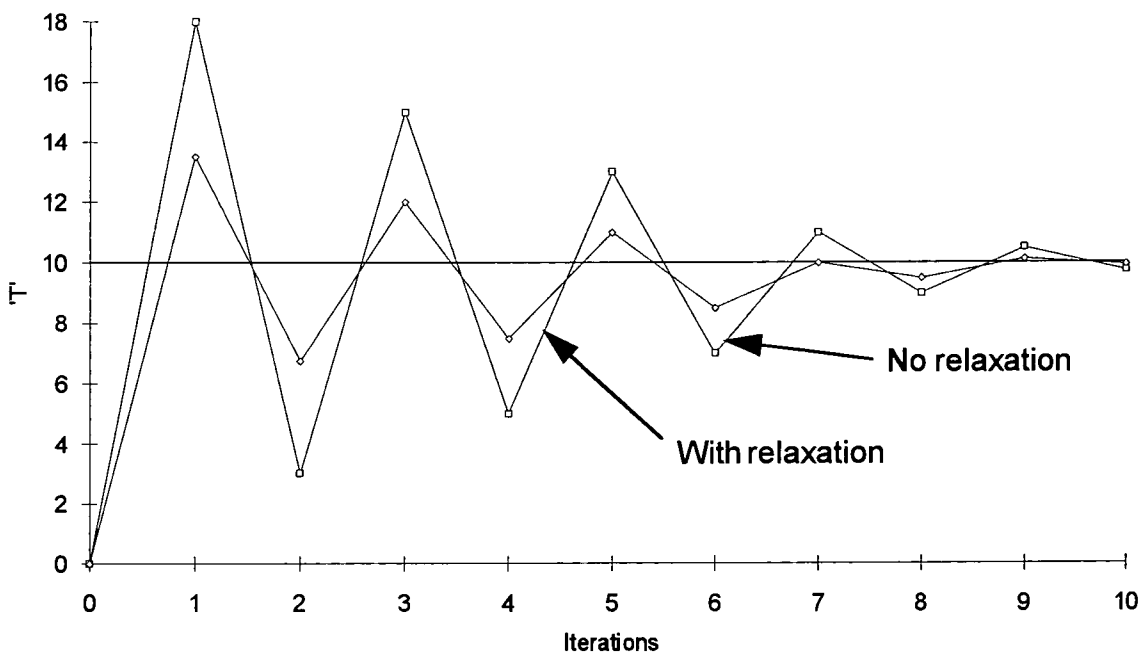

Figure 4.13: Convergence of an algorithm with relaxation of 0.75

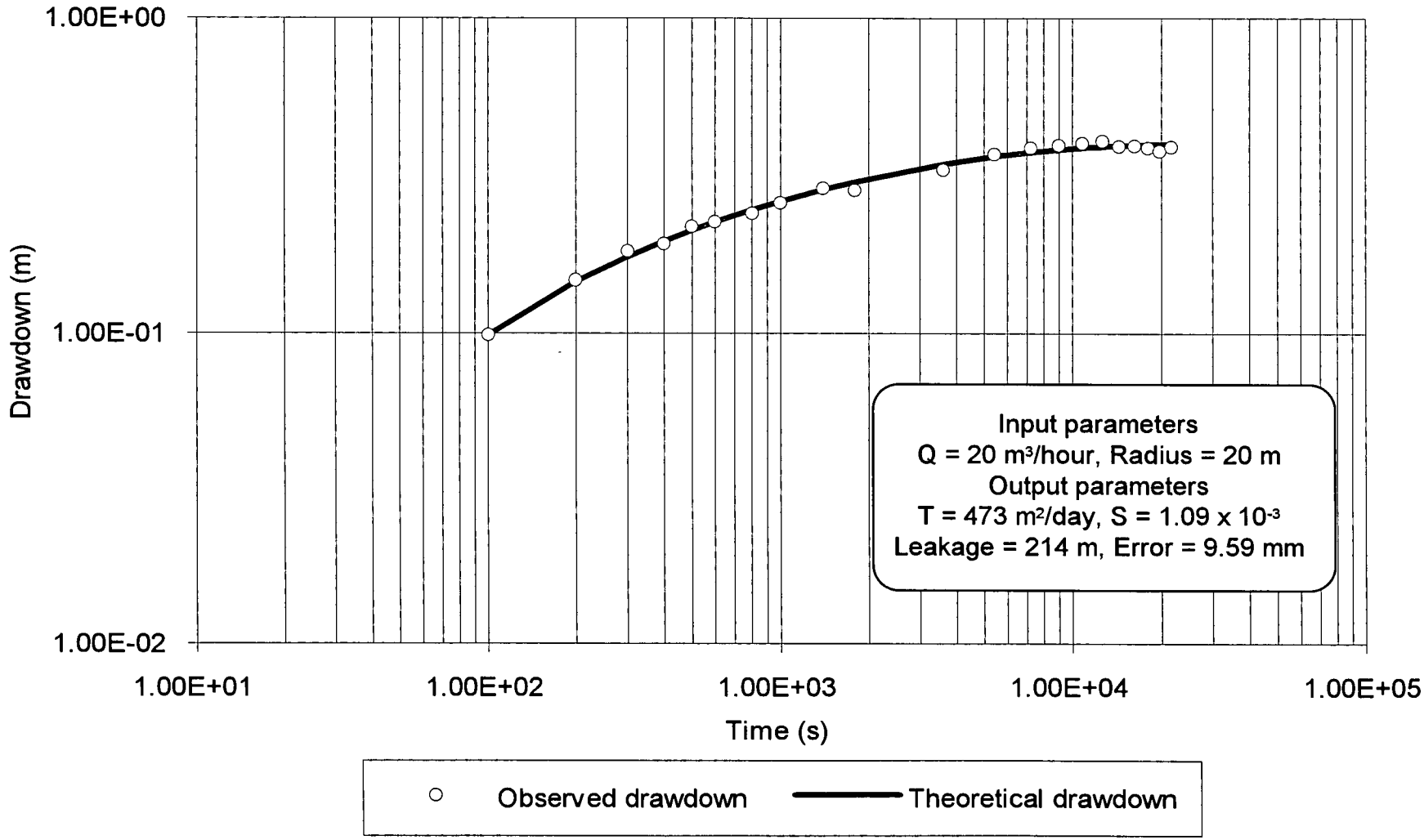

Figure 4.14: Results of a hypothetical pumping test using the WALPUTS programme

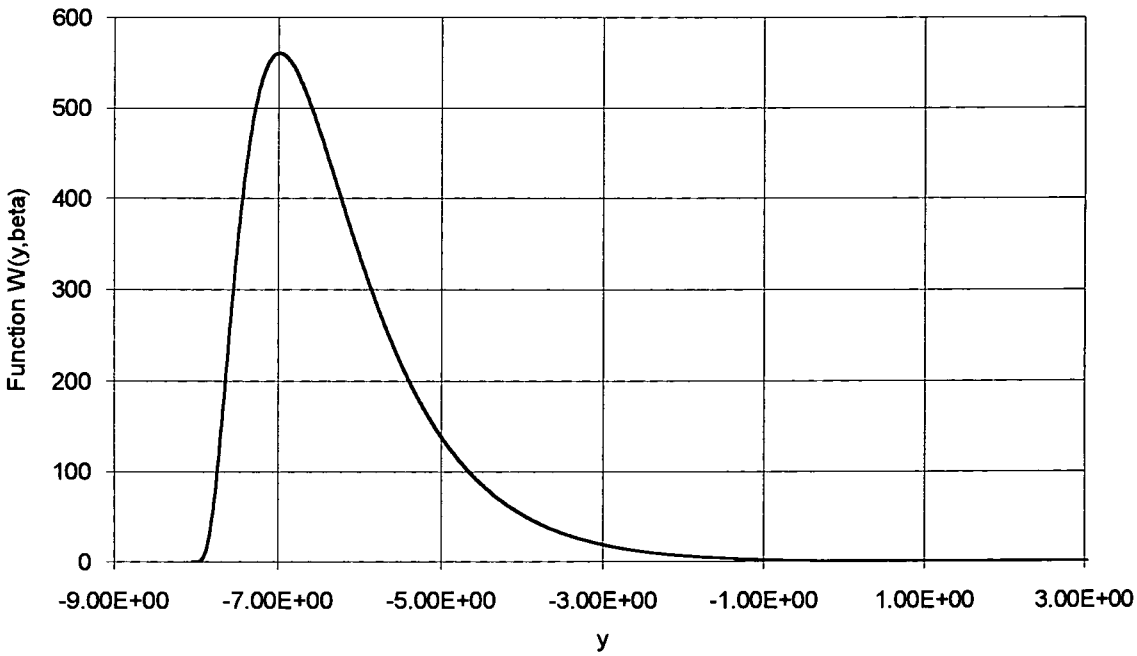

Figure 4.15: Evaluation of the function W(u,beta) using the trapezoidal rule

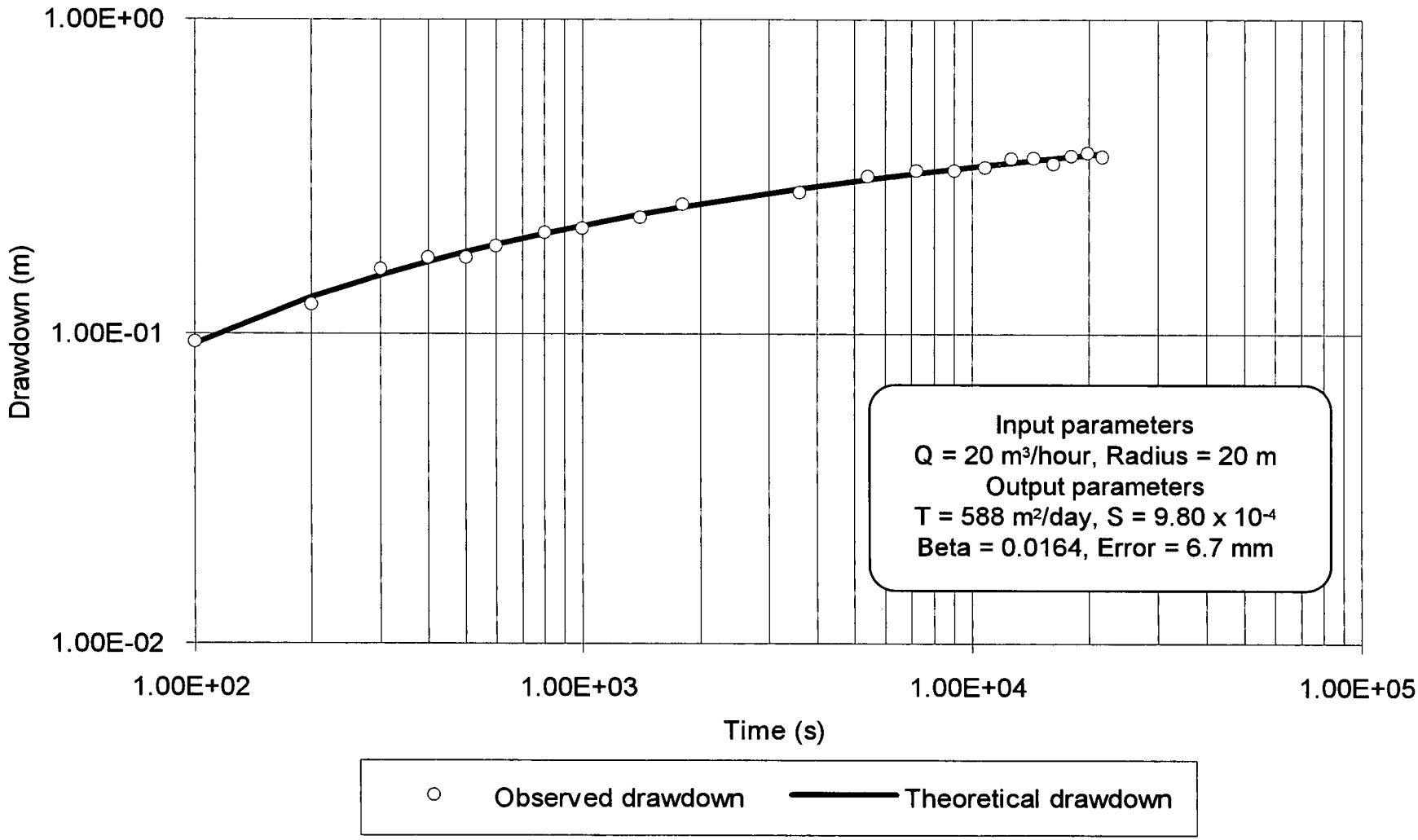

Figure 4.16: Results of a hypothetical pumping test using the HANPUTS programme

Chapter 5

Hermitian interpolation

5.1. Introduction

The previous chapter described the algorithms that were developed to analyse pumping test data by calculating parameters that give a best fit between the observed and theoretical values of drawdown. The computer programmes that calculate leaky parameters, WALPUTS and HANPUTS, are slow due to the numerous calculations that are performed to evaluate the well functions. To increase the speed of these programmes, Hermitian interpolation is incorporated with the least squares algorithms to estimate the well function. The technique uses a grid of previously calculated values, from which it interpolates to estimate the required values at any point.

Once this technique was incorporated as part of the WALPUTS and HANPUTS programmes, the time taken to run the least squares algorithm was much reduced. The Walton least squares programme including Hermitian interpolation was 16 times faster than the analytical solution. The example used to demonstrate the Hantush solution was 74 times faster. In both cases there was a small loss in accuracy, but this may be considered as negligible.

5.2. Background

The Theis well function may be represented by a single line, on a graph of $1/u$ vs. $W(u)$, as shown in Figure 5.1. The type curves of the Walton and Hantush well functions are similar, but consist of a series of curves, as shown in Figures 5.2 and 5.3 respectively. These leaky well functions may also be represented by a contour plot. Figure 5.4 shows the Walton well function, plotted against ln (u) and ln (r/L). Similarly, the Hantush well function is shown in Figure 5.5, plotted against ln (u) and ln (β). These contour plots represent the data used by

the Hermitian interpolation algorithm. The value of the well function is stored at a series of points, in the form of a grid. The algorithm calculates the well function at any point by interpolating between these grid points.

This may be further expanded by plotting the well functions as a three dimensional surface, with *1/u* and *r/L* or β on the *x* and *y* axes. The magnitude of the well function at any point is then represented by the elevation of this surface. Each of the type curves from Figures 5.2 or 5.3 thus represents a cross-section through the three dimensional surface at a constant value of *r/L* or β. Three dimensional surface plots of the Walton well function, W(u,r/L), and the Hantush well function, W(u,β), are shown in Figures 5.6 and 5.7 respectively.

Examining Figure 5.6, the Walton well function, it can be seen that the value of *W(u,r/L)* is constant for certain combinations of *u* and *r/L*. This represents the point where all discharge from the pumped well is from leakage through the aquitard, so no more drawdown takes place. As the value of *r/L* reduces, the point at which the leakage term dominates occurs at smaller and smaller values of *u*, which corresponds to later time. The point where *r/L* is smallest represents no leakage, where the system is analogous to Theis and the drawdown will never reach a steady state value.

Figure 5.7 shows the three dimensional surface plot of the Hantush well function. This function takes the storage of the aquitard into account, an important factor. It is more complex than the Walton case, as β is calculated from the transmissivity and storativity of the aquifer, and the vertical permeability and storativity of the aquitard. Neuman and Witherspoon (1969b) discussed the assumptions on which the two methods are based and concluded that for early time the Walton method would be inaccurate. The slight discontinuities that may be seen on both graphs are caused by the calculation of the function at values of *r/L* and β, not the logarithms of these values.

If a section of the grid is examined more closely, as shown in Figure 5.8, the well function is plotted from a series of grid points where the magnitude of this function is known. If the value of the function was required at a point within the grid, it could be calculated by interpolating between the four grid points that surround it. These four nodes are considered as the four nodes of a rectangular Hermitian element. In a similar way, the derivative of the well function is calculated by considering the slope of the well function at the four nodes.

The type of element used for Hermitian interpolation is important. A C_0 element is linear, so the function is continuous but the first derivative is not. The second type is a C_1 element. This element is continuous across both the function and the first derivative. As the first derivative of the function is required by the least squares algorithm, a C_1 element will be used. The second derivative is required as part of this technique to establish the continuity of the first derivative. The third type, a C_2 element, is continuous across the function, first and second derivatives.

To increase the speed of the least squares algorithms, the well function and first derivatives must be calculated using Hermitian interpolation. Thus if the well function W is a function of two variables, x and y, the Hermitian interpolation algorithm must calculate the values of $W(x,y)$, $\partial W(x,y)/\partial x$ and $\partial W(x,y)/\partial y$. Hermitian interpolation using C_1 elements is thus most appropriate. At each of the grid nodes, the values of $W(x,y)$, $\partial W(x,y)/\partial x$, $\partial W(x,y)/\partial y$ and $\partial^2 W(x,y)/\partial x \partial y$ will be stored. All these nodal values must be determined before the Hermitian interpolation algorithm may be used.

5.3. Theory of Hermitian interpolation

The theory of Hermitian interpolation will first be considered for a one dimensional C_1 element. This will then be expanded to consider the case of a rectangular (two dimensional) C_1 element.

5.3.1. One Dimensional elements

The Hermitian interpolation technique uses the function and its derivatives as nodal freedoms. Hence Hermitian interpolation functions are such that their derivatives are equal to zero at one end of the region of interpolation, and one at the other. Figure 5.9 shows the nodal freedoms of a one dimensional Hermitian element.

The polynomial equation can be described by using a dimensionless co-ordinate system to simplify the calculations. Thus the interpolation is carried out over the element from $\xi = -1$ to $\xi = +1$. Thus if the element is of length $2a$, the value of ξ at any point x may be determined from:

$$\xi = \frac{x - x_c}{a}$$ where x_c is the co-ordinate at the centre of the element.

If we required the value of the function, $W(x,y)$, at a point ξ, the interpolation polynomial or displacement function is written:

$$\begin{aligned} W &= \alpha_1 + \alpha_2\xi + \alpha_3\xi^2 + \alpha_4\xi^3 \\ &= \{M\}^T\{\alpha\} \end{aligned} \tag{5.1}$$

and

$$\begin{aligned} \phi &= \frac{dw}{d\xi} \\ &= \alpha_2 + 2\alpha_3\xi + 3\alpha_4\xi^2 \end{aligned} \tag{5.2}$$

Substituting the nodal values W_1, ϕ_1, W_2, ϕ_2, on the left hand side of equations 5.1 and 5.2, and the appropriate nodal co-ordinates on the right hand side of the equation, gives four simultaneous equations:

$$\begin{aligned} W_1 &= \alpha_1 - \alpha_2 + \alpha_3 - \alpha_4 \\ \phi_1 &= \alpha_2 - 2\alpha_3 + 3\alpha_4 \\ W_2 &= \alpha_1 + \alpha_2 + \alpha_3 + \alpha_4 \\ \phi_2 &= \alpha_2 + 2\alpha_3 + 3\alpha_4 \end{aligned}$$

These equations may be written in matrix form to give

$$\{d\}=\begin{bmatrix} W_1 \\ \phi_1 \\ W_2 \\ \phi_2 \end{bmatrix}=\begin{bmatrix} 1 & -1 & 1 & -1 \\ 0 & 1 & -2 & 3 \\ 1 & 1 & 1 & 1 \\ 0 & 1 & 2 & 3 \end{bmatrix}\begin{bmatrix} \alpha_1 \\ \alpha_2 \\ \alpha_3 \\ \alpha_4 \end{bmatrix}=A^{-1}\{\alpha\} \tag{5.3}$$

We also know that:

$$W=\{f\}^T\{d\} \tag{5.4}$$

where $\{f\}$ is the shape function. This shape function may be determined from:

$$\begin{aligned}\{f\}^T &= \{M\}^T A \\ &= \begin{bmatrix} 1 \\ \xi \\ \xi^2 \\ \xi^3 \end{bmatrix}^T \cdot \frac{1}{4}\begin{bmatrix} 2 & 1 & 2 & -1 \\ -3 & -1 & 3 & -1 \\ 0 & -1 & 0 & 1 \\ 1 & 1 & -1 & 1 \end{bmatrix}\end{aligned} \tag{5.5}$$

Combining equations 5.4 and 5.5, the value of W at any point ξ may be determined from:

$$W=f_1W_1+f_2\left(\frac{dW}{d\xi}\right)_1+f_3W_2+f_4\left(\frac{dW}{d\xi}\right)_2 \tag{5.6}$$

where

$$f_1=\frac{1}{4}(2-3\xi+\xi^3)$$
$$f_2=\frac{1}{4}(1-\xi-\xi^2+\xi^3)$$
$$f_3=\frac{1}{4}(2+3\xi-\xi^3)$$
$$f_4=\frac{1}{4}(-1-\xi+\xi^2+\xi^3)$$

5.3.2. Two dimensional elements

The theory of two dimensional elements is developed in a similar manner. Each element will have 16 degrees of freedom and 4 nodes, as shown in Figure 5.10. The interpolation is effectively a combination of two one dimensional elements, the first in the x and the second in the y direction.

The shape function f is defined in the x direction, with dimensionless co-ordinate ξ, whilst shape function g is defined in the y direction, with dimensionless co-ordinate η. The

element is of length $2a$ in the x direction, and $2b$ in the y direction. The value of the shape function at any point may be defined from equation 5.5 as:

$$\begin{bmatrix} f_1 \\ f_2 \\ f_3 \\ f_4 \end{bmatrix} = \begin{bmatrix} 1 \\ \xi \\ \xi^2 \\ \xi^3 \end{bmatrix}^T \cdot \frac{1}{4} \begin{bmatrix} 2 & 1 & 2 & -1 \\ -3 & -1 & 3 & -1 \\ 0 & -1 & 0 & 1 \\ 1 & 1 & -1 & 1 \end{bmatrix} \tag{5.7}$$

and

$$\begin{bmatrix} g_1 \\ g_2 \\ g_3 \\ g_4 \end{bmatrix} = \begin{bmatrix} 1 \\ \eta \\ \eta^2 \\ \eta^3 \end{bmatrix}^T \cdot \frac{1}{4} \begin{bmatrix} 2 & 1 & 2 & -1 \\ -3 & -1 & 3 & -1 \\ 0 & -1 & 0 & 1 \\ 1 & 1 & -1 & 1 \end{bmatrix} \tag{5.8}$$

These two shape functions may then be combined to give **N**, the two dimensional shape function. The value of W may then be calculated from

$$\begin{aligned} W(x,y) &= \mathbf{Nd} \\ &= [\mathbf{N}_1, \ \mathbf{N}_2, \ \mathbf{N}_3, \ \mathbf{N}_4] \begin{bmatrix} \mathbf{d}_1 \\ \mathbf{d}_2 \\ \mathbf{d}_3 \\ \mathbf{d}_4 \end{bmatrix} \end{aligned} \tag{5.9}$$

where

$$\mathbf{d}_i = \left[w_i, \ \left(\frac{\partial w}{\partial x}\right)_i, \ \left(\frac{\partial w}{\partial y}\right)_i, \ \left(\frac{\partial^2 w}{\partial x \partial y}\right)_i \right]$$

The value of **N** may be established by combining the shape functions for each side:

$$\begin{aligned} \mathbf{N}_1 &= [f_1 g_1, \ f_2 g_1, \ f_1 g_2, \ f_2 g_2] \\ \mathbf{N}_2 &= [f_3 g_1, \ f_4 g_1, \ f_3 g_2, \ f_4 g_2] \\ \mathbf{N}_3 &= [f_3 g_3, \ f_4 g_3, \ f_3 g_4, \ f_4 g_4] \\ \mathbf{N}_4 &= [f_1 g_3, \ f_2 g_3, \ f_1 g_4, \ f_2 g_4] \end{aligned} \tag{5.10}$$

The first derivatives may also be calculated by differentiating the shape functions and using these values in equation 5.9. Thus when differentiating with respect to ξ equation 5.7 becomes:

$$\begin{bmatrix} f_1 \\ f_2 \\ f_3 \\ f_4 \end{bmatrix} = \begin{bmatrix} 0 \\ 1 \\ 2\xi \\ 3\xi^2 \end{bmatrix}^T \cdot \frac{1}{4} \begin{bmatrix} 2 & 1 & 2 & -1 \\ -3 & -1 & 3 & -1 \\ 0 & -1 & 0 & 1 \\ 1 & 1 & -1 & 1 \end{bmatrix} \tag{5.11}$$

and similarly when differentiating with respect to η equation 5.8 becomes:

$$\begin{bmatrix} g_1 \\ g_2 \\ g_3 \\ g_4 \end{bmatrix} = \begin{bmatrix} 0 \\ 1 \\ 2\eta \\ 3\eta^2 \end{bmatrix}^T \cdot \frac{1}{4} \begin{bmatrix} 2 & 1 & 2 & -1 \\ -3 & -1 & 3 & -1 \\ 0 & -1 & 0 & 1 \\ 1 & 1 & -1 & 1 \end{bmatrix} \tag{5.12}$$

The values of $\partial W(\xi,\eta)/\partial\xi$ and $\partial W(\xi,\eta)/\partial\eta$ are then evaluated using equation 5.9, after the new values of the two dimensional shape function have been calculated using equation 5.10. The required values of $\partial W(x,y)/\partial x$ and $\partial W(x,y)/\partial y$ may then be calculated from:

$$\frac{\partial W(x,y)}{\partial x} = \frac{\partial W(\xi,\eta)}{\partial \xi} \Big/ a \tag{5.13}$$

and

$$\frac{\partial W(x,y)}{\partial y} = \frac{\partial W(\xi,\eta)}{\partial \eta} \Big/ b \tag{5.14}$$

5.4. The Hermitian interpolation algorithms

5.4.1. Programmes to calculate the well functions - WALTHERM and HANTHERM

Two programmes were written to evaluate the well function and its' first derivatives, one for the Walton and the second the Hantush case. These are identical, except they use different input data to establish the well function details at each of the nodal points.

The range of values of u and r/L or β over which the programmes would interpolate, must be ascertained. The objective of using Hermitian interpolation is to increase the speed at which the least squares algorithms operate. Thus the interpolation function should be available

over a wide range of values. Also, Hermitian interpolation should retain the same accuracy in calculating the well functions that was achieved by the trapezoidal rule. This would indicate a small grid spacing. However, a huge number of data points would slow the algorithm, and so render the inclusion of the interpolation technique pointless.

Using the same technique as in the least squares programmes, the functions were calculated at different values of v, where $v = ln(u)$. The Walton well function was evaluated over the range:

$$-13.8 < v < 1.0$$

which relates to values of u between 1.0×10^{-6} and 2.7. The Hantush well function was evaluated over a similar range, of:

$$-13.9 < v < 2.0$$

which relates to a value of u between 9.2×10^{-7} and 7.3.

If the Walton well function is examined, if $r/L < 1.0 \times 10^{-3}$ the function tends to Theis, so this was chosen as the lower limit of r/L. The upper limit was chosen as 9.0, as values greater than this would be likely to lead to a high leakage factor, i.e. where the vertical permeability of the aquitard is high. This would contradict the assumptions on which the analysis is based. In a similar way, the Hantush variables were calculated for values in the range $1.0 \times 10^{-3} < \beta < 9.0$.

The grid spacing was chosen so that accuracy would be maintained, but without the use of a large number of points. In the 'v' direction, the spacing was chosen as 0.1 units. As this is a logarithmic scale, the grid spacing is thus closer together where u is small, which coincides with where the gradient of the well functions are greatest. In the second direction (r/L or β), the upper and lower values of the grid are 1.0×10^{-3} and 9.0. The grid was chosen at 1.0×10^{-3}, 2.0×10^{-3}, etc., to 9.0×10^{-9}. This pattern was then repeated for one multiple of ten greater, and so on, up to the value of 9. This grid spacing over a portion of the datafile is illustrated in Figure 5.11.

A computer programme was written to generate the values of the well functions and their derivatives at each of the nodal points using the methods devised in the last chapter. This consisted of calculating the well function using the trapezoidal rule, and the first derivatives from the slope of the function in each respective direction. The second derivatives were then evaluated from the gradient of the first derivatives. Considering the Walton function, the following variables were calculated and stored in datafiles:-

$$W\left(v,r/L\right),\ \frac{\partial W\left(v,r/L\right)}{\partial v},\ \frac{\partial W\left(v,r/L\right)}{\partial\left(r/L\right)},\ \frac{\partial^2 W\left(v,r/L\right)}{\partial v\partial\left(r/L\right)} \text{ and } \frac{\partial^2 W\left(v,r/L\right)}{\partial\left(r/L\right)\partial v}$$

Similarly, for the Hantush function:

$$W(v,\beta),\ \frac{\partial W(v,\beta)}{\partial v},\ \frac{\partial W(v,\beta)}{\partial \beta},\ \frac{\partial^2 W(v,\beta)}{\partial v\partial\beta} \text{ and } \frac{\partial^2 W(v,\beta)}{\partial\beta\partial v}$$

If the second derivatives, for example $\partial^2 W(u,\beta)/\partial u\partial\beta$ and $\partial^2 W(u,\beta)/\partial\beta\partial u$, are considered, the values should be identical. Examining the results of the calculations above this was seen to be true, thus validating the differentiation procedure. This was the case for both the Walton and Hantush data.

Two programmes were written using the Hermitian interpolation theory to evaluate the well function and first derivatives at any point within the previously specified grid. Given a point with *x* and *y* co-ordinates, *u* and *r/L* or β, the programmes use the previously calculated nodal data from the datafiles to determine the variables at this required point.

A number of different functions are used within this operation. First the previously calculated nodal data is read from the datafiles and stored in arrays. In this way all of the data may be accessed quickly. The next stage evaluates the four grid points that form the nodes of the rectangular element that surrounds the data point. The data from these nodes are then retrieved, and the variables at the required point calculated using the Hermitian

interpolation algorithm. Flowcharts describing this procedure are shown in Figures 5.12 and 5.13. The code and documentation for the programme interpolating to find data for the Walton case, WALTHERM, are included on the floppy disc in Appendix D17. The algorithm is identical for the Hantush case, except for the use of different nodal data.

5.4.2. Testing the Hermitian interpolation algorithms

The accuracy of the Hermitian interpolation algorithm was tested by calculating a range of values of both the Hantush and Walton well functions, and their first derivatives, using the subroutines that were written as part of the WALPUTS and HANPUTS programmes. These values were then compared against those calculated using the Hermitian interpolation algorithms, using the programmes WALTHERM and HANTHERM. The results of these tests are presented in Appendices E1 and E2 respectively.

These tables show that the Hermitian algorithm calculates the required parameters accurately. Any inaccuracies that occur are very small. These errors may have a slight influence on the aquifer parameters that the programmes converge to. However, it is unlikely that these errors would be substantial, and this inaccuracy is offset by the increase in speed of the least squares programmes. The impact of the introduction of these inaccuracies is considered later.

5.5. Combining Hermitian interpolation with the least squares algorithms

The Hermitian interpolation algorithm was then included in both least squares programmes, WALPUTS and HANPUTS. The result of this is the speeds of these programmes are greatly increased, with minimal loss in accuracy. Both programmes are run in a similar manner to the WALPUTS and HANPUTS programmes. The input files are identical, except they should be renamed WALTIN2.DAT and HANTIN2.DAT. The results are presented in WALTOUT2.DAT and HANTOUT2.DAT. The individual programmes are discussed below.

5.5.1. The Walton programme - WALPUTS2

The Hermitian interpolation algorithm, WALTHERM, is combined with the least squares programme, WALPUTS, to produce a new programme, WALPUTS2. This calculates the variables $W(u,r/L)$, $\partial W(u,r/L))/\partial u$ and $\partial W(u,r/L))/\partial(r/L)$ using Hermitian interpolation over the range:

$-13.8 < v < 1.0$ and $1.0 \times 10^{-3} < r/L < 9.0$

where $v = ln(u)$. Figure 5.14 shows graphically the different methods used to evaluate the well function. If the value of $r/L < 1.0 \times 10^{-3}$ then the value of the well function is calculated from the Theis solution. Variables outside the Hermitian interpolation range are calculated analytically using the trapezoidal rule. A listing of WALPUTS2 is included on the floppy disc (Appendix D17).

The accuracy of this programme may be shown by comparing the results of the two Walton least squares programmes, using the input data from the hypothetical pumping test presented in Appendix D8. The same initial values of parameters were used as those used to test the WALPUTS programme. The results from running the two programmes are summarised in table 5.1 below.

Parameter	WALPUTS - (normal)	WALPUTS2 - (Interpolation)
No. of iterations	10	10
Transmissivity (m^2/day)	472.96	472.97
Storativity	1.092×10^{-3}	1.092×10^{-3}
Leakage factor (m)	214.03	214.03
Average error (m)	9.59×10^{-3}	9.59×10^{-3}
Time taken (s)	80	5

Table 5.1: Comparison of the results from the analytical and Hermitian interpolation least squares programmes

Table 5.1 shows that the small errors introduced by Hermitian interpolation are negligible when incorporated as part of the least squares programme. The time taken is reduced by a factor of sixteen, from 80 to 5 seconds over 10 iterations. The purpose of the inclusion of the Hermitian interpolation algorithm is achieved. The time taken for the algorithm to converge has been reduced, with minimal loss of accuracy.

A number of other tests were also completed, to observe the convergence properties of the new algorithm and compare the increase in speed with data from previous tests. The results are shown in table 5.2 below.

T guess m^2/day	S guess	L guess	Converge (Y/N) ?	WALPUTS (normal)		WALPUTS2 - with interpolation	
				Iterations	Time(s)	Iterations	Time(s)
250	$1.0x10^{-2}$	100	Y	10	70	10	5
250	$1.0x10^{-4}$	800	Y	12	105	12	5
750	$1.0x10^{-4}$	800	Y	12	100	12	5
1000	$1.0x10^{-2}$	100	N	20	180	20	5

Table 5.2: Comparison of the convergence properties from the analytical and Hermitian interpolation least squares programmes

These tests show that the Hermitian interpolation algorithm does not affect the convergence of the least squares algorithm. The processing time of the Hermitian interpolation programme is not greatly affected by the number of iterations performed. The majority of the time is taken loading the datafiles into the computer memory, and the additional time taken to complete the algorithm is small compared to this.

5.5.2. The Hantush programme - HANPUTS2

The least squares algorithm HANPUTS was combined with the Hermitian interpolation algorithm to produce HANPUTS2, in the same manner as the Walton case. This programme uses Hermitian interpolation to calculate the values of $W(u,\beta)$, $\partial W(u,\beta)/\partial u$ and $\partial W(u,\beta)/\partial \beta$ over the range:

$-13.9 < v < 2.0$ and $1.0 \times 10^{-3} < \beta < 9.0$

where $v = \ln(u)$. If the variables are required to be calculated outside of the above range, then they are calculated using the trapezoidal rule. A listing of the HANPUTS2 programme is included on the floppy disc in Appendix D17.

The results from the analysis of the hypothetical pumping test were compared for both programmes, to compare the accuracy and speed. The results are shown in table 5.3 below.

Parameter	HANPUTS - (normal)	HANPUTS2 - (Interpolation)
No. of iterations	8	8
Transmissivity (m^2/day)	588.47	588.82
Storativity	9.804×10^{-4}	9.799×10^{-4}
Beta (m/s^2)	1.637×10^{-2}	1.629×10^{-2}
Average error (m)	6.69×10^{-3}	6.69×10^{-3}
Time taken (s)	370	5

Table 5.3: Comparison of the results from the analytical and Hermitian interpolation least squares programmes

From this table it can be seen that the inclusion of Hermitian interpolation does not affect the accuracy of the least squares programme. However, the time taken for the programme to run has been substantially reduced. Thus the inclusion of the Hermitian interpolation algorithm is successful. The convergence of the least square algorithm was tested and

compared against some of the data used for testing the HANPUTS programme. The results of these tests are summarised in table 5.4 below.

T guess m^2/day	S guess	Beta guess	Converge (Y/N) ?	HANPUTS (normal)		HANPUTS2 - with interpolation	
				Iterations	Time(s)	Iterations	Time(s)
50	$5.0x10^{-4}$	$1.0x10^{-1}$	Y	10	540	13	5
250	$5.0x10^{-3}$	$2.0x10^{-3}$	Y	19	960	20	5
750	$5.0x10^{-4}$	$2.0x10^{-2}$	Y	6	350	6	5
1000	$5.0x10^{-3}$	$2.0x10^{-2}$	Y	9	480	10	5

Table 5.4: Comparison of the convergence properties from the analytical and Hermitian interpolation least squares programmes

These results show that the inclusion of Hermitian interpolation in the least squares algorithm does not affect the convergence. The HANPUTS programme takes 540 seconds to converge for 10 iterations, which is reduced to 5 seconds by the HANPUTS2 programme. Thus the new programme is a much faster solution, with negligible loss of accuracy.

5.6. Conclusions

Two programmes have been developed using the Walton and Hantush leaky solutions which estimate the parameters which lead to the best fit between the observed and calculated values of drawdown. The programmes use the theory of least squares, and calculate the well functions and first order derivatives using the technique of Hermitian interpolation.

Some small errors are introduced when the well function and first derivatives are calculated by Hermitian interpolation. The errors calculated by comparing the analytical values of the well function and the first derivatives with those estimated by Hermitian interpolation were within 1%. The nature of the aquifers under investigation will be such that they are

heterogeneous, and so will not conform to the initial assumptions on which these methods of analysis are based. The results of the analysis of pumping tests should only be taken as a guide to the aquifer parameters, remembering that it is quite possible for them to change over very small distances, for example due to lenses of different material within the aquifer. Thus the inaccuracies introduced by Hermitian interpolation when compared to the variable nature of aquifer properties may be considered as negligible.

The new programmes, WALPUTS2 and HANPUTS2, were shown to converge to the same parameters as the initial programmes. They were also shown to converge from a variety of starting values. Hence the inclusion of Hermitian interpolation is successful. The least squares algorithms to calculate aquifer parameters work in a much reduced time with negligible loss of accuracy.

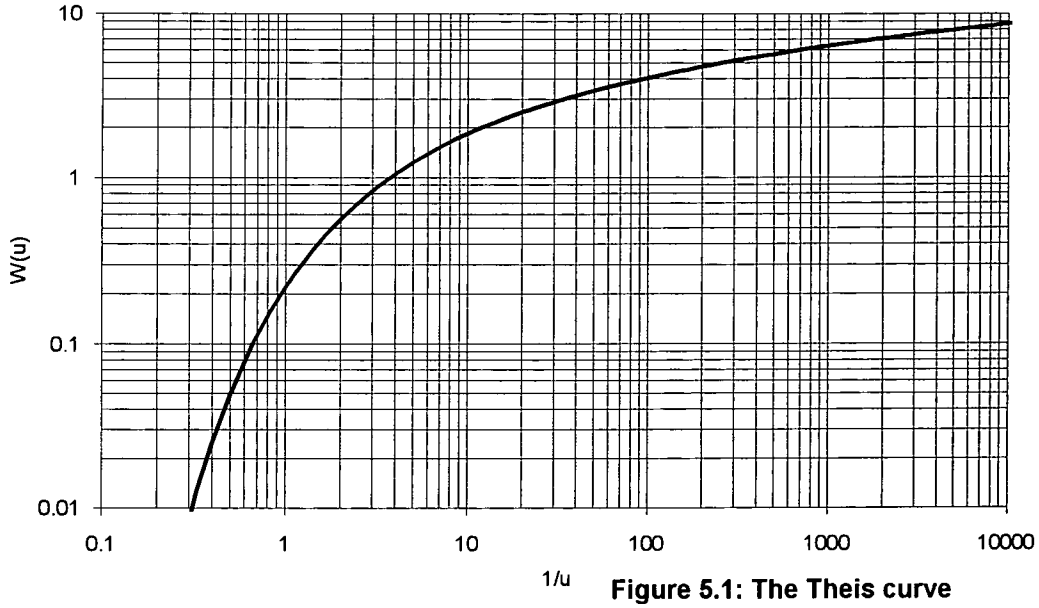

Figure 5.1: The Theis curve

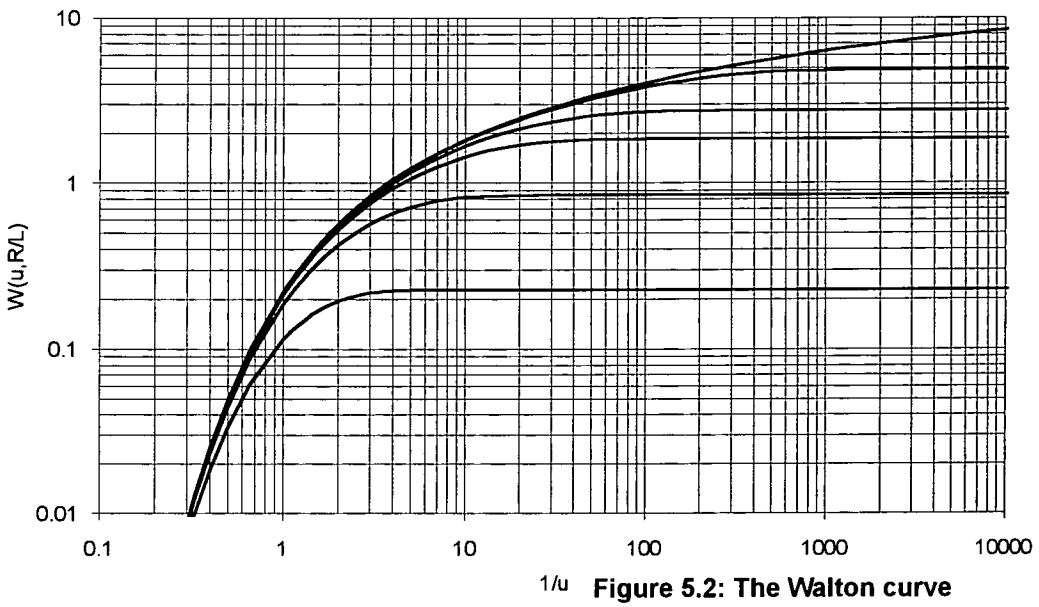

Figure 5.2: The Walton curve

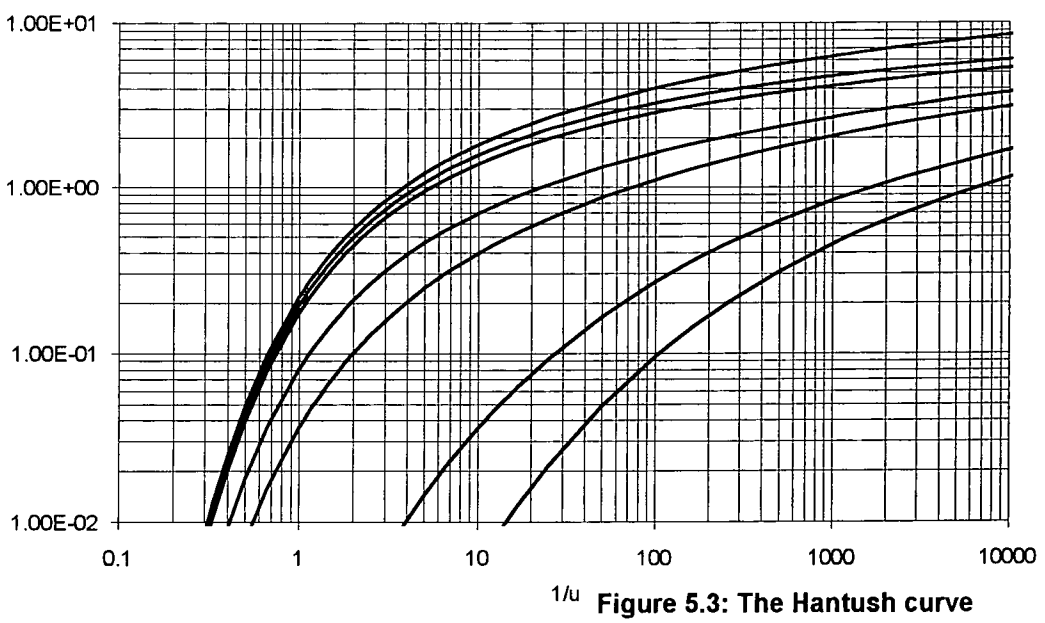

Figure 5.3: The Hantush curve

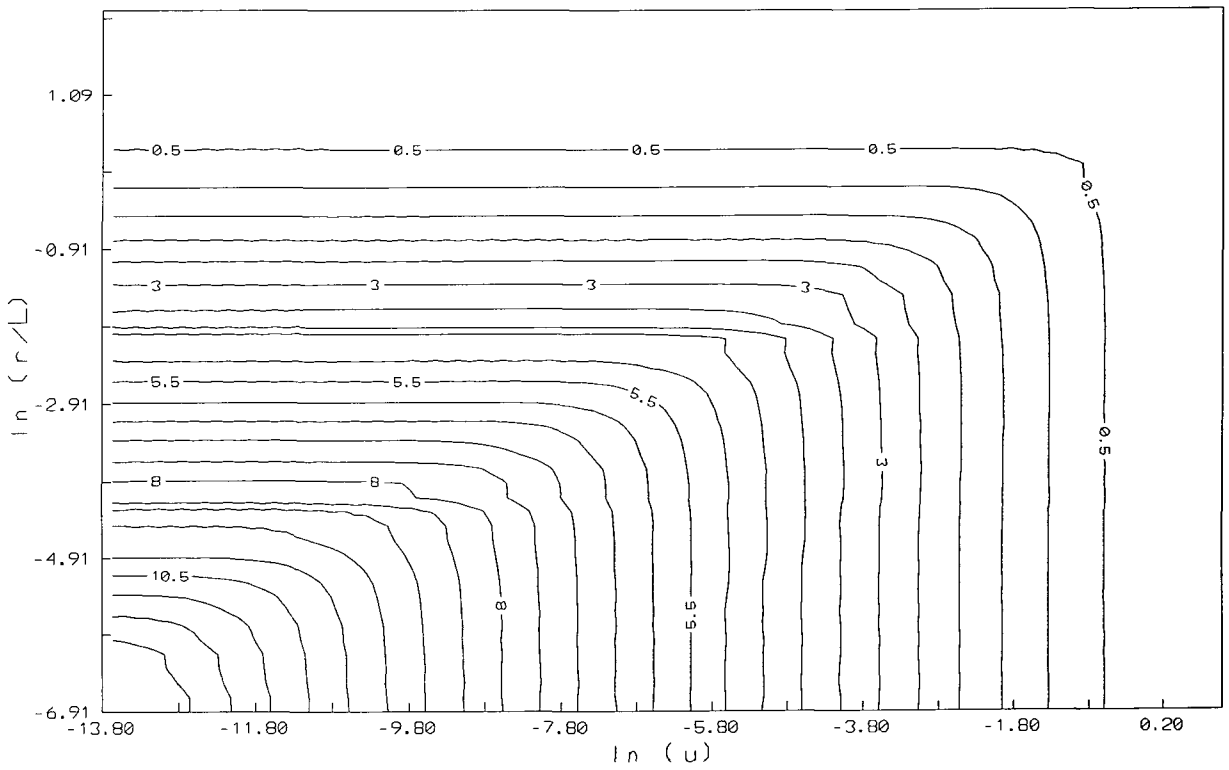

Figure 5.4: Contour plot of the Walton well function

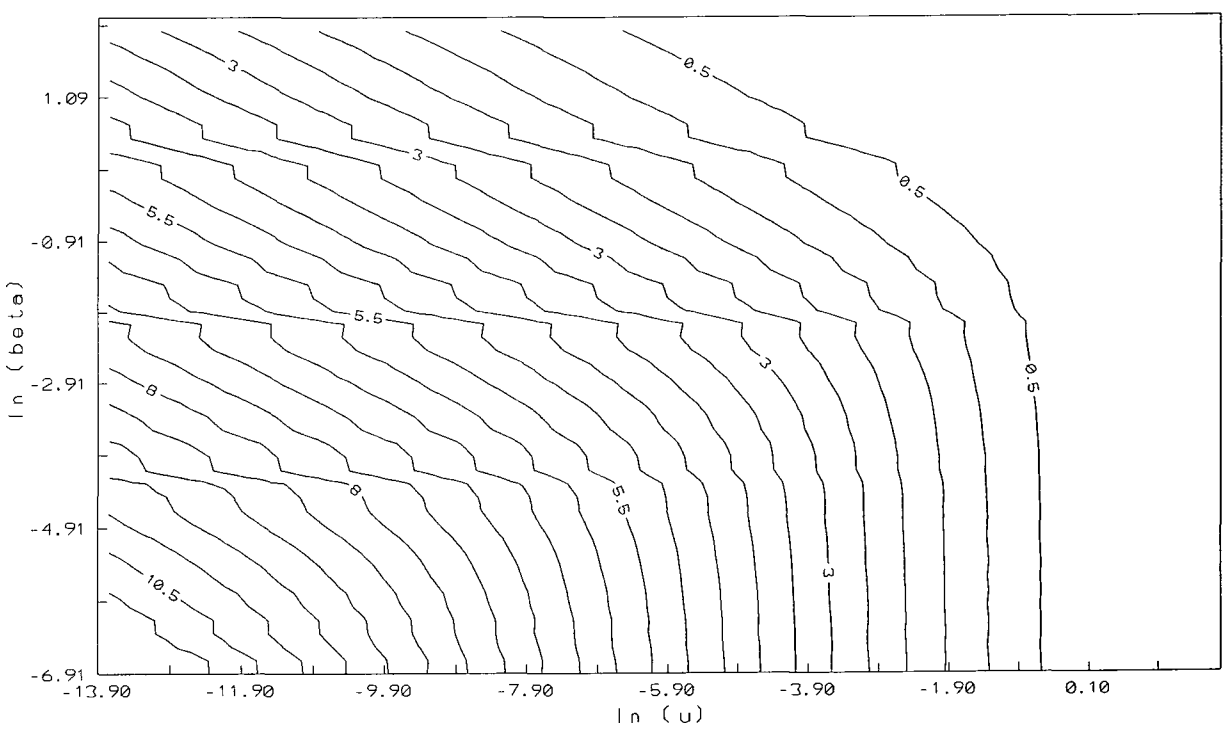

Figure 5.5: Contour plot of the Hantush well function

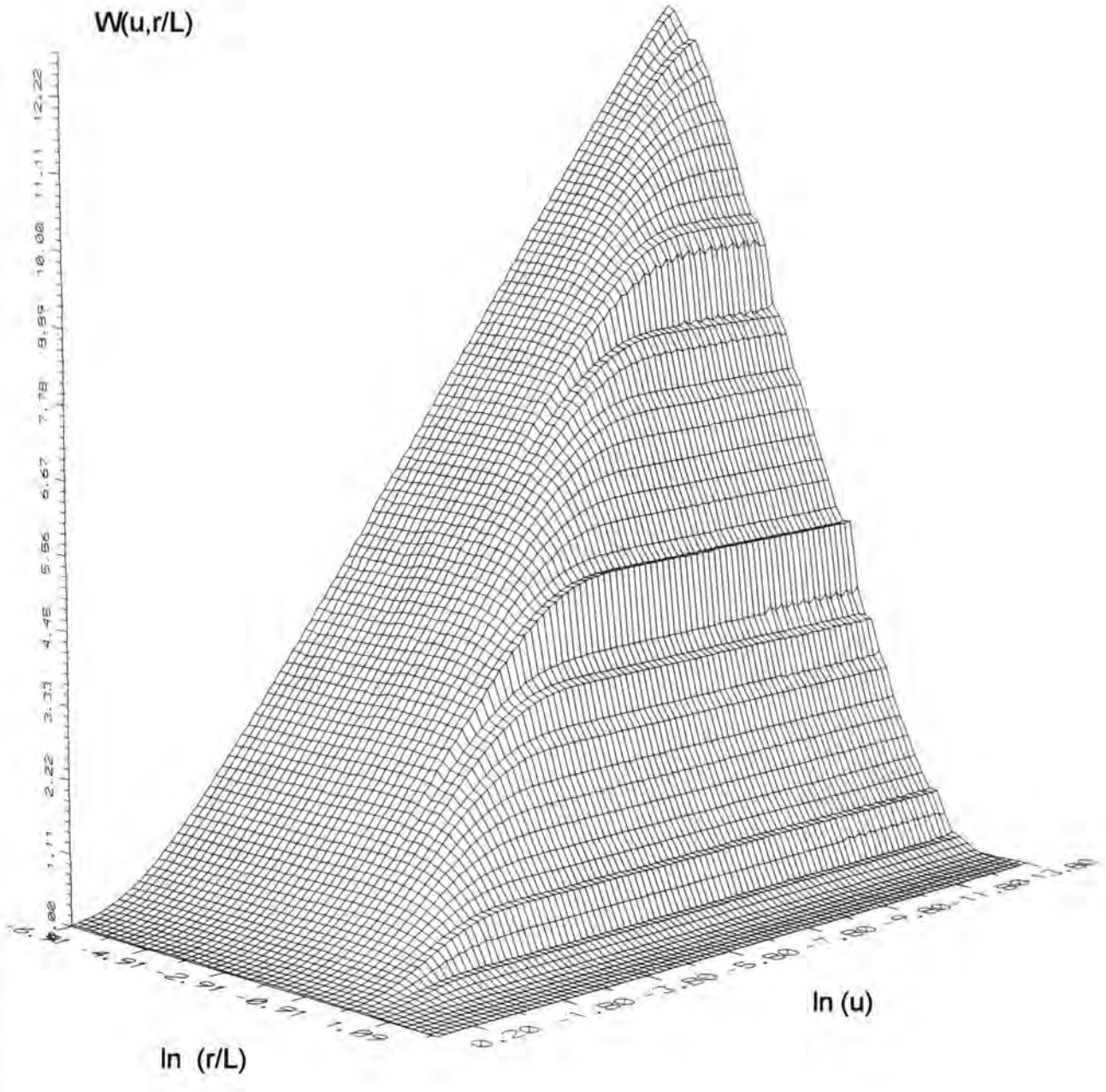

Figure 5.6:The Walton well function W(u,r/L)

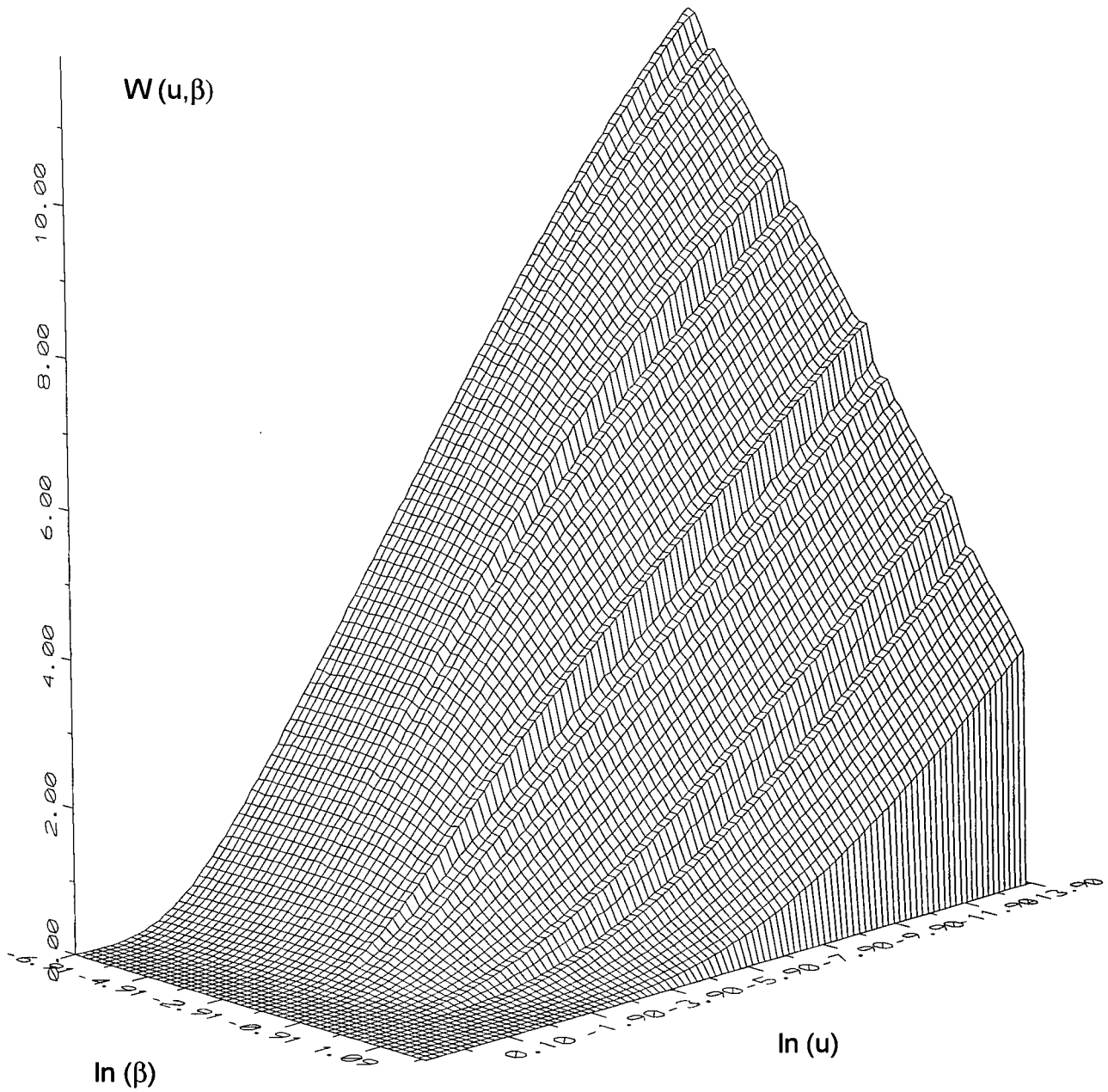

Figure 5.7: The Hantush well function W (u,β)

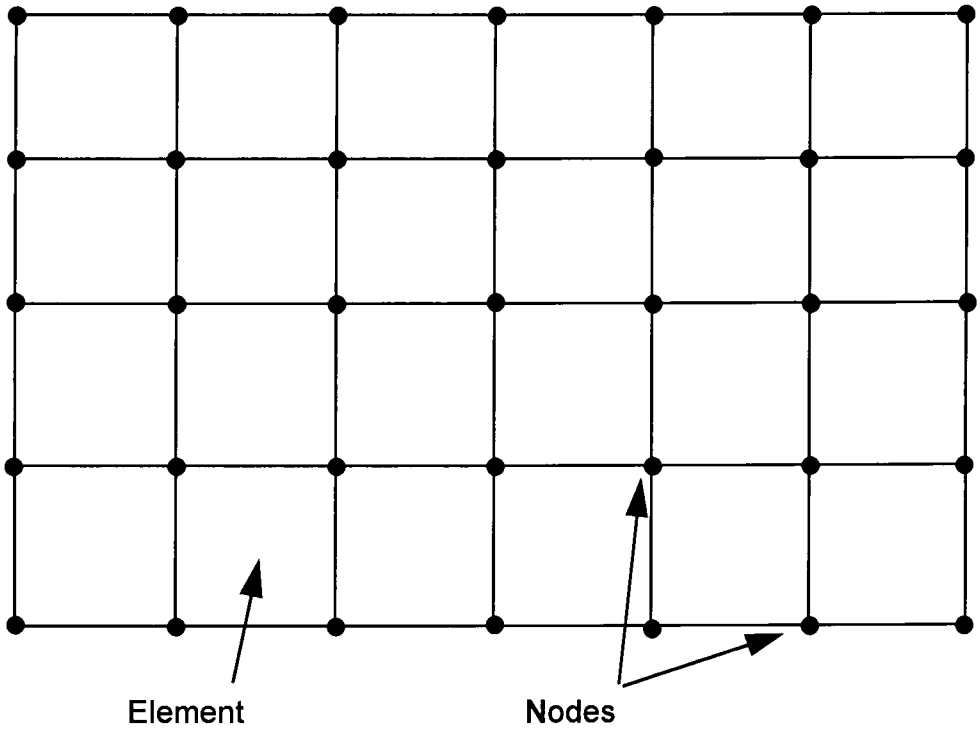

Figure 5.8: Grid of Hermitian elements

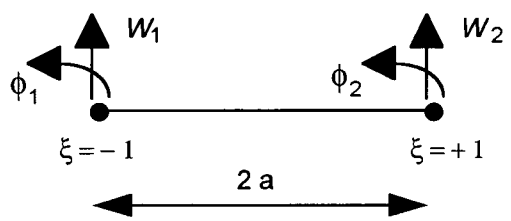

Figure 5.9: Nodal freedoms of a one dimensional Hermitian element

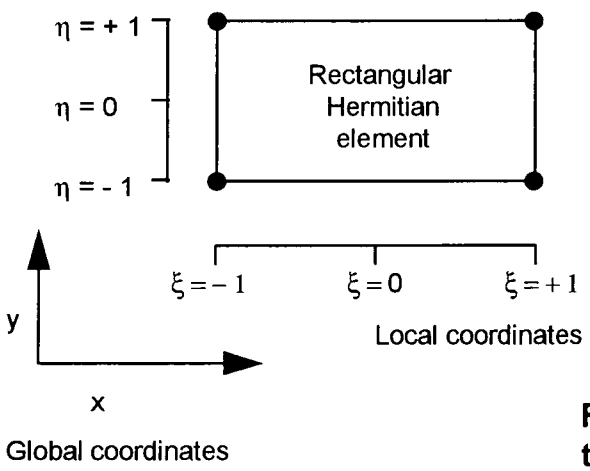

At each node there are 4 degrees of freedom:

1) W

2) $\frac{\partial W}{\partial x}$

3) $\frac{\partial W}{\partial y}$

4) $\frac{\partial^2 W}{\partial x \partial y}$

Figure 5.10: Nodal freedoms of a two dimensional Hermitian element

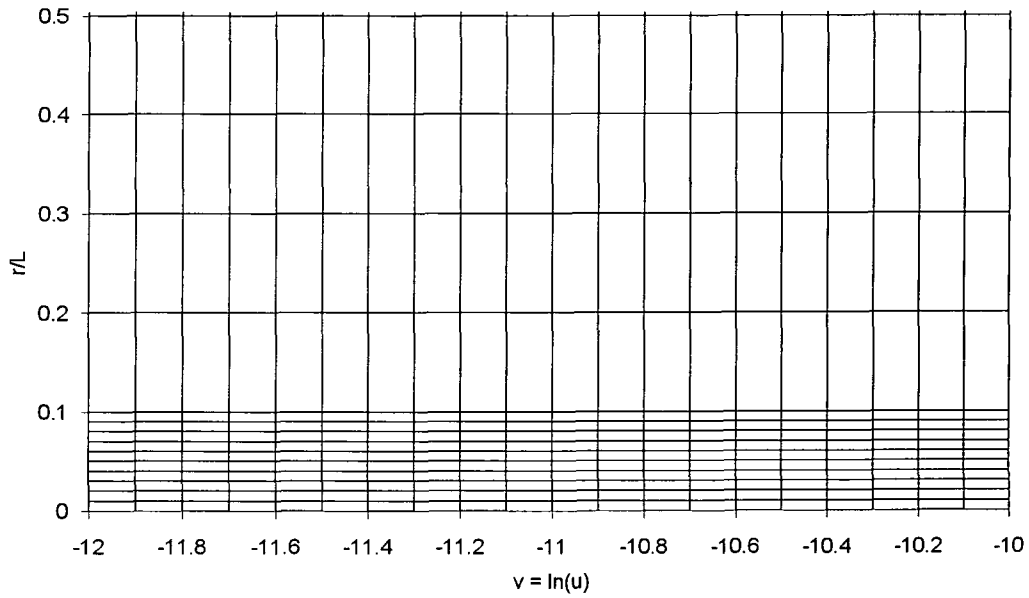

Figure 5.11: Illustration of the grid spacing for the Hermitian interpolation datafiles

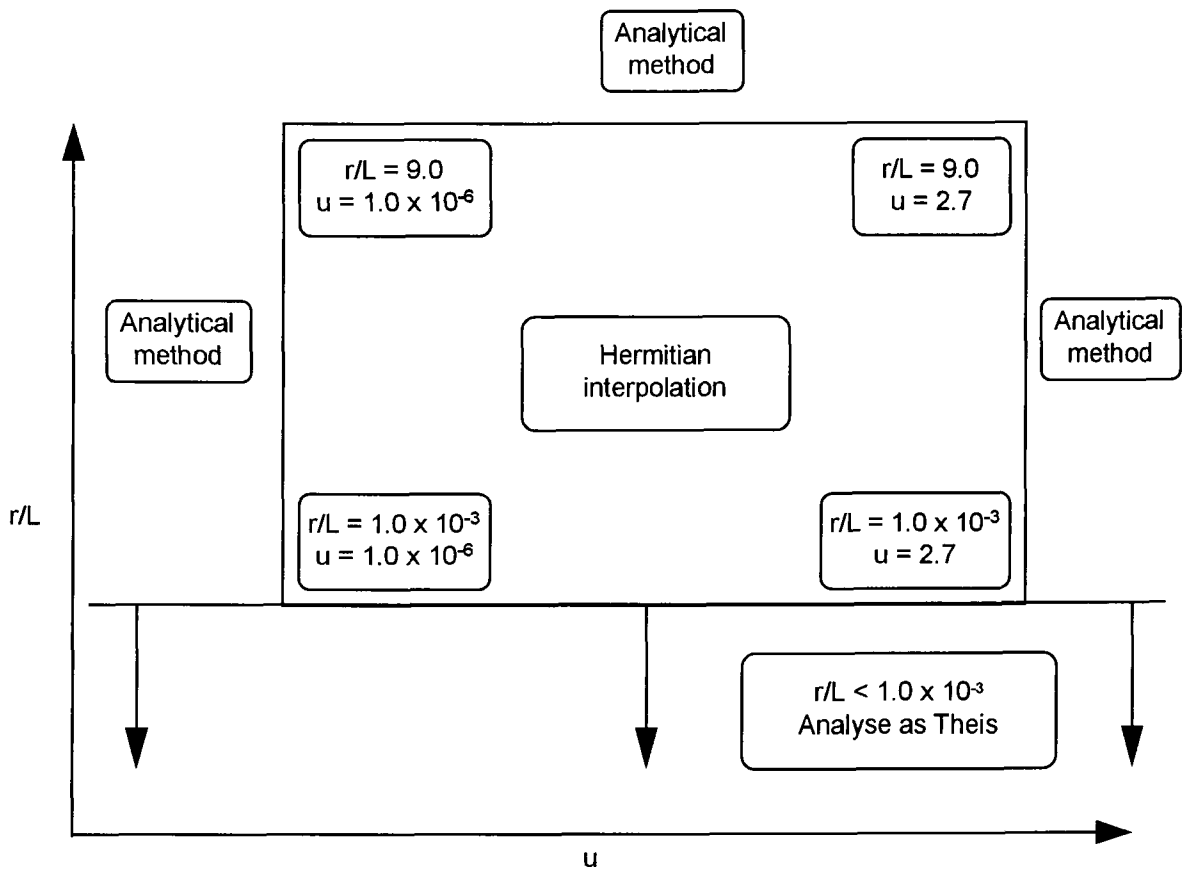

Figure 5.14: Illustration of the methods used to evaluate the well function

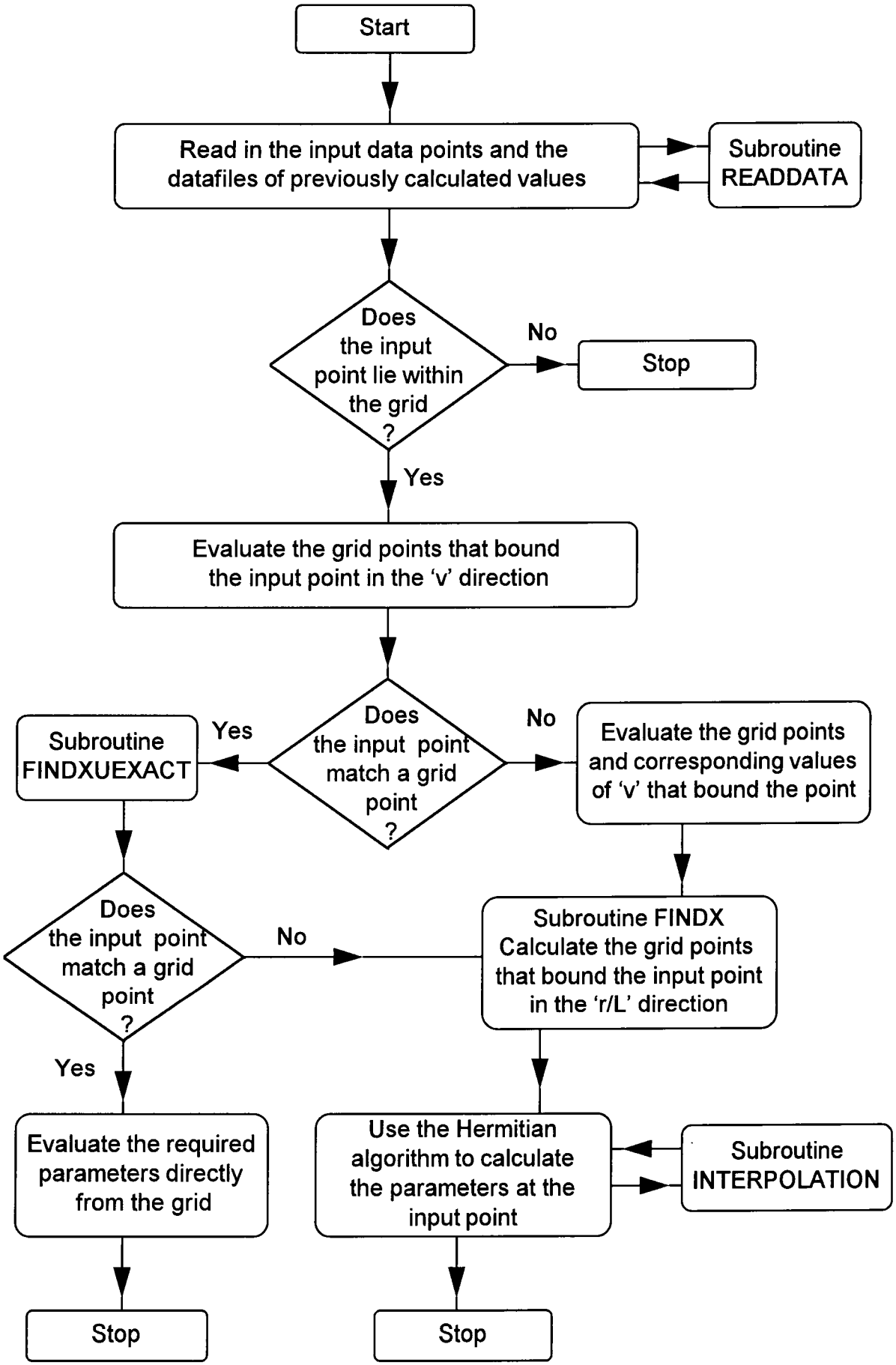

Figure 5.12: Flowchart showing the WALTHERM programme

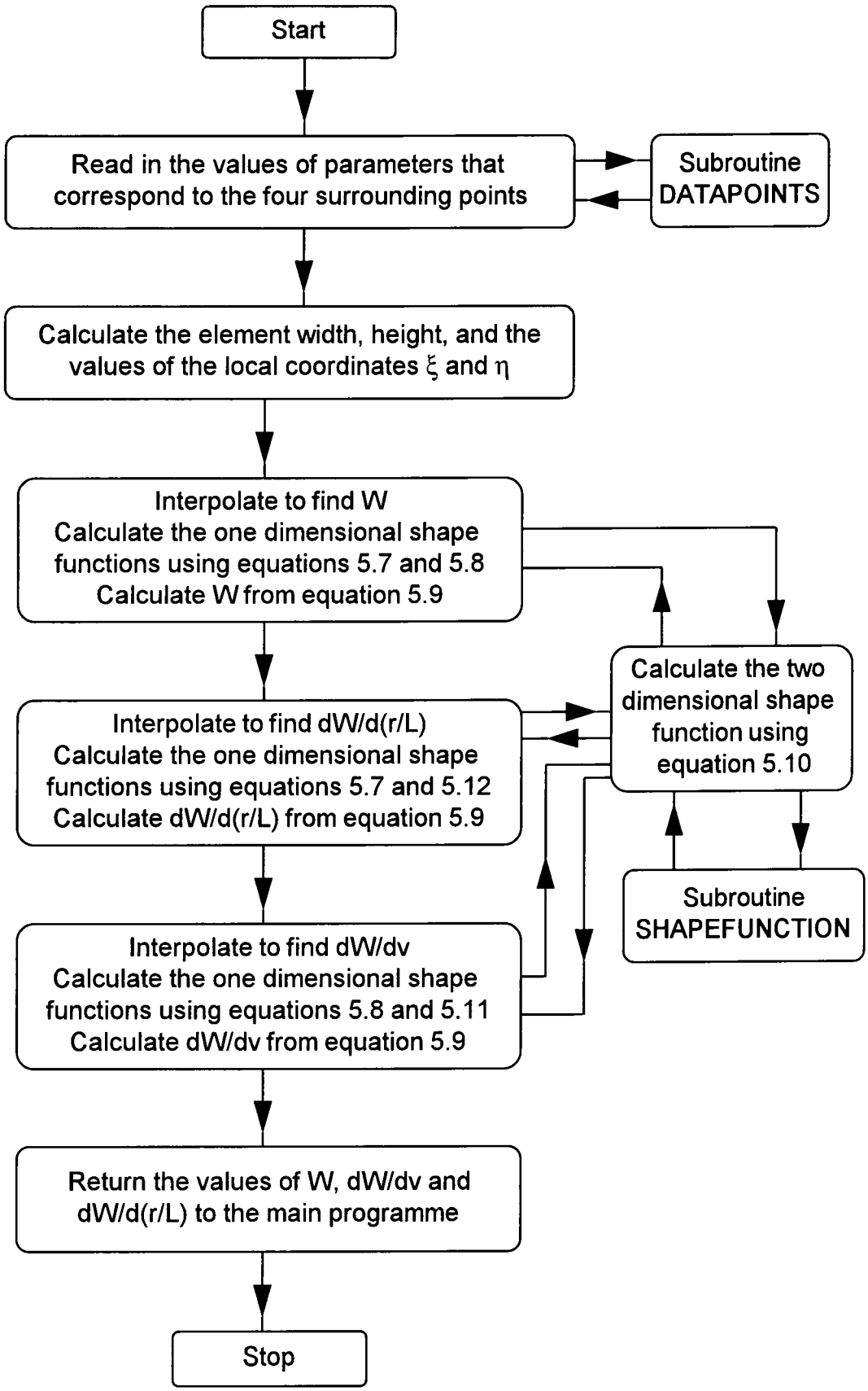

Figure 5.13: Flowchart showing subroutine INTERPOLATION

Chapter 6

Pump test analysis and results

6.1. Introduction

This chapter presents the results of the analysis of pumping test data using the three least squares algorithms that were developed. The main focus of the work is the analysis of the data from the fieldwork described in Chapter 3, but in addition three well documented pump tests from other literature are analysed. This demonstrates the range of the calculated parameters using a number of different methods of analysis. A three dimensional groundwater modelling package is used to validate the results obtained by these methods.

6.2. Parameter estimation using published pump test data

This section presents the results of different methods of analysis to determine aquifer parameters. Two well documented pump tests in confined aquifers are analysed, and one in a leaky aquifer.

6.2.1. Confined pump test analysis

The first pumping test was conducted in the polder 'Oude Korendijk', south of Rotterdam, the Netherlands, and is taken from Kruseman and de Ridder (1990). The aquifer is a coarse sandy gravel, of 7 m thickness, bounded above and below by clayey aquicludes. The aquifer was pumped for 14 hours at an average pumping rate of 32.8 m^3/hour. Details of the second pumping test from Todd were reported by Bardsley (1991). A confined aquifer was pumped for 4 hours at an average rate of 104 m^3/hour. The pumping test data of time vs. drawdown are presented in Appendix F1.

Both pumping tests have been used by different authors in order to validate methods of pump test analysis. Pump test 'Oude Korendijk' was analysed using the data from

observation boreholes at 30 and 90 m radius from the pumped well. The results of the analysis of this test are summarised in Table 6.1 below.

Author	Method of analysis	Radius (m)	Results		Error (mm)
			T (m^2/day)	S	
Kruseman and de Ridder	Theis hand curve matching	30	392	1.6×10^{-4}	N/A
Kruseman and de Ridder	Cooper/Jacob (equation 2.8)	30, 90	370	4.1×10^{-4}	N/A
Kruseman and de Ridder	Cooper/Jacob (equation 2.9)	30	385	1.7×10^{-4}	N/A
Kruseman and de Ridder	Cooper/Jacob (equation 2.10)	30, 90	437	1.7×10^{-4}	N/A
Srivastava and Guzman (1994)	Slope matching	30	517	1.9×10^{-4}	N/A
Reed (CONPUTS)	Least squares curve matching	30	475	1.17×10^{-4}	31.0
Reed (CONPUTS)	Least squares curve matching	90	487	2.11×10^{-4}	22.0

Table 6.1: Results of different methods of analysis for pumping test 'Oude Korendijk'

A comparison of the observed and theoretical drawdown using the final parameters calculated from the CONPUTS programme for both the 30 and 90 m observation boreholes is shown in Figures 6.1 and 6.2 respectively. The same procedure was taken to evaluate aquifer parameters using the data from Todd, reported by Bardsley (1991). The results of the different methods of analysis are presented below in Table 6.2. A graph showing the observed and theoretical drawdown calculated using the final parameters from the CONPUTS programme is shown in Figure 6.3.

Author	Method of analysis	Results		Error
		T (m^2/day)	S	(mm)
Mukhopadhyay (1985)	Cooper/Jacob linear least squares	1161	1.8×10^{-4}	N/A
Yeh (1987)	Least squares finite difference Newton	1139	1.93×10^{-4}	N/A
Bardsley (1991)	Two point curve matching	1134	1.96×10^{-4}	N/A
Srivastava and Guzman (1994)	Slope matching	1145	2.09×10^{-4}	N/A
CONPUTS	Least squares curve matching	1138	1.93×10^{-4}	0.0052

Table 6.2: Results of different methods of analysis of pumping test from Todd

The analysis of these pumping tests show that the computer programme, CONPUTS, converges to values close to those calculated by other methods. This is also shown by Figures 6.4 and 6.5. These show schematically the values of transmissivity and storativity calculated by the different methods in each of the above tests. This shows that the results from the CONPUTS programme agree with other methods.

6.2.2. Leaky aquifer pump test analysis

Pumping test data from Kruseman and de Ridder (1990) was used to compare the results of the analysis of pumping test data from a leaky aquifer. There were observation wells at four different radii from the pumped well; 30, 60, 90 and 120 m. The site of the pumping test is at 'Dalem', The Netherlands. The geology consists of a sandy aquifer overlying an aquiclude. The aquifer is confined by a clayey peat that acts as the aquitard. The aquifer was pumped for 8 hours at 31.70 m^3/hour. The recorded drawdown is presented in

Appendix F2. This pumping test has been analysed by a number of authors and is well documented. Table 6.3 summarises the results from the methods of analysis based on the Walton solution, and includes the results of the curve matching programme WALPUTS2. Table 6.4 summarises the results based on the Hantush methods of analysis, and includes the results from the curve matching programme HANPUTS2.

Author	Method	Radius (m)	*T* m^2/day	*S*	*L* (m)	*K'/d'* ($days^{-1}$)	Error (mm)
Kruseman & de Ridder	Walton curve match	90	1731	1.9×10^{-3}	900	2.14×10^{-3}	N/A
Kruseman & de Ridder	Hantush inflection	All	1883	1.6×10^{-3}	1043	1.73×10^{-3}	N/A
Chander et al (1981)	Marquardt algorithm	90	1763	1.57×10^{-3}	882	2.27×10^{-3}	2.17
Sen (1986)	Slope matching	All	1576	2.4×10^{-3}	505	6.18×10^{-3}	N/A
Rushton & Chan(1976)	Discrete space/time	All	1680 $\pm$50	$1.5 \pm 0.2 \times 10^{-3}$	850 $\pm$ 100	2.33×10^{-3}	N/A
WALPUTS	Least squares curve matching	30	1927	9.47×10^{-4}	1938	5.13×10^{-4}	0.88
WALPUTS		60	1843	1.92×10^{-3}	1000	1.84×10^{-4}	1.12
WALPUTS		90	1663	1.78×10^{-3}	739	3.05×10^{-3}	1.26
WALPUTS		120	1757	1.51×10^{-3}	1039	1.63×10^{-3}	1.54

Table 6.3: Results of the analysis of pumping test Dalem by the Walton solution

Author	Method	Radius (m)	T m^2/day	S	β	$K' S'/d'$ ($days^{-1}$)	Error (mm)
Kruseman & de Ridder	Hantush curve match	90	1515	1.5×10^{-3}	0.05	1.1×10^{-5}	N/A
HANPUTS	Least squares curve matching	30	1087	1.02×10^{-3}	0.134	0.02	0.98
HANPUTS		60	1626	1.88×10^{-3}	0.026	9.2×10^{-6}	1.21
HANPUTS		90	1325	1.73×10^{-3}	0.038	1.1×10^{-4}	0.62
HANPUTS		120	1437	1.32×10^{-3}	0.048	5.03×10^{-6}	1.67

Table 6.4: Results of the analysis of pumping test Dalem by the Hantush solution

Graphs comparing the observed and theoretical values of drawdown calculated from the final parameters using the curve matching programmes are presented in Figures 6.6 to 6.13.

6.3. Parameter estimation using the fieldwork pump test data

A number of different pumping tests were conducted during the fieldwork, as detailed in chapter 3. The majority of the tests pumped water from the gravel layer, but some pump tests were also conducted in the sand. The details of the analysis of these tests are given in the following sections. Only those pump tests with results from observation wells are included, due to the inherent errors involved with the analysis of data from a pumped well.

Four different types of analysis were carried out on each of the sets of data. The first was a hand analysis using the Cooper/Jacob formula, which formed the analysis included in a report on the fieldwork. The CONPUTS programme was also used to determine these parameters. The leaky programmes, WALPUTS2 and HANPUTS2, were then used to evaluate the aquifer parameters by analysing the system as a leaky aquifer. The Walputs

programme calculates the aquitard characteristic K'/d' from r/L, and the HANPUTS programme determines $K'S'/d'$, after evaluating β.

If the geology of the site is recalled from chapter 3, the aquifer consists of a gravel bed, saturated to 2 metres thickness. This is underlain by a sandy clay which extends to uncertain depth. The validity of the analysis of this system as a leaky confined aquifer must be questioned. However, the drawdown due to the low pumping rate was small when compared to the saturated thickness of the aquifer. The principal difference between the leaky confined, and the unconfined solution is the effect of the storativity term. When pumping an unconfined system, the actual water table, not the piezometric surface, is reduced. Discharge derived from drainage of the pores, not expansion of the water and compression of the aquifer as a confined system. This leads to the situation of delayed yield and much greater values of storativity. However, as the drawdown is minimised by the pump test method, the analysis by Walton and Hantush is the most appropriate. They take the leakage from the aquitard into account, which must have a significant effect.

6.3.1. Pump borehole 16 - material: sand

The following results were obtained from the analysis of a pumping test in borehole no. 16, which was pumped for 4 hours at an average discharge of 0.511 m^3/hour. The drawdown was observed in two piezometers at different depths in borehole no. 18. The results from the observations in the lower piezometer are presented in Table 6.5, and from the middle piezometer are presented in Table 6.6.

Method of analysis	Aquifer Properties		Aquitard properties			Error (mm)
	T (m^2/day)	S	r/L or β	K'/d' (d^{-1})	$K'S'/d'$ (d^{-1})	
Theis hand	173	1.0×10^{-1}	N/A	N/A	N/A	N/A
CONPUTS	111	1.14×10^{-1}	N/A	N/A	N/A	0.34
WALPUTS	51	7.2×10^{-1}	0.063	2.0×10^{-3}	N/A	0.40
HANPUTS	3	3.8×10^{-2}	10.47	N/A	2.0	9.14

Table 6.5: Results of the analysis of the pumping test in BH16 sand, observed from the bottom sand piezometer in borehole 18.

Diagrams comparing the observed and theoretical drawdown curves using the values calculated from the computer analysis are shown in Figures 6.14, 6.15 and 6.16.

Method of analysis	Aquifer Properties		Aquitard properties			Error (mm)
	T (m^2/day)	S	r/L or β	K'/d' (d^{-1})	$K'S'/d'$ (d^{-1})	
Theis hand	52	5.0×10^{-3}	N/A	N/A	N/A	N/A
CONPUTS	54	5.7×10^{-3}	N/A	N/A	N/A	1.7
WALPUTS	38	6.05×10^{-3}	0.33	4.22×10^{-2}	N/A	0.68
HANPUTS	44	6.26×10^{-3}	6.9×10^{-3}	N/A	2.10×10^{-6}	?.?

Table 6.6: Results of the analysis of the pumping test in BH16 sand, observed from the middle sand piezometer in borehole 18.

Diagrams comparing the observed and theoretical drawdown curves using the values calculated from the computer analysis are shown in Figures 6.17, 6.18 and 6.19.

6.3.2. Pump borehole 16 - material: gravel

The pumping test in borehole 16 lasted for 5 hours at a pumping rate of 1.32 m^3/hour. The drawdown was analysed using the observations in boreholes 17 and 18, at radii of 7 and 10

metres respectively. The results of the analysis of the drawdown recorded in borehole 17 are shown in Table 6.7 and from borehole 18 in Table 6.8.

Method of	Aquifer Properties		Aquitard properties			Error
analysis	T (m^2/day)	S	r/L or β	K'/d' (d^{-1})	$K'S'/d'$ (d^{-1})	(mm)
Theis hand	241	1.3×10^{-1}	N/A	N/A	N/A	N/A
CONPUTS	370	5.5×10^{-2}	N/A	N/A	N/A	1.7
WALPUTS	202	1.66×10^{-1}	1.5×10^{-2}	9.0×10^{-4}	N/A	0.2
HANPUTS	73	5.5×10^{-2}	5.9×10^{-1}	N/A	4.55×10^{-1}	0.2

Table 6.7: Results of the analysis of the pumping test in borehole 16, observed from borehole 17.

Method of	Aquifer Properties		Aquitard properties			Error
analysis	T (m^2/day)	S	r/L or β	K'/d' (d^{-1})	$K'S'/d'$ (d^{-1})	(mm)
Theis hand	223	0.10	N/A	N/A	N/A	N/A
CONPUTS	231	1.03×10^{-1}	N/A	N/A	N/A	1.0
WALPUTS	250	1.01×10^{-1}	?.?	3.45×10^{-3}	N/A	1.0
HANPUTS	170	3.3×10^{-2}	1.4×10^{-1}	N/A	1.76×10^{-2}	2.9

Table 6.8: Results of the analysis of the pumping test in borehole 16, observed from borehole 18.

These leaky solutions were obtained by using the late time data only. Diagrams comparing the observed and theoretical drawdown for each solution from borehole 17 are presented in Figures 6.20, 6.21, 6.22. Similarly, these diagrams for the results of the analysis from borehole 18 are presented in Figures 6.23, 6.24 and 6.25.

6.3.3. Pump borehole 17 - material: gravel

The results of the pumping test in borehole 17 are presented below. The pumping test was of 4 hours duration , at an average pumping rate of 1.34 m^3/hour. The results of the analysis of the drawdown in borehole 16 at 7 m radius is shown in Table 6.9, and from borehole 18 at 3 m radius in Table 6.10.

Method of	Aquifer Properties		Aquitard properties			Error
analysis	T (m^2/day)	S	r/L or β	K'/d' (d^{-1})	$K'S'/d'$ (d^{-1})	(mm)
Theis hand	327	0.087	N/A	N/A	N/A	N/A
CONPUTS	283	1.10×10^{-1}	N/A	N/A	N/A	0.18
WALPUTS	267	1.14×10^{-1}	1.1×10^{-1}	6.9×10^{-2}	N/A	0.17
HANPUTS	240	1.05×10^{-1}	3.6×10^{-2}	N/A	1.07×10^{-2}	0.17

Table 6.9: Results of the analysis of the pumping test in borehole 17, observed from borehole 16.

Method of	Aquifer Properties		Aquitard properties			Error
analysis	T (m^2/day)	S	r/L or β	K'/d' (d^{-1})	$K'S'/d'$ (d^{-1})	(mm)
Theis hand	310	0.27	N/A	N/A	N/A	N/A
CONPUTS	310	2.0×10^{-1}	N/A	N/A	N/A	0.37
WALPUTS	242	2.65×10^{-1}	0.179	8.6×10^{-1}	N/A	0.26
HANPUTS	263	1.47×10^{-1}	5.3×10^{-2}	N/A	1.93×10^{-1}	4.53

Table 6.10: Results of the analysis of the pumping test in borehole 17, observed from borehole 18.

Again, the accuracy of the estimated parameters may be evaluated by plotting the observed drawdown with the theoretical drawdown using the calculated parameters. These graphs for the results of the analysis from borehole 16 are shown in Figures 6.26, 6.27 and 6.28. The results from borehole 18 are shown in Figures 6.29, 6.30 and 6.31.

6.3.4. Pump borehole 18 - material: gravel

The results of the pumping test in borehole 18 are presented below. The pumping test was of 6.5 hours duration, at an average pumping rate of 1.33 m^3/hour. The drawdown in borehole 17, at 3 m radius, and borehole 16 at 10 m radius from the pumped well were analysed. This gave the results presented in Tables 6.11 and 6.12 respectively:

Method of	Aquifer Properties		Aquitard properties			Error
analysis	T (m^2/day)	S	r/L or β	K'/d' (d^{-1})	$K'S'/d'$ (d^{-1})	(mm)
Theis hand	208	1.14	N/A	N/A	N/A	N/A
CONPUTS	162	9.92×10^{-1}	N/A	N/A	N/A	0.80
WALPUTS	42	8.78×10^{-1}	1.2×10^{-1}	6.6	N/A	0.36
HANPUTS	111	3.77×10^{-1}	1.5×10^{-1}	N/A	1.674	3.79

Table 6.11: Results of the analysis of the pumping test in borehole 18, observed from borehole 17.

Method of	**Aquifer Properties**		**Aquitard properties**			**Error**
analysis	T (m^2/day)	S	r/L or β	K'/d' (d^{-1})	$K'S'/d'$ (d^{-1})	**(mm)**
Theis hand	325	0.068	N/A	N/A	N/A	N/A
CONPUTS	288	7.47×10^{-2}	N/A	N/A	N/A	0.82
WALPUTS	755	4.75×10^{-3}	7.1×10^{2}	3.8×10^{-2}	N/A	4.42
HANPUTS	3887	3.16×10^{-3}	3.2×10^{-3}	N/A	2.05×10^{-5}	13.9

Table 6.12: Results of the analysis of the pumping test in borehole 18, observed from borehole 16.

Diagrams comparing the observed and theoretical drawdown from borehole 17 are shown in Figures 6.32, 6.33 and 6.34, and borehole 16 are shown in Figures 6.35, 6.36 and 6.37.

6.3.5. Summary of the aquifer parameters from the pumping tests

The aim of the fieldwork is to estimate the aquifer parameters. These parameters are the permeability and storativity of both the gravel and sand layers. The permeability of a formation is made up of two directions, vertically and horizontally. The vertical permeability of the sand layer is very important, as it is the vertical flow of water that recharges the gravel layer. This parameter is the most difficult parameter to estimate accurately from these tests. It is only measured in the form of K'/d' or $K'S'/d'$, from the Walton or Hantush pumping tests. In addition, the depth of the aquitard, d', is unknown.

Some of the gravel characteristics calculated from the leaky aquifer analysis are obviously inaccurate, due to pumping test results that do not conform with the Walton or Hantush solutions. When evaluating the aquifer parameters, the hydrologist needs to use experience and common sense to determine which results are likely to be accurate, and those which are not. Table 6.13 presents those parameters which the author considers accurate, from the analysis of the pumping test data from the gravel formation as a leaky aquifer. The results from the Theis analysis are not included in this table, because of the innacuracies introduced with this method when the contribution to discharge from the aquitard is ignored.

Results from Table no:	Transmissivity (m^2/day)	Storativity
6.7	202	1.66×10^{-1}
	73	5.5×10^{-2}
6.8	250	1.01×10^{-1}
	170	3.30×10^{-2}
6.9	267	1.14×10^{-1}
	240	1.05×10^{-1}
6.10	242	2.65×10^{-1}
	263	1.47×10^{-1}
Average values	213.4	1.23×10^{-1}

Table 6.13: Summary of the results of the leaky analysis of pumping test data from the gravel formation

The values calculated from the analysis of the data from the pumping tests in the sand formation are presented in Table 6.14.

Results from Table no:	Transmissivity (m^2/day)	Storativity	*K'/d'* ($days^{-1}$)	*K'S'/d'* ($days^{-1}$)
6.6	38	6.05×10^{-3}	N/A	N/A
	44	6.26×10^{-3}	N/A	N/A
6.7	N/A	N/A	9.0×10^{-4}	4.55×10^{-1}
6.8	N/A	N/A	3.45×10^{-3}	1.76×10^{-2}
6.9	N/A	N/A	6.9×10^{-2}	1.07×10^{-2}
6.10	N/A	N/A	8.6×10^{-1}	1.93×10^{-1}
Average values	41	6.16×10^{-3}	2.3×10^{-1}	1.69×10^{-1}

Table 6.14: Summary of the results of aquifer parameters calculated for the sand formation

The gravel parameters have been evaluated, and values determined which are feasible when compared with standard values. To evaluate the validity of these results further, Figure 6.38 plots each of the transmissivity vs. storativity pairs presented in Table 6.13. The Hantush results give generally lower transmissivity results than the Walton analysis, but there are not enough results to make any conclusions from this graph. The average values of transmissivity and storativity calculated do coinicide with the centre of the results. However, it is possible that the trend of the results indicate that the average value of transmissivity should be slightly greater.

The quantification of the vertical permeability of the sand layer is more difficult. A wide range of values of the parameter K'/d' have been determined from the Walton method. It is also difficult to determine d' as the depth of the sand is unknown, the border with the underlying, less permeable formation is gradational and so generally permeability is likely to reduce with depth.

If an assumption is made that the thickness of the sand layer is 10 metres, then the horizontal permeability is approximately 4 m/day. The borehole logs suggest that 10 metres thickness is a reasonable estimate. The Walton solution gives an average value of K' of 2.3 m/day. If the Hantush solution is examined, the average value of $K'S'/d'$ calculated from the analysis is 0.169. Using $S' = 6.16 \times 10^{-3}$ and $d' = 10.0$ m, the average value of K' calculated is 274 m/day. This is two orders of magnitude greater than the values calculated by the other methods. It is almost certainly far too great.

This problem could derive from the analysis of the gravel, which is unconfined, as a confined leaky system. As the pumping rate is very low, the drawdown is small and the effects of delayed yield are minimised. However, the average storativity term of the aquifer is very high, greater than 10%. Thus when this is included in the Hantush equation to evaluate $K'S'/d'$ from β, the resulting parameter may be too great. It is unfortunate that the

geology where this fieldwork took place represents a non standard pump test situation. However, field tests are very unlikely to ever conform to theoretical conditions.

The values of vertical permeability could be different if the depth of the aquitard or the storativity were changed. However, a value calculated close to the first two methods was chosen, of 2.5 m/day.

In conclusion, the following average parameters have been calculated for the gravel and sand formations where fieldwork was conducted.

GRAVEL

Transmissivity, T = 213.4 m^2/day

Storativity, S = 1.23 x 10^{-1}

SAND

Leakage factor, K'/d' = 2.5 x 10^{-1} $days^{-1}$

Storativity, S' = 6.16 x 10^{-3}

To observe the accuracy of these results, a finite element method is used to simulate the pumping tests using the calculated parameters, and so the theoretical and observed drawdown may be compared. This allows the validity of the assumptions made during the analysis to be examined.

6.4. Finite element evaluation of parameters from leaky aquifer pump tests

Aquifer parameters for the fieldwork completed as part of this project were evaluated in section 6.3.5. The validity of these parameters is evaluated by modelling the pump tests using the calculated parameters.

6.4.1. Verification of the finite element model

A two dimensional finite element modelling package, SEFTRANS[1], was used to model the pumping tests. The model was set up in cross-section, with axisymmetric flow conditions. To ensure that the model is representative of the analytical solution a hypothetical pump test was run using the following parameters:-

Aquifer

$T = 200\ m^2/day$ $S = 0.10$

Aquitard

$K' = 1.0 \times 10^{-3}\ m/day$ $S' = 5.0 \times 10^{-3}$

The thickness of the aquifer was set at 2.0 m, and the aquitard 10.0 m. The aquifer overlies the aquitard, in a similar way to the geology encountered during the fieldwork. A discharge rate of 20 m^3/hour was set, and the drawdown observed at a radius of 10.0 m.

The analytical solution was evaluated using the Hantush equation for drawdown in a leaky aquifer. The well function was evaluated using the appropriate subroutine from the HANPUTS programme. This is compared against the numerical results in Figure 6.39. This figure shows that the SEFTRANS numerical solution gives a good match to the analytical solution.

As the parameters are known, it is possible to evaluate the validity of the Hantush solution over time. Recalling this from chapter 2, the Hantush solution is only valid if the time,

$$t < \frac{d'S'}{10K'} \qquad (6.1)$$

The values used in this problem give an upper time limit of 5 days. Thus the analytical solution and the numerical model are both correct.

---

[1]Oxford Geotechnica Limited, 1993

6.4.2. Validation of the experimental results

The values of aquifer parameters calculated in section 6.3.5 were used in the SEFTRANS model. If these values of parameters are correct, then the Hantush solution is only valid if the time,

$$t < \frac{d'S'}{10K'}$$
$$< \frac{10 \cdot 6.16x10^{-3}}{10 \cdot 2.5}$$
$$< 2.464x10^{-3} \text{ days}^{-1}$$

Thus the Hantush solution is only valid if the time, $t < 210$ seconds. This could be a further reason for the high values of $K'S'/d'$ that were calculated in the previous section. However, the numerical solution will not be affected by the validity of the analytical solution.

The pumping rate in each of the three gravel pumping rates was very similar. The model was run with a pumping rate of 1.33 m^3/hour and the drawdown recorded at radii of 3, 7 and 10 metres from the pumped well. These were then compared against the field data recorded during the pumping tests.

The graphs of these results are shown in Figures 6.40 to 6.45, for the pumping in boreholes 16, 17 and 18. Each of the radii at 7 and 10 metres fit very well to the recorded data. Only the observations from 3 metres do not match exactly, even though it is reasonably close. This could be because a slightly different combination of parameters is required, or there may be an error introduced in the measurement when an observation well records the drawdown at just 3 metres from the pumped well.

6.5. Conclusions

This chapter has shown that the three least squares programmes are able to accurately calculate aquifer parameters using pump test data. The results from the analysis of published pump test data allow these methods to be compared against other methods of

pump test analysis. These show that the parameters calculated are close to those of other methods.

The data from the fieldwork were also successfully analysed. The average results from this analysis were validated by a numerical method. A finite element model was used to calculate the theoretical drawdown for the field pump tests. These results were compared with the field data, and a very close match was found.

The results of the numerical analysis indicate that the relevant parameters have been evaluated accurately. However, a number of errors have occurred in the analysis. For some of the tests the least squares algorithm did not converge to values of parameters which give drawdown close to the recorded values. The reason for this may be that the algorithm is calculating the parameters that give the average minimum drawdown between the theoretical and observed values of drawdown. A solution may be possible which fits some but not all of the data.

Another source of error could be the application of confined leaky aquifer solutions, of Walton and Hantush, to data from pumping tests that were carried out in a leaky unconfined system. Also, the Hantush solution is the most accurate pumping test solution used, but it is only theoretically accurate at early time. The time after which the theoretical solution is no longer valid is calculated from equation 6.1. However, this uses the two aquitard parameters, K' and S'. If these parameters are to be evaluated using the Hantush equation, it is impossible to know over what time period the solution is valid for.

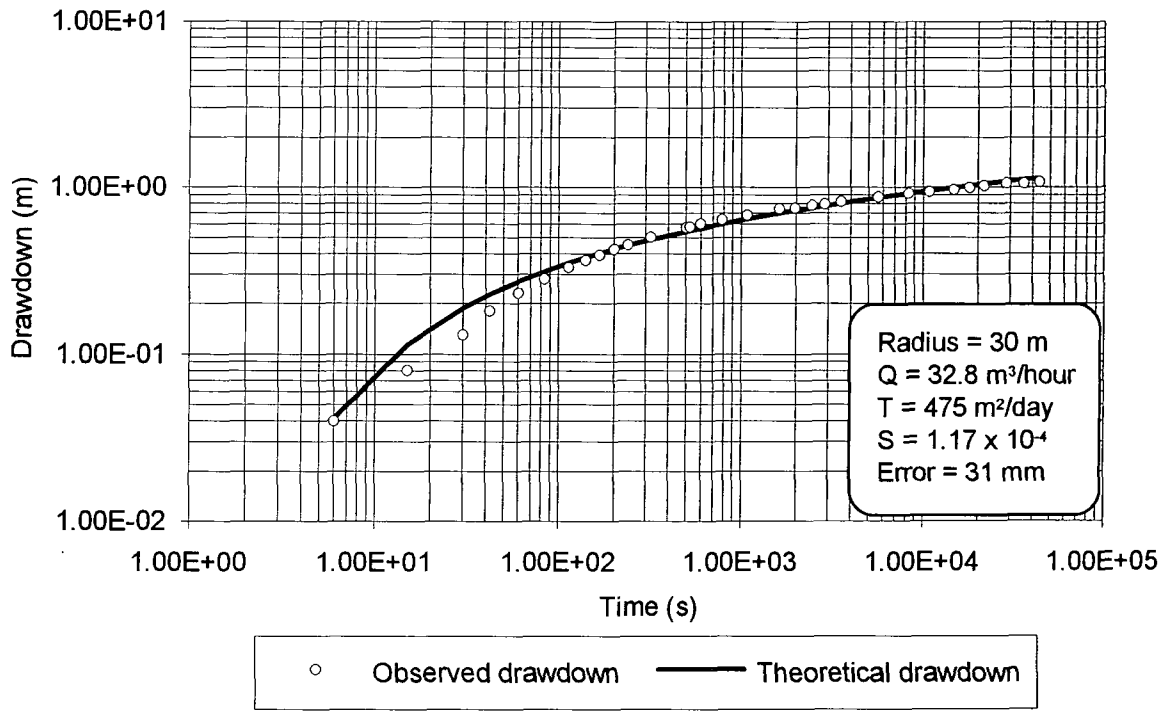

Figure 6.1: Observed and theoretical drawdown results from pumping test 'Oude Korendijk' (confined aquifer).

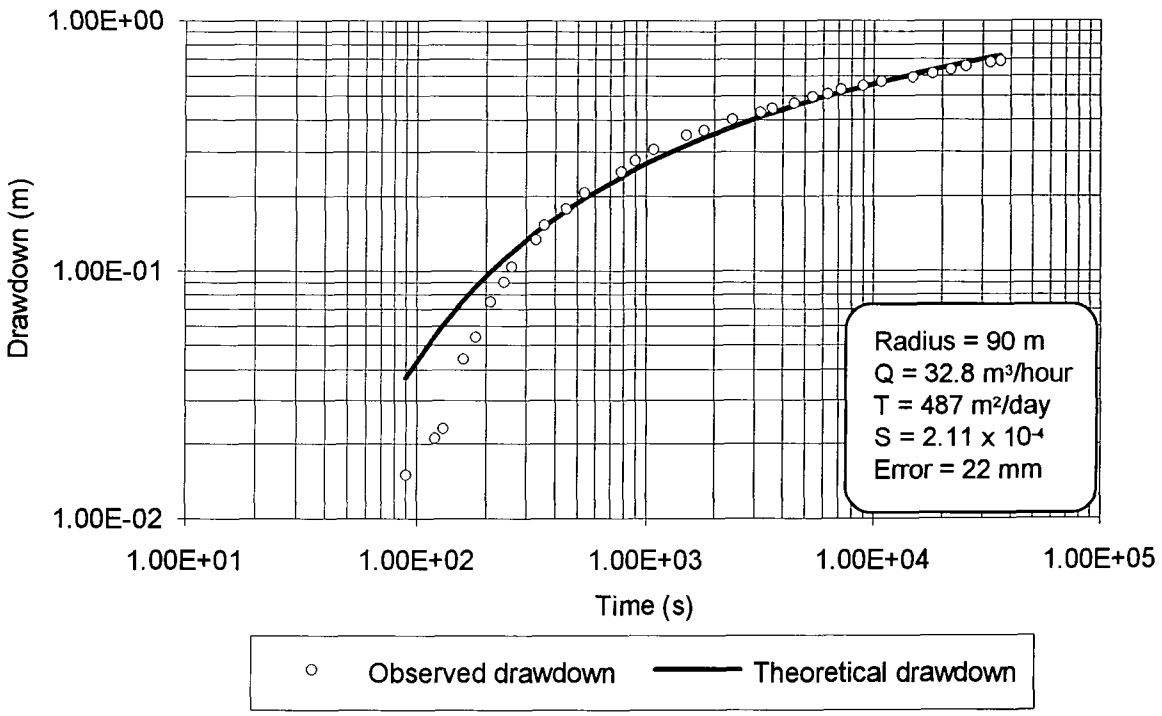

Figure 6.2: Observed and theoretical drawdown results from pumping test 'Oude Korendijk' (confined aquifer).

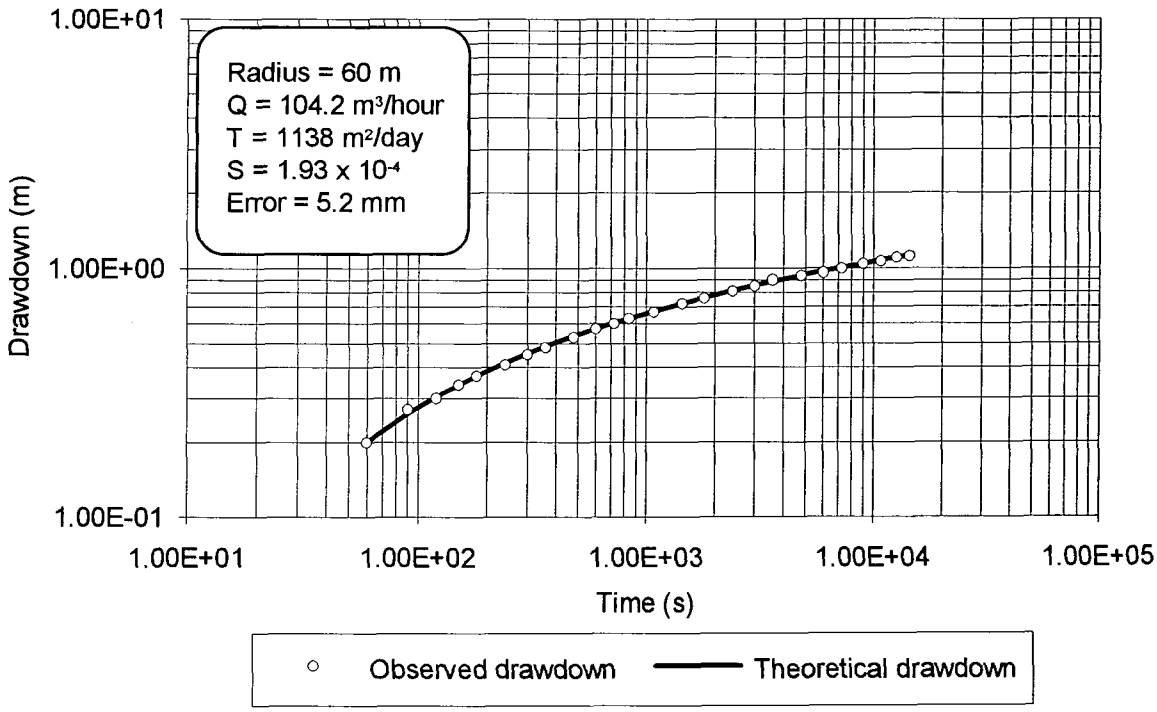

Figure 6.3: Observed and theoretical drawdown for Todd pumping test (confined aquifer).

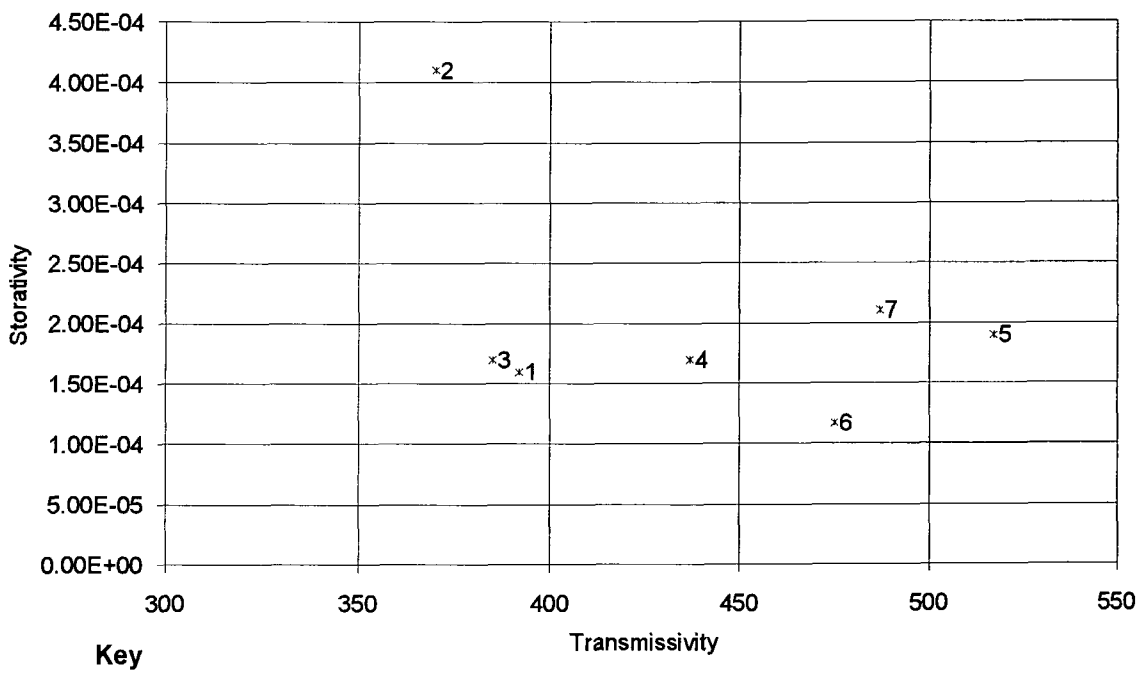

Key

1. Theis curve matching
2. Cooper/Jacob (constant time)
3. Cooper/Jacob (constant radius)
4. Cooper/Jacob (constant r^2/t)
5. Slope matching
6. CONPUTS curve matching
7. CONPUTS curve matching

Figure 6.4: Comparsion of the results of the different methods of analysis of pumping test 'Oude Korendijk'

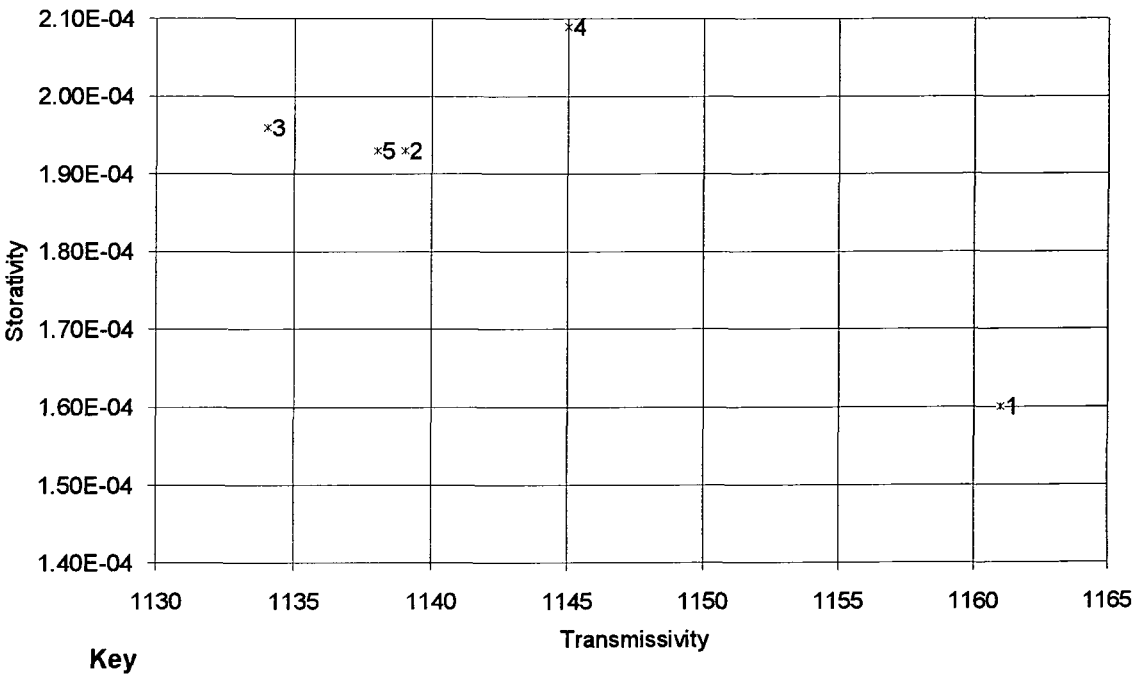

Key

1. Cooper/Jacob linear least squares
2. Least squares finite difference Newton
3. Two point curve matching
4. Slope matching
5. CONPUTS curve matching

Figure 6.5: Comparsion of the results of the different methods of analysis of the pumping test from Todd

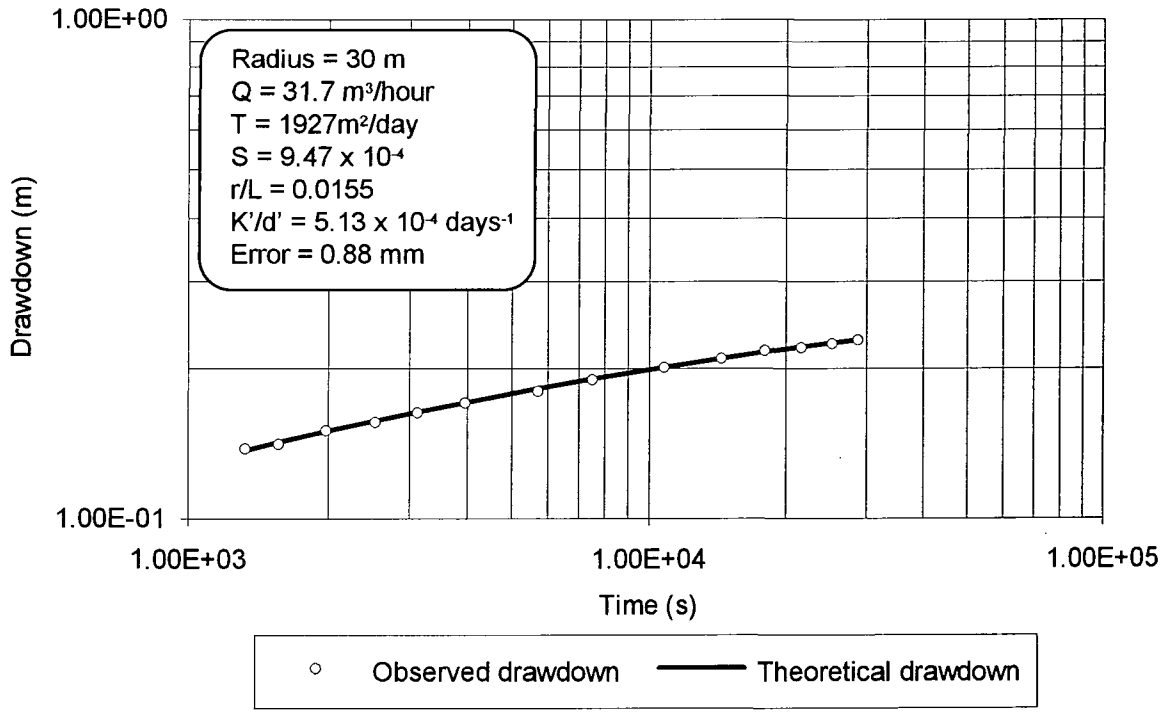

Figure 6.6: Observed and theoretical drawdown results of pumping test Dalem by Walton (leaky aquifer).

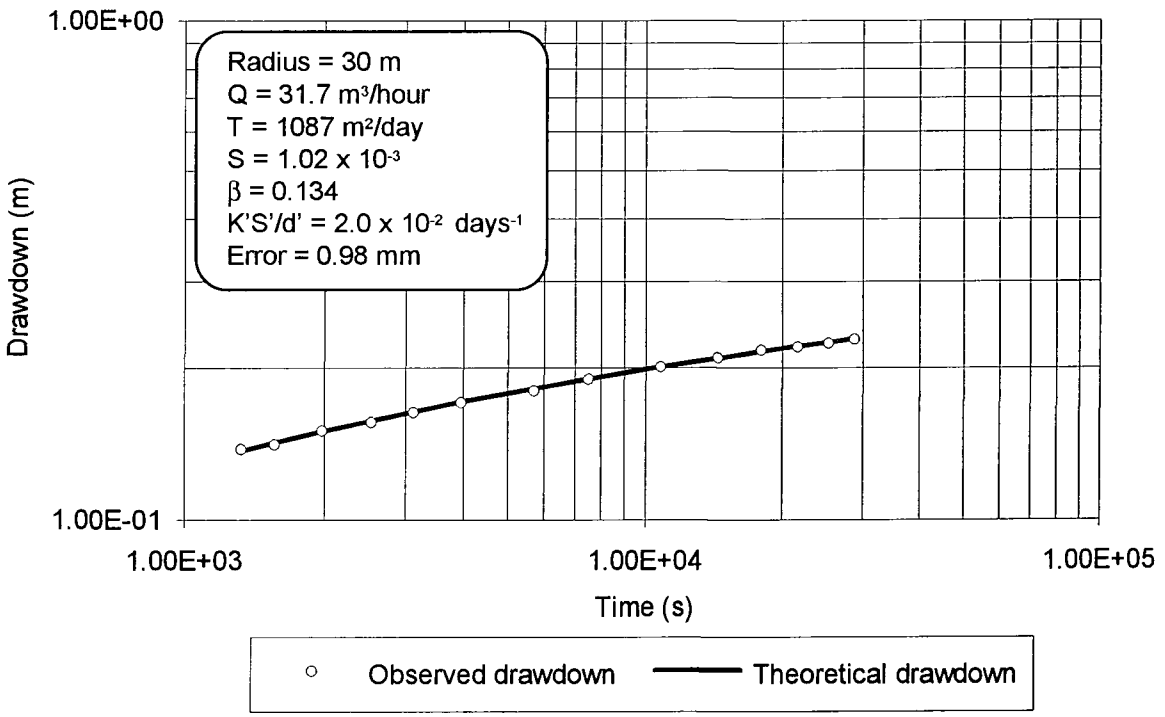

Figure 6.7: Observed and theoretical drawdown results of pumping test Dalem by Hantush (leaky aquifer).

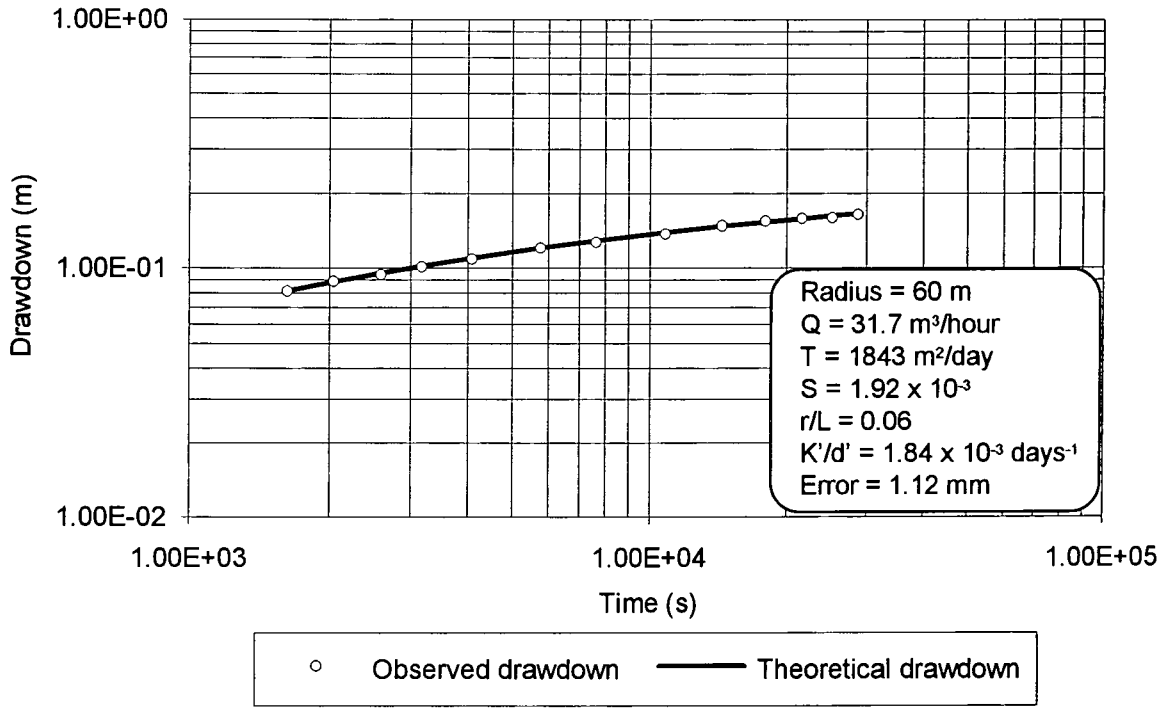

Figure 6.8: Observed and theoretical drawdown results of pumping test Dalem by Walton (leaky aquifer).

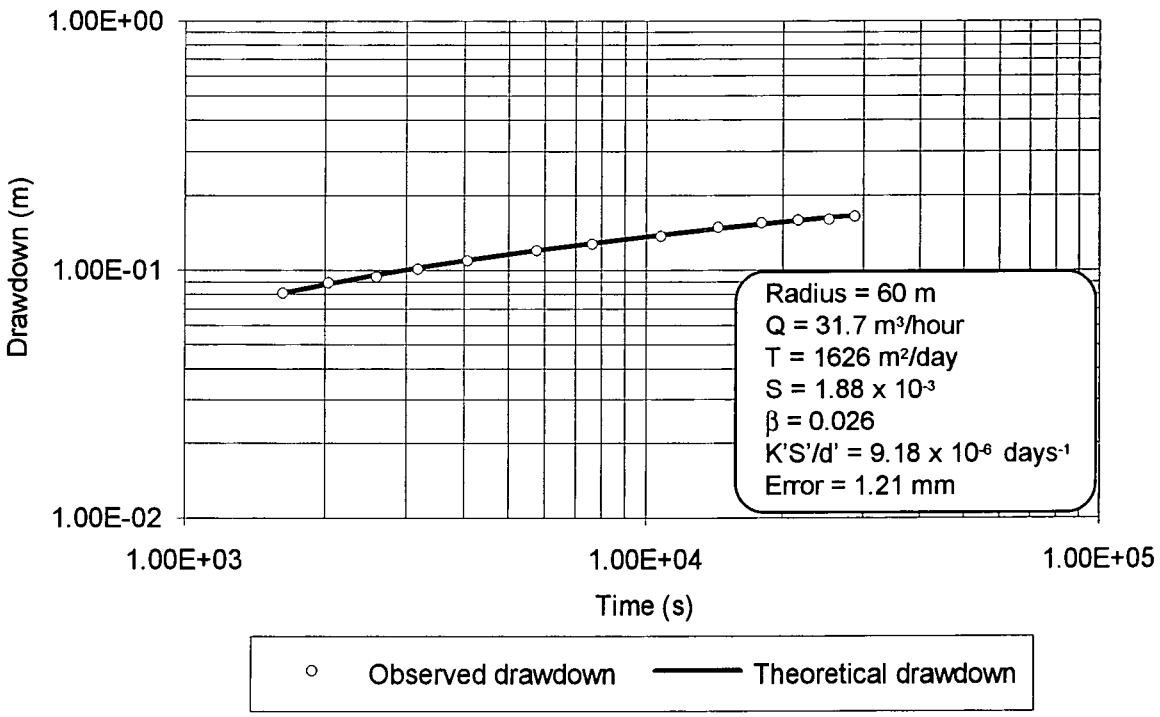

Figure 6.9: Observed and theoretical drawdown results of pumping test Dalem by Hantush (leaky aquifer).

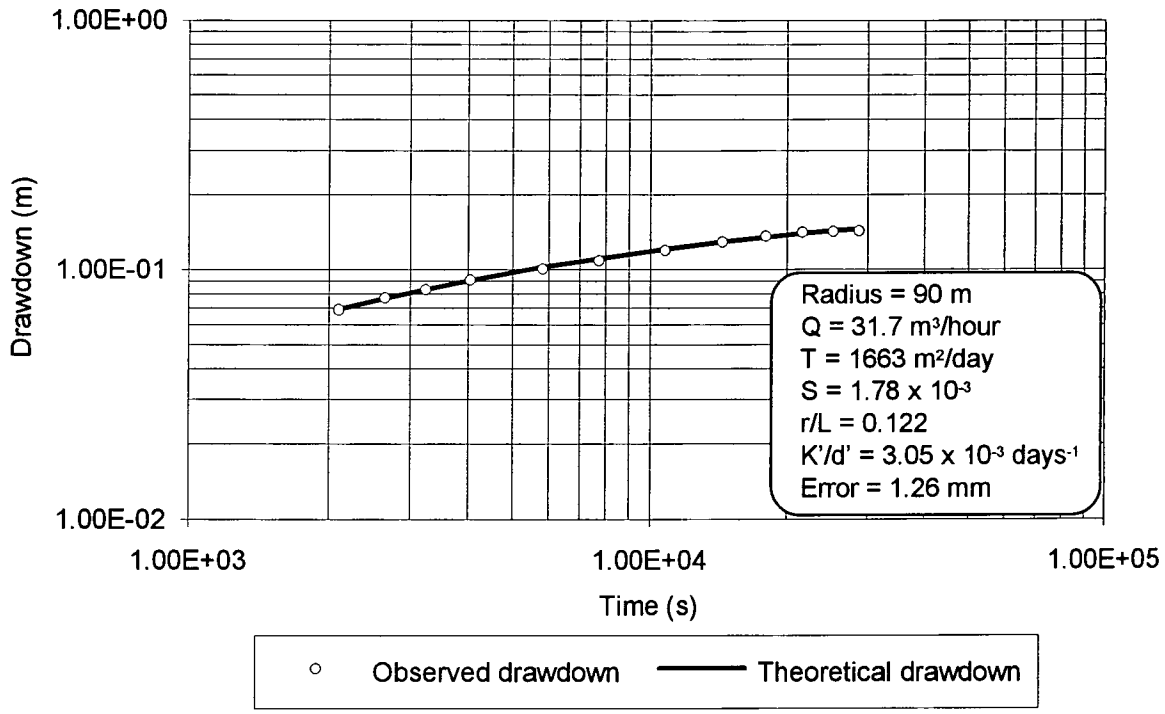

Figure 6.10: Observed and theoretical drawdown results of pumping test Dalem by Walton (leaky aquifer).

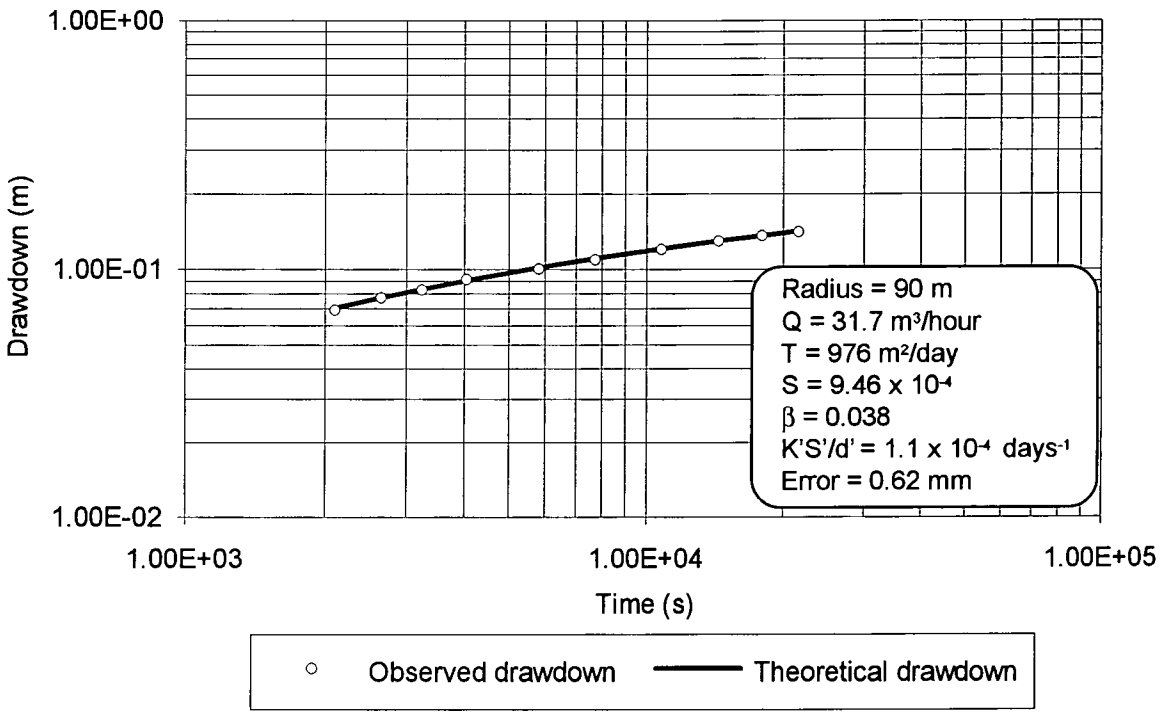

Figure 6.11: Observed and theoretical drawdown results of pumping test Dalem by Hantush (leaky aquifer).

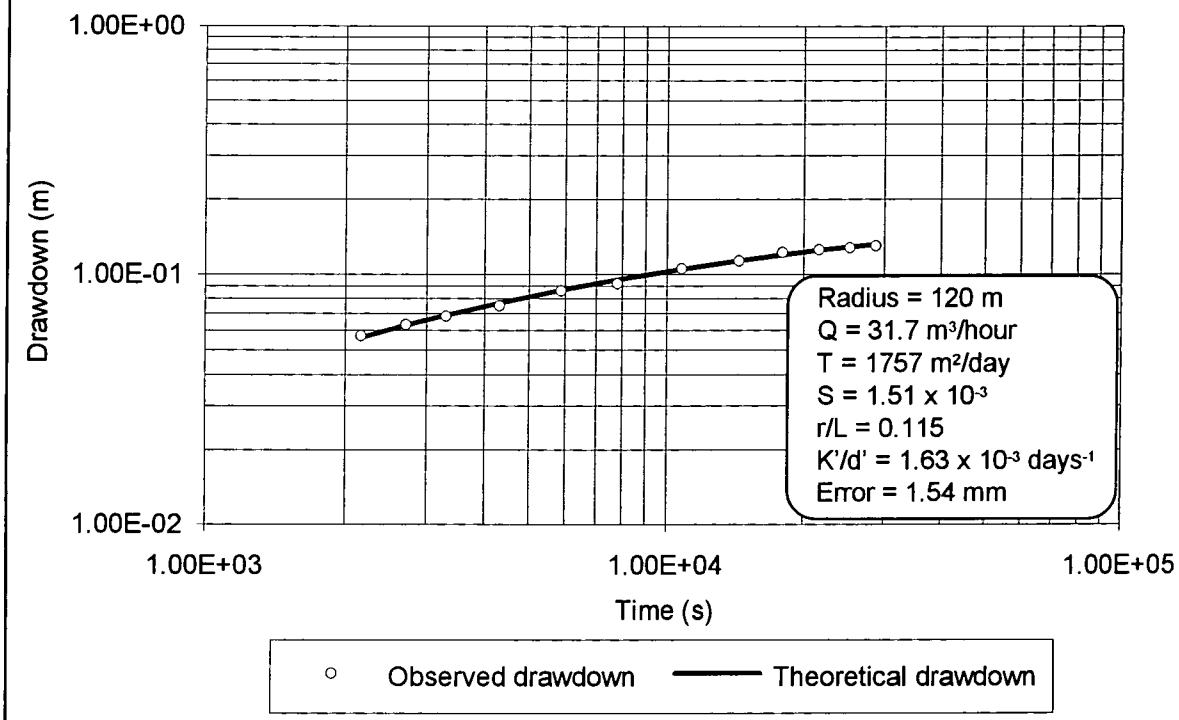

Figure 6.12: Observed and theoretical drawdown results of pumping test Dalem by Walton (leaky aquifer).

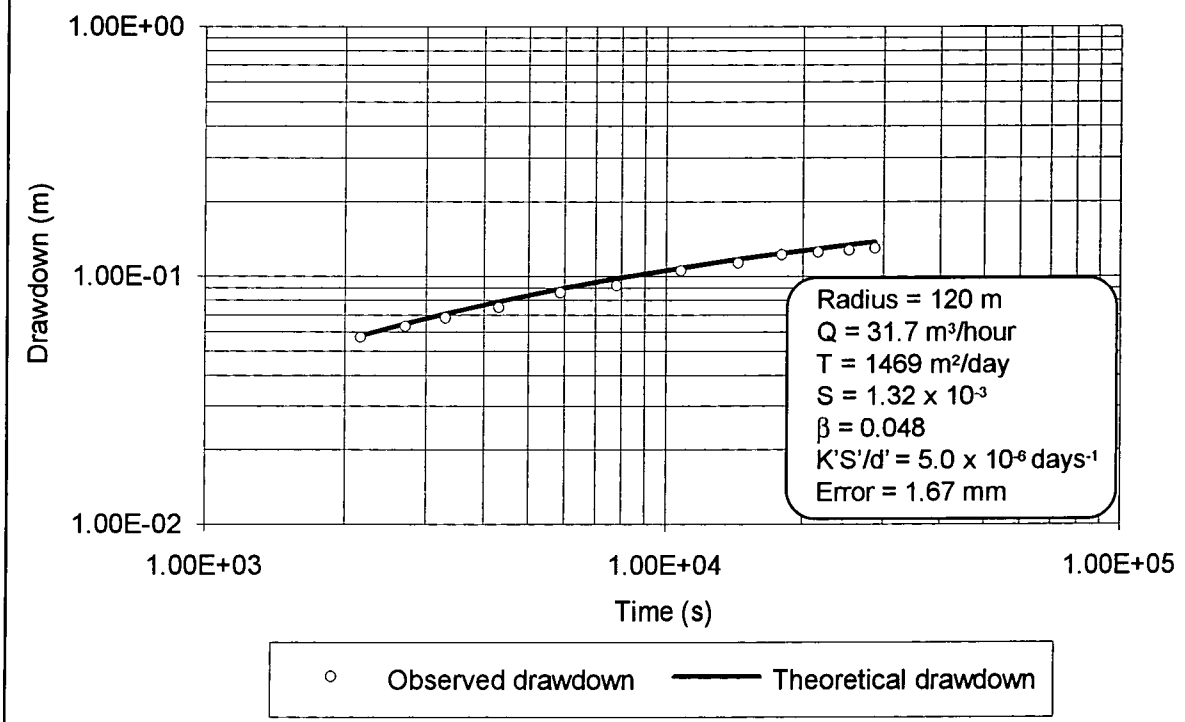

Figure 6.13: Observed and theoretical drawdown results of pumping test Dalem by Hantush (leaky aquifer).

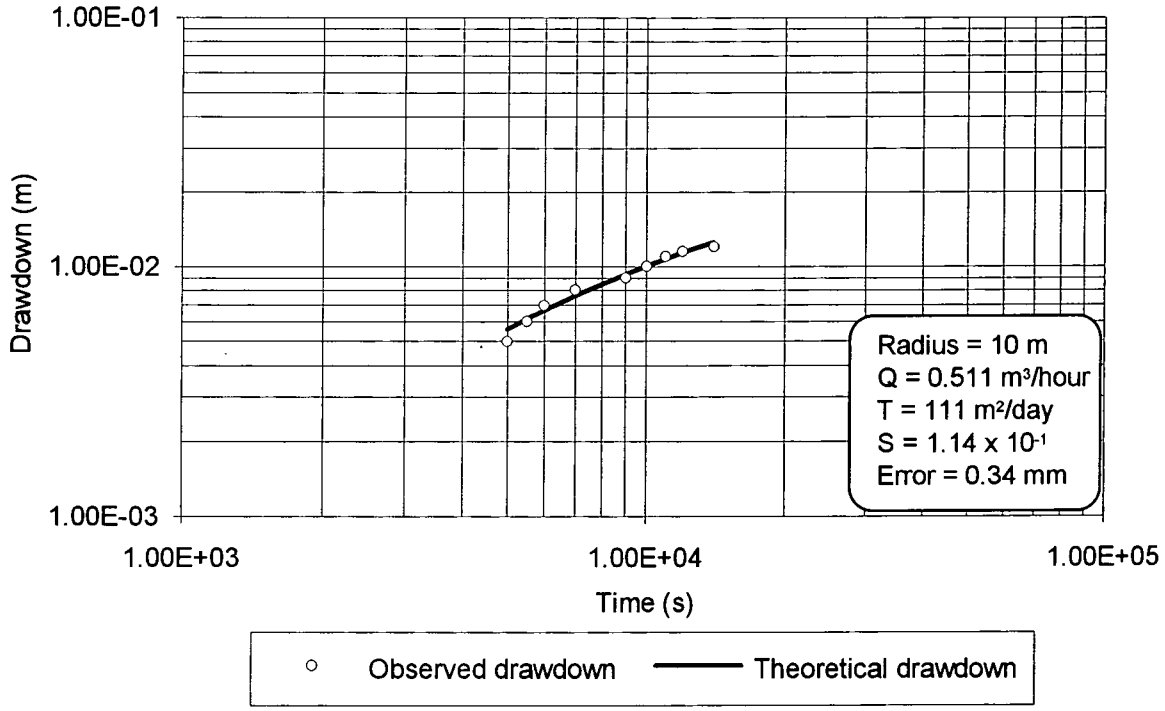

Figure 6.14: THEIS analysis of field pump test
Borehole pumped: 16 Material: Sand
Borehole observed: 18 (Bottom piezometer)

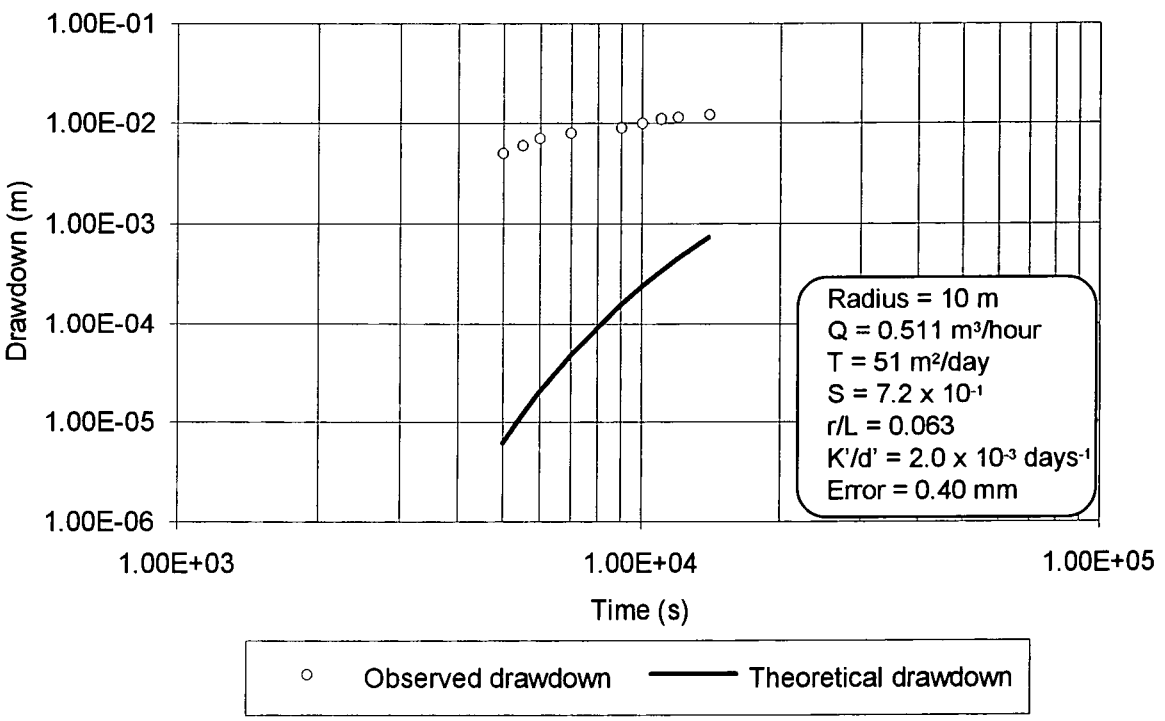

Figure 6.15: WALTON analysis of field pump test
Borehole pumped: 16 Material: Sand
Borehole observed: 18 (Bottom piezometer)

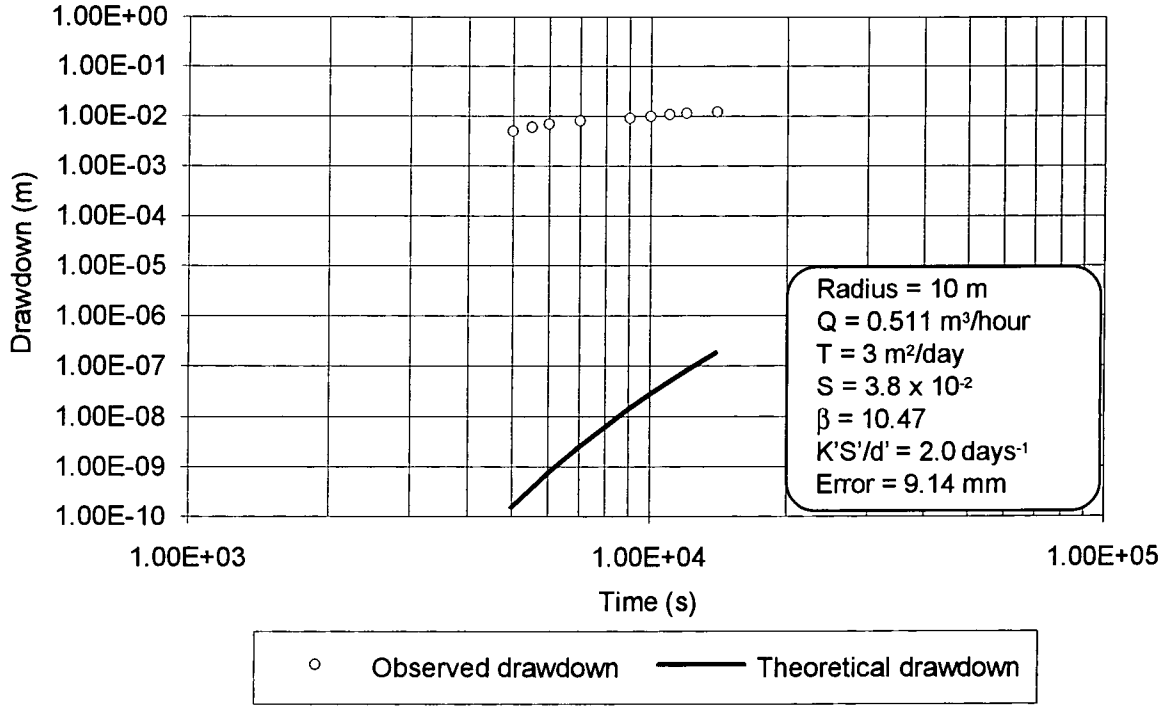

Figure 6.16: HANTUSH analysis of field pump test
Borehole pumped: 16 Material: Sand
Borehole observed: 18 (Bottom piezometer)

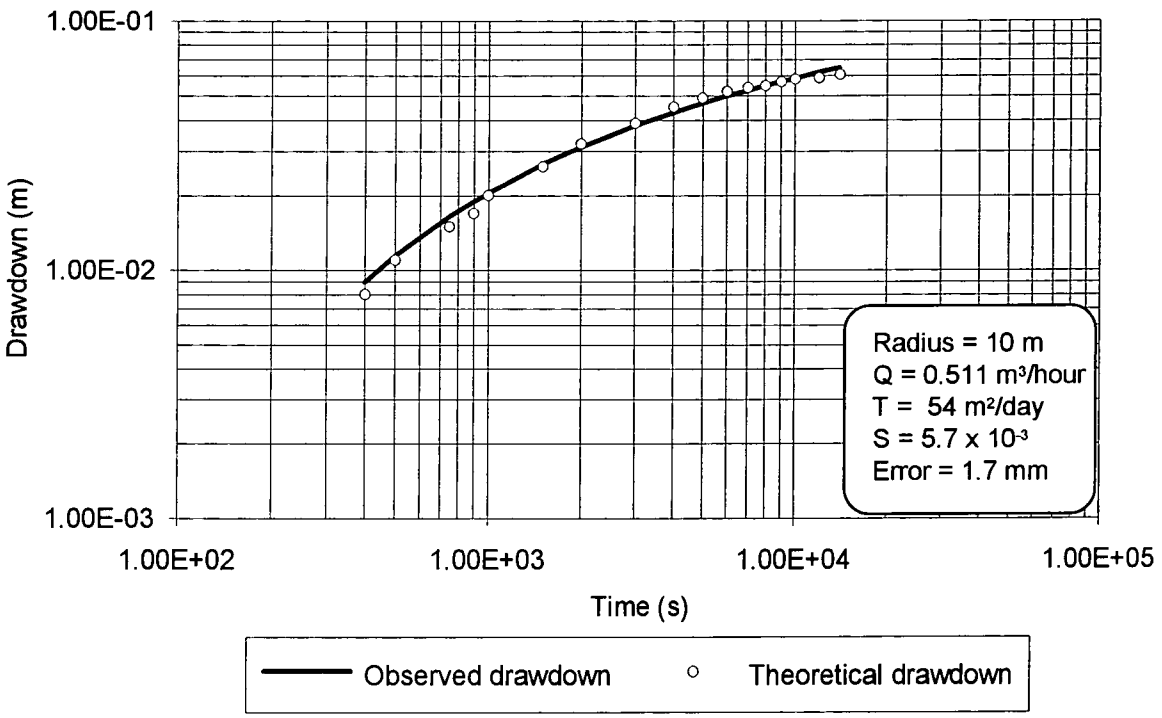

Figure 6.17: THEIS analysis of field pump test
Borehole pumped: 16 Material: Sand
Borehole observed: 18 (Middle piezometer)

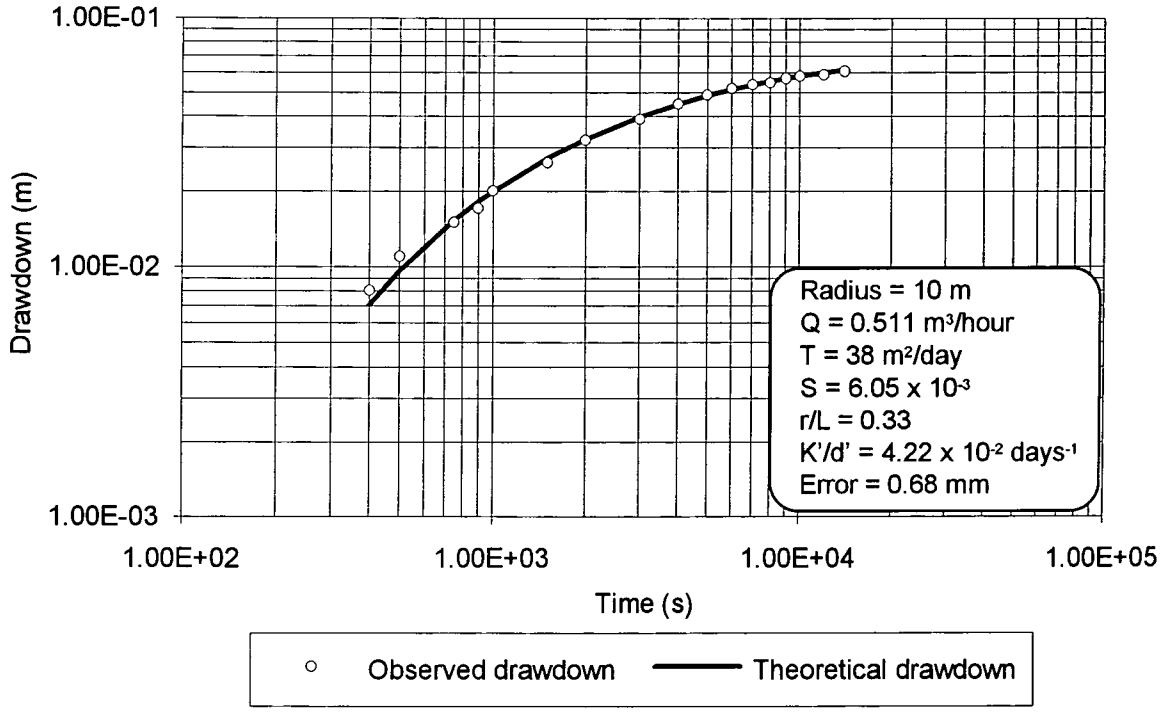

Figure 6.18: WALTON analysis of field pump test
Borehole pumped: 16 Material: Sand
Borehole observed: 18 (Middle piezometer)

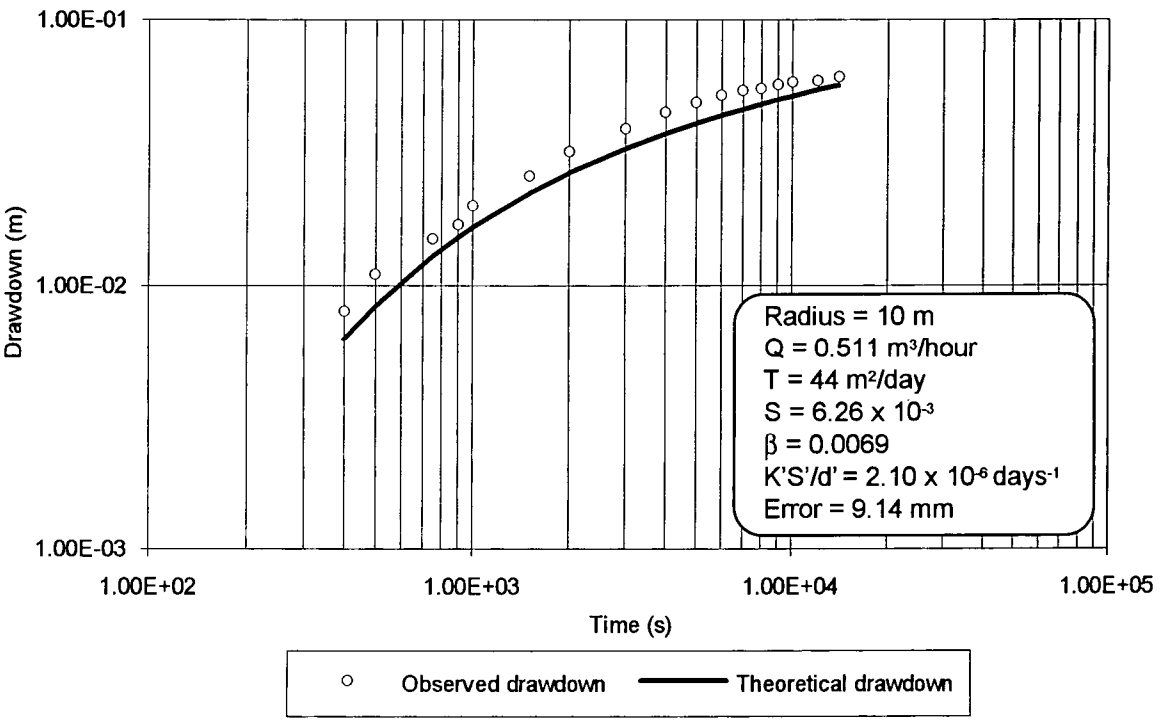

Figure 6.19: HANTUSH analysis of field pump test
Borehole pumped: 16 Material: Sand
Borehole observed: 18 (Middle piezometer)

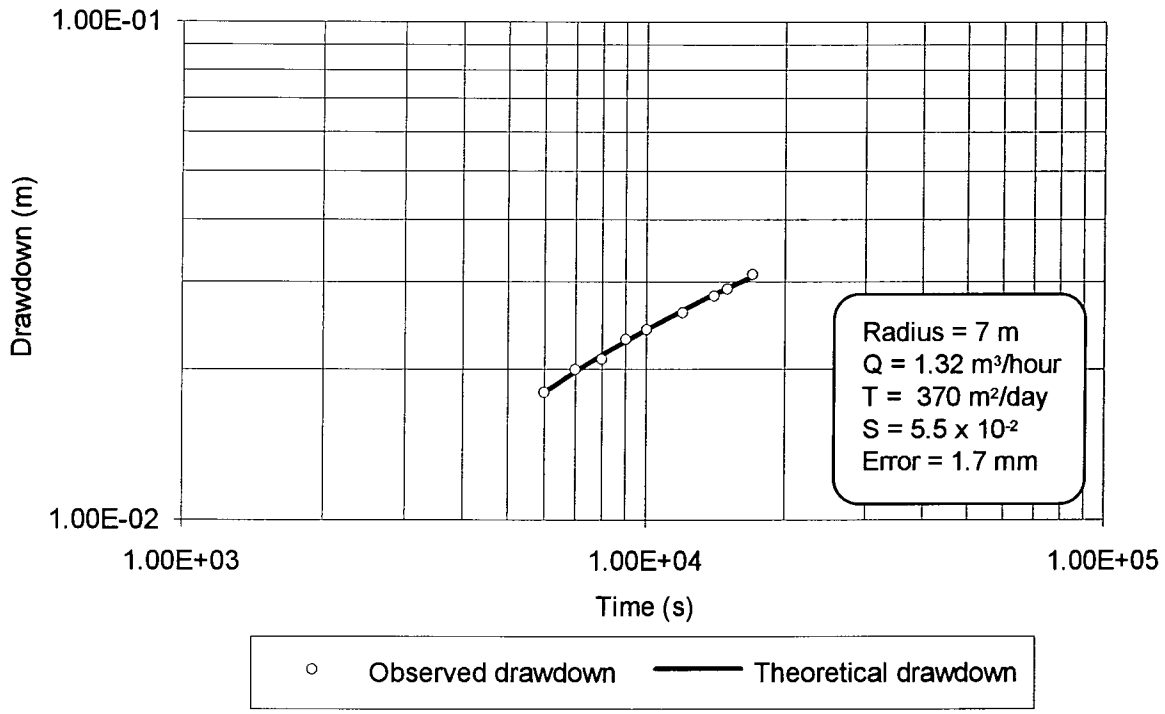

Figure 6.20: THEIS analysis of field pump test
Borehole pumped: 16 Material: Gravel
Borehole observed: 17

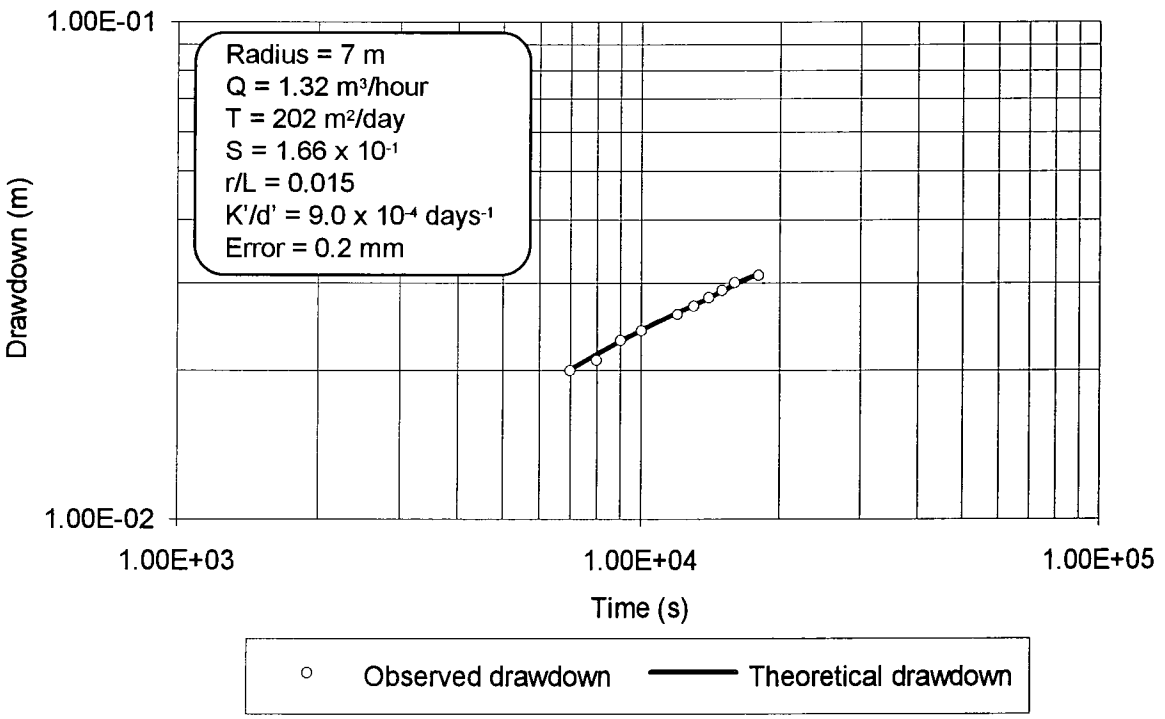

Figure 6.21: WALTON analysis of field pump test
Borehole pumped: 16 Material: Gravel
Borehole observed: 17

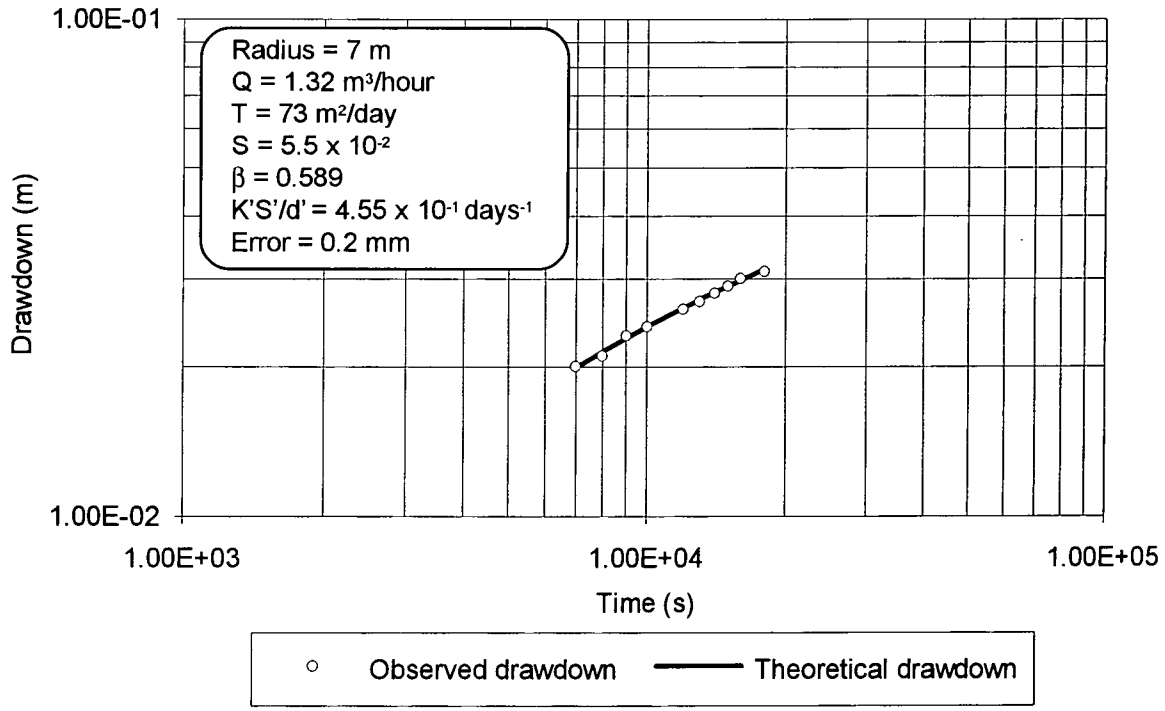

Figure 6.22: HANTUSH analysis of field pump test
Borehole pumped: 16 Material : Gravel
Borehole observed: 17

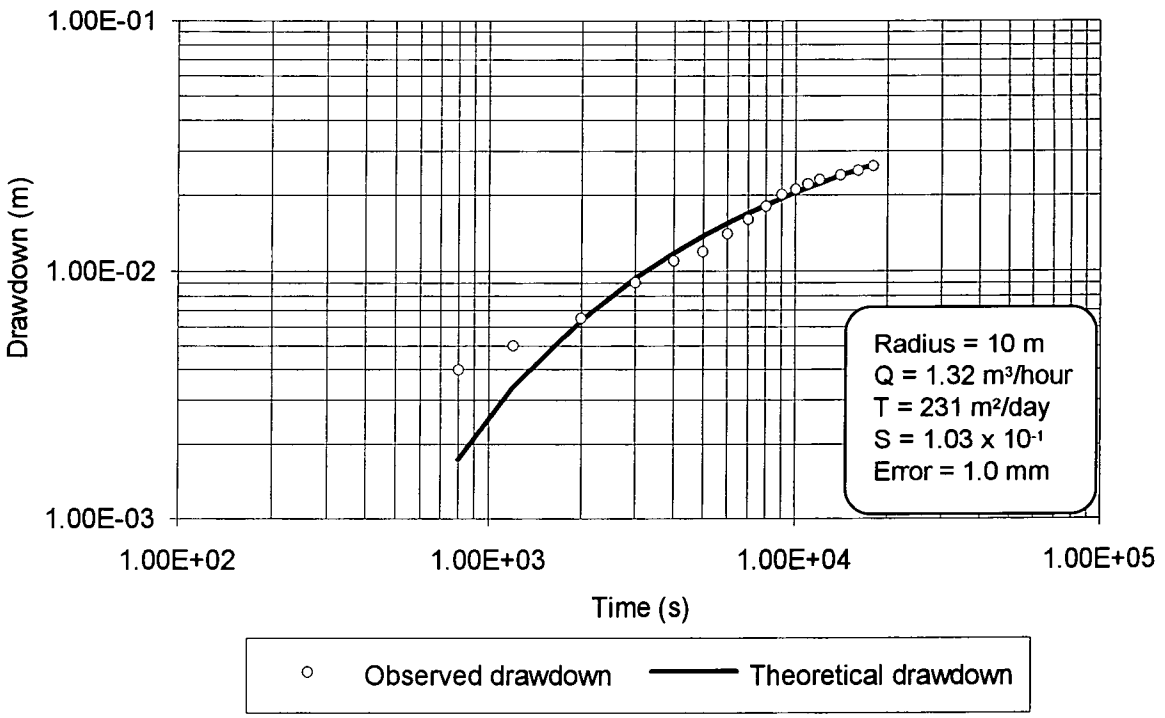

Figure 6.23: THEIS analysis of field pump test
Borehole pumped: 16 Material: Gravel
Borehole observed: 18

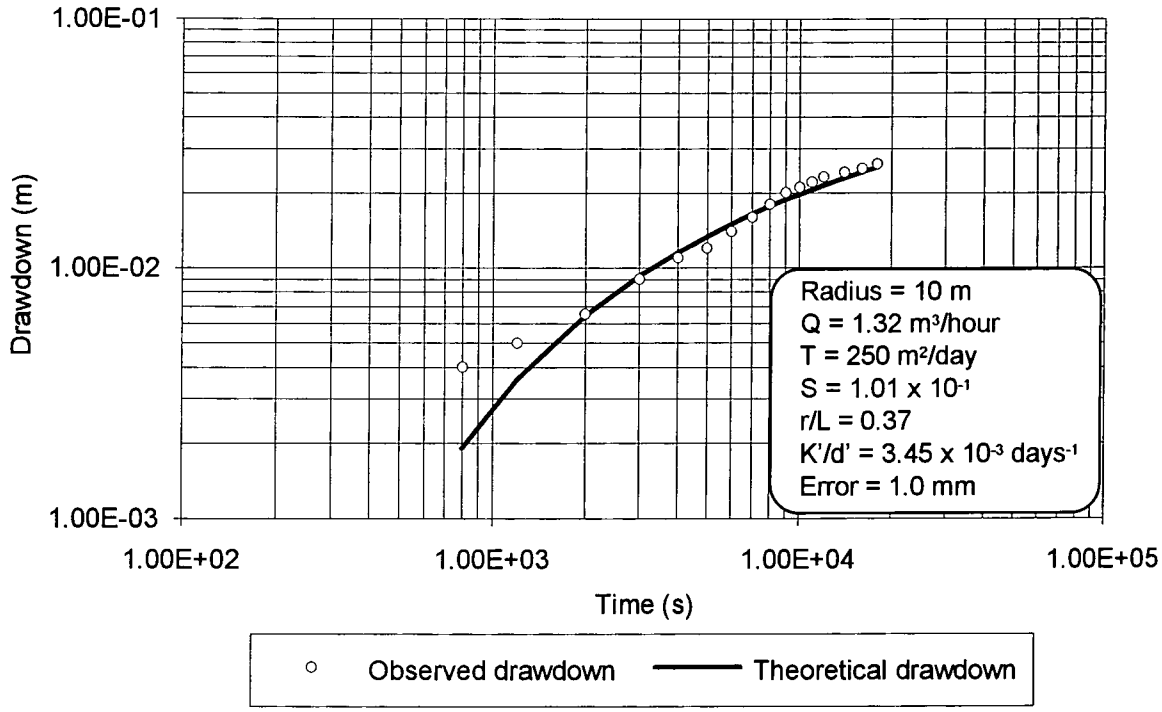

Figure 6.24: WALTON analysis of field pump test
Borehole pumped: 16 Material: Gravel
Borehole observed: 18

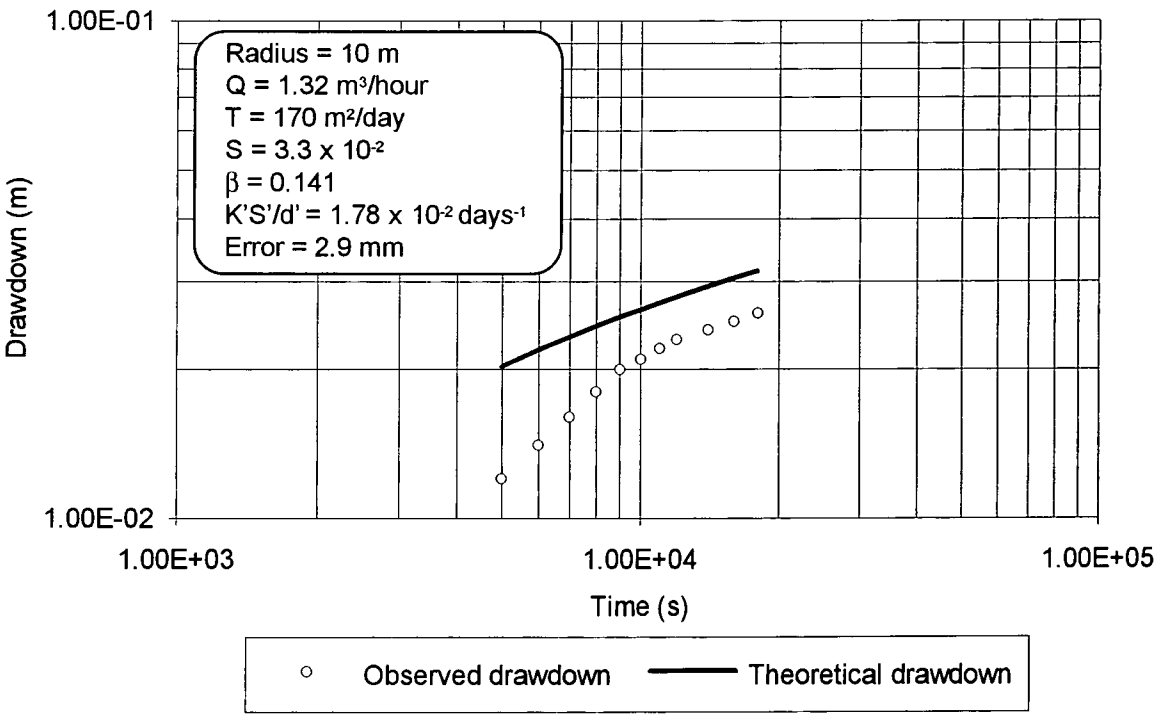

Figure 6.25: HANTUSH analysis of field pump test
Borehole pumped: 16 Material: Gravel
Borehole observed: 18

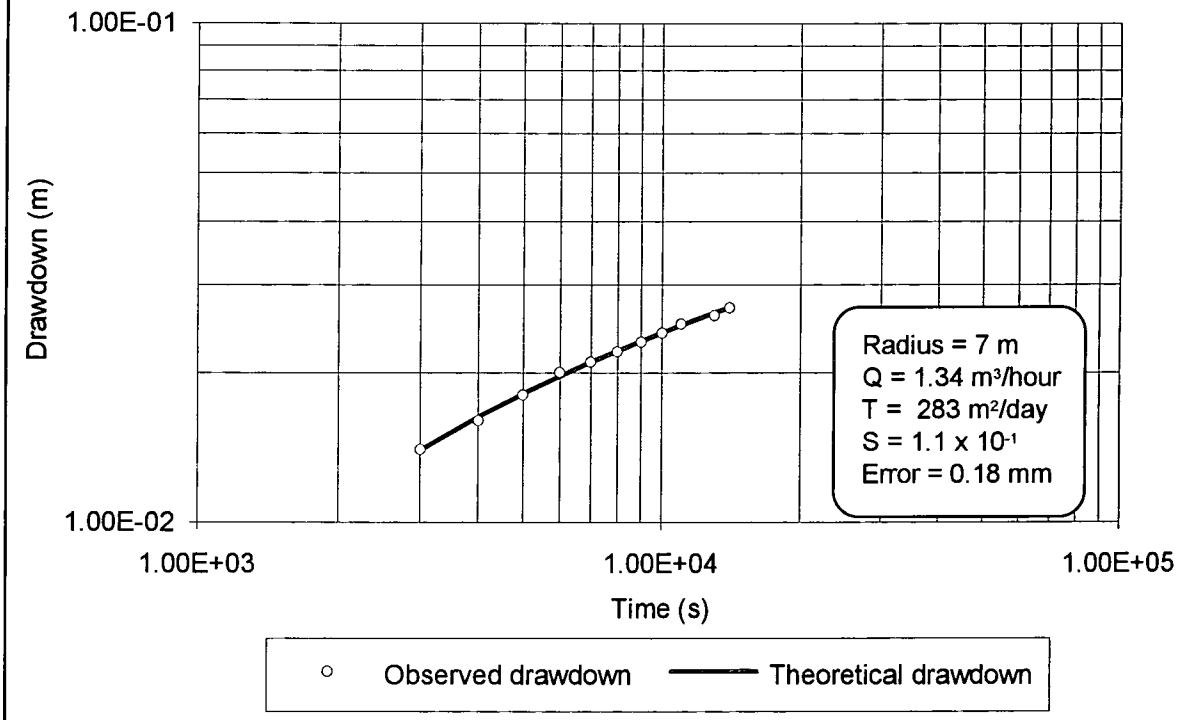

Figure 6.26: THEIS analysis of field pump test:
Borehole pumped: 17 Material: Gravel
Borehole observed: 16

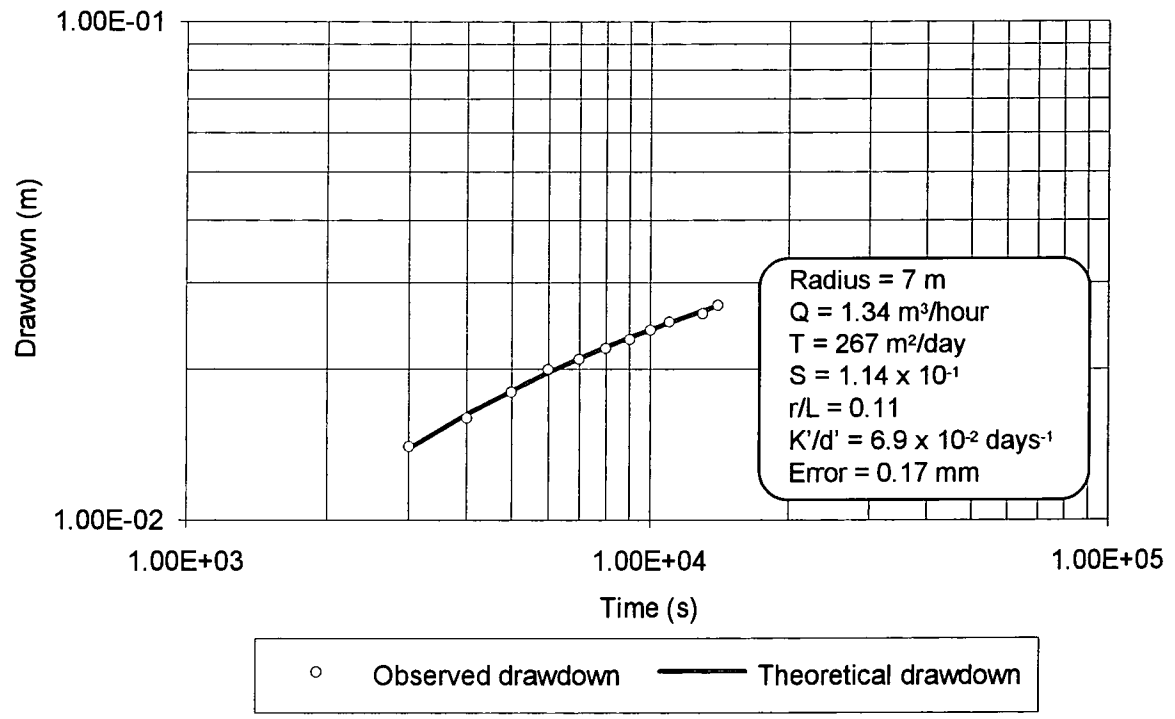

Figure 6.27: WALTON analysis of field pump test
Borehole pumped: 17 Material: Gravel
Borehole observed: 16

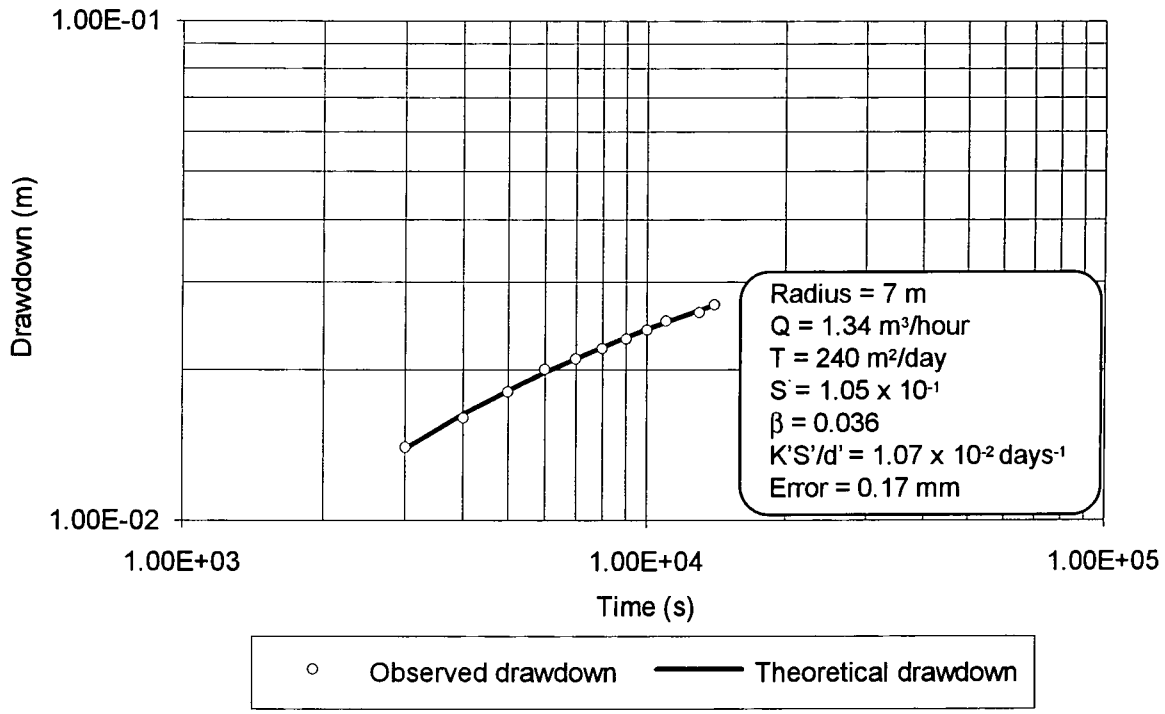

Figure 6.28: HANTUSH analysis of field pump test
Borehole pumped: 17 Material: Gravel
Borehole observed: 16

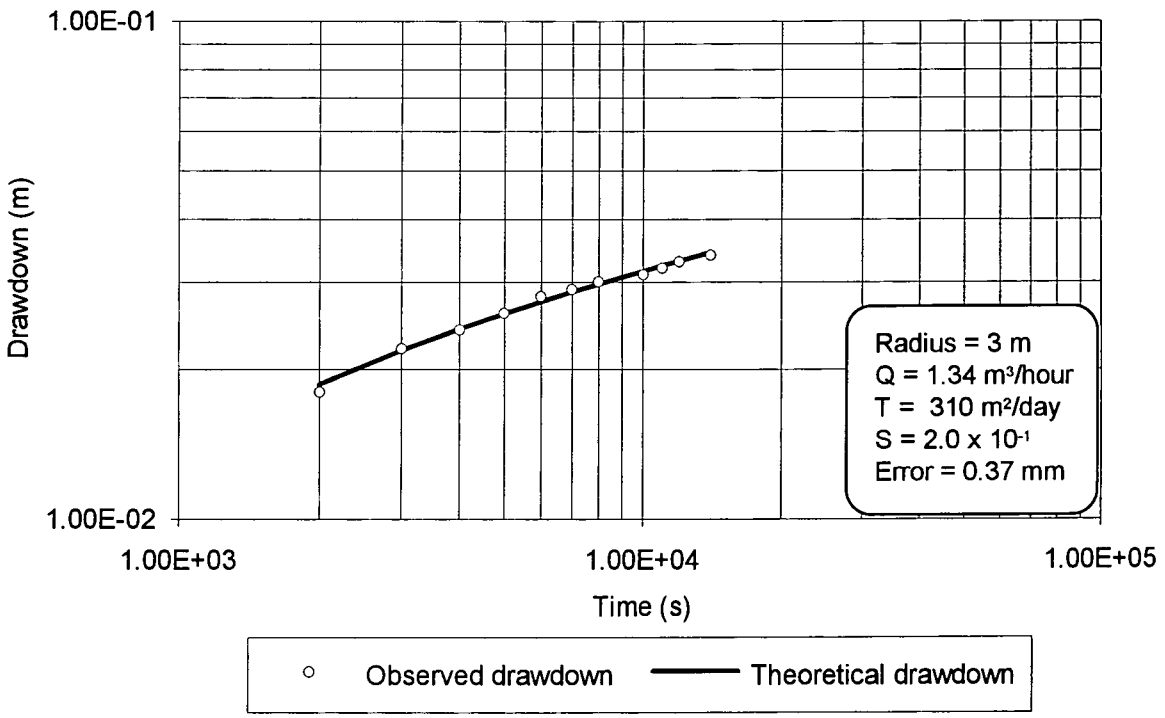

Figure 6.29: THEIS analysis of field pump test
Borehole pumped: 17 Material: Gravel
Borehole observed: 18

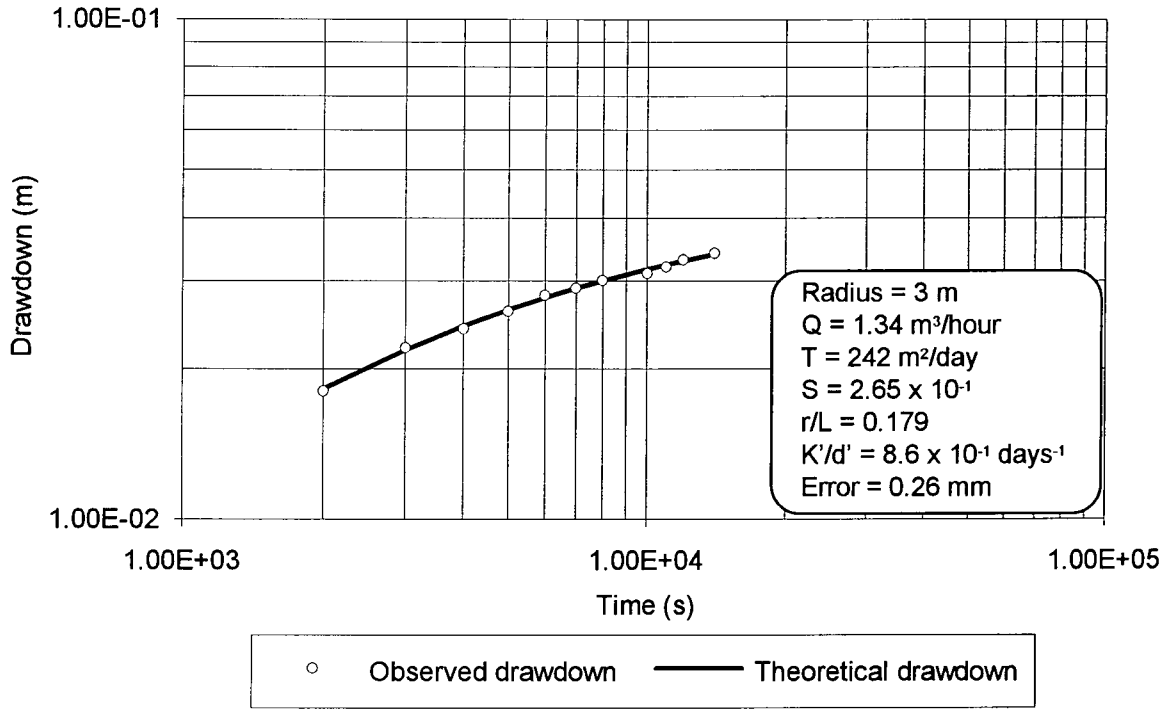

Figure 6.30: WALTON analysis of field pump test
Borehole pumped: 17 Material: Gravel
Borehole observed: 18

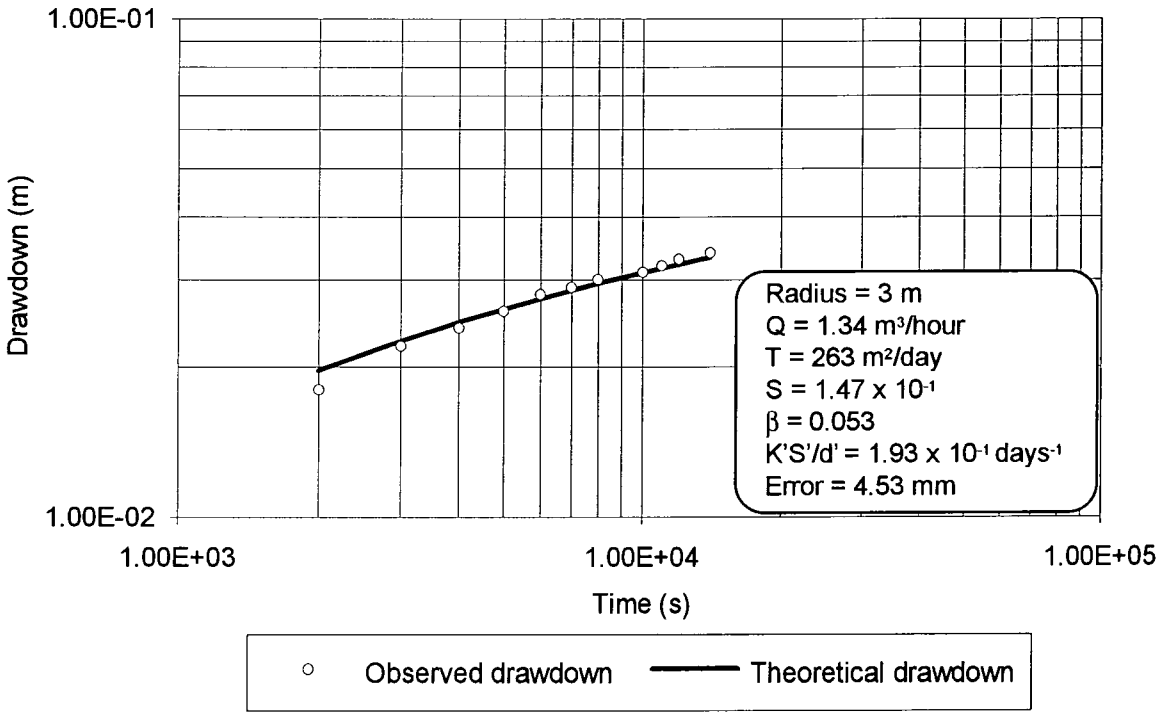

Figure 6.31: HANTUSH analysis of field pump test
Borehole pumped: 17 Material: Gravel
Borehole observed: 18

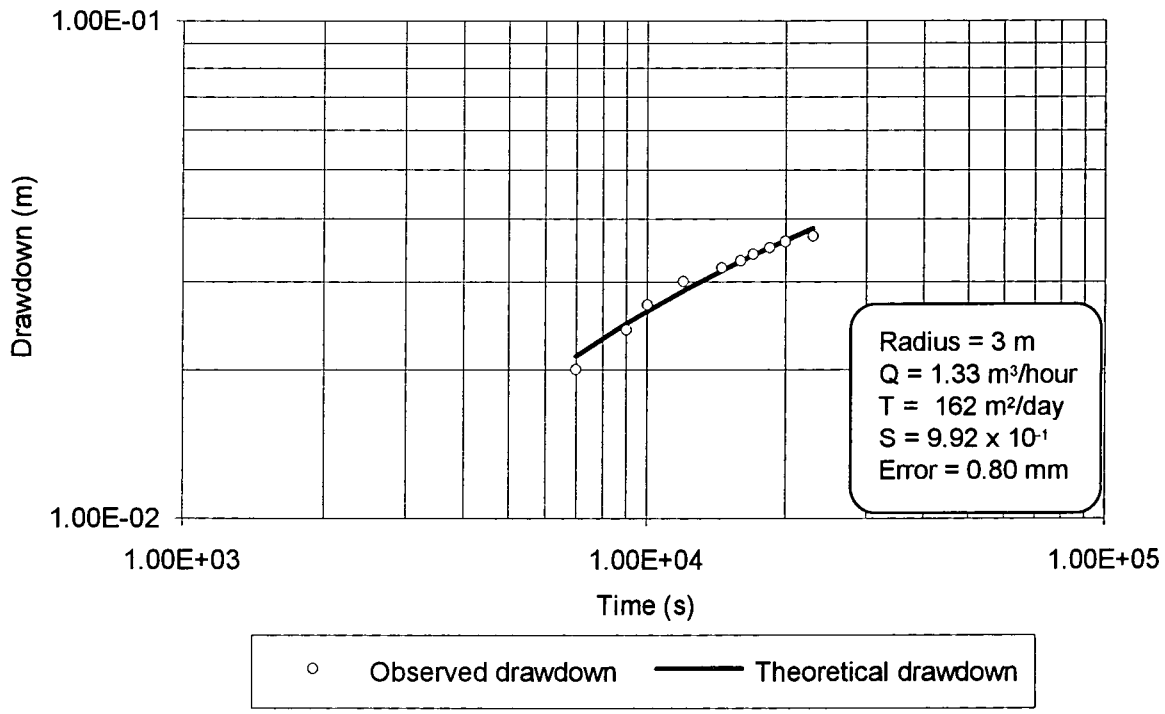

Figure 6.32: THEIS analysis of field pump test
Borehole pumped: 18 Material: Gravel
Borehole observed: 17

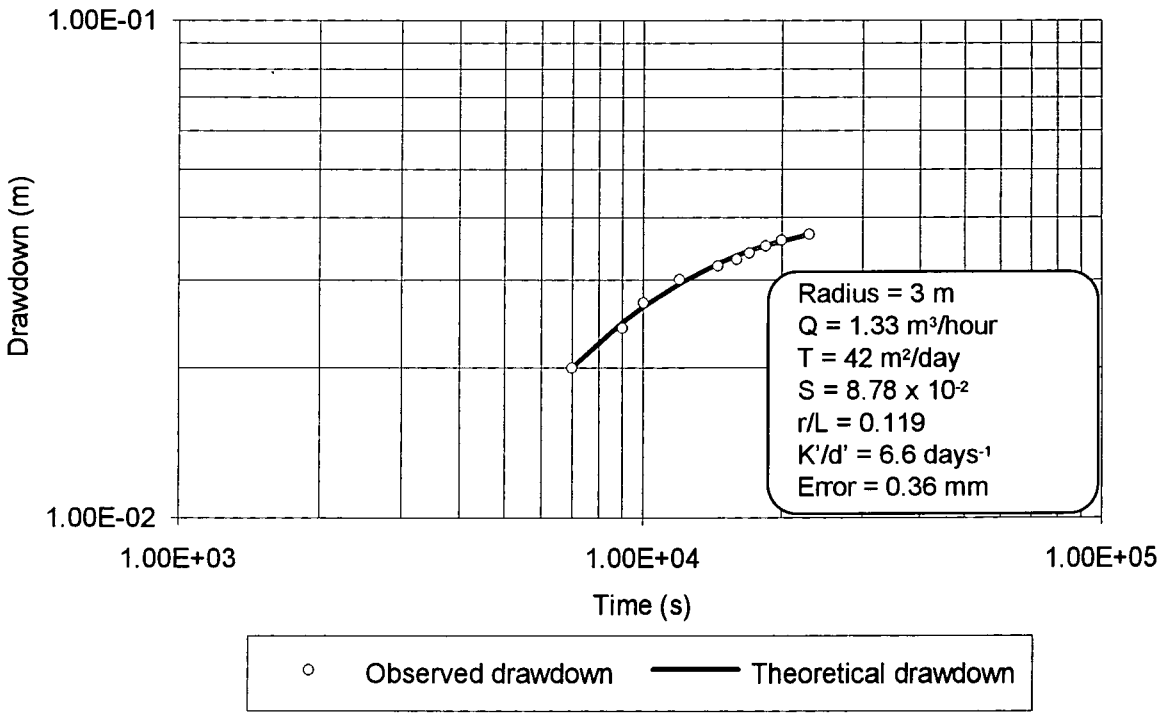

Figure 6.33: WALTON analysis of field pump test
Borehole pumped: 18 Material: Gravel
Borehole observed: 17

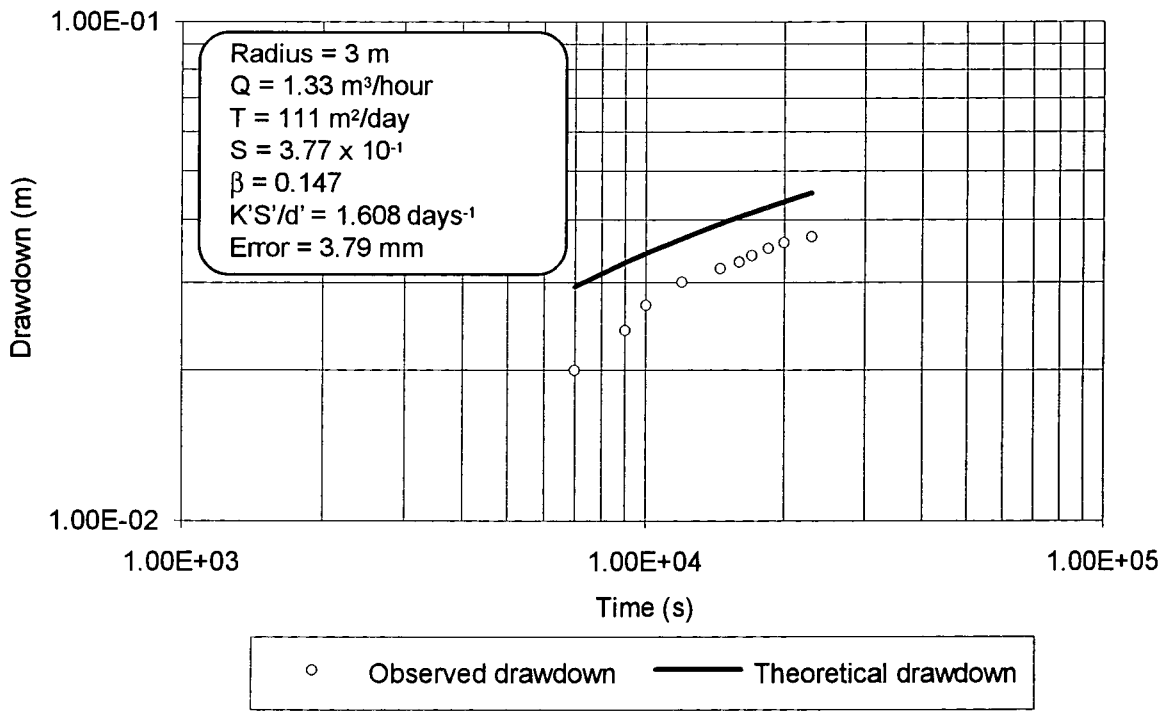

Figure 6.34: HANTUSH analysis of field pump test
Borehole pumped: 18 Material: Gravel
Borehole observed: 17

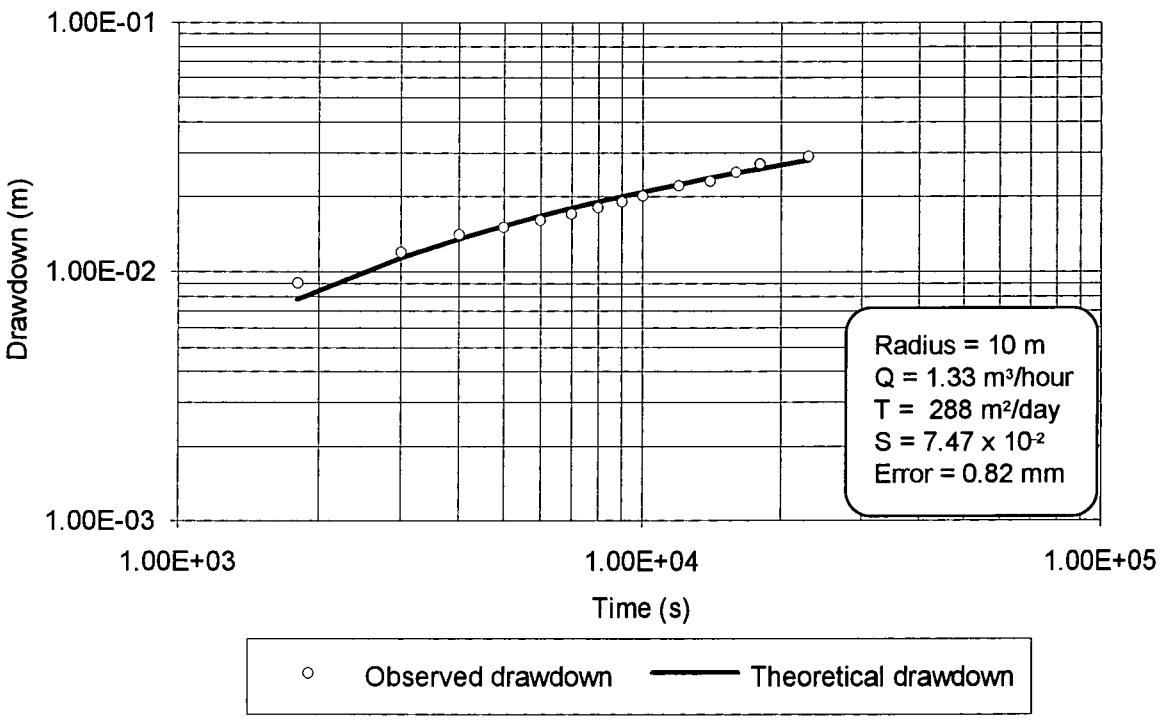

Figure 6.35: THEIS analysis of field pump test
Borehole pumped: 18 Material: Gravel
Borehole observed: 16

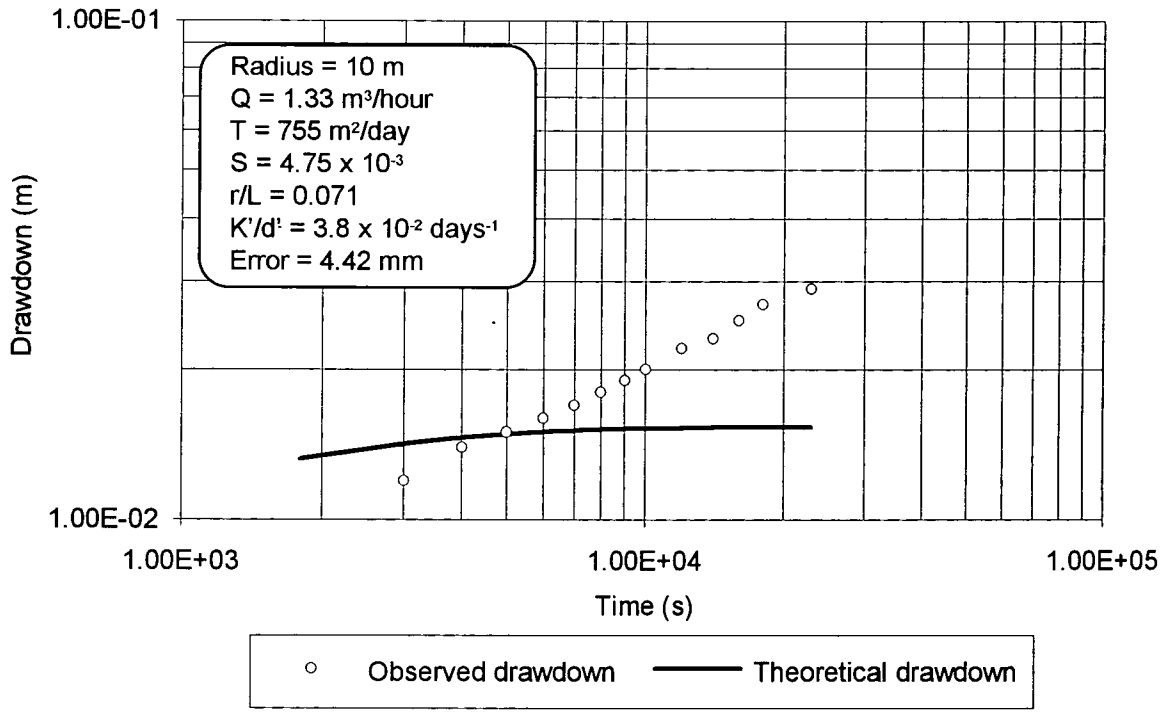

Figure 6.36: Walton analysis of field pump test
Borehole pumped: 18 Material: Gravel
Borehole observed: 16

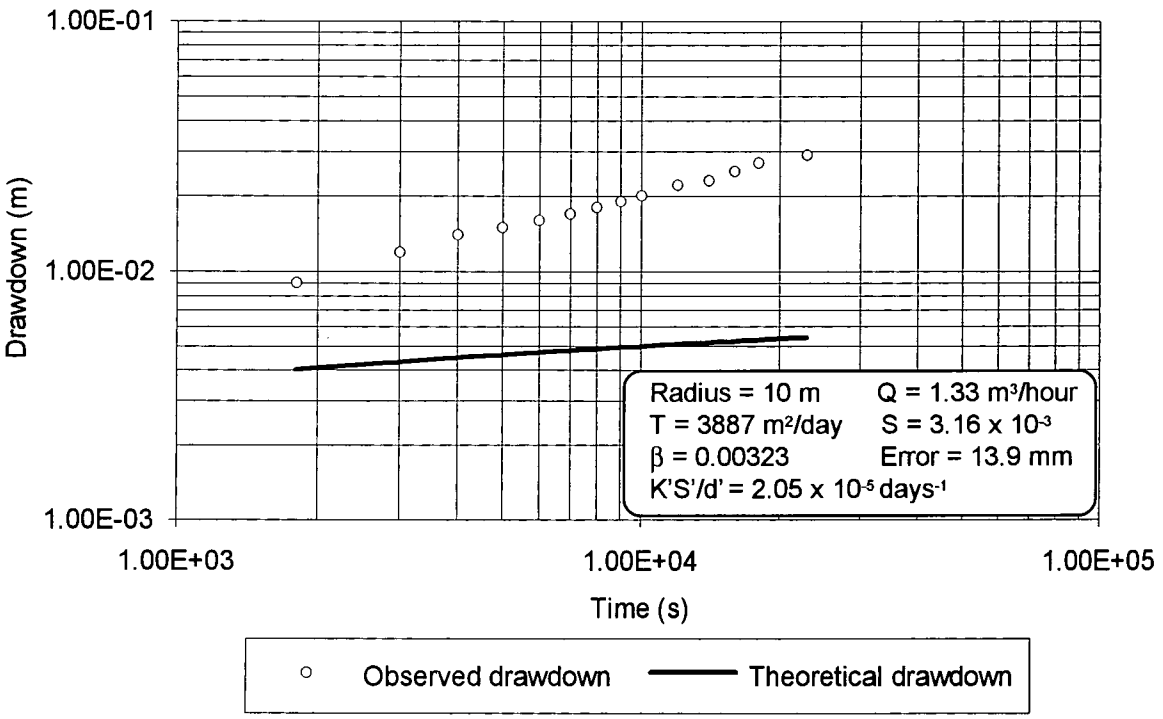

Figure 6.37: Hantush analysis of field pump test
Borehole pumped: 18 Material: Gravel
Borehole observed: 16

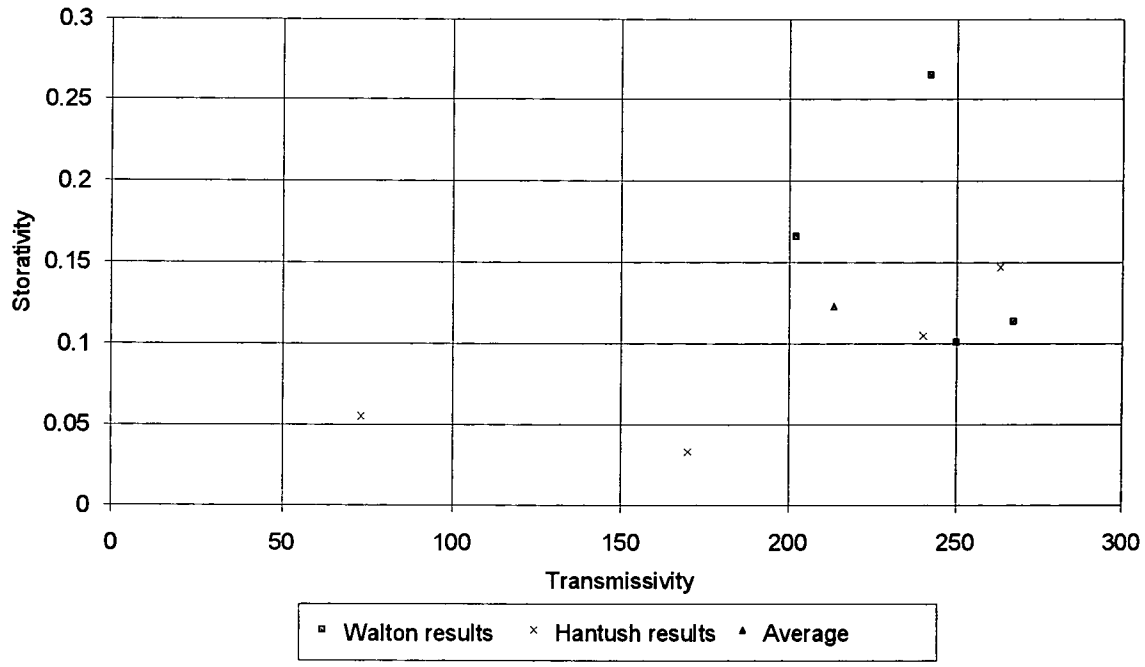

Figure 6.38: Comparison of aquifer parameters in the gravel layer

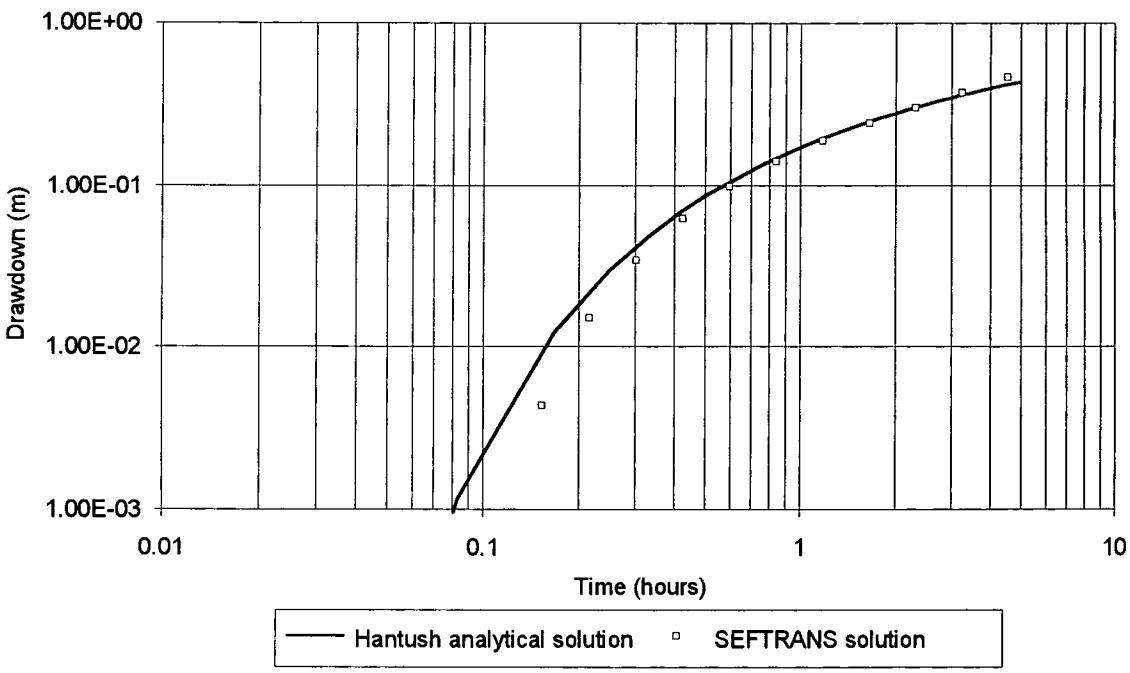

Figure 6.39: Comparison of the Hantush analytical and the SEFTRANS numerical solutions

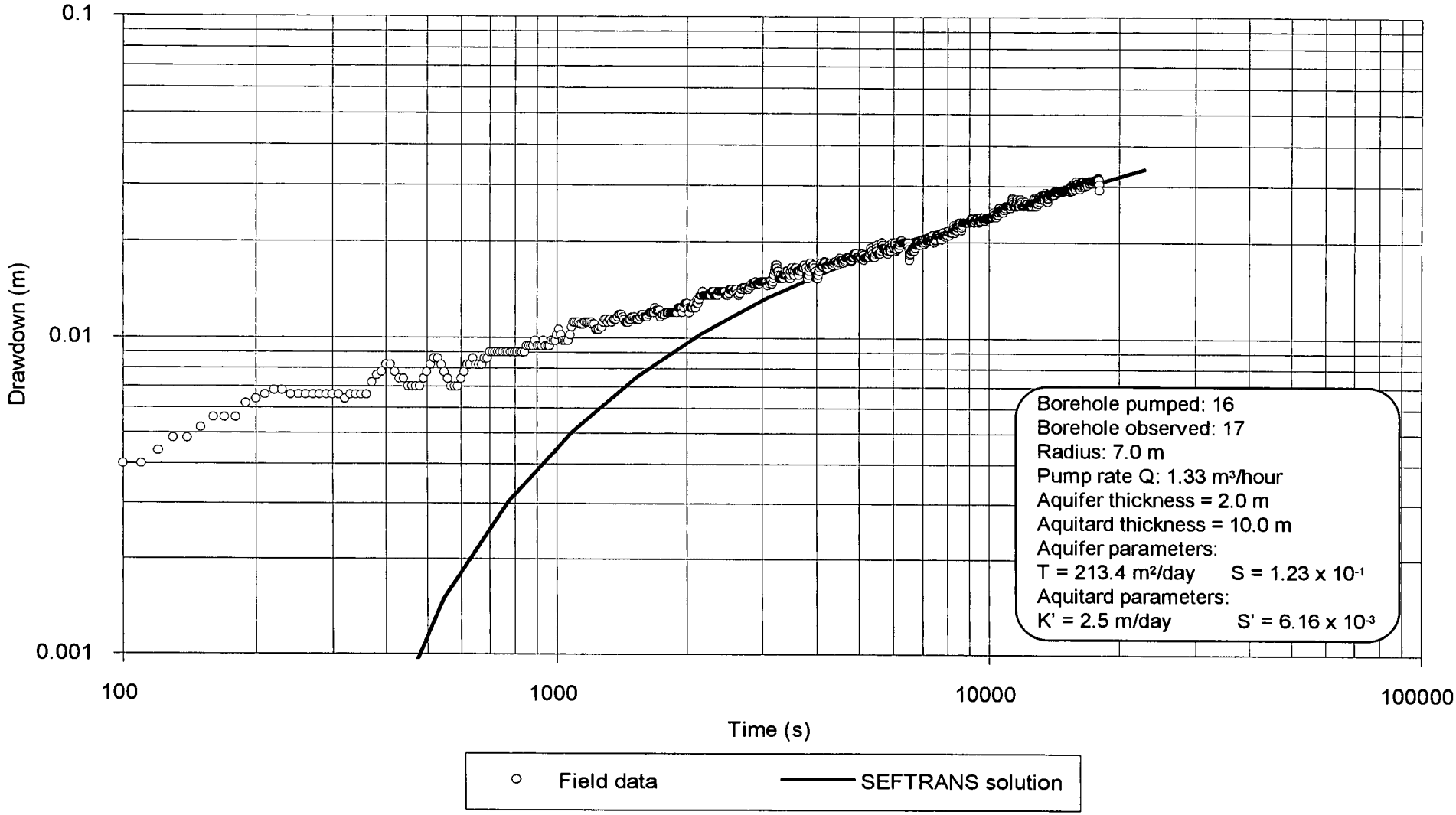

Figure 6.40: Comparison of pump test field data and the SEFTRANS numerical solution

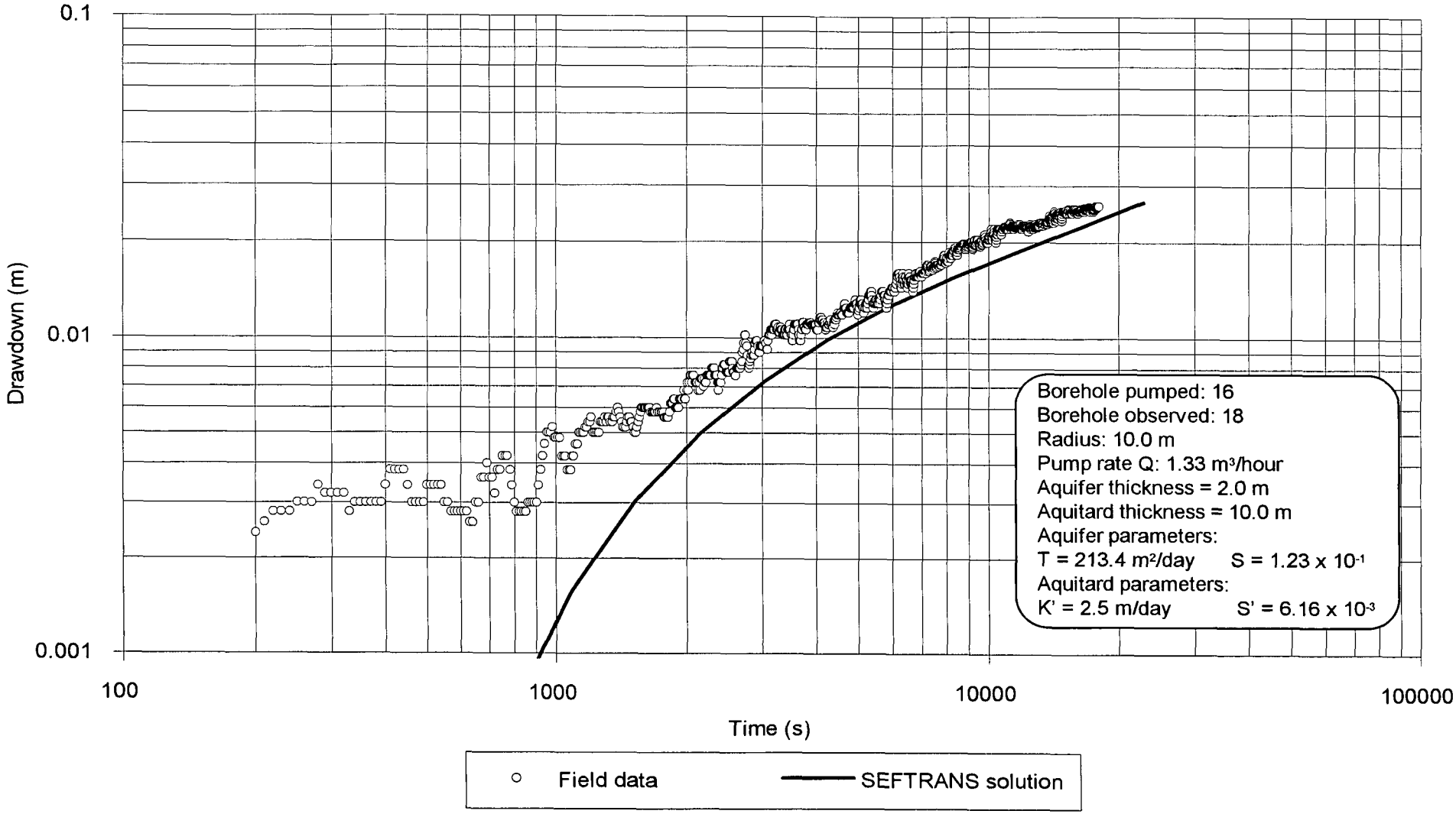

Figure 6.41: Comparison of pump test field data and the SEFTRANS numerical solution

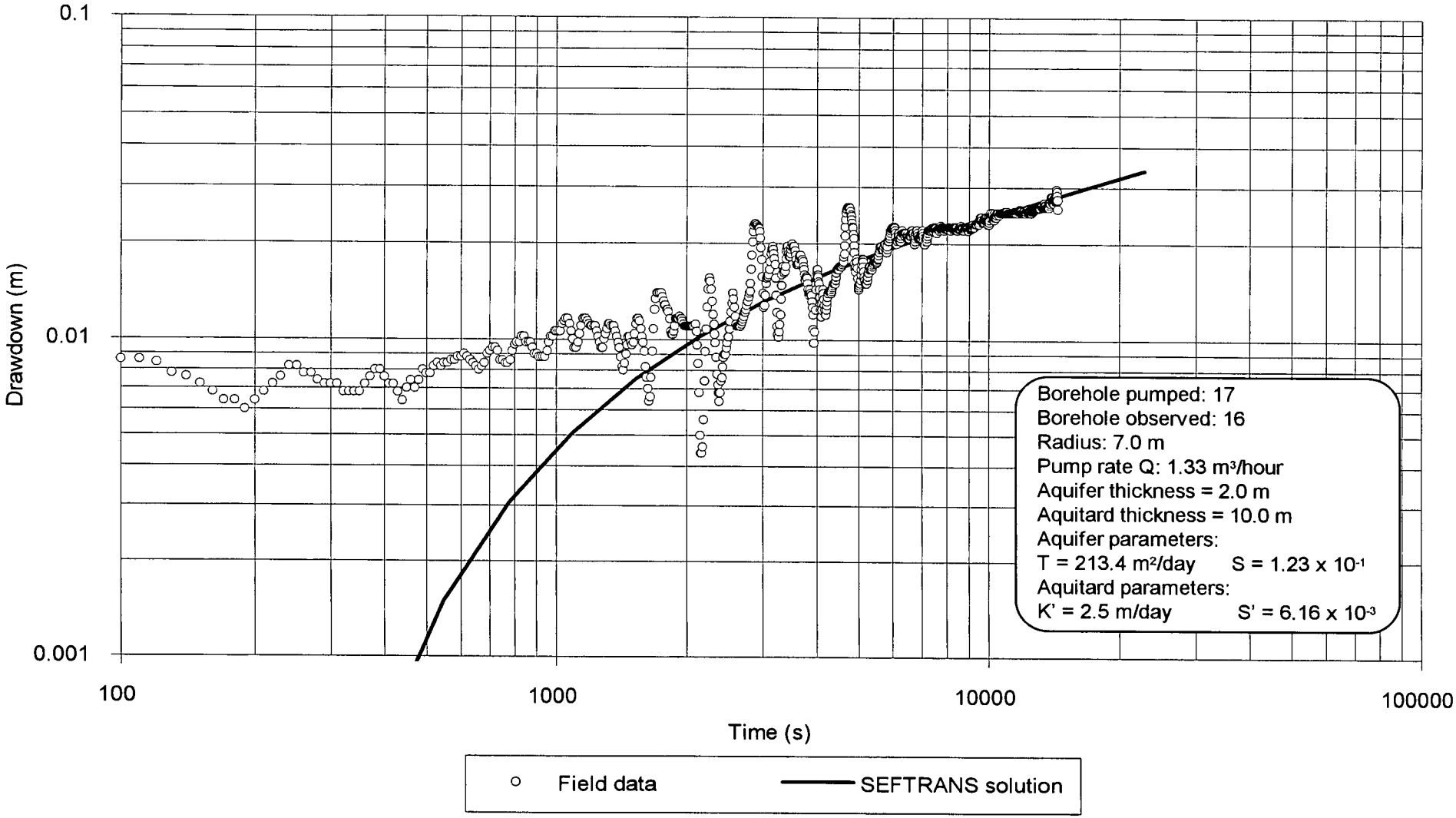

Figure 6.42: Comparison of pump test field data and the SEFTRANS numerical solution

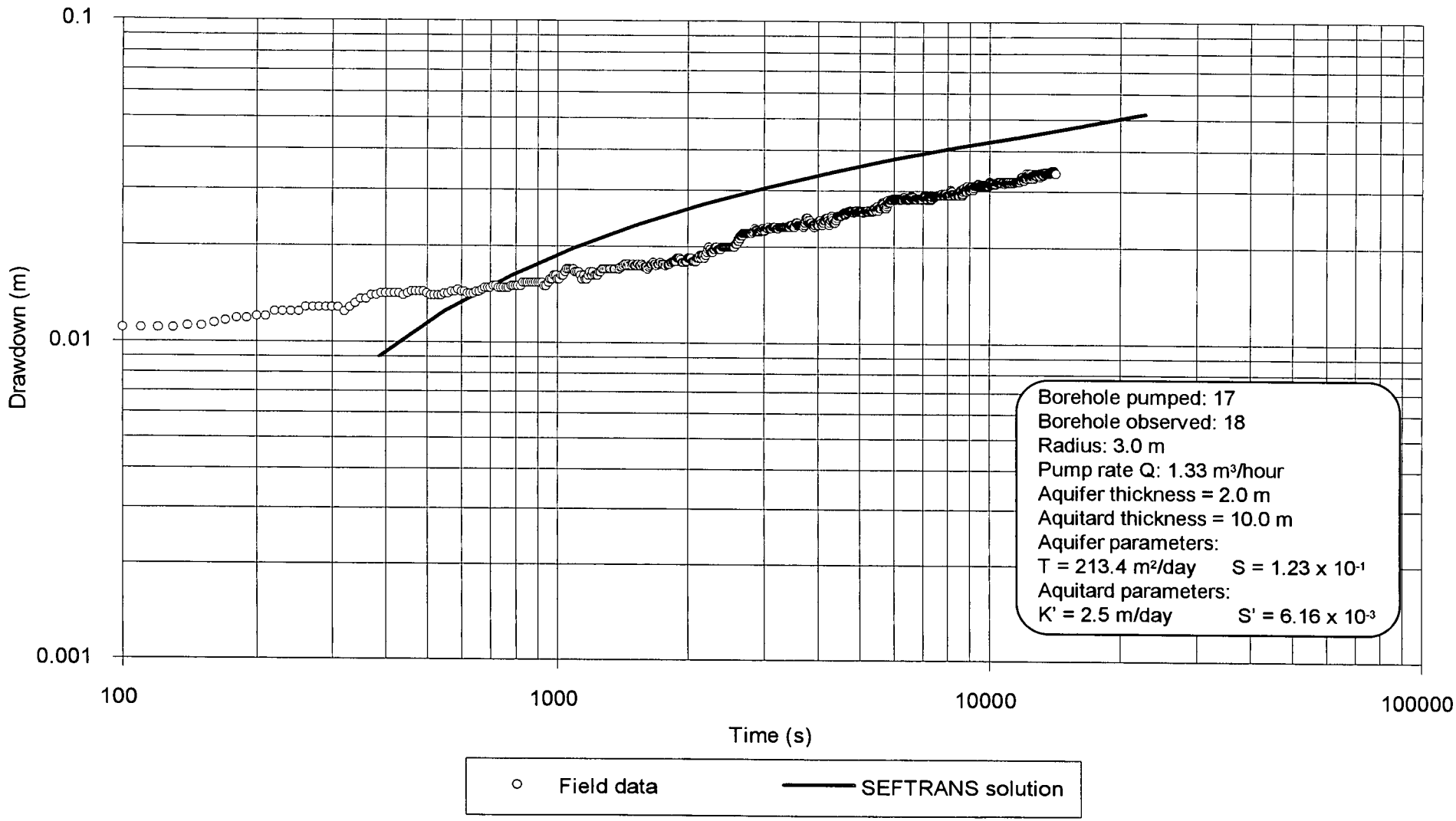

Figure 6.43: Comparison of pump test field data and the SEFTRANS numerical solution

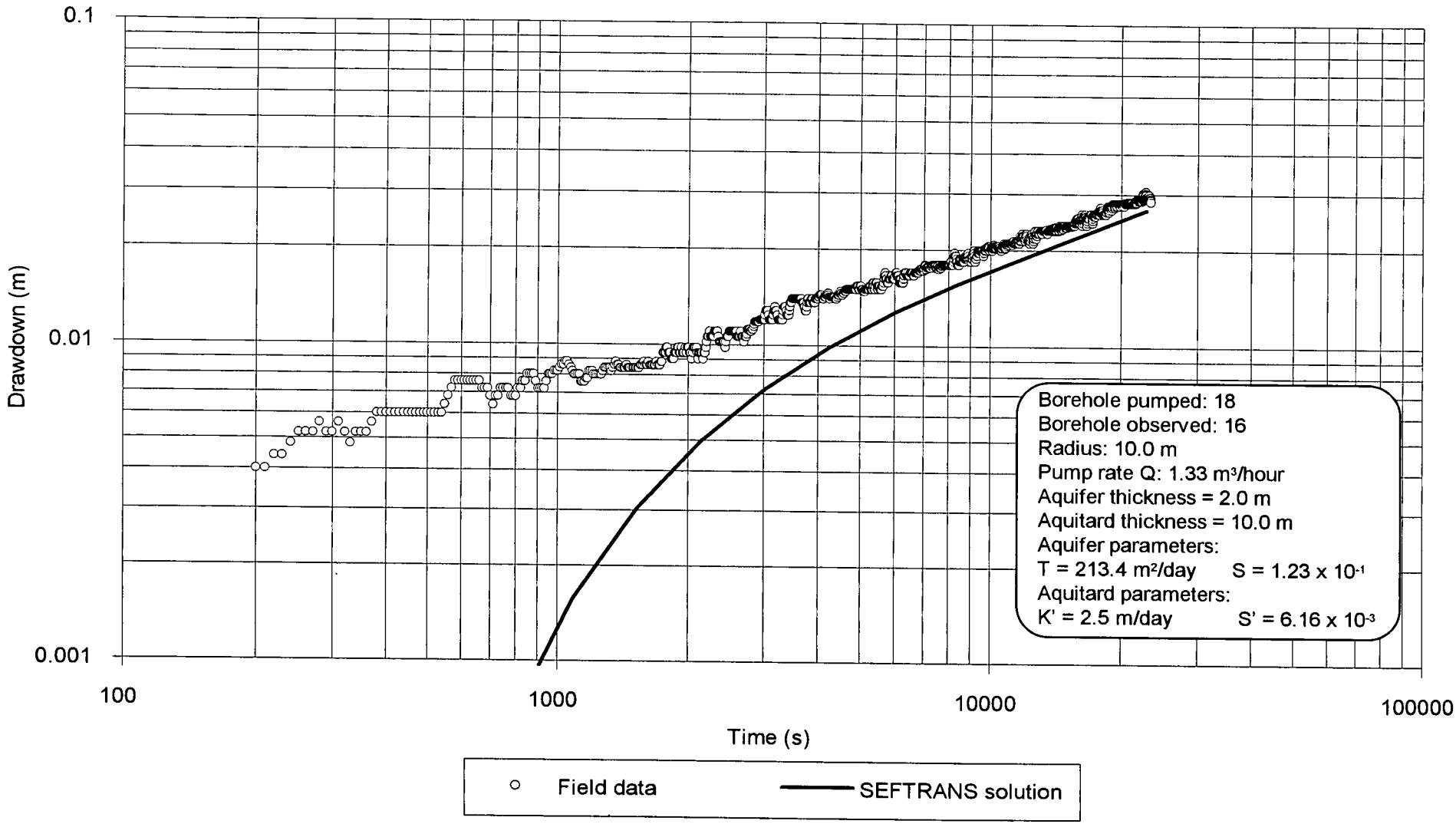

Figure 6.44: Comparison of pump test field data and the SEFTRANS numerical solution

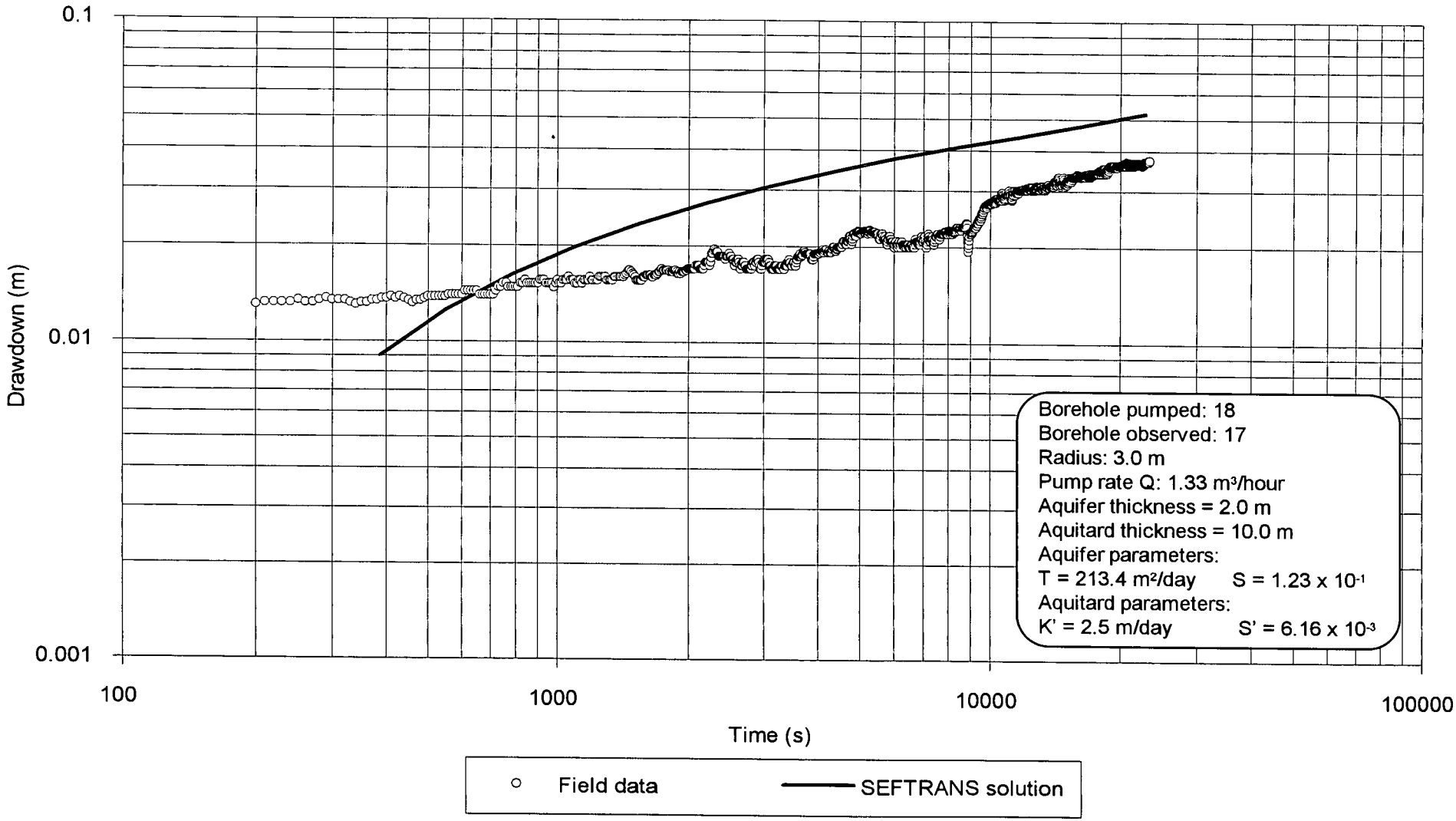

Figure 6.45: Comparison of pump test field data and the SEFTRANS numerical solution

Chapter 7

Sensitivity of groundwater models to parameter variation

7.1. Introduction

The least squares analysis used by the programmes developed during this research calculate the parameters which give the best fit between the observed and theoretical values of drawdown. This technique is based on the calculation of the change in theoretical drawdown due to a change in the aquifer parameters. This chapter examines the importance of the derivatives of drawdown with respect to these parameters, or the sensitivity of a theoretical aquifer system to a change in the aquifer parameters.

The drawdown in any pumping test can be determined if a number of parameters are known. For a confined system, this drawdown may be written as a function of the following variables:

$$s = f\{Q, t, r, T, S\}$$

The flowrate, time and radius may all be easily measured. In confined aquifers, the transmissivity and storativity must be evaluated. It is unlikely that these will be estimated accurately, due, for example, to measurement errors during aquifer tests or inconsistency of the aquifer geology. When leaky aquifers are investigated, the vertical permeability and storativity of the aquitard present further unknowns. If the sensitivity coefficients are evaluated and understood, a hydrogeologist will understand more fully the mechanism of flow within an aquifer system. The coefficients may also be used to evaluate the significance of errors, as the coefficients represent the potential change in theoretical drawdown for a small change in the relevant parameter.

7.2. Previous work

A significant amount of work has been completed previously in this area, notably by McElwee and Yukler (1978) and Cobb, McElwee and Butt (1982). They defined the 'sensitivity coefficients' for confined (Theis) and leaky (Walton) systems, and examined how these parameters vary in space and time. This work will be expanded in this chapter to include the leaky solution from Hantush.

Cheng and Ouazar (1995) also developed a method of determining the drawdown due to pumping in a confined aquifer using stochastic analysis. This takes into account the uncertainty in the information about the hydrogeological properties. The stochastic solution includes this estimated variation in the aquifer parameters, corrects the drawdown and calculates its variance. It thus gives a solution to drawdown, including the errors that are involved in the evaluation procedure.

7.3. Confined aquifers - sensitivity of the Theis solution

The sensitivity of the drawdown to changes in parameters for the Theis solution was examined by McElwee and Yukler (1978). A theoretical pumping test is used in all the following examples to demonstrate the concepts being discussed. The parameters used to generate these values are as follows:

Transmissivity (T) = 500 m^2/day

Storativity (S) = 1.0×10^{-3}

Discharge rate (Q) = 25 m^3/hour

7.3.1. Sensitivity to transmissivity

The theoretical distribution of drawdown with radius after 30 minutes of pumping in a confined aquifer is presented in Figure 7.1. The curve represents a cross-section through the cone of depression. These curves show how the influence of the pumping has not

effected the drawdown further than 500 metres from the well. As pumping continues, the cone of depression will expand, thus creating drawdown further and further from the well.

Figure 7.2 examines more closely the portion of the curve between 100 and 200 metres from the well. This is the region where the curves for different values of transmissivity cross. As an equal amount of water has been removed from the aquifer, the cone of depression for each value of transmissivity must be of equal volume. For the case of reduced transmissivity, the drawdown near the well is greater. Further from the well, this drawdown reduces to zero. If the case of increased transmissivity is considered, near the well the drawdown will be less. Both curves tend to zero drawdown at a finite distance from the well. However, in order that the volume of the cone of depression is equal for both cases, the curves swap over, which is seen at a radius of 140 metres from the pumped well.

The sensitivity to transmissivity can be further examined by considering the first derivative of the theoretical Theis solution with respect to transmissivity. This was defined in section 4.2.5 as:

$$\frac{\partial s}{\partial T} = \frac{Q}{4\pi T^2} \cdot \left(e^{-u} - W(u)\right) \qquad (7.1)$$

Figure 7.3 shows how $\partial s/\partial T$ varies with radius. It is obvious that it diverges near the well, and so this is the region where the theoretical drawdown is particularly sensitive to a change of transmissivity. It can also be seen that the sign of the function becomes positive at a radius of 140 m. The radius where the function becomes positive corresponds with the radius where the curves in Figure 7.2 cross. Figures 7.2 and 7.3 show that changing the transmissivity will theoretically lead to a shallower cone of depression in some regions, whereas in others it will deepen.

Figure 7.4 investigates the effect of radius and transmissivity on the time dependence of $\partial s/\partial T$. This shows that at different values of radius, the curves have an identical shape,

and further from the well $\partial s/\partial T$ has less effect at any given time. In the region of 10 m radius, the effect of varying the transmissivity on $\partial s/\partial T$ is plotted. This shows that a reduction in transmissivity decreases the sensitivity, and an increase in transmissivity increases the sensitivity. This is because an increase in transmissivity will reduce drawdown, and so changing the transmissivity will create a change in drawdown that is proportionately greater.

7.3.2. Sensitivity to storativity

A similar approach may be taken to observe the sensitivity of confined aquifers to the storage coefficient. Figure 7.5 shows the effect of varying storage on drawdown. Unlike the transmissivity case, changing the storativity just causes a general raising or lowering of the water table. The changes in drawdown due to a 20% change in the storage coefficient are much less than those for a 20% change in the transmissivity. However, the changes in drawdown due to varying the storage coefficient are significant over a greater radius, shown by the comparison of Figures 7.1 and 7.5.

The first derivative of the Theis equation with respect to storativity may be recalled from section 4.2.5 as:

$$\frac{\partial s}{\partial S} = -\frac{Q}{4\pi TS} \cdot e^{-u} \qquad (7.2)$$

The radial variation of $\partial s/\partial S$ is shown in Figure 7.6. There is no change in sign, just a general raising or lowering of the water table, the effect of which decreases with distance from the well. The time dependence of $\partial s/\partial S$, shown in Figure 7.7 for radii of 10, 100 and 250 m shows that $\partial s/\partial S$ tends towards a steady state value. The curves are identical, but displaced in time as the distance from the well increases.

7.4. Leaky aquifers - sensitivity of the Walton solution

The sensitivity coefficients for the Walton solution were examined by Cobb, McElwee and Butt (1982). This was part of a least squares programme which estimated aquifer parameters using the Walton solution. A theoretical pumping test is used to examine and compare the sensitivity coefficients for the Walton solution. The parameters used in the theoretical pumping test are:

Transmissivity (T)	= 500 m^2/day
Storativity (S)	= 1.0 x 10^{-3}
Discharge rate (Q)	= 25 m^3/hour
Leakage factor (K'/d')	= 1.0 x 10^{-3} $days^{-1}$

7.4.1. Sensitivity to transmissivity

The Walton equation was differentiated with respect to transmissivity in section 4.3. Recalling this equation:

$$\frac{\partial s}{\partial T} = -\frac{Q}{4\pi T^2} \cdot \left\{ W(u,r/L) + \frac{\partial W(u,r/L)}{\partial u} \cdot u + \frac{\partial W(u,r/L)}{\partial r/L} \cdot \frac{r/L}{2} \right\} \qquad (7.3)$$

The effect of increasing radius on this function is shown in Figure 7.8. The function exhibits a similar curve to that of the confined condition. The variation of $\partial s/\partial T$ with time is shown in Figure 7.9, at radii of 10 and 50 m. This diagram also shows the effect of increasing and reducing the transmissivity by 20%. They show that towards late time, the value of $\partial s/\partial T$ tends to a steady state value. This is the time where all the discharge is derived from leakage through the aquitard, rather than from the aquifer itself.

7.4.2. Sensitivity to storativity

The first derivative of the Walton solution with respect to storativity was derived in section 4.3. Recalling this equation:

$$\frac{\partial s}{\partial S} = \frac{Qr^2}{4\pi T} \cdot \left(\frac{\partial W(u, r/L)}{\partial u} \right) \tag{7.4}$$

The radial dependence of $\partial s/\partial S$, and the sensitivity to changes in S are shown in Figure 7.10. The graph is similar to the Theis case, as the distance from the pumped well increases the effect of $\partial s/\partial S$ is decreased. The effect of reducing S is to increase the value of $\partial s/\partial S$, and vice-versa. The time dependence of $\partial s/\partial S$ at radii of 10, 100 and 250 metres is shown in Figure 7.11. The maximum value of $\partial s/\partial S$ is achieved at a time proportional to the radial distance from the well. At early time, storage from the aquifer supplies the discharge, so the value of $\partial s/\partial S$ increases. However, leakage through the aquitard begins to contribute to discharge. The value of $\partial s/\partial S$ reaches a peak value, and then tends to zero. Before the curves tend to zero there is a dual source of leakage and storage supply the discharge.

7.4.3. Sensitivity to leakage

The first derivative of the Walton equation with respect to the dimensionless variable r/L was evaluated in section 4.3 as:

$$\frac{\partial s}{\partial (r/L)} = \frac{Q}{4\pi T} \cdot \left(\frac{\partial W(u, r/L)}{\partial (r/L)} \right) \tag{7.5}$$

The radial dependence of $\partial s/\partial (r/L)$ is shown in Figure 7.12. The curves are not divergent near the well, and the effect of $\partial s/\partial (r/L)$ is reduced as the distance from the well increases. Figure 7.13 shows the time dependence of $\partial s/\partial (r/L)$ at radii of 10 and 50 metres from the well. The effect of varying L is also shown for the 10 metre case. The curves show that $\partial s/\partial (r/L)$ increases and then tends to steady state. This is where the entire discharge is from leakage. The curves at 10 metre radius and different values of L cross after approximately one day. This crossover point is again because of the dual source to discharge. The L + 20% curve represents less leakage, or a higher aquitard vertical permeability. Thus when water is released from storage in the aquifer at early time, the $\partial s/\partial (r/L)$ term is less important. However, when all the discharge is derived from

leakage, the sensitivity of drawdown to changing L is greater, so the steady state value of $\partial s/\partial(r/L)$ is of greater magnitude. The inverse is true for the case of L - 20%.

7.5. Leaky aquifers - sensitivity of the Hantush solution

The sensitivity coefficients of the Hantush solution are examined in the same manner. The parameters used in the pumping test used to demonstrate the features of the sensitivity coefficients are:

Transmissivity (T)	= 500 m^2/day
Storativity (S)	= 1.0×10^{-3}
Discharge rate (Q)	= 25 m^3/hour
Aquitard permeability (K'/d')	= 1.0×10^{-3} $days^{-1}$
Aquitard storativity (S')	= 1.0×10^{-3}

7.5.1. Sensitivity to transmissivity

The Hantush solution to drawdown in a leaky aquifer was differentiated with respect to transmissivity in section 4.4.3. This was presented as:

$$\frac{\partial s}{\partial T} = -\frac{Q}{4\pi T^2} \cdot \left\{ W(u,\beta) + \frac{\partial W(u,\beta)}{\partial u} \cdot u + \frac{\partial W(u,\beta)}{\partial \beta} \cdot \frac{\beta}{2} \right\} \qquad (7.6)$$

The change in $\partial s/\partial T$ with radius is shown in Figure 7.14. The curve, as for both the Theis and Walton case, is divergent near the well and changes sign. Figure 7.15 shows the effect of time and transmissivity on the time dependence of $\partial s/\partial T$. These curves show that the effect of reducing the transmissivity increases the sensitivity of the system to changes in transmissivity, and vice-versa. Also, the effect is more pronounced for an increase than a reduction in transmissivity.

7.5.2. Sensitivity to storativity

The sensitivity to storativity was evaluated in section 4.4.3, and reported as:

$$\frac{\partial s}{\partial S} = \frac{Q}{4\pi T} \cdot \left\{ \frac{\partial W(u,\beta)}{\partial u} \cdot \frac{u}{S} - \frac{\partial W(u,\beta)}{\partial \beta} \cdot \left(\frac{\beta}{2S} \right) \right\} \qquad (7.7)$$

The change in $\partial s/\partial S$ with radius is shown in Figure 7.16. This is similar to the Walton case, as near the well $\partial s/\partial S$ is not divergent, and the value tends to zero as distance from the pumped well increases. However, the curves of S + 20% and S - 20% cross at a radius of 100 metres. The reason for this can be evaluated by considering the process of the flow of water to a well within a theoretical Hantush leaky system. For the case of S + 20%, the drawdown in the aquifer will be less as a greater proportion of water is released from storage. This in turn reduces the head difference between the aquifer and aquitard, thus reducing the leakage from the aquitard. The effect of changing the storativity of the aquifer on the drawdown will be greater, as the contribution to discharge from the aquifer storage is now a proportionally larger part.

As the distance from the pumped well increases, the head difference between the aquifer and the aquitard is reduced as the effects of pumping have not yet reached this area. The value of $\partial s/\partial S$ is then similar to that of the confined case, and the curves of S + 20% and S - 20% change sides. It is interesting to note that the Walton case does not exhibit the same behaviour. This is because the Hantush case takes the storage of the aquitard into account. The leakage at early time comes from storage in the aquitard. The leakage for the Walton solution is derived from water leaking through the aquitard from an overlying aquifer to the pumped aquifer. Thus the effect of changing the head between the aquifer and aquitard is different in the two cases, reflected by these figures.

Figure 7.17 shows the change of $\partial s/\partial S$ with time. This again shows the dual source which supplies discharge in leaky aquifers. The effect of changing the storativity near the front of the cone of depression is great. This is reduced as time increases.

7.5.3. Sensitivity to aquitard parameters

The sensitivity to the aquitard parameters, *K'S'/d'*, was presented in section 4.4.3 as:

$$\frac{\partial s}{\partial \gamma} = \frac{Q}{4\pi T} \cdot \frac{\partial W(u,\beta)}{\partial \beta} \cdot \frac{\beta}{2\gamma} \qquad (7.8)$$

where $\gamma = K'S'/d'$

Figure 7.18 shows the variation of $\partial s/\partial \gamma$ with radius, and the effect of increasing and decreasing γ. Increasing γ leads to greater leakage through the aquitard to the aquifer for any given head difference. Thus for the case of γ + 20%, the magnitude of $\partial s/\partial \gamma$ is reduced as changing γ when there is more leakage will have less effect on the aquifer drawdown. The reverse is true for the case of γ - 20%.

The variation of $\partial s/\partial \gamma$ with time in a leaky aquifer is shown in Figure 7.19 for the Hantush solution. The effect of increasing the leakage is again to reduce $\partial s/\partial \gamma$, and reducing the leakage increases $\partial s/\partial \gamma$. The graph shows $\partial s/\partial \gamma$ at radii of 10 and 50 metres. These curves are coincident. This implies that the distance from the pumping well does not affect the value of $\partial s/\partial \gamma$. The values calculated of $\partial s/\partial \gamma$ are very high, in the order of 1.0×10^9, whereas the values of other sensitivity coefficients calculated are many magnitudes smaller, in the region of 1.0×10^2.

7.6. Comparison of common aquifer parameters

In this section the parameters common to all three aquifer types, $\partial s/\partial T$ and $\partial s/\partial S$, are compared as they change with radius and time. This enables the differences between the solutions to be evaluated.

Figure 7.20 shows how $\partial s/\partial T$ varies with radius. All of these curves are coincident, which shows that the difference between $\partial s/\partial T$ is negligible, when a confined or leaky system is considered. The variation of $\partial s/\partial T$ with time is shown in Figure 7.21 at a radius of 10 metres. This shows that $\partial s/\partial T$ continues increasing for the confined system, and does not achieve steady state. The Walton and Hantush curves are far more similar. They tend to

the same steady state value after a pumping period of one day. The value of $\partial s/\partial T$ is slightly less at early time for the Hantush case. This is because of the increased leakage as the aquitard storage is taken into account. However after the water has been released from storage at that radius in the aquitard, the two solutions converge.

The effect of radius on the value of $\partial s/\partial S$ is shown in Figure 7.22. All of the curves are a similar shape, tending to zero as distance from the pumped well increases. The initial value of the Walton curve is slightly less than the Theis curve, due to some leakage. The Hantush curve is a similar shape, but the effect of including the aquitard storage term is obvious. The initial value of $\partial s/\partial S$ is 15% less than the other two curves at the well. This difference reduces as distance from the well increases. This difference is the effect of including the storage of the aquitard, which contributes to discharge near the well where drawdown is greatest.

Figure 7.23 shows the variation of $\partial s/\partial S$ with time for each of the solutions. The confined solution is very different, as the value of $\partial s/\partial S$ tends towards a steady state value greater than zero. This is because in the confined solution, this is the only supply to discharge, so the effect of changing the storativity will always effect the drawdown. The Walton solution follows the confined solution at early time, but then leakage begins to contribute to discharge and the effect of the storage coefficient is reduced. Thus the impact on drawdown of changing the storage coefficient is reduced, and $\partial s/\partial S$ tends to zero. The Hantush curve does not follow the confined solution at all. The leakage from the aquitard storage at early time reduces the value of $\partial s/\partial S$. The peak value of $\partial s/\partial S$ occurs at an earlier time than the Walton case, but it tends to zero at a later time than the Walton curve. This is because of the added contribution to discharge from the aquitard storage, which reduces the quantity of water from the aquifer storage which is discharged during any period of time. Thus the effect of changing storativity will affect the aquifer drawdown over a longer period of time. The time when $\partial s/\partial S$ tends to zero is thus much later for the Hantush than the Walton case.

7.7. Discussion

The sensitivity coefficients may be used to examine the influence of a change of aquifer parameters on the drawdown due to pumping. The coefficients form an important part of the least squares algorithm developed during this research, which calculates the 'best fit' aquifer parameters.

If a confined system is considered, the change in drawdown, Δs, due to a small change in an aquifer parameter, was defined in section 4.2.4 as:

$$(s+\Delta s)_i = s_i + \frac{\partial s}{\partial T}\cdot \Delta T + \frac{\partial s}{\partial S}\cdot \Delta S \qquad (7.9)$$

Thus the sensitivity coefficients, $\partial s/\partial T$ and $\partial s/\partial S$, control the magnitude of the change in drawdown, Δs. These coefficients may also be examined when considering a groundwater flow model. If a range of possible parameters is being investigated, knowledge of the sensitivity coefficients allows the hydrogeologist to easily evaluate the effect of changing any particular parameter.

The magnitude of the sensitivity coefficients change with the different solutions to drawdown that are examined, and are in proportion to the magnitude of the parameters themselves. The magnitude of the Hantush sensitivity coefficient, $\partial s/\partial \gamma$, is particularly large. However, this is multiplied by the small leakage factor, γ ($K'S'/d'$), to evaluate the change in drawdown.

For certain cases the convergence of the leaky aquifer programme, HANPUTS, was more difficult than for the CONPUTS or WALPUTS programmes when using the same input data. Either a number of different starting values were used, or several data points removed, before convergence was achieved. This may be explained by the nature of the sensitivity coefficient, $\partial s/\partial \gamma$. The magnitude of this coefficient is much greater than the other coefficients, $\partial s/\partial T$ and $\partial s/\partial S$.

The least squares algorithm calculates changes to each of the aquifer parameters which minimise the difference between the observed and theoretical values of drawdown. These changes, ΔT, ΔS and $\Delta\gamma$, are calculated by a series of mathematical formulae. As the best fit parameters are calculated the magnitude of the $\partial s/\partial\gamma$ term may prevent the parameter changes, ΔT, ΔS and $\Delta\gamma$ from tending to zero. This may be particularly evident where the theoretical drawdown curve does not fit the observed data well. This may induce an oscillation around the best fit parameters, or divergence from them. Oscillation in the calculated parameters was observed in the results from the HANPUTS programme on several occasions.

The difference between the Walton and Hantush cases is evident in a number of the graphs of the sensitivity coefficients. It is obvious that the effect of the storage of the aquitard does significantly impact the drawdown, especially at early time.

A practical application of the sensitivity coefficients could be to that of modelling the fieldwork. The two dimensional groundwater flow model was shown in chapter 6 to accurately model the recorded drawdown at 7 and 10 m from the well, but slightly over estimate it at 3 m from the well. The sensitivity coefficients for this system could be plotted against radius from the well. It may be possible to adjust one parameter so that the drawdown at a radius of 3 m would be slightly reduced, without significantly changing the drawdown at a greater distance. The impact of errors in the parameters could also be examined, from the change in drawdown that would result from a slight change in the calculated parameters.

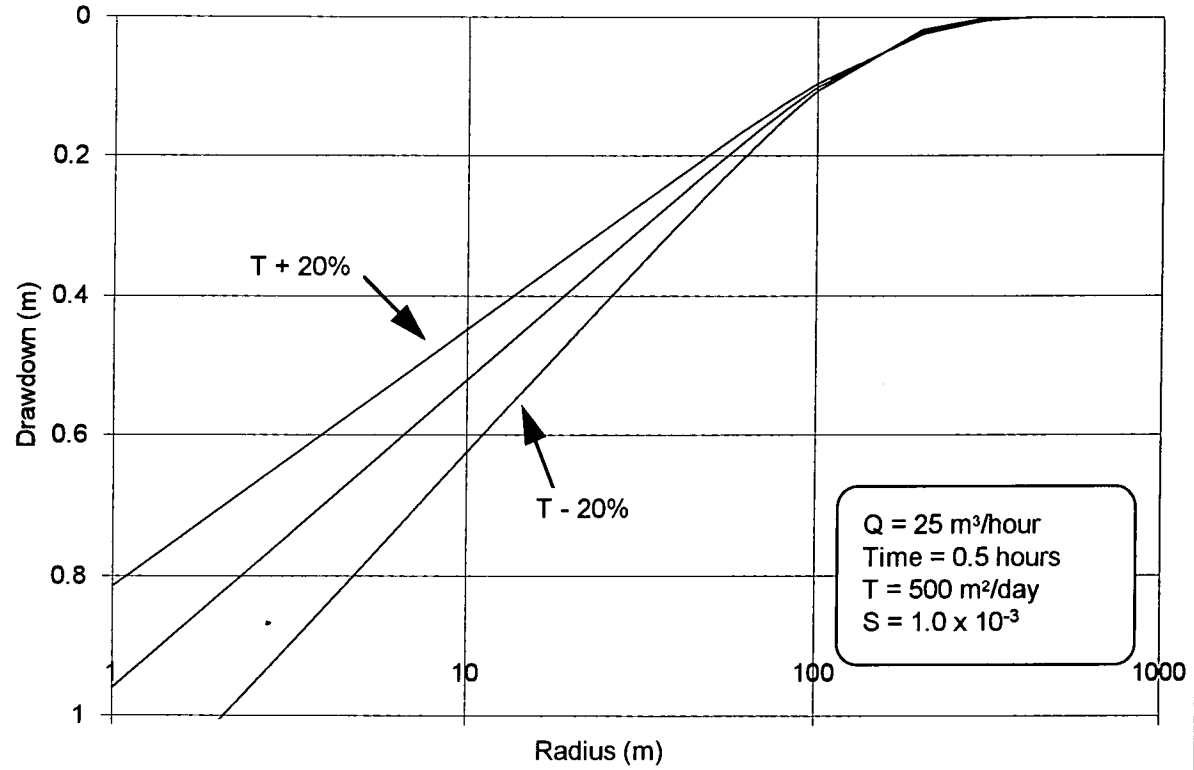

Figure 7.1: The effect of varying transmissivity on drawdown in a confined aquifer.

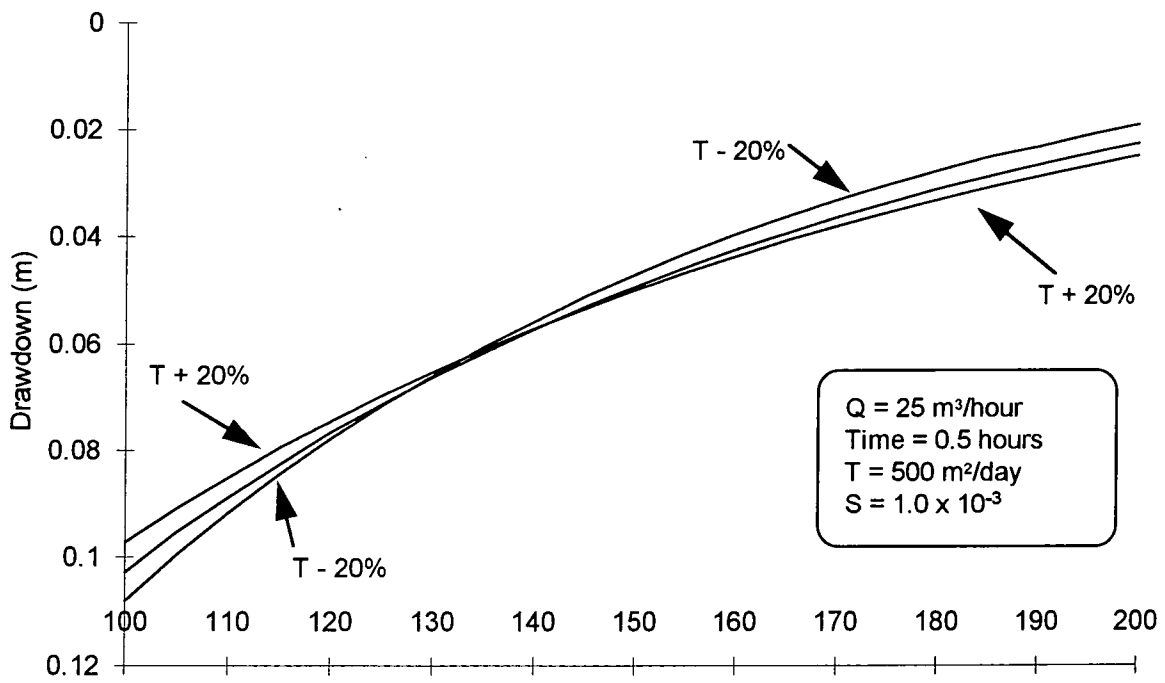

Figure 7.2: The effect of varying transmissivity on drawdown in a confined aquifer for radii between 100 and 200 metres.

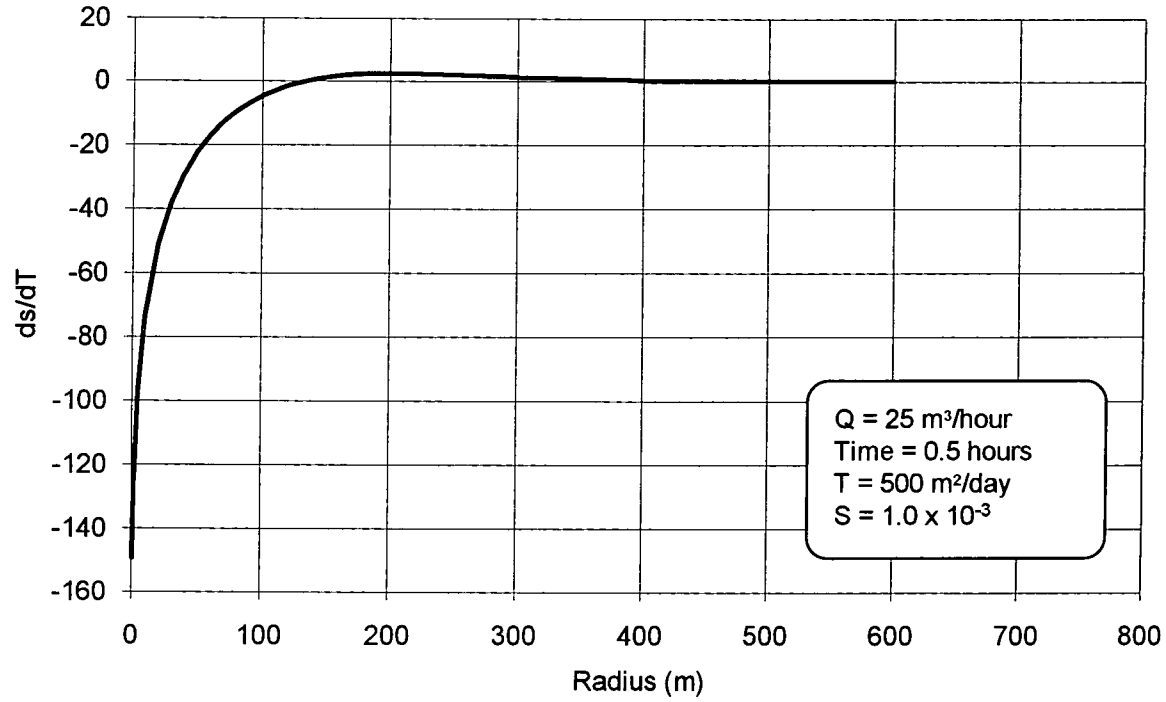

Figure 7.3: The variation of ds/dT with radius in a confined aquifer.

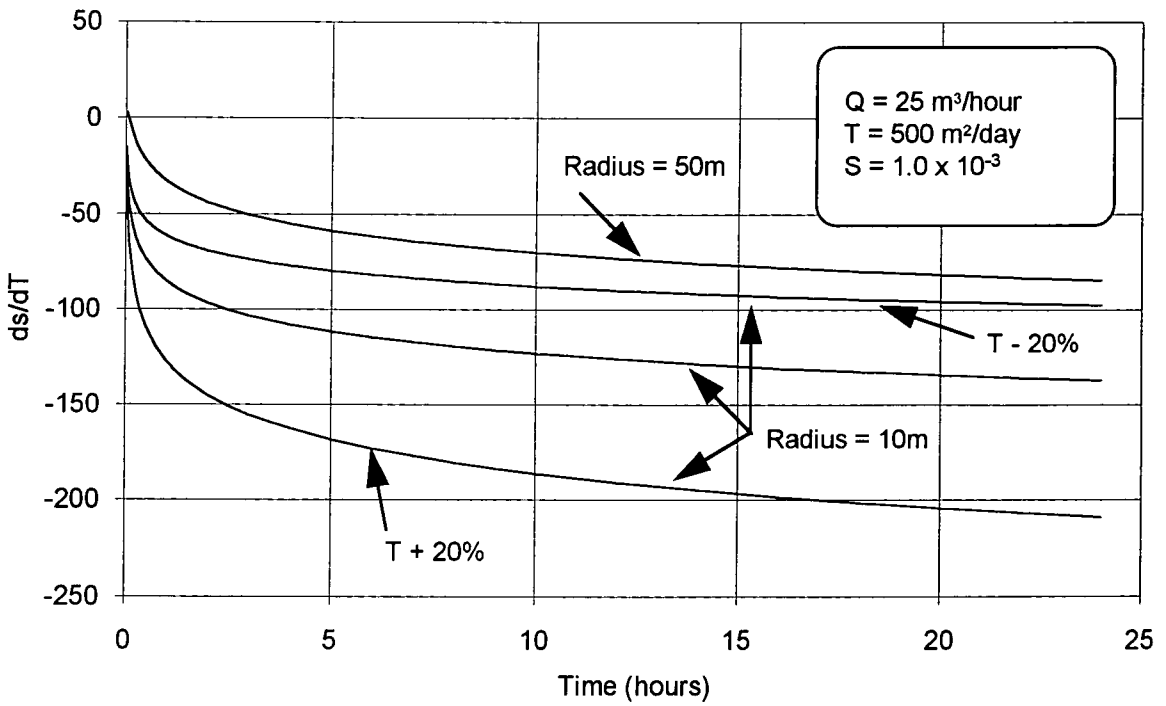

Figure 7.4: The variation of ds/dT with time in a confined aquifer.

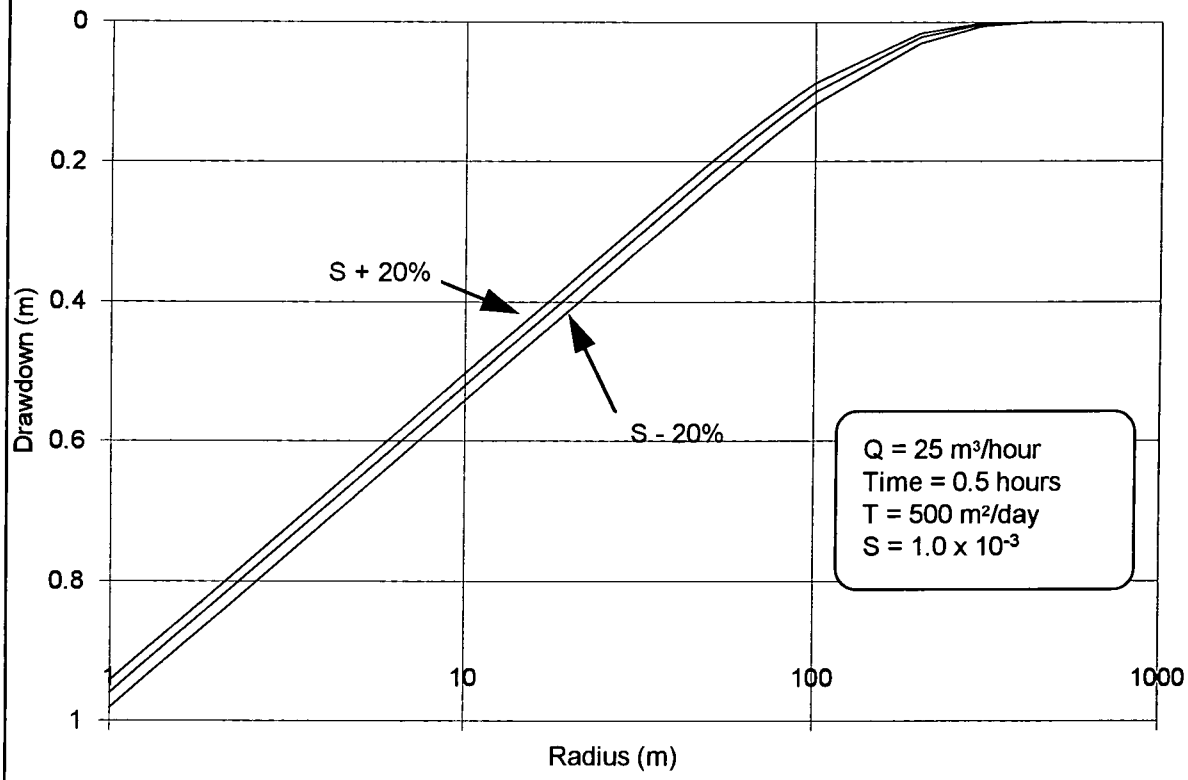

Figure 7.5: The effect of varying the storage coefficient on drawdown in a confined aquifer.

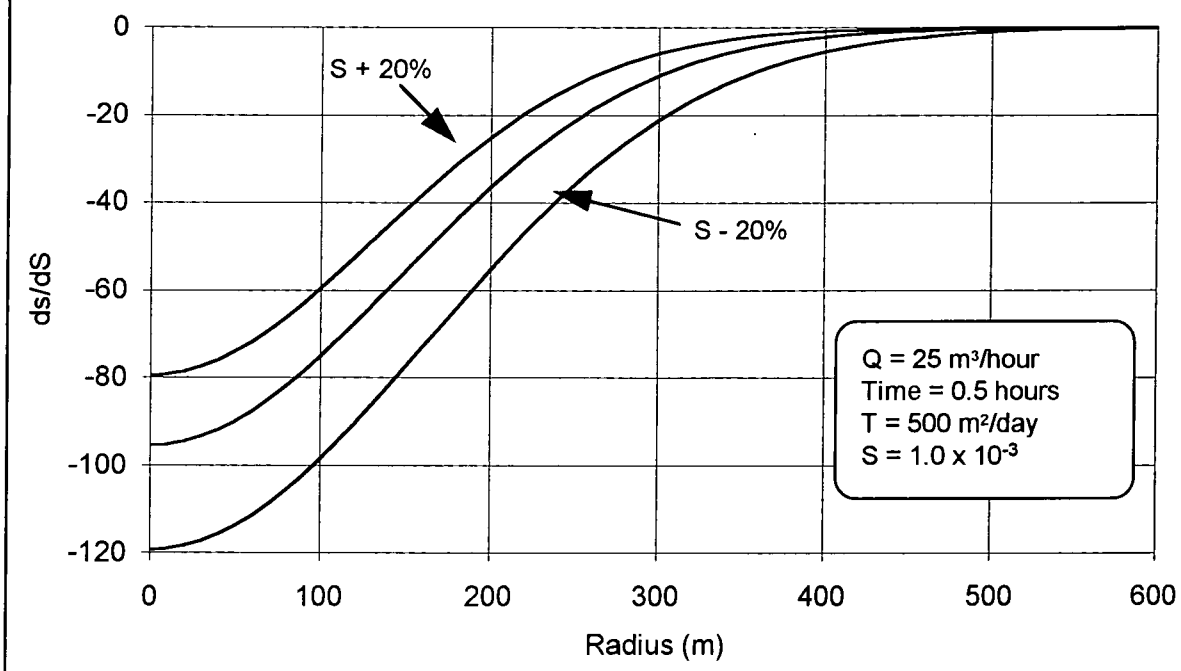

Figure 7.6: The variation of ds/dS with radius in a confined aquifer.

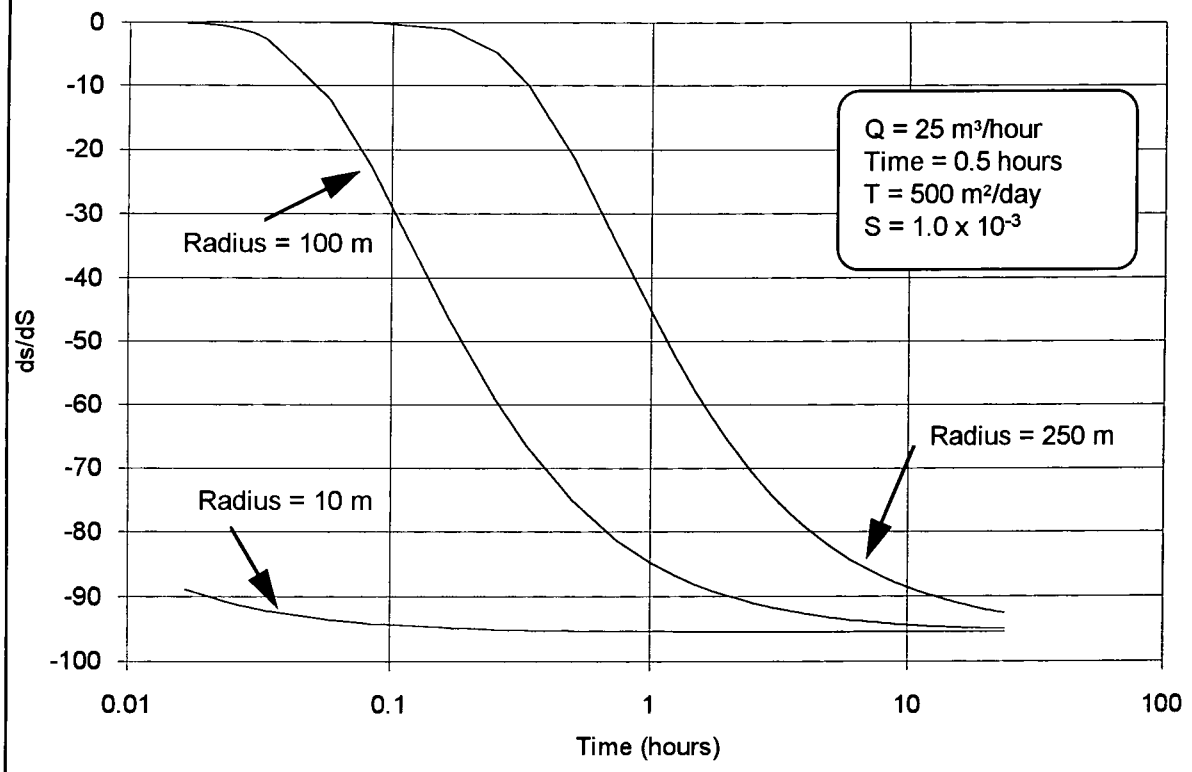

Figure 7.7: The variation of ds/dS with time in a confined aquifer.

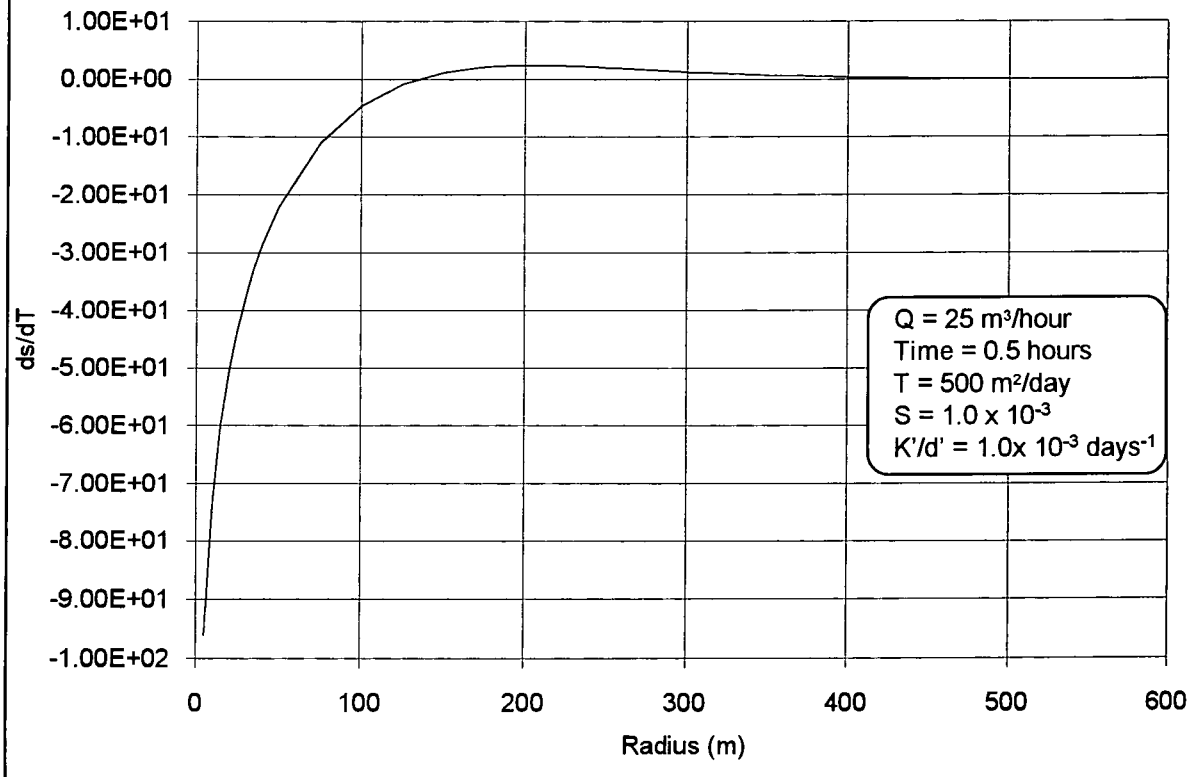

Figure 7.8: The variation of ds/dT with radius in a leaky(Walton) aquifer.

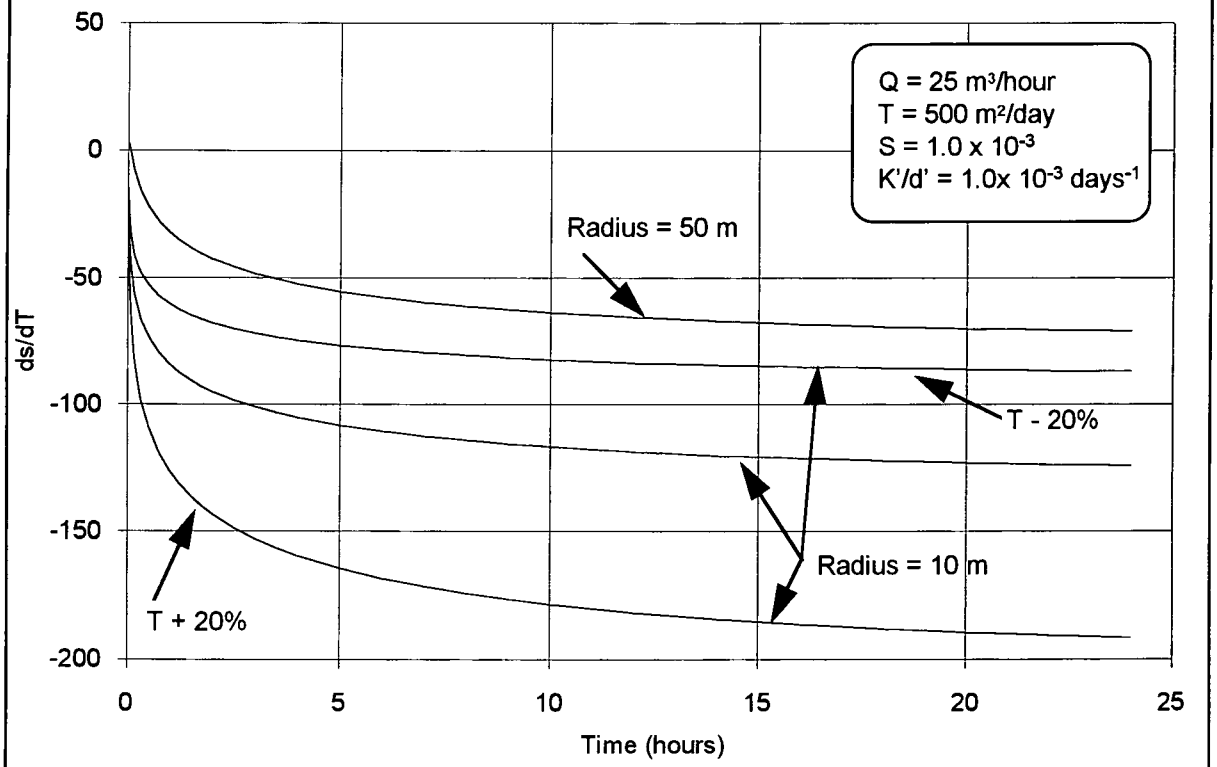

Figure 7.9: The variation of ds/dT with time in a leaky (Walton) aquifer.

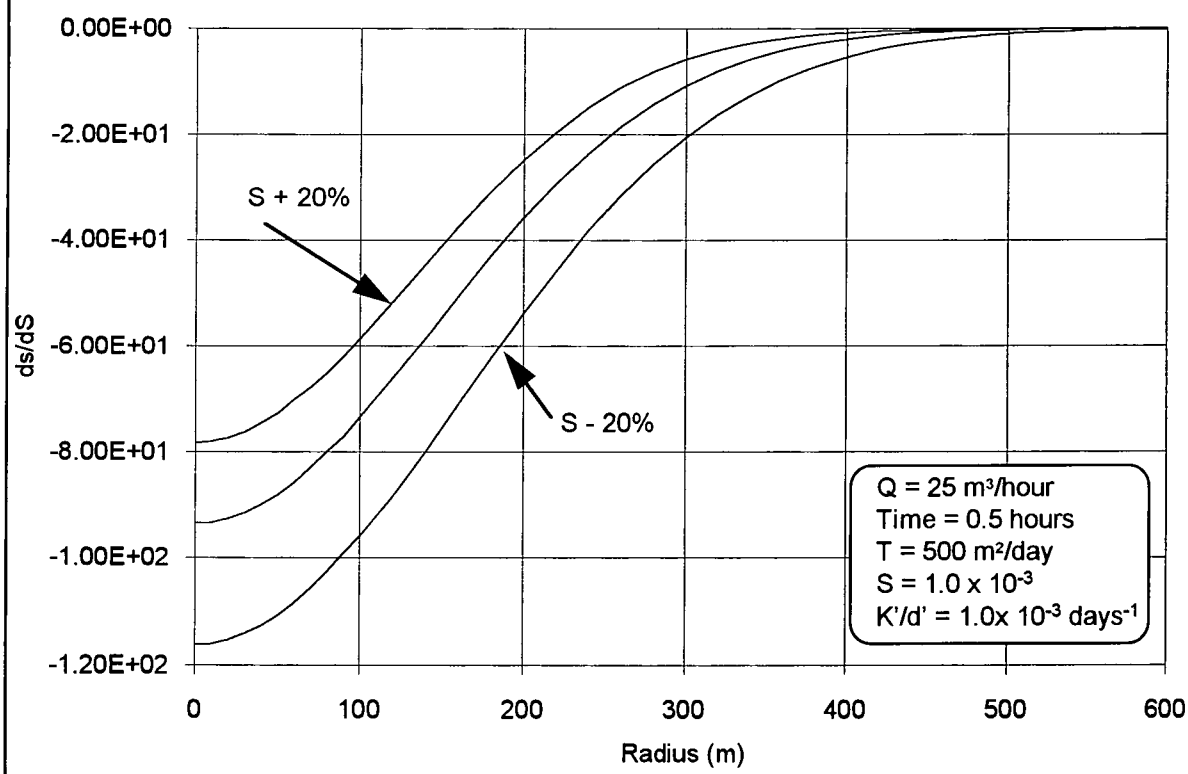

Figure 7.10: The variation of ds/dS with radius in a leaky (Walton) aquifer.

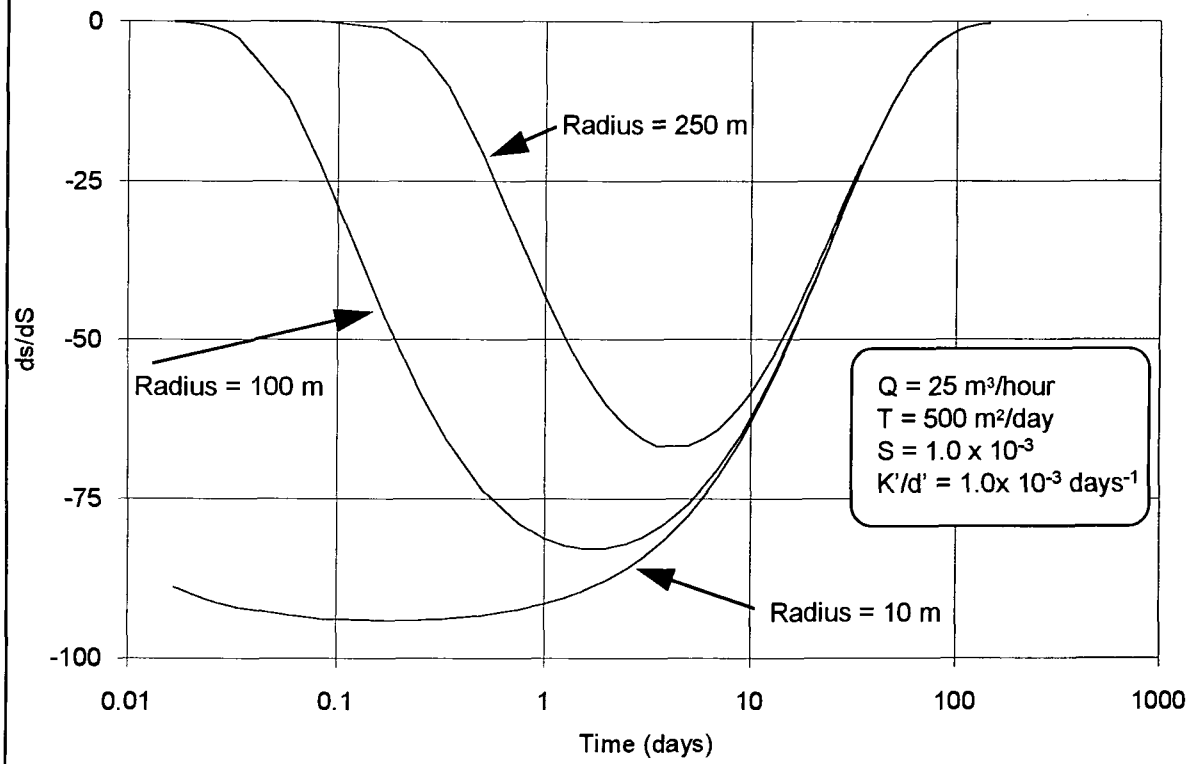

Figure 7.11: The variation of ds/dS with time in a leaky (Walton) aquifer.

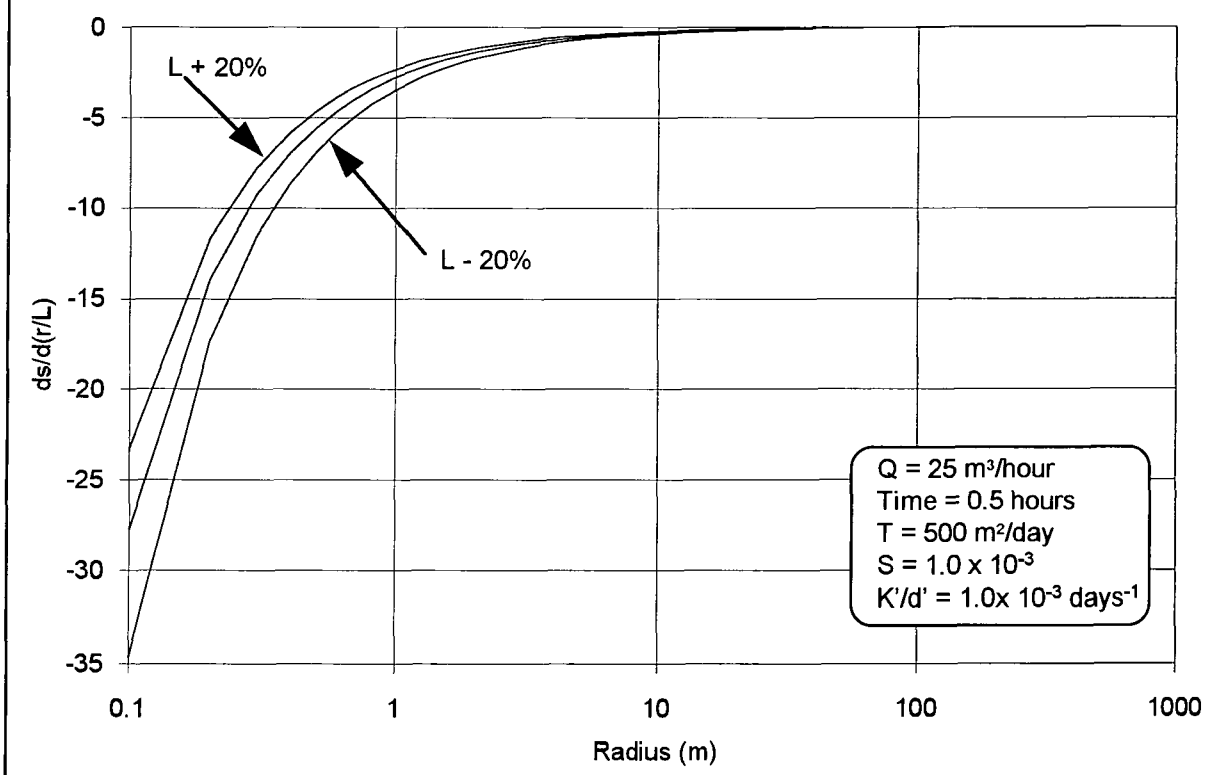

Figure 7.12: The variation of ds/d(r/L) with radius in a leaky (Walton) aquifer.

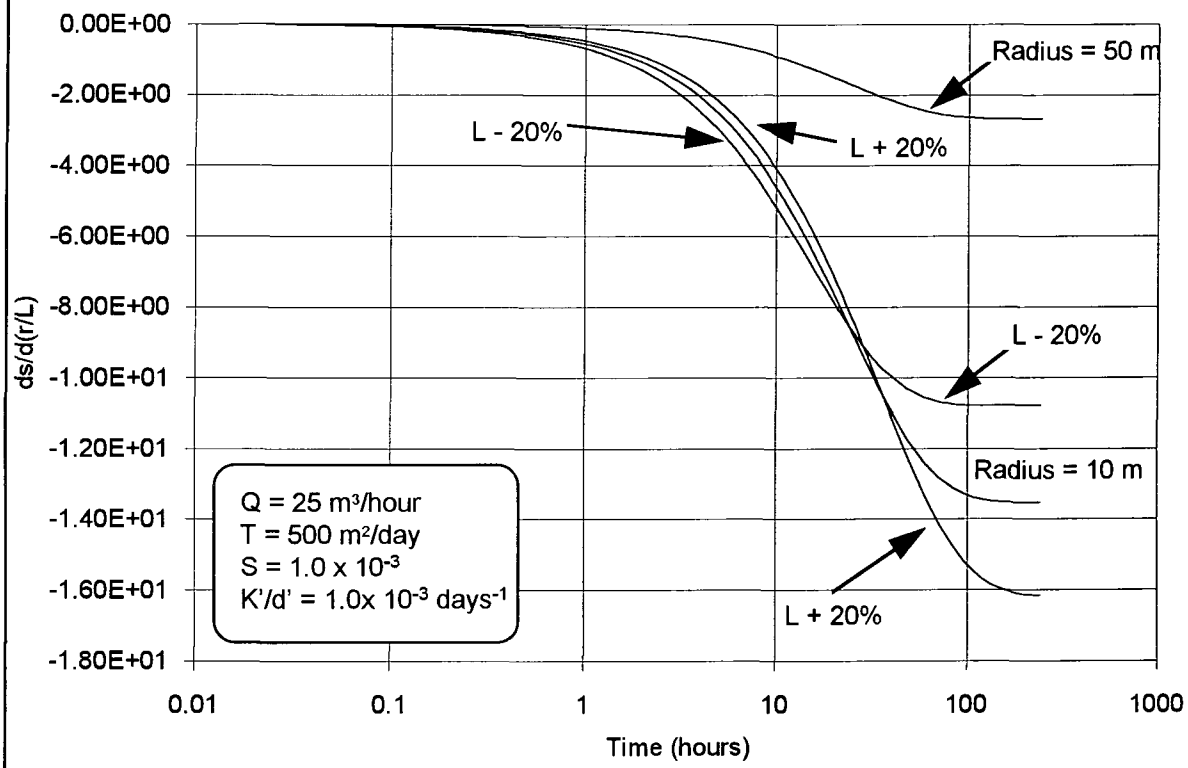

Figure 7.13: The variation of ds/d(r/L) with time in a leaky (Walton) aquifer.

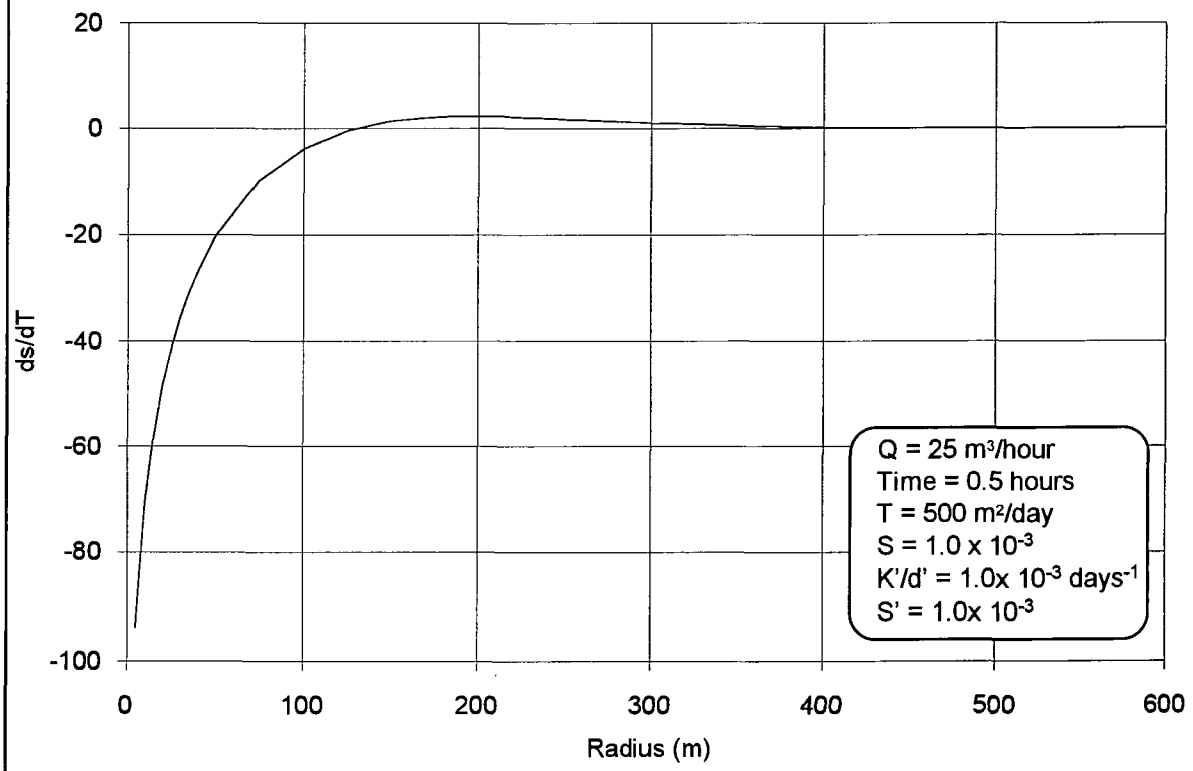

Figure 7.14: The variation of ds/dT with radius in a leaky (Hantush) aquifer.

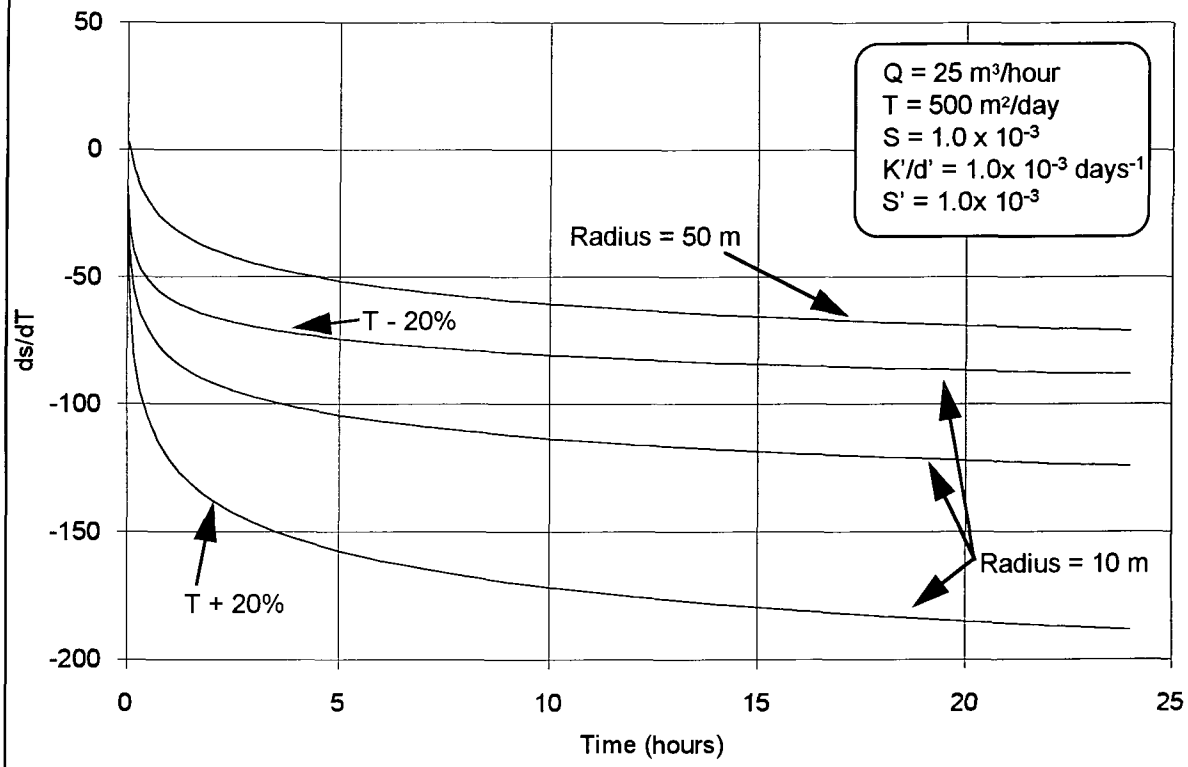

Figure 7.15: The variation of ds/dT with time in a leaky (Hantush) aquifer.

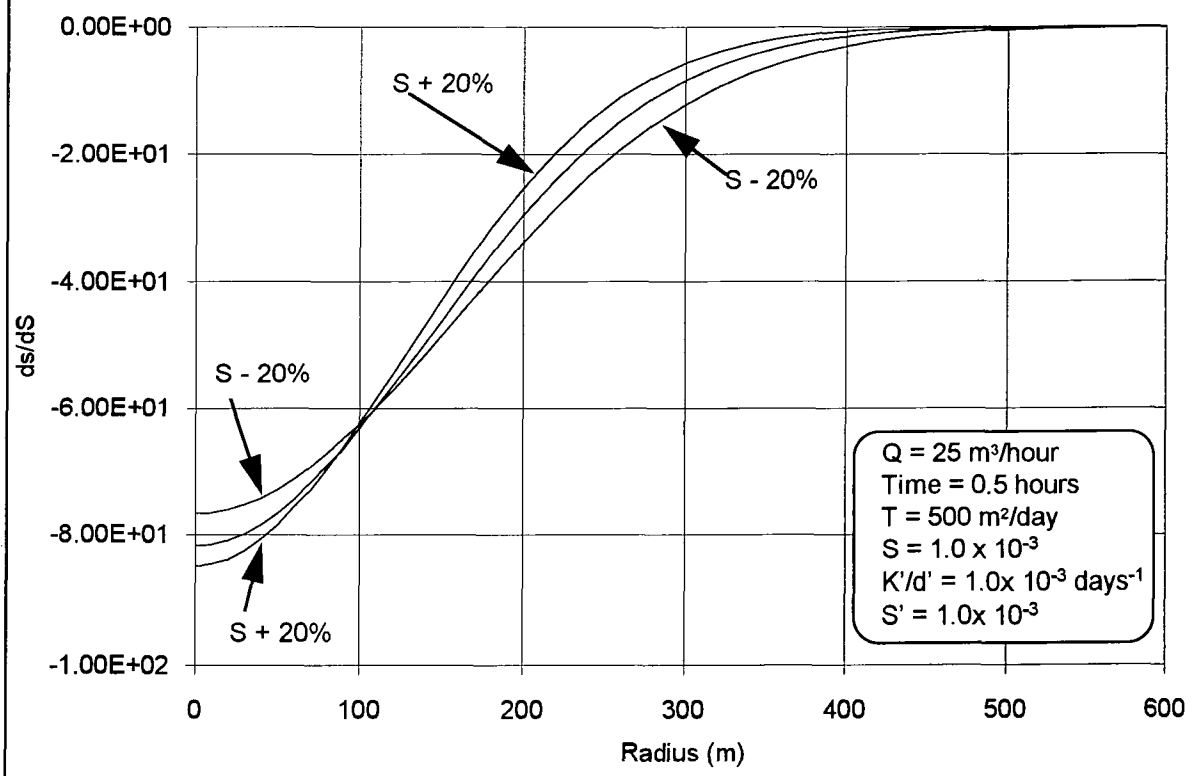

Figure 7.16: The variation of ds/dS with radius in a leaky (Hantush) aquifer.

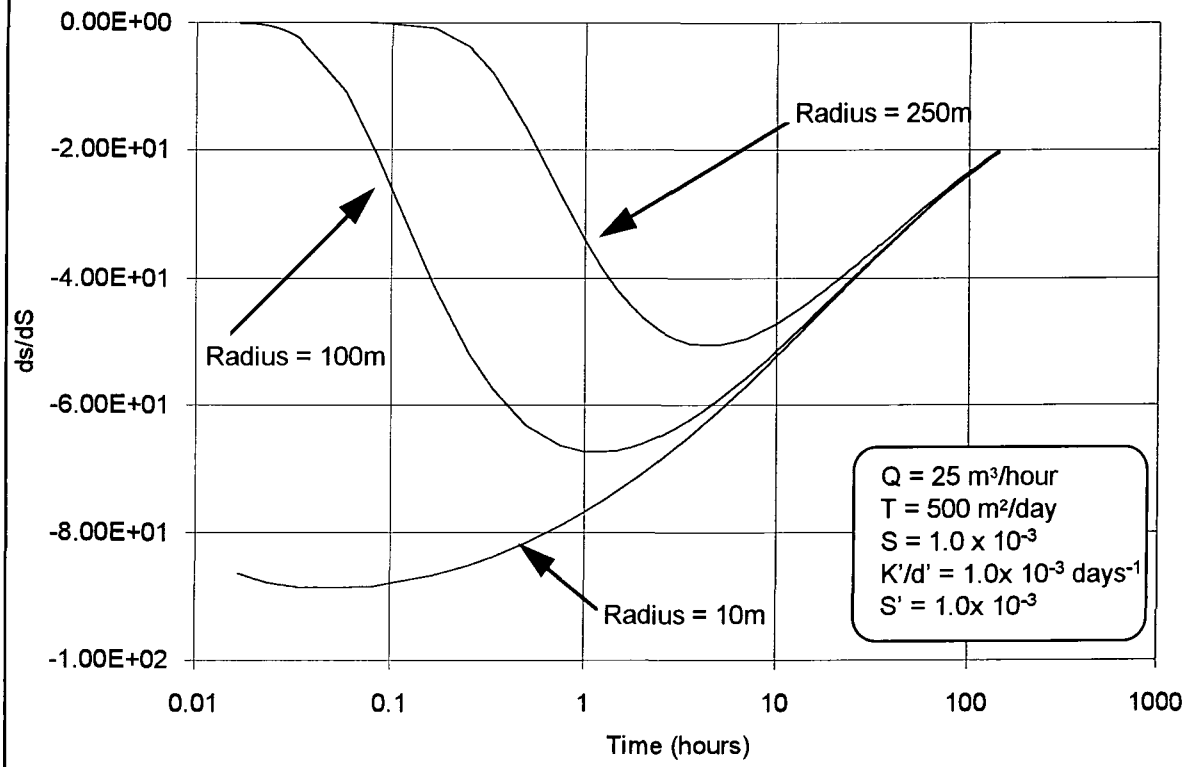

Figure 7.17: The variation of ds/dS with time in a leaky (Hantush) aquifer.

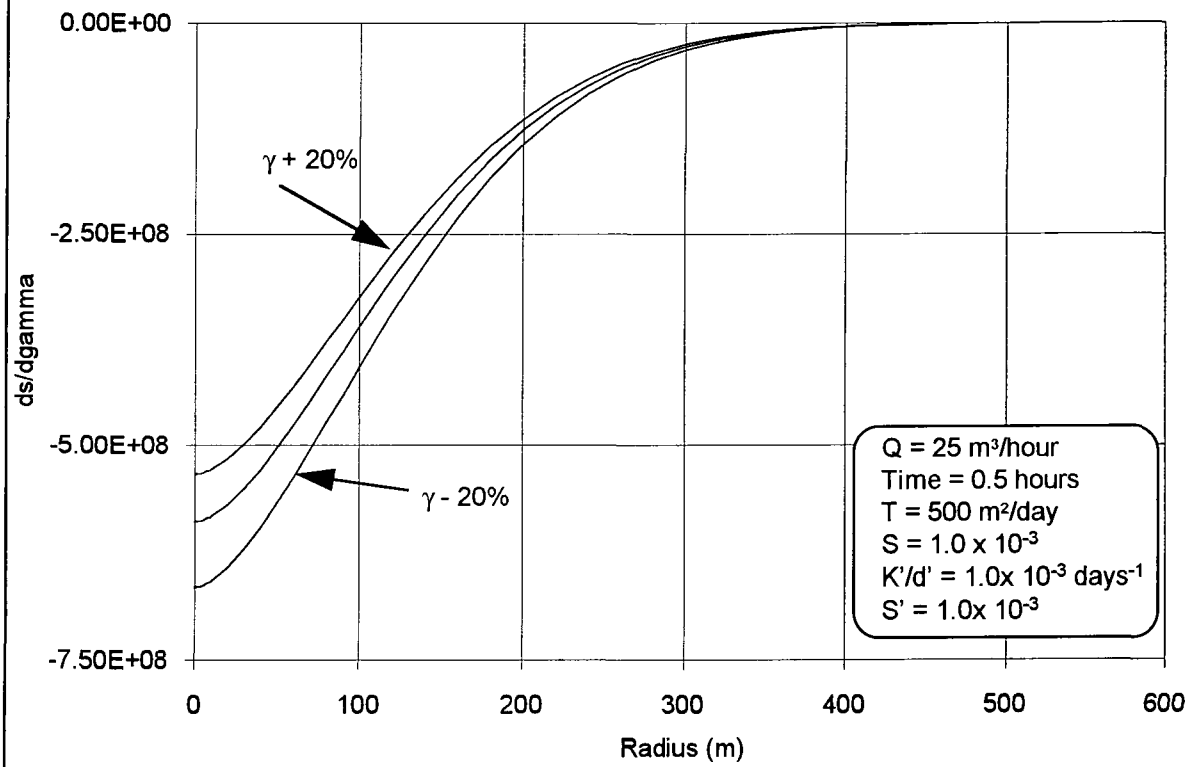

Figure 7.18: The variation of ds/dγ with radius in a leaky (Hantush) aquifer.

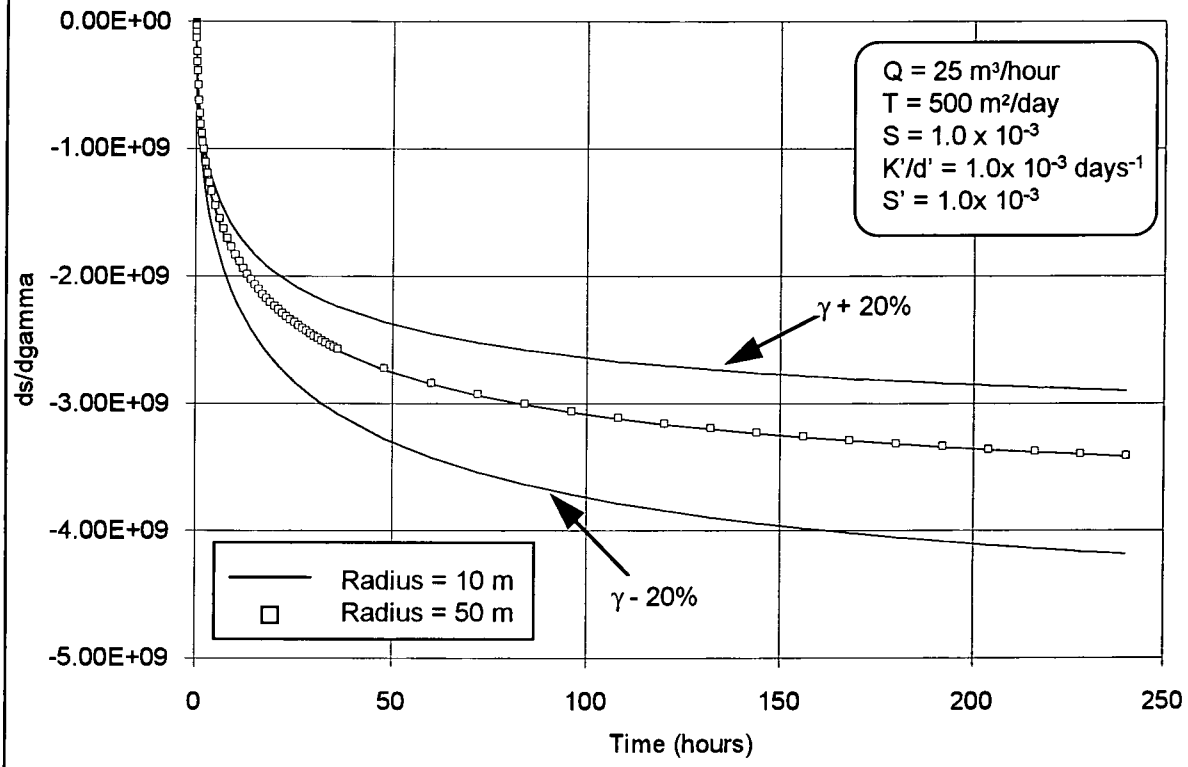

Figure 7.19: The variation of ds/dγ with time in a leaky (Hantush) aquifer.

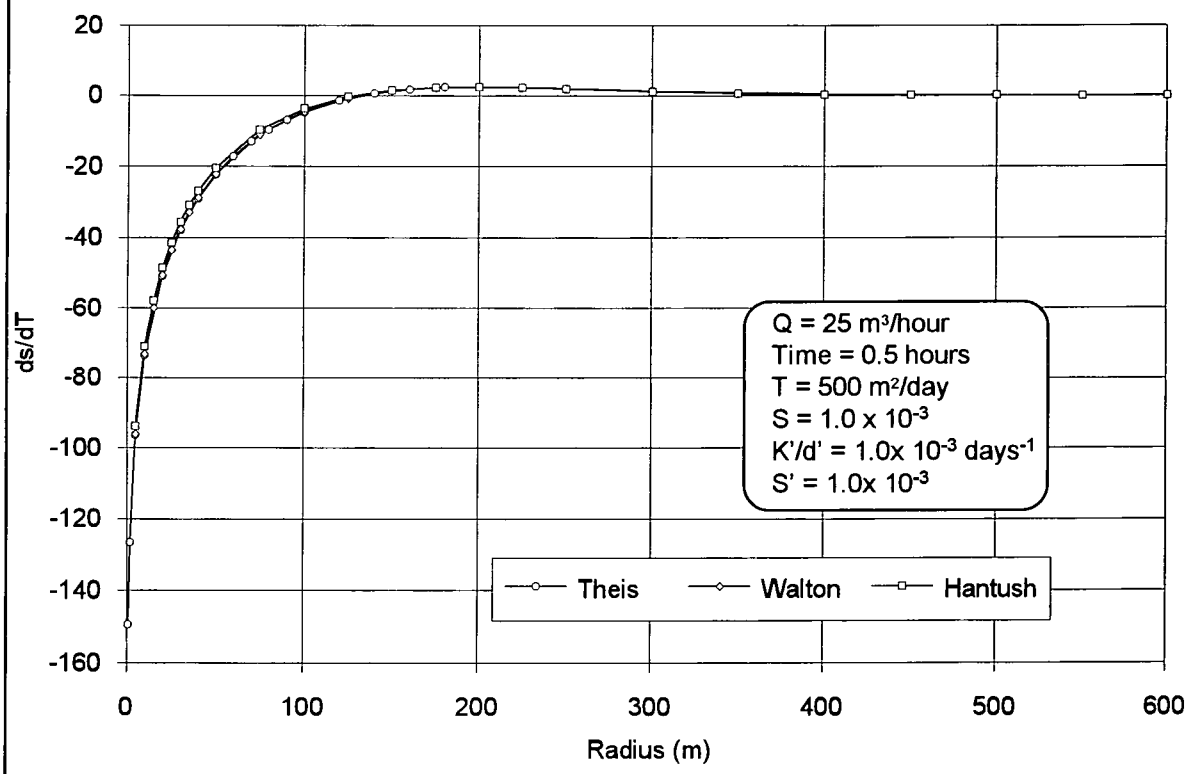

Figure 7.20: A comparison of the variation of ds/dT with radius in confined and leaky aquifers.

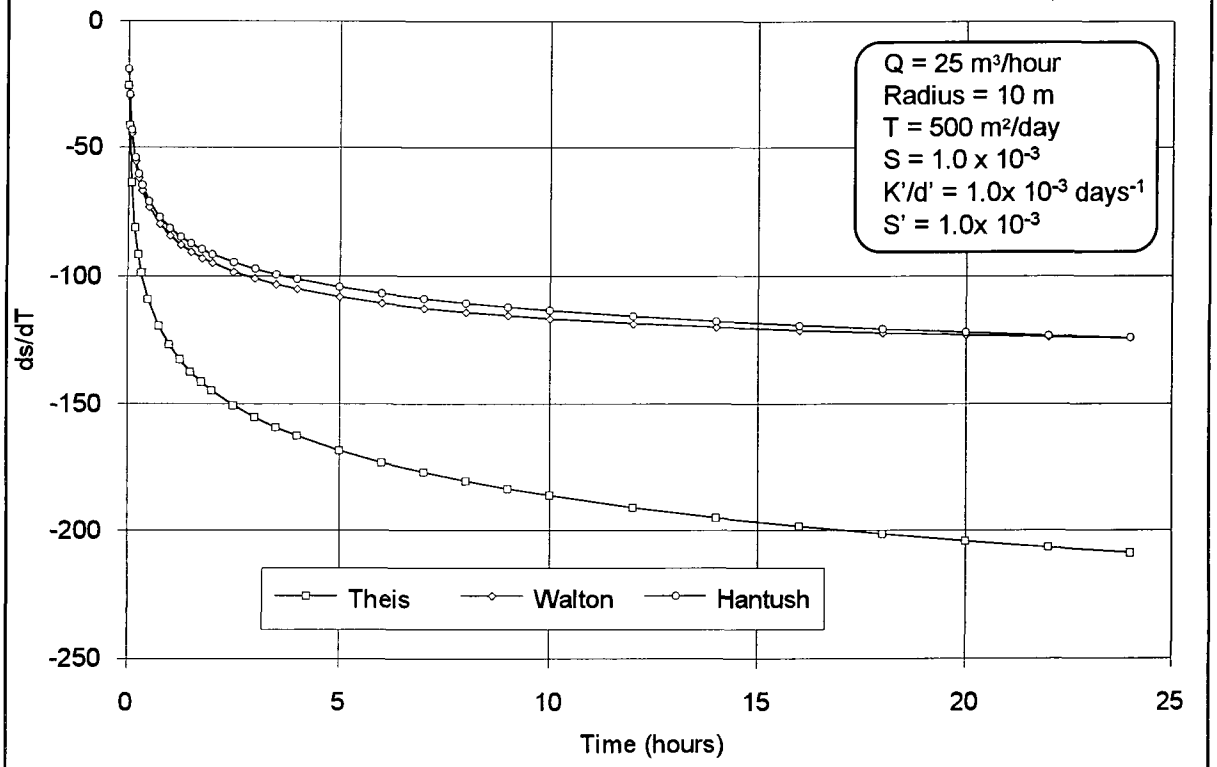

Figure 7.21: A comparison of the variation of ds/dT with time in confined and leaky aquifers.

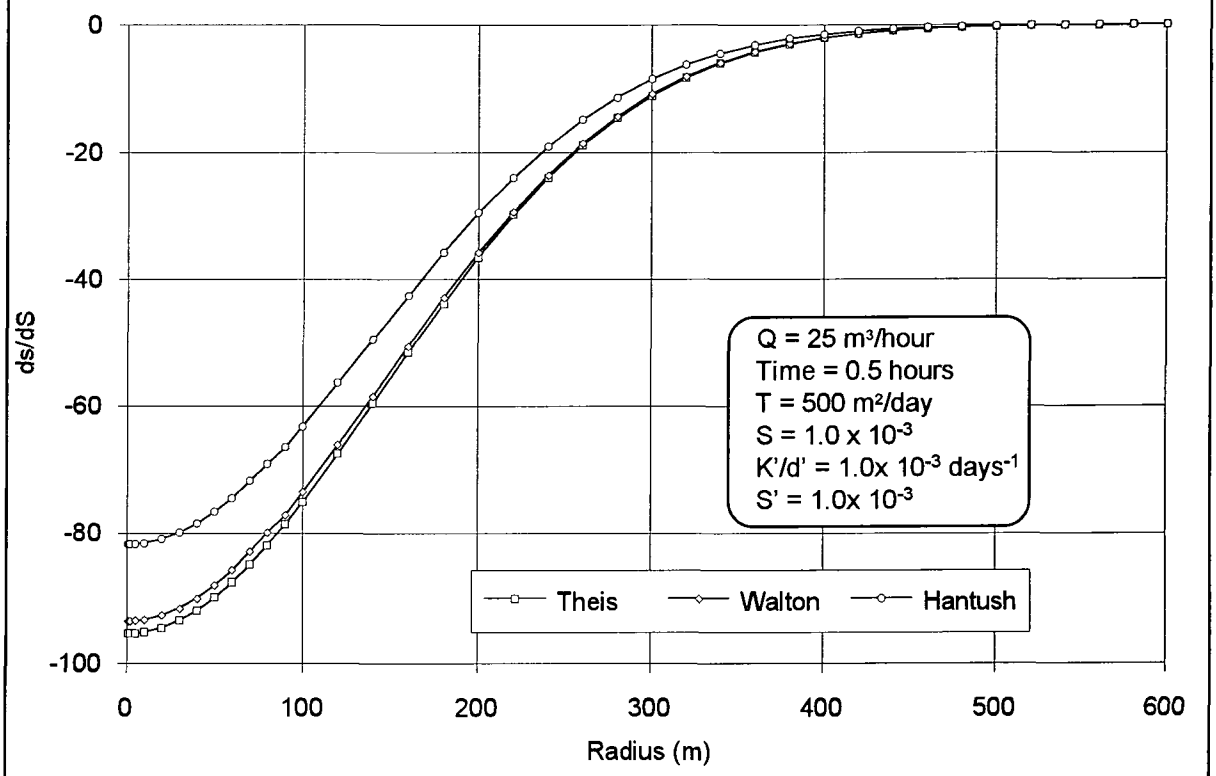

Figure 7.22: A comparison of the variation of ds/dS with radius in confined and leaky aquifers.

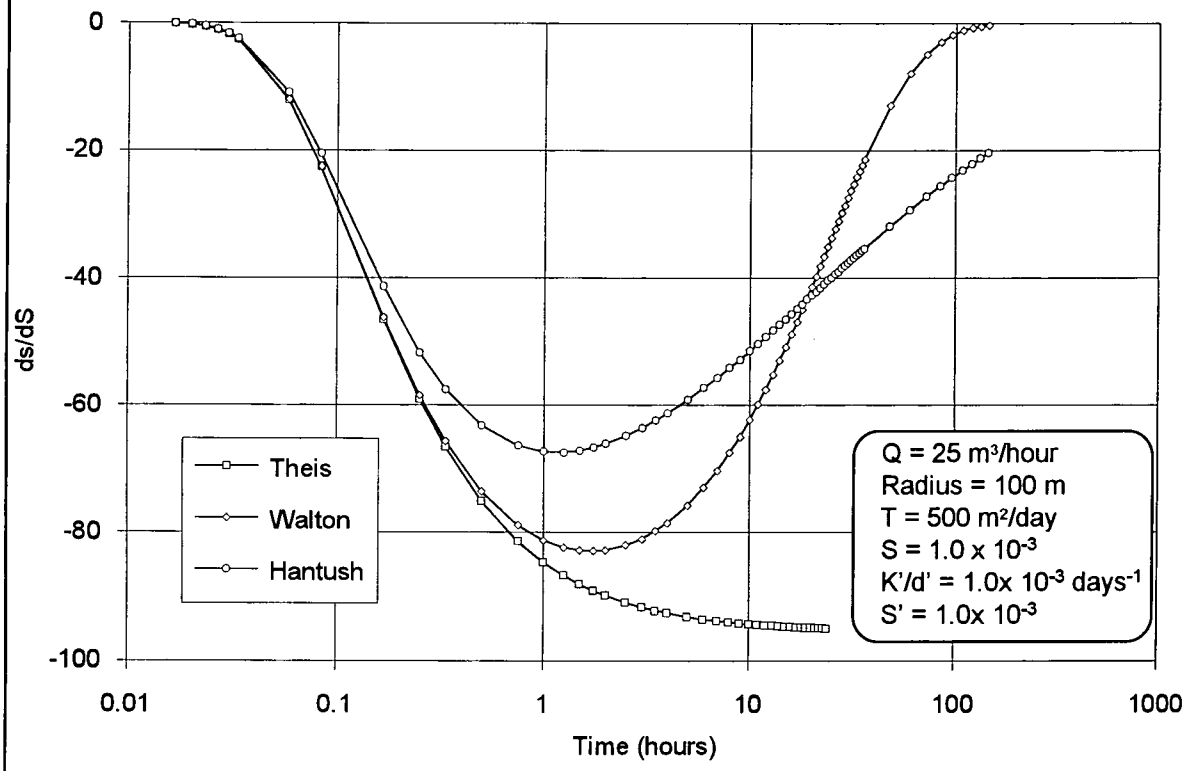

Figure 7.23: A comparison of the variation of ds/dS with time in confined and leaky aquifers.

Chapter 8

Discussion

8.1. Introduction

The aim of this research was to produce an efficient method of calculating aquifer parameters from pumping test data . As a large amount of fieldwork was completed in a leaky aquifer system, confined and leaky systems were examined.

8.2. Achievements

The method of least squares curve fitting was used to estimate aquifer parameters for both confined and leaky aquifers. This method estimates the parameters that minimise the difference between the observed and theoretical values of drawdown. The Theis solution is used in the confined programme, CONPUTS, where the transmissivity and storativity of a confined aquifer are estimated.

Two different methods were used to calculate parameters for a leaky aquifer. The first, WALPUTS, uses the Walton solution to estimate the transmissivity and storativity of the pumped aquifer, and the leakage coefficient (K'/d') of the aquitard. The second method, HANPUTS, uses the Hantush solution. For this case in addition to calculating the aquifer parameters of transmissivity and storativity, a leakage coefficient is calculated which includes both the vertical permeability and the storativity of the aquitard.

The leaky aquifer least square algorithms are slow due to the huge number of calculations performed to evaluate the well functions. To reduce the running time of the programmes, the numerical method of Hermitian interpolation was included. This method evaluates all the parameters used in the least squares algorithm from previously prepared grids of values. This reduced the running time for the majority of problems to 5 seconds.

These programmes were verified using data from synthesised pumping tests, and were found to quickly converge to a 'best fit' solution. Convergence was achieved from a wide range of input parameter values, although, the range reduced as the number of parameters increased.

In addition to the theoretical and computer work, a three week programme of field pumping tests was undertaken. The geology varied across the site and so a number of different methods were used to estimate the relevant geological parameters. The data from the pumping tests using an electric pump in an area where observation wells recorded the drawdown are used to validate the least squares programmes.

A number of accurately documented pumping tests, which other authors have used to test methods of pump test analysis, were also used to test the least squares programmes. The parameters estimated by the programmes gave similar values to those previously reported. The programmes were further validated by calculating the leaky aquifer parameters using the pumping test data from the fieldwork. The results of the analysis of a number of pump tests enabled average parameter values to be evaluated. These parameter values were used in a two dimensional finite element model, and the field pump tests simulated. The resulting theoretical drawdown curves gave a close match to the drawdown data recorded during the tests.

8.3. Considerations for accurately evaluating aquifer parameters

For some civil engineering applications an accurate knowledge of aquifer parameters and how they change in space and time is an important factor. If this is the case, then a rigorous testing and analysis technique should be employed in order that the correct parameters are evaluated.

Often the most difficult factor is the quantification of the geology. The cost of a large number of possibly deep exploration boreholes may often be prohibitive. However, if an accurate analysis of pump test data is required, the first step is to accurately develop a conceptual model of the regional geology.

Some of the differences between the theoretical confined and leaky solutions have been discussed in previous chapters. For example, if a confined aquifer is pumped, the drawdown in the aquifer keeps increasing. When a leaky aquifer is considered, the recharge through the aquitard contributes to discharge, and at late time the drawdown in the aquifer reaches steady state and all the discharge is derived from leakage. The inaccuracies introduced by analysing a leaky aquifer as a confined aquifer could lead to significant errors. Even the use of the Walton instead of the Hantush solution at early time to analyse leaky aquifers can introduce errors, as the Walton solution does not include the storage of the aquitard. This shows that a significant period of time should be spent evaluating all the geological information available, in order that the correct approach is taken.

The purpose of the evaluation of the aquifer parameters should be examined before the fieldwork is undertaken. A different approach may be more suitable, for different applications. For example, the fieldwork conducted as part of this research required accurate parameters for use in a hydrogeological model. The pump test method employed was one where the drawdown was limited by using a low pumping rate. To achieve high accuracy, a sensitive measuring system was used to record the drawdown during the pumping test. In this way, the actual groundwater conditions were not significantly altered during the test.

Conversely, a much higher pumping rate creating a greater drawdown could have been used. This would lead to the calculation of aquifer parameters, where the aquifer is significantly altered from its usual state. The analysis of these results could present

different values of aquifer parameters. A test of this kind would be more appropriate if the potential well yield was being investigated. The aquifer parameters should be calculated for the condition that is being evaluated.

Different numerical methods were used to evaluate the well functions in each case. The most simple case is that of Theis, where the well function is calculated using a simple power series. The first derivatives of the Theis equation, with respect to transmissivity and storativity, were solved analytically. The leaky solutions were more complex. In each case the evaluation of the well function was achieved using the trapezoidal rule to calculate the integral. The Hantush well function also entailed the solution of the complementary error function, using a power series. The first derivatives of the leaky drawdown equations could not be solved analytically, and so they were calculated by determining the slope of the tangent.

The evaluation of the leaky well functions using the trapezoidal rule led to numerous calculations. The running time of the least squares algorithm was increased to several minutes for the leaky cases. The actual least squares algorithm is very fast, as shown by the CONPUTS programme, the running time of which is negligible. The Hermitian interpolation algorithm was included into the leaky programmes, which accurately evaluates the well functions and its derivatives, which would otherwise be calculated using the trapezoidal rule. The Hermitian interpolation algorithm is very fast, and reduced the running time of these programmes from a number of minutes to an average of 5 seconds. This is because the calculation of the well function and its derivatives only requires a small number of calculations from a database created from previous solutions.

The significance of this approach is that a quick but accurate method of pump test analysis for leaky aquifers is available. The least squares method, a technique which has previously been used extensively, is simple and powerful. A significant number of previous methods have been developed to evaluate pumping test data in confined aquifers. There are also

some methods available which use the Walton solution to determine parameters for leaky aquifers. However, as a more realistic approach is taken to pump test analysis, by using a method which accurately represents the conceptual model, it is likely that the complexity of the analysis is increased.

This additional complexity of analysis may prevent the hydrogeologist from using an appropriate method. Significant errors may be introduced by using a method of analysis that does not reflect the conceptual model. The introduction of a fast, accurate, method of pump test analysis, using the least squares algorithm for both confined and leaky aquifers, gives the hydrogeologist greater freedom to use a more appropriate method. The concepts of the least squares method are simple, yet it is a very powerful tool.

The least squares method uses the first derivatives of the relevant drawdown equation with respect to each of the aquifer parameters. These derivatives are termed the sensitivity coefficients. The significance of these parameters was examined in chapter 7, and shows how their effect on drawdown changes in space and time. These parameters can help to evaluate the stability of mathematical models that are developed to model groundwater flow. They show the effect of changing certain parameters on the drawdown due to pumping. Thus the effect of errors in the calculated parameters may be evaluated. If a small error in any particular parameter could lead to a significant change in drawdown, then further work could be completed to ensure a greater accuracy is accomplished.

The HANPUTS computer programme, which uses the Hantush solution to drawdown in a leaky aquifer due to pumping, is considered accurate as it minimises the number of assumptions made about the leaky aquifer flow regime. There are several problems with this method. Theoretically, it is only valid for early time solutions, which may be calculated from equation 6.1. This equation uses the parameters calculated by the Hantush solution, so it is difficult to evaluate the for time which this method is valid.

The Hantush solution takes the permeability and storativity of both the aquitard and aquifer into account. In certain cases the evaluation of the aquitard parameters, in addition to the aquifer parameters, will be important. However, the Hantush solution effectively combines the aquitard parameters, and the value of $K'S'/d'$ is calculated. The separation of these parameters is difficult.

One method which may be used is to analyse the same data using both the Walton and Hantush method. The Walton method evaluates the leakage coefficient, K'/d'. If the value of $K'S'/d'$ is known from the Hantush analysis, it is simple to evaluate S'. However, there are significant differences between the two methods of analysis. Errors are introduced by the Walton equation. Thus the validity of the value of K'/d' calculated by this method is questionable. To use these values in conjunction with the Hantush equation could lead to inaccurate values.

The method used to determine the parameters from the fieldwork would be accurate. A pumping test was carried out in the aquitard material. Even though the aquitard is of lower permeability than the aquifer, it is often possible to conduct a pumping test at a low discharge rate. The analysis of these results gave the transmissivity and storativity of the aquitard. It is important to differentiate between the horizontal and vertical permeability of the aquitard. The values may be significantly different. However, the storativity term is not affected in this manner. Thus, this value of S' may be used in conjunction with the Hantush results to calculate the leakage coefficient, K'/d'.

This method was not used successfully to analyse the fieldwork data due to the high values of $K'S'/d'$ calculated by the Hantush analysis. The reasons for this were discussed in chapter 6. These were that the conceptual geological model is a leaky unconfined system, and the Hantush solution is for a leaky confined system. Also, the parameters calculated led to the Hantush solution only being valid for very early time, the first four minutes of the pumping test. A combination of these factors may have introduced inaccuracy. However,

the analysis of the published pump tests led to parameter values in the same region as other authors.

A third solution in order to accurately evaluate leaky aquifer parameters is to further develop the least squares solution to solve for four variables. This would be possible but would require a significant change in the matrix manipulation within the computer code. This is discussed more fully in section 8.4.

The computer programmes have presented methods of calculating aquifer parameters accurately. However, a solution must be used which reflects the geological conceptual model. Also, the theoretical solutions to drawdown in a pumped aquifer were developed for homogeneous materials. In practice, the geology is likely to exhibit a high degree of heterogeneity, so the hydrogeologist should use experience and common sense when considering the results of any pump test analysis.

8.4. Further Work

The strengths of the least squares technique to calculate aquifer parameters have been demonstrated by the algorithms developed in this project. The number of parameters solved was limited to three, but there should be no theoretical limit to the number of parameters that are solved using this method. However, as the solution became more complex, the convergence of the algorithm became more difficult.

The least squares algorithm could be expanded to four variables. If this were applied to the Hantush solution in a leaky aquifer, the aquifer parameters of transmissivity and storativity, and aquitard parameters of vertical permeability and storativity, could be independently assessed. It would be interesting to compare the increase in accuracy of calculation of the aquitard parameters using this method.

If the least squares technique was expanded to four variables, the solution could also be applied to the case of an unconfined or water table aquifer. In this case, delayed yield significantly affects the drawdown in a pumped aquifer. The methods of determining aquifer parameters using this method are complex. If some of these difficulties could be removed by the use of a least squares technique, a significant improvement in the accuracy of the calculation of unconfined parameters may be possible.

The accuracy and speed of the least squares algorithms have been discussed in this section. The computer programmes, however, have been written using FORTRAN77, and the data is entered using previously prepared datafiles. The output is again in the form of a datafile. If these algorithms are to be developed for much wider use, a more 'user friendly' approach should be taken to the software.

To make greater use of the potential of this project, a simple improvement would be to include a data entry programme, which would operate in a 'Windows' environment. This would write all the relevant information to the input datafiles. This interface could then run the appropriate least squares programme, and then present the results. A simple way of demonstrating the accuracy of the solution would be to include a graphical section, which compares the theoretical curve using the 'best fit' parameters against the input data. This would enable the user to ascertain easily the accuracy of the solution.

Overall, this project has shown the strength and potential of the least squares algorithm. Coupled with other numerical techniques, it can produce quick and accurate estimations of aquifer parameters. There are many other types of tests and problems where this algorithm could be applied within the field of groundwater engineering.

Chapter 9

Conclusions

Three methods of determining aquifer parameters have been devised. They use the least squares algorithm to estimate the aquifer parameters that give the 'best fit' between the observed and theoretical drawdown.

The cases of both confined and leaky confined aquifers are solved. These use the Theis, Walton and Hantush solutions to drawdown in a pumped aquifer. The technique of Hermitian interpolation is incorporated with the leaky solutions to produce fast and accurate programmes.

A programme of fieldwork was carried out. The geology of the area consisted of a gravel aquifer underlain by a clayey sand aquitard. The least squares programmes were used to analyse the pumping test data. The following average parameters were estimated as a result of this analysis.

GRAVEL

Transmissivity, T = 213.4 m^2/day

Storativity, S = 1.23×10^{-1}

SAND

Leakage factor, K'/d' = 2.5×10^{-1} $days^{-1}$

Storativity, S' = 6.16×10^{-3}

The results of the analysis of these and other pump tests validate the least squares programmes. Additionally, a two dimensional finite element model was used to simulate the field pump tests. The results from this were compared with the field data. The finite

element solution matched the observed data well. This again validates the results of the least squares programmes.

The solutions of groundwater flow during a pumping test vary due to different geological conditions. The analysis of pump test data using an inappropriate solution may lead to inaccurate results. An accurate geological conceptual model is necessary, so that an appropriate approach may be taken.

The leaky least squares programmes offer a simple and fast method of calculating leaky aquifer properties. This further allows the use of a method of analysis that reflects the conceptual model.

The leaky solutions offer an accurate method of calculating the aquifer parameters. The evaluation of the aquitard properties is more difficult. Further work should expand the current least squares algorithm to estimate individually each of the leaky aquifer parameters.

References

Alvarez, A., and F. Kohlbeck, 1991, A method to determine the formation constants of leaky aquifers, and its application to pumping test data, Ground Water, v. 29 no. 3, pp 425 - 429.

Atkinson, L. V., P. J. Horley and J. D. Hudson, 1989, *Numerical methods with FORTRAN 77*, Addison-Wesley, England.

Bardsley, W. E., 1991, Graphical estimation of the Theis drawdown function, Journal of Hydrology, v. 128 pp 357 - 367.

Butler, J. J., (1990), The role of pumping test in site characterization: some theoretical considerations, Ground Water, v. 28, no. 3, pp. 394 - 402.

Butt, M. A., P. M. Cobb and C. D. McElwee, 1982, Analysis of leaky aquifer pumping test data: an automated numerical solution using sensitivity analysis, Ground Water, v. 20, no. 3, pp 325 - 333.

Chan, Y. K. and K. R. Rushton, 1976, A numerical model for pumping test analysis, Proc. Institution of Civil Engineers, part 2 pp 281 - 296.

Chander S., S. K. Goyal and P. N. Kapoor, 1981, Analysis of pumping test data using Marquardt Algorithm, Ground Water, v. 19, no. 3, pp 275 - 278.

Cheng, A. H-D., and D. Ouazar, 1995, Theis solution under aquifer parameter uncertainty, Ground Water, v. 33, no. 1, pp 11 - 15.

Chow, V. T., 1952, On the determination of transmissibility and storage coefficients from pumping test data, Trans. Amer. Geophysical Union, v. 33, no. 3, pp 397 - 404.

Cooper, H. H., and C. E. Jacob, 1946, A generalized method for evaluating the formation constants and summarizing well-field history, Trans. Amer. Geophysical Union, v. 27, no. 4, pp 526 - 534.

Das Gupta, A. and S. G. Joshi, (1984), Algorithm for Theis solution, Ground Water, v. 22, no. 2, pp 199 - 206.

Doherty, J., 1990, The interpretation of pump-test data from a disused underground mine, Journal of Hydrology, v. 114, pp 109 - 123.

Etter, D. M., 1990, *Structured Fortran for Engineers and Scientists*, 3rd edition, Benjamin Cummings Publishing Co.

Freeze, R. A. and J. A. Cherry, 1979, *Groundwater*, 1st Edition, Prentice-Hall, New Jersey, 604 pp.

Grimestad, G., 1981, Inverse solutions of the Theis equation determined with programmable calculators, Ground Water, v. 19, no. 4, pp 387 - 391.

Guzman-Guzman, A. and R. Srivastava, 1994, Analysis of slope-matching methods for aquifer parameter determination, Ground Water, v. 32, no. 4, pp 570 - 575.

Hantush, M. S., and C. E. Jacob, 1955, Non-steady radial flow in an infinite leaky aquifer, Trans. Amer. Geophysical Union, v. 36, no. 1, pp 95 - 100.

Hantush, M. S., 1956, Analysis of data from pumping tests in leaky aquifers, Trans. Amer. Geophysical Union, v. 37, no. 6, pp 702 - 714.

Hantush, M. S., 1960, Modification of the theory of leaky aquifers, Trans. Amer. Geophysical Union, v. 27, no. 4, pp 3713 - 3725.

Hinton, E. and D. R. J. Owen, 1979, *An Introduction to Finite Element Computations*, First Edition, Pineridge Press Ltd, Swansea, 385 pp.

Holzschuh, J. C., 1976, A simple computer program for the determination of aquifer characteristics from pump test data, Ground Water, v. 14, no. 5, pp 283 - 285.

Jacob, C.E., 1940, On the flow of water in an elastic artesian aquifer, Trans. Amer. Geophysical Union, v. 21, pp 574 - 586.

Jacob, C. E., 1946, Radial flow in a leaky artesian aquifer, Trans. Amer. Geophysical Union, v. 27, no. 2, pp 198 - 208.

Jennings, A., 1977, *Matrix computations for Engineers and Scientists*, Wiley.

Kreyszig, E., 1988, *Advanced Engineering Mathematics*, Wiley, 1400 pp.

Kruseman, G. P. and N. A. de Ridder, 1990, *Analysis and Evaluation of Pumping Test Data*, Second Edition, The International Institute for Land Reclamation and Improvement, Wageningen, The Netherlands.

McElwee, C. D., and M. A. Yukler, 1978, Sensitivity of groundwater models with respect to variations in transmissivity and storage, Water Resources Research, v. 14, no. 3, pp 451 - 459.

McElwee, C. D., 1980, Theis parameter evaluation from pumping tests by sensitivity analysis, Ground Water, v. 18, no. 1, pp 56 - 60.

McElwee, C. D., and J. Paschetto, 1982, Hand calculator program for evaluating Theis parameters from a pumping test, Ground Water, v. 20, no. 5, pp 551 - 555.

Milton, A. and I. A. Stegun, (Eds.), 1972, *Handbook of Mathematical Functions*, US department of Commerce, National Bureau of Standards, 10th edition.

Mohr, G. A., 1992, *Finite Elements for Solids, Fluids and Optimization*, First Edition, Oxford University Press, 604 pp.

Motz, L. H., 1990, Aquifer parameters from a one-dimensional steady-leaky type curve, Ground Water, v. 28, no. 3, pp 350 - 356.

Mukhopadhyay, A., 1985, Automated derivation of parameters in a nonleaky confined aquifer with transient flow, Ground Water, v. 23, no. 6, pp 806 - 811.

Neuman, S. P., and P. A. Witherspoon, 1969a, Theory of flow in a confined two aquifer system, Water Resources Research, v. 5, no. 4, pp 803 - 816.

Neuman, S. P., and P. A. Witherspoon, 1969b, Applicability of current theories of flow in leaky aquifers, Water Resources Research, v. 5, no. 4, pp 817 - 829.

Rai, S. P., 1985, Numerical determination of aquifer constants, Journal of Hydraulic Engineering, v. 111, no. 7, pp 1110 - 1114.

Rayner, F. A., !980, Pumping test analysis with a hand-held calculator, Ground Water, v. 18, no. 6, pp 562 - 568.

Saleem, Z. A., 1970, A computer method for puming-test analysis, Ground Water, v. 8, no. 5, pp 21- 24.

Sen, Z., 1986, Determination of aquifer parameters by the slope matching method, Ground Water. v. 24, no. 2, pp 217 - 223.

Theis, C. V., 1935, The relation between the lowering of the piezometric surface and the rate and duration of discharge of a well using groundwater storage, Trans. Amer. Geophysical Union, v. 16, pp 519 - 524.

Theis, C. V., 1940, The source of water derived from wells, Civil Engineering, v. 10, no. 5, pp. 519 - 524.

Thomas, S. D., 1985, Evaluation of the parameters of the capillary head - saturation curve using least squares techniques, GeoTrans, Inc., unpublished paper.

Thomas, S. D., 1993, *SEFTRANS, A Simple and Efficient Flow and TRANSport Model*, Oxford Geotechnica International Software Documentation.

Walton, W. C., 1970, *Groundwater resource evaluation*, First Edition, McGraw-Hill, New York, 664 pp.

Walton, W. C., 1979, Review of leaky artesian aquifer test evaluation methods, Ground Water, v. 17, no. 3, pp 270 - 283.

Wilson, E. M., 1993, *Engineering Hydrology,* Fourth Edition, Macmillan, London, 348 pp.

Yeh, H., 1987a, Theis' solution be nonlinear least-squares and finite-difference Newton's method, Ground Water, v. 25, no. 6, pp 710 - 715.

Yeh, H., 1987b, Discussion on numerical determination of aquifer constants, by S.P. Rai, Journal of Hydraulic Engineering, ASCE, v. 111, no. 7.

APPENDICES

Details of each Appendix are shown in a Table of Contents

at the front of each Appendix

Appendix C

C 1: Pump test equipment

Appendix C1

Pump test equipment

Grundfos MP1 Pump

The pump tests in the 50 mm boreholes were carried out using a Grundfos MP1 electric pump. This was connected to 50 m of riser. The pump was connected to the end of the riser, and so was lowered to the bottom of the borehole. The pump itself is a 2 stage centrifugal pump with radial impellers. The minimum borehole diameter in which it can be used is 50 mm (2"). A gauge on the outlet pipe records the total volume of water that is extracted, from which the flowrate may be calculated. This gauge measures to an accuracy of 0.0001 m^3.

Converter BTI/MP1

The power to the Grundfos MP1 pump was supplied through a converter. The converter changed the two phase alternating input current to three phase power in order to drive the pump. The pumping rate may then be changed by altering the frequency of the three phase supply. The maximum frequency is 400 Hz. The pump rate is also governed by the distance through which the water must be raised. For shallow boreholes (less than 10 m), the maximum pump rate is nearly 2 m^3/hour.

Haverhill Power Unit

The power was supplied to the converter by a portable Haverhill power unit. This was made up of a Honda engine which ran on unleaded petrol and a Markon A.C. generator. The output was 50 Hz and 240 V.

Technolog logging system

The Technolog Newlog logging system was used. This comprised a pressure transducer in the borehole which recorded the water level. This was connected by electrical cable to a logging unit which was mounted inside the top of the borehole. The information was held in the logging unit until it was downloaded to a portable computer on site at the end of the test. The logger is self contained with an internal battery.

Druck pressure transducer

A PDCR 800 series pressure transducer was used. This was placed in the borehole and observed the change in water level by measuring the change in pressure. The accuracy of the transducer was within $\pm$ 0.06%. The transducer is thus able to record a 1 mm change in water level.

Land Rover (4 x 4)

A four wheel drive Land Rover vehicle was used to transport the pump equipment to the site. A vehicle of this type is necessary when the difficult terrain is considered.

Waterra pump

A standard Waterra hand pump system was used for pump tests in 19 mm piezometer tubes. This consisted of a 10 metre length of 16 mm tubing made of high density polyethylene. An internal fitting stainless steel foot valve was screwed to the end of the tubing. The Waterra pump was operated manually and the quantity pumped measured by collecting it in a calibrated vessel.

Dipmeter

A dipmeter was used to record the depth below ground level of the water within a borehole. A dipmeter is a sensor which is connected to a buzzer by a measuring tape. When the sensor reaches water, the buzzer sounds and the depth of the water may be recorded.

More technical details follow about some of this equipment.

Grundfos Environmental Pumps

MP1 & SPE

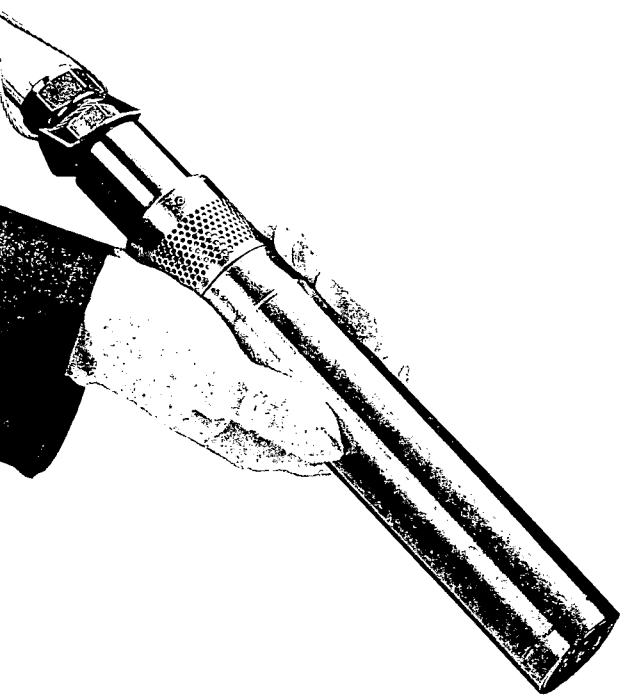

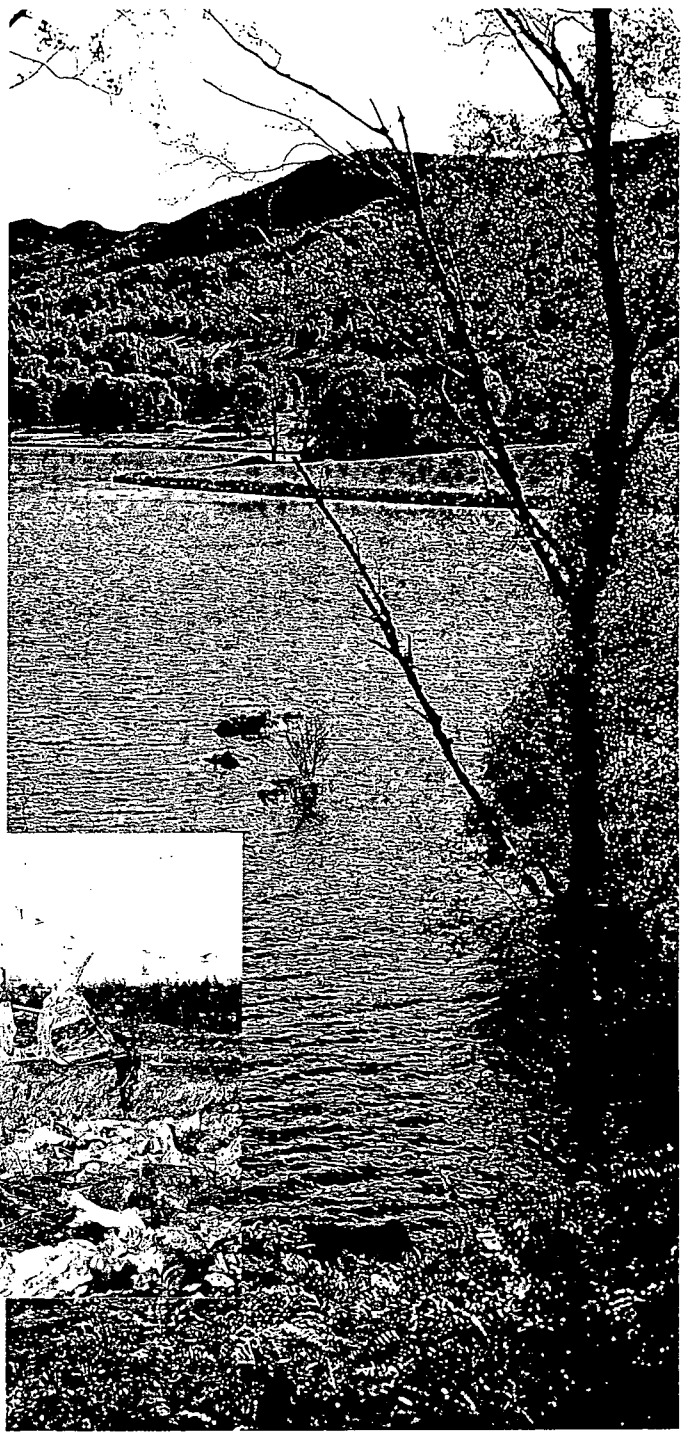

GRUNDFOS®

Accessories

In addition to the pump Grundfos can, in most cases, supply the accessories requisite for carrying through sampling.
If the wells are situated far from electricity supplies, the MP1 pump can be driven by a transportable generator.

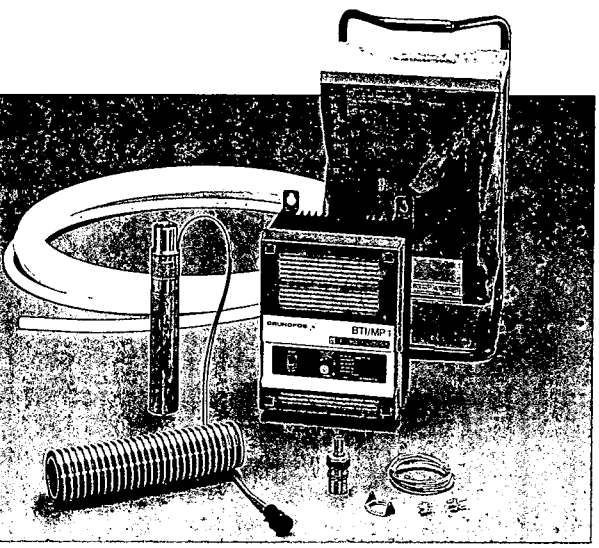

Photo shows a selection of accessories for the MP1 pump.

Frequency Converter
For continuously variable adjustment of MP1 pump performance. Operating frequency and fault readings can be read in the display and there is built-in motor protection.

Frequency Converter Stand
The specially designed converter stand protects the frequency converter against rain, dust etc. The stand features a handle facilitating transport of the converter during sampling.

Motor Cable
The MP1 pump is available with cable lengths varying from 10 to 90 metres. The cable insulation is made of teflon.

Flexible Hoses/Riser Pipes
If required, flexible hoses or riser pipes of teflon, PVC or similar materials are available for connection to the pump.

Straining Wire
In spite of the low pump weight, it is recommended to secure the pump with a steel wire when lowering the pump into the well. Wire and holder are available as accessories.

Service Kit
A service kit consisting of two complete pump stages is available for repairs and replacements.

Remedial Action

When laboratory analyses of water samples have revealed a contamination, the next step will often be to withdraw the contaminated ground water. To cope with this job, use the specially designed Grundfos SPE pump.
Aggressive liquids from refuse dumps and chemical waste dumps etc. contaminate the ground water but, in most cases, do not affect the function and life of the SPE pump.
The SPE pump is made exclusively of highly resistant stainless steel and other resistant materials and is a special variant of Grundfos' reliable and efficient submersible pumps.
The SPE pumps are applicable for performances ranging from 0.8 to 22 m³ per hour at heads up to 200 metres.

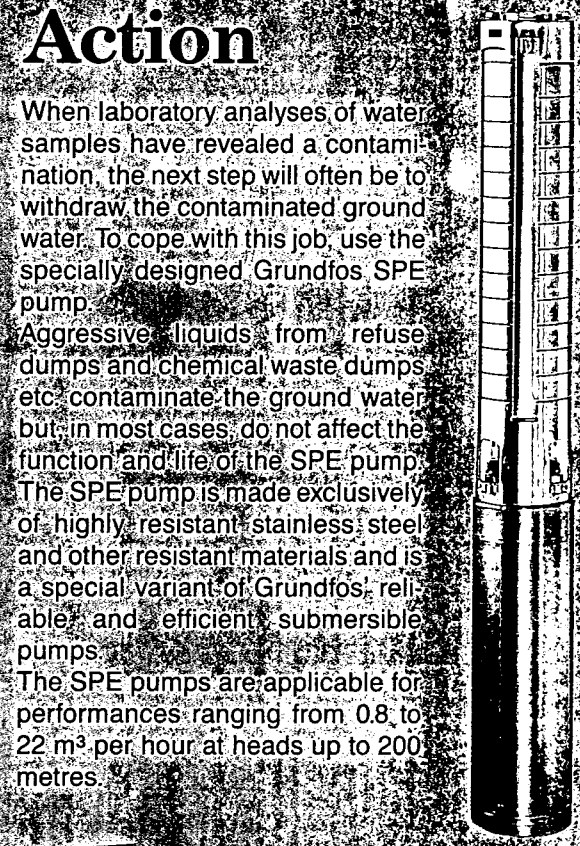

Operating Control
When the SPE pump is installed in the well, the Grundfos Control Unit CU2 constantly monitors the operating conditions of the pump to ensure problem-free operation and long life.

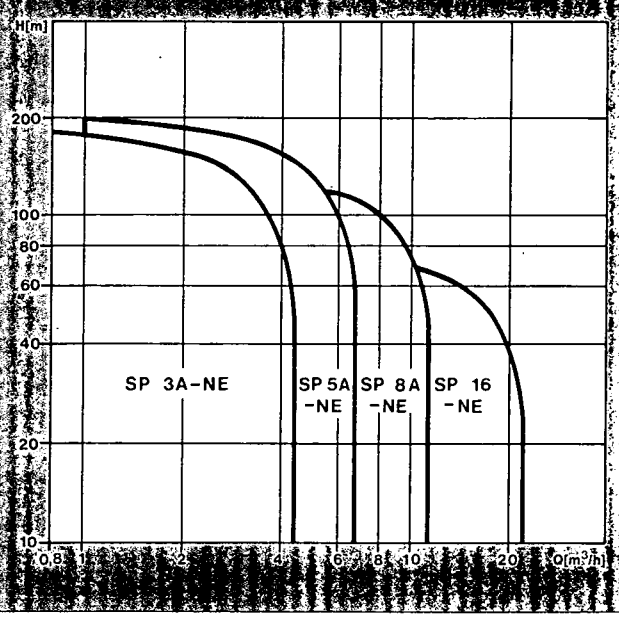

Technical Data MP1

Application

The MP1 is designed for the purging and sampling of contaminated ground water.

Water samples are sent to the laboratory for analysis in order to establish:

- Content of contaminants,
- Concentration of contaminants,
- Extension of contamination plume.

Operating Data

Borehole diameter:	Min. 48 mm (2'')
Temperature of pumped liquid:	+1°C to +30°C.
Ambient temperature:	0°C to +40°C.

The pump is run via an adjustable frequency converter, BTI/MP1, in the 50 to 400 Hz frequency range. This gives the pump a rated performance of 1 m^3/h at 65 m head.

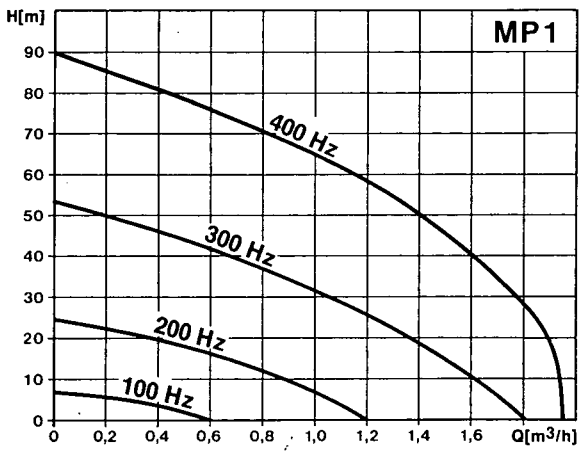

MP1

The MP1 is an integral motor/pump unit made of inert materials. The pumped liquid will thus only be in contact with stainless steel and teflon.

The pump is a 2-stage centrifugal pump with radial impellers. The pump chambers are kept in place by a screwed-on pump housing with connecting thread (Rp ¾). Into the connecting thread can be fitted a riser pipe, compression coupling for flexible hose or possibly a holder for fastening of straining wire.

The suction interconnector connecting motor and pump is equipped with a strainer preventing large particles from entering and blocking the pump.

The motor has a built-in thermal switch which will switch off the motor if the motor temperature exceeds the maximum permissible temperature.

The motor is filled with demineralised water for lubrication of bearings and cooling of rotor. The motor bearings are ceramic and tungsten carbide. This combination of materials gives increased resistance to wear and extended working life.

The cable connecting the motor and the converter is fitted on delivery. The cable is available in several lengths so that cable joints can be avoided.

Converter BTI/MP1

The BTI/MP1 converter, which has been specially made for Grundfos, is a frequency converter for power supply and speed control of GRUNDFOS monitor pump, type MP1. The BTI/MP1 enables continuously variable frequency adjustment corresponding to a speed of the MP1 ranging from approx. 2,800 to approx. 23,000 rpm.

The converter has built-in motor protection for the MP1 pump, and therefore no further overload or short circuit protection of the pump is required.

The small outer dimensions and low weight of the converter makes it especially suitable for being transported from job to job. Before start-up the converter just has to be connected to a 1 × 220 V, 50 Hz electricity supply either from a transportable generator or from an ordinary single-phase household installation.

Sampling

Prior to sampling the well must be purged. By using MP1 the time consumption for this can be reduced considerably compared to other methods, as a high pump performance is achieved when the frequency is raised. When the water sample is taken, the pump performance can be lowered by means of the frequency converter. It is therefore unnecessary to fit a valve for performance adjustment. Through adjustment of the frequency, a steady water flow with minimum risk of degassing is achieved.

In order to avoid cross-contamination, dedicated installation of the pump is recommended. This will save valuable time for the sampling technician as he can quickly disconnect the converter and proceed to the next MP1 installation. However, it is quite all right to use the same MP1 in several wells as lowering and lifting of the pump is quick and easy.

In these cases the pump can be easily dismantled and cleaned or fitted with pre-cleaned parts from service kits.

V7 022011 02.93 GB

GRUNDFOS International a/s . DK-8850 Bjerringbro . Denmark
Telephone: +45 86 68 14 00 . Telefax: +45 86 68 44 72

GRUNDFOS®

The Waterra Inertial Pump . . . simply better.

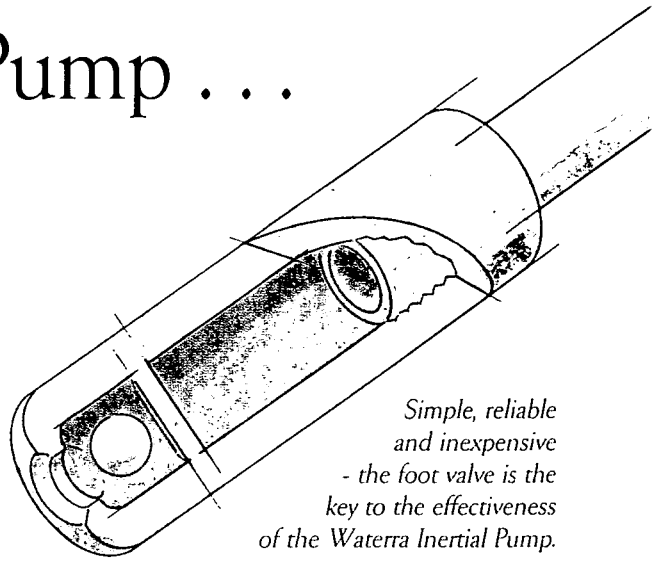

Simple, reliable and inexpensive - the foot valve is the key to the effectiveness of the Waterra Inertial Pump.

Since its conception and development in Canada in the mid 1980's, the Waterra groundwater sampling system has rapidly become the first choice of groundwater professionals around the world.

The Waterra Inertial Pump has proved to be a cost-effective, high performance tool for developing, purging, sampling and hydraulic testing of monitoring wells. So before you invest in expensive and over-sophisticated sampling systems, look seriously at the 'simply better' solution - the Waterra Inertial Pump.

KEY FEATURES:

- Inexpensive and highly reliable.
- Dedicated or portable.
- Manual or power operation.
- Designed for well diameters from 11mm to 150mm.
- Flow rates up to 15 litres/minute.
- Lift capability 70m and greater.
- Highly effective for volatile organic sampling.
- Excellent tool for developing and cleaning sediment-laden wells.

THE WATERRA SYSTEM

The Waterra Inertial Pump consists of 3 components:

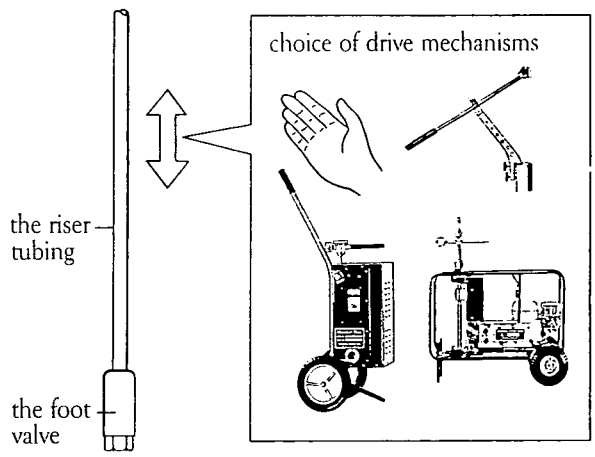

Installation and Operation

The foot valves have self-tapping threads which screw directly on to the tubing without the need for any couplings. A valve wrench (WVR-1) can be used to ensure the valve is securely fastened to the tubing.

In a typical well the tubing and foot valve assembly is lowered to the bottom of the well and the tubing then cut flush with the top of the casing to allow capping of the well when not in use. This takes a matter of minutes to complete - and the only tool required is a sharp knife! The tube will stand unsupported on the base of the well.

To pump water, the tube is oscillated vertically a few centimetres using one of the drive mechanisms or simply by hand. The system requires no priming, and is not limited by suction depth. The water will rise rapidly up the tubing to discharge at surface.

PUMPING CYCLE

1. Tube/Valve assembly is installed in well. Water level inside tube rises to that in the well.
2. A rapid upstroke closes the foot valve and lifts the water column inside the tubing a distance equal to the stroke.
3. At the end of the upstroke, the water column continues to rise due to its momentum. A further column of water is thus simultaneously drawn into the tube.
4. Pushing the tubing down immediately after the upstroke forces a further column of water into the tubing due to the inertia of the water column.
5. The cycle is repeated and water rises in pulses to discharge at the surface.

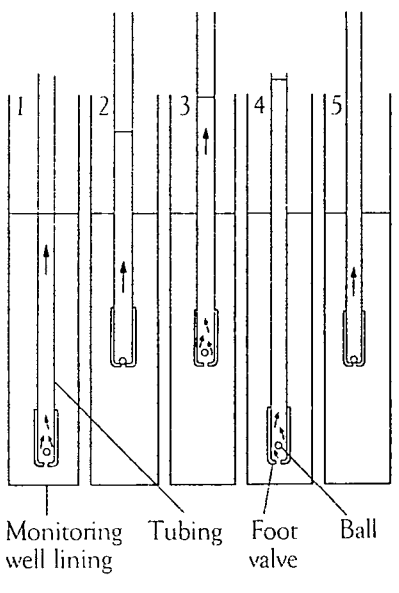

Tubing and Foot Valves

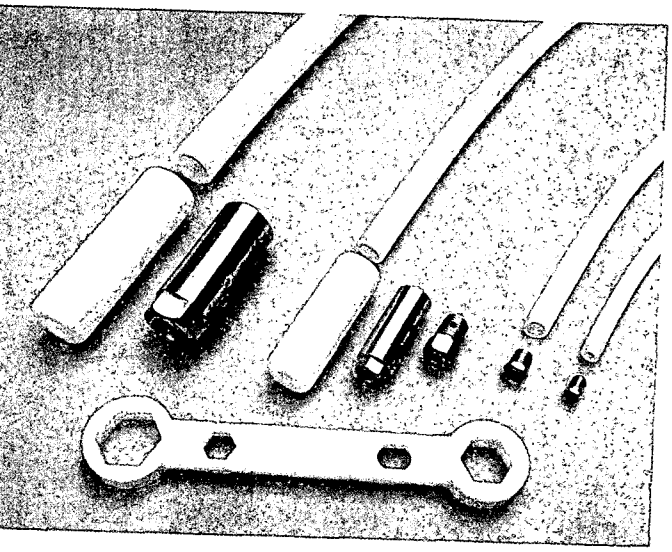

UBING

Waterra tubing is usually sold in coiled lengths of 30m d 60m in a selection of 4 tubing diameters: 10mm (Mini III tem), 13mm (Mini II System), 16mm (Standard System) and mm (High Capacity System). High density polyethylene DPE) is the most commonly used material because of its n strength, durability and low cost. Teflon® tubing is also lable for the Standard System.

OT VALVES

To facilitate the use of the system in a wide variety of well neters or different sampling situations, a selection of rnal and external fitting foot valves in stainless steel and in® plastic are available. Typically the Standard and High acity Systems are used with the Delrin® external fitting valves (D-25 and D-32). Where greater physical wear is cted (eg well development or prolonged purging in nent filled wells) or for specialist applications (eg some nic sampling) stainless steel foot valves are the preferred n (SS-19 and SS-32).

ll internal fitting foot valves for the Mini III, Mini II and dard Systems are manufactured from stainless steel 0, SS-13 and SS-16).

Manual Pumping

Many customers initially purchase the Waterra Inertial Pump because of its unique ability to be operated manually. The maximum recommended depth for manual operation with the Standard System is 30 metres and with the High Capacity System, 15 metres. The Mini Systems are almost always operated manually.

OPERATION BY HAND

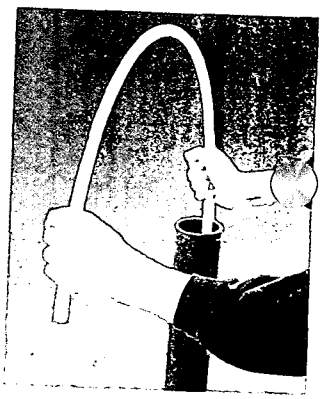

In many situations the Waterra System can literally be operated by hand without the need for any mechanical assistance. This makes the system exceptional, not only in its cost effectiveness but also in situations where access is remote or difficult and heavy equipment cannot easily be transported to site.

To use manually simply withdraw a short length of tubing from the well (add a portable extension tube if the water level is close to the bottom of the well) and oscillate vertically.

USING THE PUMPING HANDLE

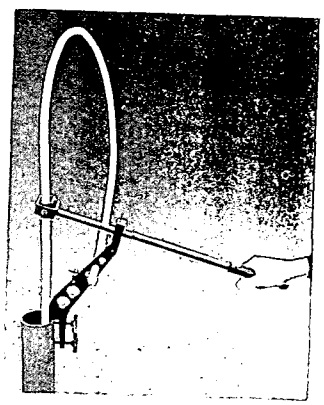

The portable steel pumping handle (WHP-301) attaches to the borehole casing or protective headworks using a simple clamp.

The lever arm can be adjusted to grip the tubing above the centre of the well. A side clamp on the handle allows the discharge end of the tubing to be held in place. The main advantage of the handle is in carrying the weight of the tubing and in allowing it to be temporarily left at rest in a fixed position. The handle is commonly used when pumping with the Standard System at depths in excess of 15 metres and with the High Capacity System at depths in excess of 7 metres.

Accessories

TENSION TUBING

C tubing. Push-fits over riser ng to provide flexible surface harge hose.

-1:
ength for Standard Tubing

-1:
ength for High Capacity Tubing

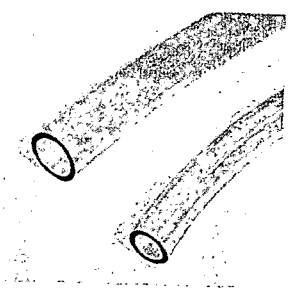

IN-LINE FILTERS & COUPLINGS

The disposable in-line filter (FHT-700) couples directly on to the standard tubing to produce instant field-filtered samples to 0.45 µm.

Coupling adapters are available for either extending the standard tubing at surface (STD/STD-5) or for use with the high capacity tubing (HC/STD-5).

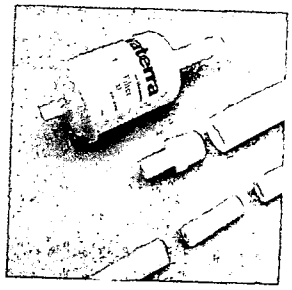

Specifications

TUBING	STANDARD	HIGH CAPACITY	MINI II	MINI III
Diameter	16mm OD/13mm ID	25mm OD/21mm ID	13mm OD/10mm ID	10mm OD/6mm ID
Material	HDPE & Teflon®	HDPE	HDPE	HDPE
Coil sizes	30m (STD-30) 60m (STD-60) Teflon®sold in 5m units	30m (HC-30) 60m (HC-60)	30m (MII-30)	30m (MIII-30)

FOOT VALVES				
External (female) fitting	25mm OD (D-25)	32mm OD (D-32)	—	—
	19mm OD (SS-19)	32mm OD (SS-32)	—	—
Internal (male) fitting	16mm OD (SS-16)	—	13mm OD (SS-13)	10mm OD (SS-10)

D = Delrin® SS = Stainless Steel HDPE = High Density Polyethylene OD = Outside Diameter ID = Inside Diameter

DRIVE MECHANISMS	PUMPING HANDLE (WHP-301)	HYDROLIFT (WHLP-500)	POWER PUMP (WPP-3500)
Motor	—	0.5 hp, 90 VDC electric	3.5hp Honda 4-stroke
Power supply	—	110 VAC, 8 Amp (~1kVA)	—
Gearbox	—	Right angle worm drive	Right angle worm drive
Weight	1.6kg	29.5 kg	60kg
Length/Height/Width	58cm long	25 x 46 x 25cm	91 x 40 x 55cm
Stroke rate per minute	0-120	0-135	70-135

	PUMPING HANDLE (WHP-301)		HYDROLIFT (WHLP-500)		POWER PUMP (WPP-3500)	
PUMP PERFORMANCE	STANDARD SYSTEM	HIGH CAPACITY SYSTEM	STANDARD SYSTEM	HIGH CAPACITY SYSTEM	STANDARD SYSTEM	HIGH CAPACITY SYSTEM
Flow rate l/min.	0-6	0-15	0-6	0-15	0-6	0-15
Lift capacity (50mm well)	50m*	15m	50m	40m	50m	75-90m**
Lift capacity (100mm well)	35m	15m	35m	40m	35m	75m

Notes: * Maximum pumping depth for efficient operation with standard tubing is 50m due to elasticity of tubing below this depth.
**Maximum pumping depth for efficient operation with high capacity tubing is 75m.
Greater depths can be reached by using thicker walled tubing (made to order).

CHOOSING THE CORRECT PUMPING SYSTEM FOR YOUR MONITORING WELLS

Record the well depth, diameter and water level. By consulting the chart below you should be able to determine which system is best suited for your wells. Alternatively, give us a call. Waterra is run by professional hydrogeologists with over 10 years experience of groundwater sampling in a wide variety of environments and all our sales staff have gained practical field experience in using the system on sampling surveys. We will be delighted to help you choose the optimum system for your sampling needs.

STANDARD SYSTEM (16mm HDPE tubing)

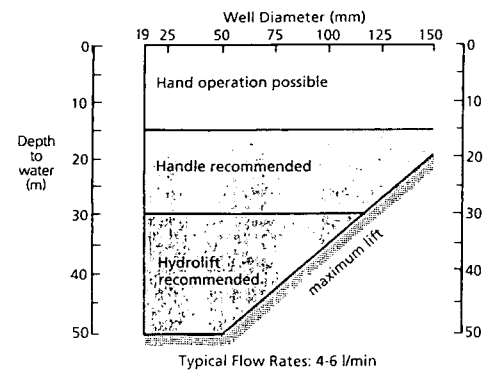

HIGH CAPACITY SYSTEM (25mm HDPE tubing)

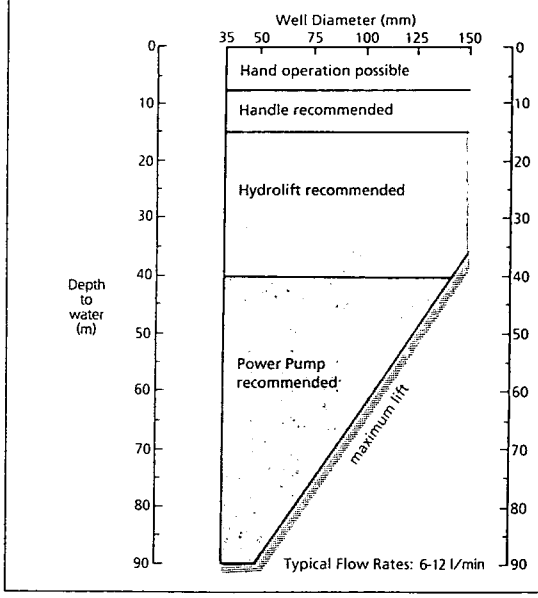

®Teflon and Delrin are trademarks of Dupont

Waterra policy is one of continuous product development and improvement. We therefore reserve the right to amend specifications without notice. Some products may differ from illustrations featured in this brochure.

waterra

Waterra (UK) Limited, Marlow House, 310 Haslucks Green Road, Shirley, Solihull, West Midlands B90 2NE. Telephone: 021-733 7743 Fax: 021-733 7746.

Dedicated uses

EWLOG can be ustomised to meet pplication specific quirements

e near right photograph shows NEWLOG ed with an integral pressure transducer.

external power is required for this system ich is used for mains water pressure cording in chambers subjected to casional flooding.

e photograph far right shows NEWLOG ed with two signal input terminals and the ial port mounted on one side wall of the ger. This dedicated version is supplied to pping bucket raingauge manufacturer.

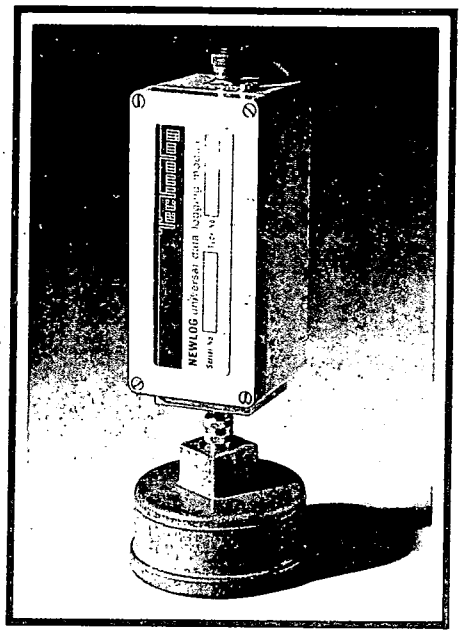

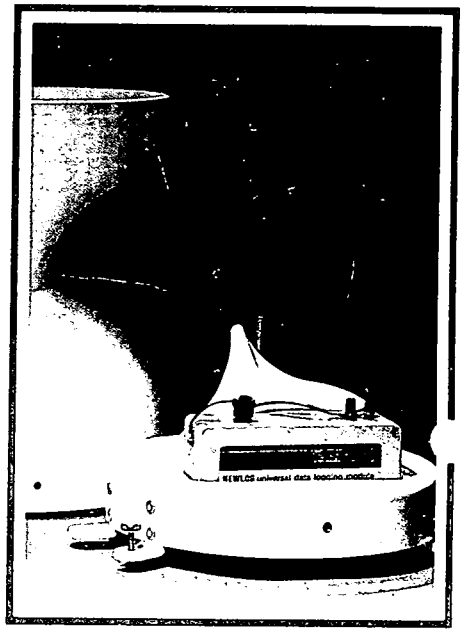

EM NEWLOGS

EWLOG is an ideal ilding block for use by anufacturers of ner equipment

a small, self contained, building block, WLOG can add logging and communi- on facilities to other manufacturers' cialist monitoring instruments.

equipment depicted on the right is a city and height recorder which utilizes WLOG as an intelligent 2 channel uency recorder capturing flow data during er surveys.

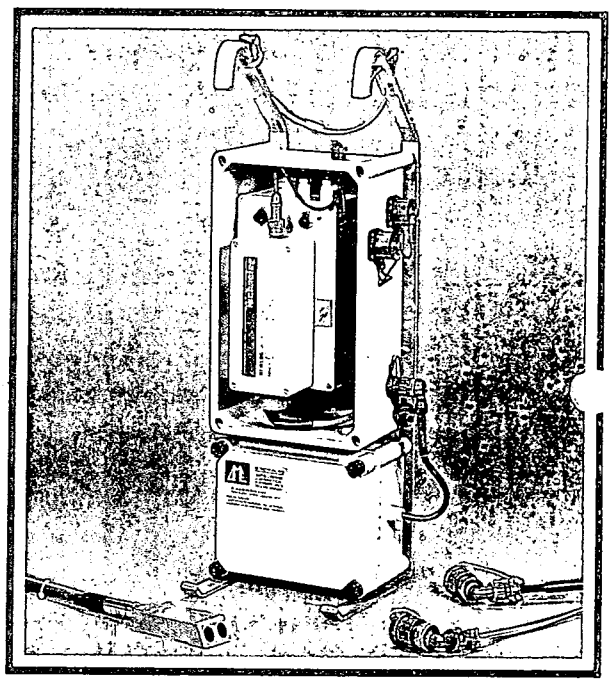

nolog is represented worldwide.
nearest sales and service location is:

Technolog Limited, Technolog House,
Mill Road, Cromford, Derbyshire
DE4 3RQ, England.
Telephone (062 982) 3611/3821

Specifications

nputs

umber of channels:	8
hannel Types:	Voltage, event, state, count, frequency. (independently selectable on each channel)
put impedance:	>300 kilohms
put protection:	Protected against reverse connection and overvoltage.
oltage input:	Range 0–2 volts, ±0.5% accuracy and resolution.
vent input:	Switch closure or logic pulse, date and time of event stored, resolution 10 secs.
tate input:	Switch closure or logic state. On state change, date, time and new state are stored, resolution 10 secs.
ount input:	Switch closures or logic pulses, maximum rate 10 per second. (Counted over and recorded at preset intervals). Resolution 0.01% Max.
requency input:	Switch closures or logic pulses, maximum frequency 16kHz, programmable sampling period of 1 to 250 seconds, independent of recording rate. Resolution 0.01% Max.

Outputs

— 2 independent digital outputs for transducer power control and alarm signalling (0 and 3 volt levels, 100k output impedance).
— 1 fixed output for 'open collector' signal bias (3 volts, 33k output impedance).

erial port

pe:	Optically isolated, full duplex, asynchronous.
ata rate:	1200/1200 baud transmit/receive, or 1200/75 baud for remote communication via modems (V23).
ommand/data format	Verbose (ASCII), or binary.

lemory

pe:	Solid state. Non-volatile.
ze:	32 Kilobyte, allocatable between channels as required.
ta retention:	5 to 10 years (i.e. life of logger).

lock

oe:	Crystal controlled calendar clock, with leap year adjustment.
curacy:	100 seconds per month maximum error over operating temperature range.

upply

oe:	Internally powered by single cell.
e:	5 to 10 years, dependent on method of use.

ecording

cording interval:	1 to 99 seconds, 1 to 99 minutes, 1 to 99 hours.
gging Method:	Time based or threshold logging.
art/stop control:	Local or remote control via serial port. Presettable start and stop date and time.
ta Storage:	Rotating store, or store until full.

nvironmental

erating temperature:	–20°C to +50°C.
otection classification:	IP68 Submersible to 2 metres for unspecified period.

onnectors

12-way input, 4-way serial port, conforming to MIL-C-26482.

echanical

mensions:	Length 160mm, width 75mm, height 35mm.
ight:	1 kg.
unting:	Two fixing holes in base, tapped M4.

rinsic Safety

xia IIC T4	BASEEFA certificate number Ex89C2060.

Druck

PDCR 800 SERIES

General Purpose Pressure Transducers

- **Excellent linearity and hysteresis**
  ±0.1% B.S.L. for ranges to 60 bar
- **High overload capability**
- **Rationalized outputs**
- **Good thermal stability**
  ±1.5% total error band –20° to +80°C
- **Parameter selection available**

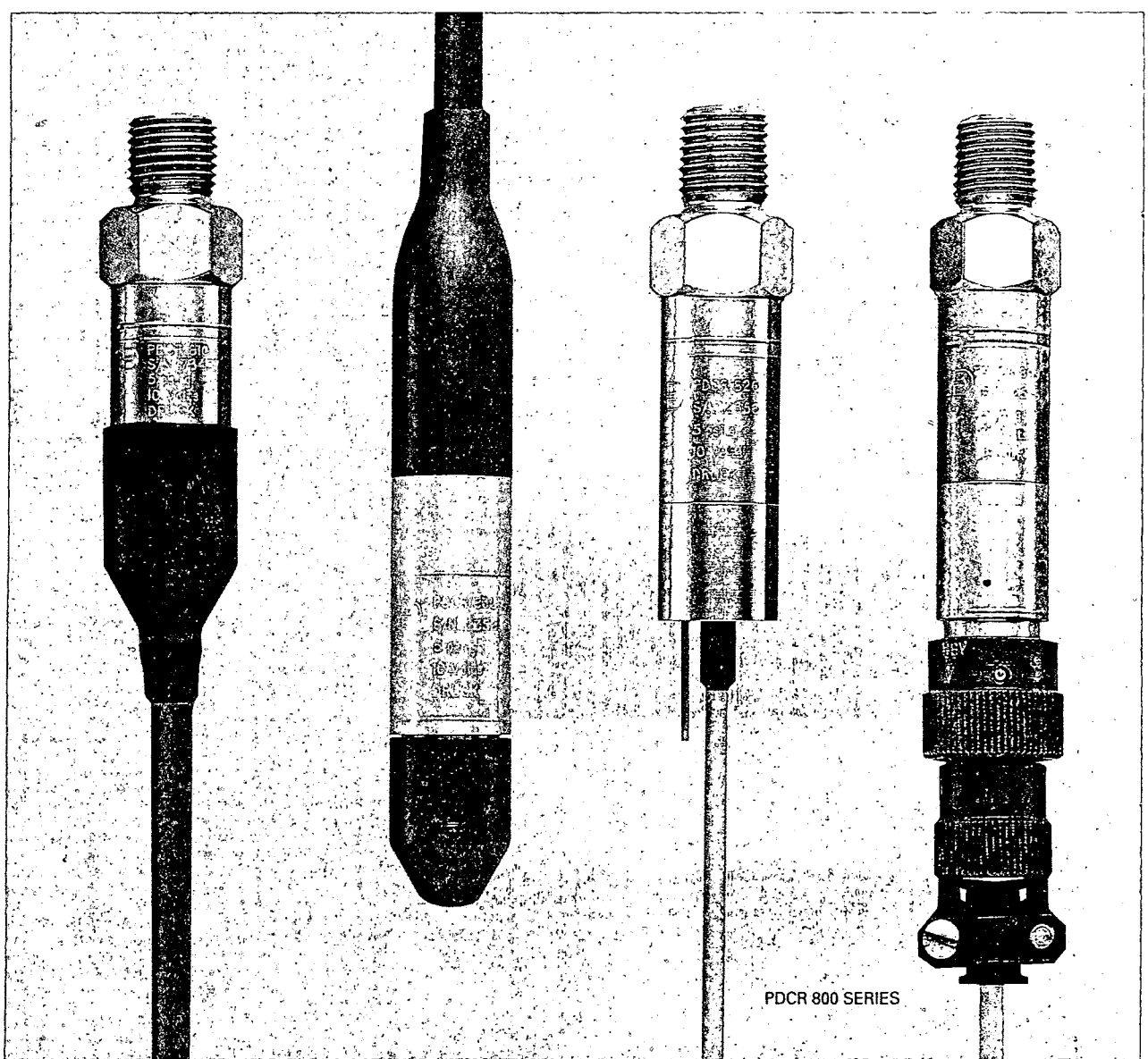

PDCR 800 SERIES

PDCR 800 SERIES: Specification Options

The following summarises the possibilities and for further details and ordering information please contact our Sales Office.

1. Parameter Selection
The PDCR 800 series transducer is calibrated to the nominal full range pressure, and the temperature effects of zero and span are monitored at five temperatures between -20° and +80°C. This information is stored in a computer and enables us, where it is important, to optimise the performance parameters to suit specific applications. Selection can either be for improved performance in accuracy or temperature drift from standard transducers or to optimise certain parameters by using the transducers in the overrange condition.

2. Improved Accuracy
The standard linearity and hysteresis is ±0.1% B.S.L., but this can be improved to ±0.06% B.S.L., or even better by selection. In some cases this may result in a reduction of the full scale output.

3. Higher Overload Pressure
The lowest overload pressure for standard devices is 400% but this can be increased up to 1000% where necessary. This will reduce the full scale output and increase the zero drift with temperature unless this is maintained by selection.

4. Higher Output
All cores can be overranged by three times nominal full scale, giving outputs of up to 300mV for most ranges. This will improve the zero stability, reduce the overload, and the linearity will be slightly degraded.

5. Excitation Voltage
The transducers can be operated from any d.c. excitation up to 12 Volts maximum. The output is proportional to excitation, but the exact offset and span should be measured at the desired excitation.

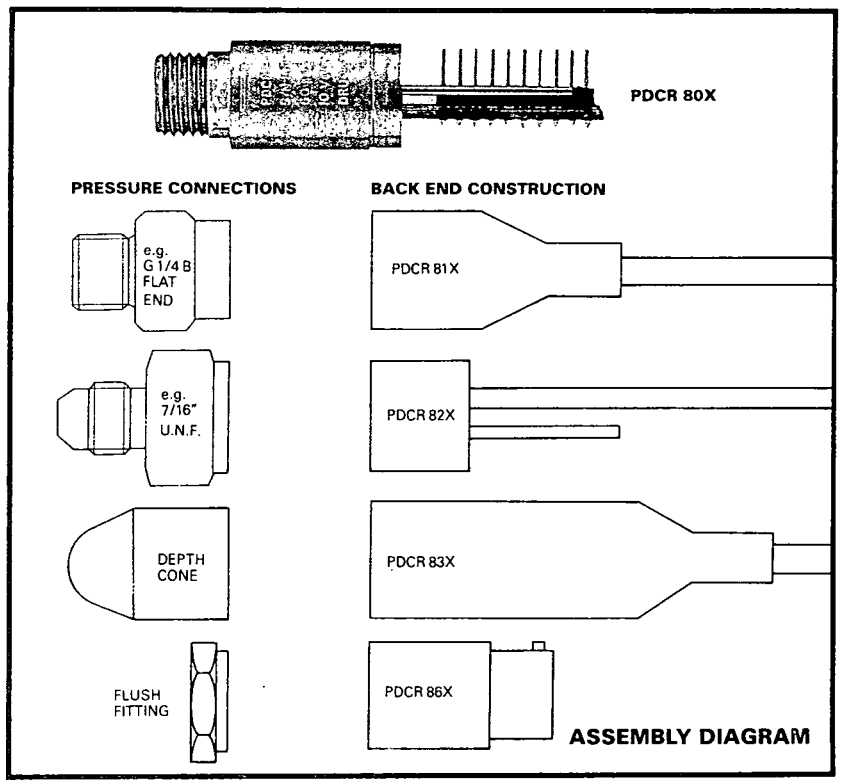

6. Improved Temperature Effects
Improved thermal error bands can be selected from the data base.
e.g. ±0.3% 0° to 50°C
±1% -20° to +80°C

Other error bands over different temperature ranges can also be selected.

7. Improved Zero Stability
Thermal zero shift and long term zero stability are improved proportionally with overload.

8. Long Term Stability
The standard PDCR 800 series offers typically 0.2mV per year stability at 10 Volt operation, but this can be improved considerably by operating in the overrange condition at a reduced supply voltage.

9. Thermal Hysteresis
The calibration of a standard transducer at room temperature will repeat within 0.2mV after cycling through the full temperature range.

10. Rationalization
The transducers can be selected such that both the zero offset and the full scale output are matched to better than 1mV where interchangeability is important.

11. Extended Temperature Range
Transducers are available which will operate between -54° and +125°C.

Please refer to PDCR 82X product note.

12. Rcal
This facility is available by connecting an external resistor across the appropriate connection. The thermal coefficient of this Rcal signal is typically 0.005% F.S./°C.

13. Calibration Print Out
Available on request relating to selected parmeters above.

ORDERING INFORMATION

Please state the following:-
(1) Type number

PDCR 8 X X

- **0** 0° to 50°C
- **1** −20° to +80°C

- **0** basic core
- **1** integral vented cable and boot
- **2** ptfe cable & reference tube
- **3** depth back end with integral vented cable which incorporates a Kevlar strain relieving core
- **6** integral connector & free mating socket

(2) Operating pressure range
(3) Pressure connection
(4) Pressure media

For non-standard requirements please specify in detail.

Examples of alternative specifications based upon a standard 10 bar g transducer

Operating pressure range bar	Overload x F.S.	Accuracy B.S.L. % F.S.	Output with 10 Volt excitation
7	x6	±0.06%	70mV
10	x4(40 bar)	±0.1%	100mV
20	x2	±0.15%	200mV
30	x1.3	±0.2%	300mV

The above example illustrates the various specification performances when using the standard 10 bar core. e.g. used at 20 bar continuously, the overload is x2, accuracy is ±0.15% B.S.L. and output 200mV

10	x4(40 bar)	±0.06%	100mV

The above example can be selected if ±0.06% is required with 100mV output for ranges up to 20 bar.

INSTALLATION DRAWINGS Dimensions: mm

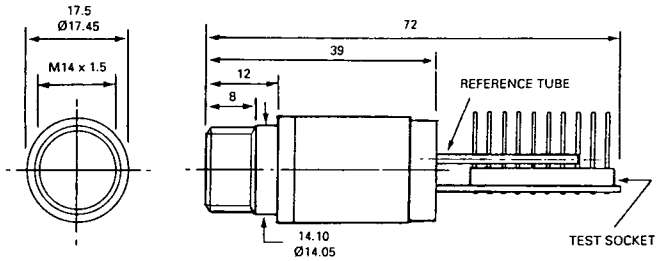

Electrical Connection
Test socket PDCR 80X

k	1	Output negative
f	3	Supply negative
e	4	Supply positive
j	5	Output positive
b	2	Rcal

PDCR 80X

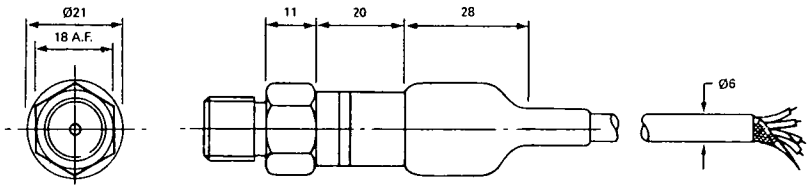

Electrical Connection
6 Core shielded/vented cable

Red	Supply positive
White	Supply negative
Yellow	Output positive
Blue	Output negative
Orange	Rcal
Screen	N/C to transducer body

Any other cores not connected.

PDCR 81X

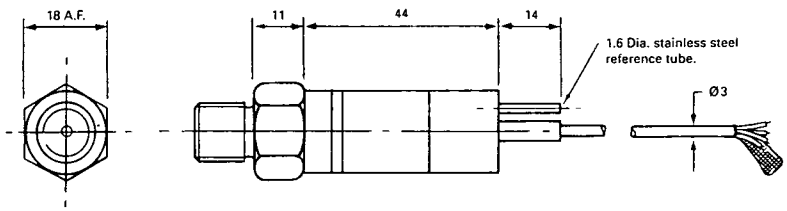

Electrical Connection
4 Core p.t.f.e.shielded cable

Red	Supply positive
Blue	Supply negative
Yellow	Output positive
Green	Output negative
Screen	N/C to transducer body

PDCR 82X

Pressure Connection
Illustrated front end depth cone fitted as standard.

This incorporates a hydraulic damper to protect the device from high pressure pulses caused by underwater impact.

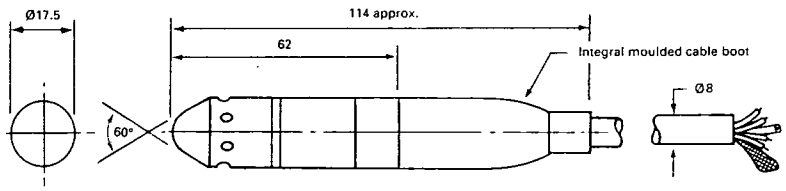

Electrical Connection
9 Core shielded/vented cable

Red	Supply positive
White	Supply negative
Yellow	Output positive
Blue	Output negative
Orange	Rcal
Black, Screen	To transducer body

Any other cores not connected.

PDCR 83X

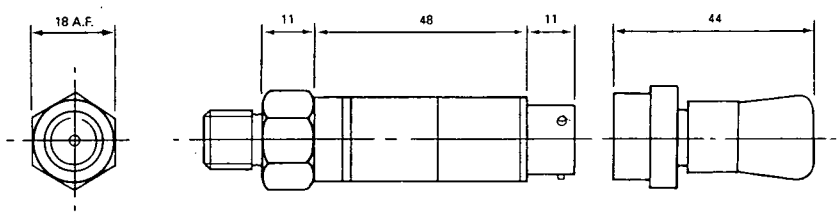

Electrical Connection

Pin A	Supply positive
Pin B	Output positive
Pin C	Output negative
Pin D	Supply negative
Pin E	Rcal

PDCR 86X

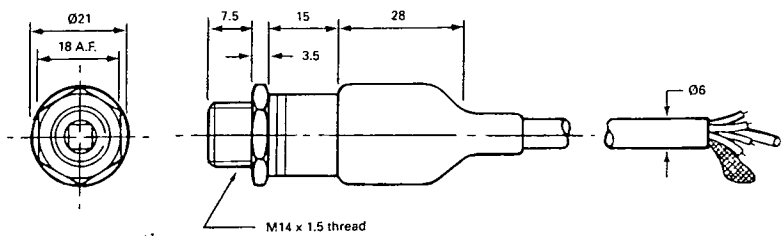

Electrical Connection
6 Core shielded/vented cable

Red	Supply positive
White	Supply negative
Yellow	Output positive
Blue	Output negative
Orange	Rcal
Screen	N/C transducer body

Any other cores not connected.

e.g. PDCR 81X
with flush fitting pressure connection

Druck Limited
Fir Tree Lane, Groby
Leicester LE6 0FH, England
Telephone: (0533) 314314
Telex: 341743 DRUCK G
Facsimile: (0533) 314192

Agent:

Appendix D

D 1:Table of values of W(u)

D 2: Comparison of values of W(u)

D 3: THEISIN.DAT - CONPUTS Input File

D 4: THEISOUT.DAT - CONPUTS Output File

D 5: Table to show the convergence properties of the CONPUTS programme

D 6: Table of values of W(u,r/L)

D 7: Comparison of computer generated values of W(u,r/L) and values taken from tables

D 8: WALTIN.DAT - WALPUTS Input File

D 9: WALTOUT.DAT - WALPUTS Output File

D 10: Table to show the convergence properties of the WALPUTS programme

D 11: Table of values of W(u,β)

D 12: Table showing the values of the complementary error function

D 13: Table comparing the values of W(u,β) from tables and the computer programme

D 14: HANTIN.DAT - HANPUTS Input File

D 15: HANTOUT.DAT - HANPUTS Output File

D 16: Convergence properties of the HANPUTS programme

D 17: Disc with copies of the computer code

		1/u=	n	n(1)	n(2)	n(3)	n(4)	n(5)	n(6)	n(7)	n(8)	n(9)	n(10)
n	N	u=	N	N(-1)	N(-2)	N(-3)	N(-4)	N(-5)	N(-6)	N(-7)	N(-8)	N(-9)	N(-10)
1.00	1.00	W(u)=	0.2194	1.823	4.038	6.332	8.633	10.94	13.24	15.44	17.84	20.15	22.45
0.83	1.20		0.1584	1.66	3.858	6.149	8.451	10.75	13.06	15.36	17.66	19.96	22.27
0.67	1.50		0.1	1.465	3.637	5.927	8.228	10.53	12.83	15.14	17.44	19.74	22.04
0.50	2.00		4.89E-02	1.223	3.355	5.639	7.94	10.24	12.55	14.85	17.15	19.45	21.76
0.40	2.50		2.49E-02	1.044	3.137	5.417	7.717	10.02	12.32	14.62	16.93	19.23	21.53
0.33	3.00		1.31E-02	9.06E-01	2.959	5.235	7.535	9.837	12.14	14.44	16.74	19.05	21.35
0.29	3.50		6.70E-03	0.7942	2.81	5.081	7.381	9.683	11.99	14.29	16.59	18.89	21.2
0.25	4.00		3.78E-03	0.7024	2.681	4.948	7.247	9.55	11.85	14.15	16.46	18.76	21.06
0.22	4.50		2.07E-03	0.6253	2.568	4.831	7.13	9.432	11.73	14.04	16.34	18.64	20.94
0.20	5.00		1.15E-03	0.5598	2.468	4.726	7.024	9.326	11.63	13.93	16.23	18.54	20.84
0.17	6.00		3.60E-04	0.4544	2.295	4.545	6.842	9.144	11.45	13.75	16.05	18.35	20.66
0.14	7.00		1.16E-04	0.3738	2.151	4.392	6.688	8.99	11.29	13.6	15.9	18.2	20.5
0.13	8.00		3.77E-05	0.3106	2.027	4.259	6.555	8.856	11.16	13.46	15.76	18.07	20.37
0.11	9.00		1.25E-05	0.2602	1.919	4.142	6.437	8.739	11.04	13.34	15.65	17.95	20.25

Appendix D1

Table of values of W(u)

Appendix D2
Comparison of values of W(u)

u	W(u) table	W(u) prog.	u	W(u) table	W(u) prog.
1.00E-06	13.24	13.23831	4.00E-03	4.948	4.948257
1.20E-06	13.06	13.05599	4.50E-03	4.831	4.830973
1.50E-06	12.83	12.83285	5.00E-03	4.726	4.726111
2.00E-06	12.55	12.54516	6.00E-03	4.545	4.544787
2.50E-06	12.32	12.32202	7.00E-03	4.392	4.391633
3.00E-06	12.14	12.1397	8.00E-03	4.259	4.259098
3.50E-06	11.99	11.98555	9.00E-03	4.142	4.14231
4.00E-06	11.85	11.85202	1.00E-02	4.038	4.037945
4.50E-06	11.73	11.73423	1.20E-02	3.858	3.857613
5.00E-06	11.63	11.62887	1.50E-02	3.637	3.637449
6.00E-06	11.45	11.44655	2.00E-02	3.355	3.354723
7.00E-06	11.29	11.2924	2.50E-02	3.137	3.136523
8.00E-06	11.16	11.15887	3.00E-02	2.959	2.959134
9.00E-06	11.04	11.04109	3.50E-02	2.81	2.809903
1.00E-05	10.94	10.93573	4.00E-02	2.681	2.681279
1.20E-05	10.75	10.7534	4.50E-02	2.568	2.568392
1.50E-05	10.53	10.53026	5.00E-02	2.468	2.467914
2.00E-05	10.24	10.24258	6.00E-02	2.295	2.295323
2.50E-05	10.02	10.01943	7.00E-02	2.151	2.150854
3.00E-05	9.837	9.837113	8.00E-02	2.027	2.026957
3.50E-05	9.683	9.682963	9.00E-02	1.919	1.918761
4.00E-05	9.55	9.549431	1.00E-01	1.823	1.82294
4.50E-05	9.432	9.431648	1.20E-01	1.66	1.659557
5.00E-05	9.326	9.326288	1.50E-01	1.465	1.464477
6.00E-05	9.144	9.143966	2.00E-01	1.223	1.222666
7.00E-05	8.99	8.989815	2.50E-01	1.044	1.044298
8.00E-05	8.856	8.856284	3.00E-01	9.06E-01	0.9056925
9.00E-05	8.739	8.738501	3.50E-01	0.7942	0.7942315
1.00E-04	8.633	8.63324	4.00E-01	0.7024	0.7023967
1.20E-04	8.451	8.450939	4.50E-01	0.6253	0.6253469
1.50E-04	8.228	8.227825	5.00E-01	0.5598	0.5597891
2.00E-04	7.94	7.940193	6.00E-01	0.4544	0.4543944
2.50E-04	7.717	7.7171	7.00E-01	0.3738	0.3737847
3.00E-04	7.535	7.534828	8.00E-01	0.3106	0.3106127
3.50E-04	7.381	7.380727	9.00E-01	0.2602	0.2601995
4.00E-04	7.247	7.247246	1.00E+00	0.2194	0.2193996
4.50E-04	7.13	7.129513	1.20E+00	0.1584	0.1584241
5.00E-04	7.024	7.024202	1.50E+00	0.1	0.1000353
6.00E-04	6.842	6.841981	2.00E+00	4.89E-02	0.0489162
7.00E-04	6.688	6.68793	2.50E+00	2.49E-02	0.0249306
8.00E-04	6.555	6.554499	3.00E+00	1.31E-02	0.0130641
9.00E-04	6.437	6.436816	3.50E+00	6.70E-03	0.0069858
1.00E-03	6.332	6.331555	4.00E+00	3.78E-03	0.003795
1.20E-03	6.149	6.149434	4.50E+00	2.07E-03	0.0020891
1.50E-03	5.927	5.92659	5.00E+00	1.15E-03	0.001164
2.00E-03	5.639	5.639407	6.00E+00	3.60E-04	0.0003758
2.50E-03	5.417	5.416763	7.00E+00	1.16E-04	0.0001312
3.00E-03	5.235	5.234941	8.00E+00	3.767E-05	5.334E-05
3.50E-03	5.081	5.081289	9.00E+00	1.245E-05	2.812E-05

Appendix D3

THEISIN.DAT

CONPUTS Input File

```
      21       100
 1.0E-10
    20.0  1.389E-3
2.894E-3    5.0E-4
1.00E+02  2.66E-02
2.00E+02  3.80E-02
3.00E+02  4.42E-02
4.00E+02  4.74E-02
5.00E+02  5.31E-02
6.00E+02  5.90E-02
8.00E+02  6.16E-02
1.00E+03  6.83E-02
1.40E+03  7.19E-02
1.80E+03  7.43E-02
3.60E+03  9.13E-02
5.40E+03  9.69E-02
7.20E+03  1.06E-01
9.00E+03  1.12E-01
1.08E+04  1.07E-01
1.26E+04  1.12E-01
1.44E+04  1.18E-01
1.62E+04  1.20E-01
1.80E+04  1.18E-01
1.98E+04  1.20E-01
2.16E+04  1.23E-01
```

Appendix D4

THEISOUT.DAT

CONPUTS Output File

```
*****************************
*                           *
*      CONPUTS - THEIS      *
*      CURVE MATCHING       *
*            BY             *
*  GROUNDWATER ENGINEERING  *
*          DURHAM           *
*                           *
*****************************



NUMBER OF OBSERVATION POINTS =   21
FLOWRATE                     =   .1389000E-02
DISTANCE FROM PUMPED WELL    =   .2000000E+02
TRANSMISSIVITY GUESS         =   .2894000E-02
STORATIVITY GUESS            =   .5000000E-03
CONVERGENCE FACTOR           =   .1000000E-09


---------------------------------
   TIME                 DRAWDOWN
```

.1000000E+03	.2660000E-01
.2000000E+03	.3800000E-01
.3000000E+03	.4420000E-01
.4000000E+03	.4740000E-01
.5000000E+03	.5310000E-01
.6000000E+03	.5900000E-01
.8000000E+03	.6160000E-01
.1000000E+04	.6830000E-01
.1400000E+04	.7190000E-01
.1800000E+04	.7430000E-01
.3600000E+04	.9130000E-01
.5400000E+04	.9690000E-01
.7200000E+04	.1060000E+00
.9000000E+04	.1120000E+00
.1080000E+05	.1070000E+00
.1260000E+05	.1120000E+00
.1440000E+05	.1180000E+00
.1620000E+05	.1200000E+00
.1800000E+05	.1180000E+00
.1980000E+05	.1200000E+00
.2160000E+05	.1230000E+00

IT. NO	ERROR	TRANS.	STORAGE

1	.8412558E-02	.3632871E-02	.7421505E-03
2	.2516269E-02	.5034912E-02	.9265856E-03
3	.1810996E-03	.5783427E-02	.9717024E-03
4	.6682498E-05	.5910697E-02	.9685771E-03
5	.4222603E-05	.5913558E-02	.9682750E-03
6	.4221703E-05	.5913561E-02	.9682741E-03
7	.4221703E-05	.5913561E-02	.9682741E-03

TIME(S)	HEAD OBSERVED(M)	HEAD CALCULATED(M)	LOG TIME	LOG HEAD OBSERVED	LOG HEAD CALCULATED
.1000000E+03	.2660000E-01	.2597291E-01	.2000000E+01	-.1575118E+01	-.1585479E+01
.2000000E+03	.3800000E-01	.3748871E-01	.2301030E+01	-.1420216E+01	-.1426100E+01
.3000000E+03	.4420000E-01	.4457436E-01	.2477121E+01	-.1354578E+01	-.1350915E+01
.4000000E+03	.4740000E-01	.4970251E-01	.2602060E+01	-.1324222E+01	-.1303622E+01
.5000000E+03	.5310000E-01	.5372315E-01	.2698970E+01	-.1274905E+01	-.1269839E+01
.6000000E+03	.5900000E-01	.5703050E-01	.2778151E+01	-.1229148E+01	-.1243893E+01
.8000000E+03	.6160000E-01	.6228168E-01	.2903090E+01	-.1210419E+01	-.1205640E+01
.1000000E+04	.6830000E-01	.6637675E-01	.3000000E+01	-.1165579E+01	-.1177984E+01
.1400000E+04	.7190000E-01	.7257908E-01	.3146128E+01	-.1143271E+01	-.1139189E+01
.1800000E+04	.7430000E-01	.7722819E-01	.3255273E+01	-.1129011E+01	-.1112224E+01
.3600000E+04	.9130000E-01	.9009940E-01	.3556303E+01	-.1039529E+01	-.1045278E+01
.5400000E+04	.9690000E-01	.9764985E-01	.3732394E+01	-.1013676E+01	-.1010328E+01
.7200000E+04	.1060000E+00	.1030129E+00	.3857332E+01	-.9746941E+00	-.9871084E+00
.9000000E+04	.1120000E+00	.1071753E+00	.3954243E+01	-.9507820E+00	-.9699053E+00
.1080000E+05	.1070000E+00	.1105775E+00	.4033424E+01	-.9706162E+00	-.9563333E+00
.1260000E+05	.1120000E+00	.1134547E+00	.4100371E+01	-.9507820E+00	-.9451773E+00
.1440000E+05	.1180000E+00	.1159476E+00	.4158362E+01	-.9281180E+00	-.9357382E+00

.1620000E+05	.1200000E+00	.1181468E+00	.4209515E+01	-.9208188E+00	-.9275781E+00
.1800000E+05	.1180000E+00	.1201142E+00	.4255273E+01	-.9281180E+00	-.9204055E+00
.1980000E+05	.1200000E+00	.1218942E+00	.4296665E+01	-.9208188E+00	-.9140170E+00
.2160000E+05	.1230000E+00	.1235193E+00	.4334454E+01	-.9100949E+00	-.9082653E+00

THE VALUE OF TRANSIMISSIVITY (MSQ/DAY) = .5109316E+03
THE VALUE OF STORATIVITY = .9682741E-03
THE AVERAGE ERROR BETWEEN THE HEADS(M) = .2054678E-02

Appendix D5

Table to show the convergence properties of the CONPUTS programme

T guess (m^2/day)	S guess	Convergence? (Y/N)	No. of iterations
5	1.0×10^{-1}	N	
5	1.0×10^{-2}	Y	20
5	1.0×10^{-3}	Y	18
5	1.0×10^{-4}	Y	17
5	1.0×10^{-5}	Y	17
50	1.0×10^{-1}	Y	16
50	1.0×10^{-2}	Y	12
50	1.0×10^{-3}	Y	12
50	1.0×10^{-4}	Y	11
50	1.0×10^{-5}	Y	19
1000	1.0×10^{-1}	Y	15
1000	1.0×10^{-2}	Y	10
1000	1.0×10^{-3}	Y	6
1000	1.0×10^{-4}	Y	12
1000	1.0×10^{-5}	Y	19
2500	1.0×10^{-1}	Y	15
2500	1.0×10^{-2}	Y	8
2500	1.0×10^{-3}	Y	8
2500	1.0×10^{-4}	Y	11
2500	1.0×10^{-5}	Y	19

In each case the programme converged to the same values:

Transmissivity = 510.9 m^2/day
Storativity = 9.68×10^{-4}
Root mean square error = 2.05 mm

u r/L=	0	0.005	0.01	0.02	0.03	0.04	0.05	0.06	0.07	0.08	0.09	0.1
0		10.8	9.44	8.06	7.25	6.67	6.23	5.87	5.56	5.29	5.06	4.85
1.00E-06	13.2											
2.00E-06	12.5											
4.00E-06	11.8	10.7										
6.00E-06	11.4	10.6					W(u,r/L) = W(0,r/L)					
8.00E-06	11.2	10.5	9.43									
1.00E-05	10.9	10.4	9.42									
2.00E-05	10.2	9.95	9.3									
4.00E-05	9.55	9.4	9.01	8.03								
6.00E-05	9.14	9.04	8.77	7.98	7.24							
8.00E-05	8.86	8.78	8.57	7.91	7.23							
1.00E-04	8.63	8.57	8.4	7.84	7.21							
2.00E-04	7.94	7.91	7.82	7.5	7.07	6.62	6.22	5.86				
4.00E-04	7.25	7.23	7.19	7.01	6.76	6.45	6.14	5.83	5.55			
6.00E-04	6.84	6.83	6.8	6.68	6.5	6.27	6.02	5.77	5.51	5.27	5.05	
8.00E-04	6.55		6.52	6.43	6.29	6.11	5.91	5.69	5.46	5.25	5.04	4.84
1.00E-03	6.33		6.31	6.23	6.12	5.97	5.8	5.61	5.41	5.21	5.01	4.83
2.00E-03	5.64		5.63	5.59	5.53	5.45	5.35	5.24	5.12	4.89	4.85	4.71
4.00E-03	4.95		4.94	4.92	4.89	4.85	4.8	4.74	4.67	4.59	4.51	4.42
6.00E-03	4.54			4.53	4.51	4.48	4.45	4.4	4.36	4.3	4.24	4.18
8.00E-03	4.26			4.25	4.23	4.21	4.19	4.15	4.12	4.08	4.03	3.98
1.00E-02	4.04			4.03	4.02	4	3.98	3.95	3.92	3.89	3.85	3.81
2.00E-02	3.35				3.34	3.34	3.33	3.31	3.3	3.28	3.26	3.24
4.00E-02	2.68					2.67	2.67	2.66	2.65	2.65	2.64	2.63
6.00E-02	2.29							2.28	2.28	2.27	2.27	2.26
8.00E-02	2.03							2.02	2.02	2.01	2.01	2
1.00E-01	1.82			W(u,r/L)=W(u,0)					1.81	1.81	1.81	1.8
2.00E-01	1.22										1.22	1.21
4.00E-01	0.702										0.7	0.7
6.00E-01	0.454											0.453
8.00E-01	0.311											0.31

Appendix D6: Table of values of W(u,r/L)

u r/L=	0	0.2	0.3	0.4	0.6	0.8	1	2	3	4	5	6
0		3.5	2.74	2.23	1.55	1.13	0.842	0.228	0.0695	0.0223	0.0074	0.0025
1.00E-04	8.63											
2.00E-04	7.94											
4.00E-04	7.25											
6.00E-04	6.84			W(u,r/L) = W(0,r/L)								
8.00E-04	6.55											
1.00E-03	6.33											
2.00E-03	5.64											
4.00E-03	4.95	3.48										
6.00E-03	4.54	3.43										
8.00E-03	4.26	3.36	2.73									
1.00E-02	4.04	3.29	2.71	2.22								
2.00E-02	3.35	2.95	2.57	2.18								
4.00E-02	2.68	2.48	2.27	2.02	1.52							
6.00E-02	2.29	2.17	2.02	1.84	1.46	1.11	0.839					
8.00E-02	2.03	1.93	1.83	1.69	1.39	1.08	0.832					
1.00E-01	1.82	1.75	1.67	1.56	1.31	1.05	0.819					
2.00E-01	1.22	1.19	1.16	1.11	0.996	0.858	0.715	0.227				
4.00E-01	0.702	0.693	0.681	0.665	0.621	0.565	0.502	0.21	0.0691			
6.00E-01	0.454	0.45	0.444	0.436	0.415	0.387	0.354	0.177	0.0664	0.0222		
8.00E-01	0.311	0.308	0.305	0.301	0.289	0.273	0.254	0.144	0.0607	0.0218		
1.00E+00	0.219	0.218	0.216	0.214	0.207	0.197	0.185	0.114	0.0534	0.0207	0.0073	
2.00E+00	0.0489	0.0487	0.0485	0.0482	0.0473	0.046	0.0444	0.0335	0.021	0.0112	0.0051	0.0021
4.00E+00	0.00378						0.0036	0.0031	0.0024	0.0016	0.001	0.0006

Appendix D6 (continued)

Table of values of W(u,r/L)

	r/L=	1.00E-02		5.00E-02		9.00E-02		3.00E-01		8.00E-01	
u		Table	Program	Table	Program	Table	Program	Table	Program	Table	Program
2.00E-06		9.44E+00	9.442572	6.23E+00	6.228497	5.06E+00	5.062044	2.74E+00	2.744891	1.13E+00	1.13064
6.00E-06		9.44E+00	9.439548	6.23E+00	6.228497	5.06E+00	5.062044	2.74E+00	2.744891	1.13E+00	1.13064
2.00E-05		9.30E+00	9.296228	6.23E+00	6.228497	5.06E+00	5.062044	2.74E+00	2.744891	1.13E+00	1.13064
6.00E-05		8.77E+00	8.767422	6.23E+00	6.22856	5.06E+00	5.062044	2.74E+00	2.744891	1.13E+00	1.13064
2.00E-04		7.82E+00	7.819342	6.22E+00	6.217428	5.06E+00	5.062106	2.74E+00	2.744891	1.13E+00	1.13064
6.00E-04		6.80E+00	6.801052	6.02E+00	6.023976	5.05E+00	5.053973	2.74E+00	2.744891	1.13E+00	1.13064
2.00E-03		5.63E+00	5.627206	5.35E+00	5.353859	4.85E+00	4.847562	2.74E+00	2.744956	1.13E+00	1.13064
6.00E-03		4.54E+00	4.540839	4.45E+00	4.446775	4.24E+00	4.244723	2.74E+00	2.739859	1.13E+00	1.13064
2.00E-02		3.35E+00	3.354723	3.33E+00	3.326477	3.26E+00	3.264734	2.57E+00	2.568813	1.13E+00	1.130667
6.00E-02		2.29E+00	2.295223	2.29E+00	2.287009	2.27E+00	2.268475	2.02E+00	2.022741	1.11E+00	1.111614
2.00E-01		1.22E+00	1.221678	1.22E+00	1.220891	1.22E+00	1.216888	1.16E+00	1.160251	8.58E-01	0.857537
6.00E-01		4.54E-01	0.4438342	4.54E-01	0.4543944	4.54E+00	0.4534634	4.44E-01	0.4441701	3.87E-01	0.3871166
2.00E+00		4.89E-02	0.0488978	4.89E-02	0.0488866	4.89E-02	0.0488603	4.85E-02	0.0484779	4.60E-02	0.0459895

Appendix D7

Comparison of computer generated values of W(u,r/L) and values taken from tables

Appendix D8

WALTIN.DAT

WALPUTS Input File

```
      21         20
  1.0E-10       1.0
     20.0
5.556E-3
2.894E-3
   5.0E-4
    500.0
1.00E+02  9.89E-02
2.00E+02  1.48E-01
3.00E+02  1.82E-01
4.00E+02  1.94E-01
5.00E+02  2.19E-01
6.00E+02  2.26E-01
8.00E+02  2.42E-01
1.00E+03  2.61E-01
1.40E+03  2.90E-01
1.80E+03  2.85E-01
3.60E+03  3.32E-01
5.40E+03  3.71E-01
7.20E+03  3.91E-01
9.00E+03  3.98E-01
1.08E+04  4.03E-01
1.26E+04  4.09E-01
1.44E+04  3.94E-01
1.62E+04  3.97E-01
1.80E+04  3.90E-01
1.98E+04  3.82E-01
2.16E+04  3.93E-01
```

Appendix D9

WALTOUT.DAT

WALPUTS Output File

```
*****************************
*                           *
*     WALPUTS - WALTON      *
*      CURVE MATCHING       *
*            BY             *
*  GROUNDWATER ENGINEERING  *
*          DURHAM           *
*                           *
*****************************
```

NUMBER OF OBSERVATION POINTS	=	21
FLOWRATE (CUB M/S)	=	.5556000E-02
DISTANCE FROM PUMPED WELL (M)	=	.2000000E+02
TRANSMISSIVITY GUESS (MSQ/S)	=	.2894000E-02
STORATIVITY GUESS	=	.5000000E-03
LEAKAGE GUESS (M)	=	.5000000E+03
R/L	=	.4000000E-01

CONVERGENCE FACTOR = .1000000E-09
RELAXATION FACTOR = .1000000E+01

TIME	MEASURED HEAD
.1000000E+03	.9890000E-01
.2000000E+03	.1480000E+00
.3000000E+03	.1820000E+00
.4000000E+03	.1940000E+00
.5000000E+03	.2190000E+00
.6000000E+03	.2260000E+00
.8000000E+03	.2420000E+00
.1000000E+04	.2610000E+00
.1400000E+04	.2900000E+00
.1800000E+04	.2850000E+00
.3600000E+04	.3320000E+00
.5400000E+04	.3710000E+00
.7200000E+04	.3910000E+00
.9000000E+04	.3980000E+00
.1080000E+05	.4030000E+00
.1260000E+05	.4090000E+00
.1440000E+05	.3940000E+00
.1620000E+05	.3970000E+00
.1800000E+05	.3900000E+00
.1980000E+05	.3820000E+00

.2160000E+05 .3930000E+00

IT NO	ERROR	TRANS.	STORAGE	R/L
1	.3789454E+00	.4270415E-02	.6368267E-03	.5973523E-01
2	.1437410E+00	.5184461E-02	.9287129E-03	.7539169E-01
3	.3961505E-01	.5410550E-02	.1087358E-02	.9577469E-01
4	.9744232E-02	.5487318E-02	.1087761E-02	.9340021E-01
5	.9605891E-02	.5475910E-02	.1091320E-02	.9324647E-01
6	.9590470E-02	.5473022E-02	.1092197E-02	.9346787E-01
7	.9590056E-02	.5474092E-02	.1091878E-02	.9344658E-01
8	.9590031E-02	.5474112E-02	.1091871E-02	.9343666E-01
9	.9590027E-02	.5474046E-02	.1091891E-02	.9343930E-01
10	.9590027E-02	.5474054E-02	.1091889E-02	.9343951E-01

TIME (S)	HEAD OBSERVED(M)	HEAD CALCULATED(M)	LOG TIME	LOG HEAD OBSERVED	LOG HEAD CALCULATED
.1000000E+03	.9890000E-01	.9842505E-01	.2000000E+01	-.1004804E+01	-.1006894E+01
.2000000E+03	.1480000E+00	.1461641E+00	.2301030E+01	-.8297383E+00	-.8351592E+00
.3000000E+03	.1820000E+00	.1755327E+00	.2477121E+01	-.7399286E+00	-.7556419E+00
.4000000E+03	.1940000E+00	.1966458E+00	.2602060E+01	-.7121983E+00	-.7063154E+00
.5000000E+03	.2190000E+00	.2130564E+00	.2698970E+01	-.6595559E+00	-.6715054E+00
.6000000E+03	.2260000E+00	.2264281E+00	.2778151E+01	-.6458916E+00	-.6450697E+00
.8000000E+03	.2420000E+00	.2473489E+00	.2903090E+01	-.6161846E+00	-.6066900E+00
.1000000E+04	.2610000E+00	.2633275E+00	.3000000E+01	-.5833595E+00	-.5795037E+00

.1400000E+04	.2900000E+00	.2867898E+00	.3146128E+01	-.5376020E+00	-.5424363E+00
.1800000E+04	.2850000E+00	.3036315E+00	.3255273E+01	-.5451551E+00	-.5176532E+00
.3600000E+04	.3320000E+00	.3454956E+00	.3556303E+01	-.4788619E+00	-.4615575E+00
.5400000E+04	.3710000E+00	.3655831E+00	.3732394E+01	-.4306261E+00	-.4370138E+00
.7200000E+04	.3910000E+00	.3772808E+00	.3857332E+01	-.4078232E+00	-.4233353E+00
.9000000E+04	.3980000E+00	.3847296E+00	.3954243E+01	-.4001169E+00	-.4148444E+00
.1080000E+05	.4030000E+00	.3897266E+00	.4033424E+01	-.3946950E+00	-.4092400E+00
.1260000E+05	.4090000E+00	.3931955E+00	.4100371E+01	-.3882767E+00	-.4053914E+00
.1440000E+05	.3940000E+00	.3956630E+00	.4158362E+01	-.4045038E+00	-.4026745E+00
.1620000E+05	.3970000E+00	.3974501E+00	.4209515E+01	-.4012095E+00	-.4007173E+00
.1800000E+05	.3900000E+00	.3987630E+00	.4255273E+01	-.4089354E+00	-.3992852E+00
.1980000E+05	.3820000E+00	.3997381E+00	.4296665E+01	-.4179366E+00	-.3982245E+00
.2160000E+05	.3930000E+00	.4004692E+00	.4334454E+01	-.4056074E+00	-.3974309E+00

BEST FIT VALUES

==========

THE VALUE OF TRANSMISSIVITY (M SQ/DAY)	=	.4729583E+03
THE VALUE OF STORATIVITY	=	.1091889E-02
THE VALUE OF R/L	=	.9343951E-01
THE LEAKAGE FACTOR (M)	=	.2140422E+03
THE AVERAGE ERROR BETWEEN CALCULATED AND OBSERVED VALUES OF DRAWDOWN (M)	=	.9590027E-02

Appendix D10

Table to show the convergence properties of the WALPUTS programme

T guess m^2/day	S guess	L guess (m)	Converge (Y/N) ?	No. of iterations	Comments
5	1.0×10^{-2}	100	N	20	Divergent
		400	N	12	Theis
		800	N	12	Theis
5	1.0×10^{-3}	100	Y	17	Converged
		400	N	11	Theis
		800	N	11	Theis
5	1.0×10^{-4}	100	N	20	Divergent
		400	Y	17	Converged
		800	Y	17	Converged
250	1.0×10^{-2}	100	Y	10	Converged
		400	N	2	Theis
		800	N	2	Theis
250	1.0×10^{-3}	100	Y	7	Converged
		400	Y	8	Converged
		800	N	1	Theis
250	1.0×10^{-4}	100	N	20	Divergent
		400	Y	12	Converged
		800	Y	12	Converged
750	1.0×10^{-2}	100	Y	10	Converged
		400	N	1	Theis
		800	N	1	Theis
750	1.0×10^{-3}	100	Y	9	Converged
		400	N	20	Divergent
		800	N	1	Divergent
750	1.0×10^{-4}	100	N	20	Divergent
		400	N	20	Divergent
		800	Y	12	Converged
1000	1.0×10^{-2}	100	N	20	Divergent
		400	N	1	Theis
		800	N	1	Theis
1000	1.0×10^{-3}	100	N	20	Divergent
		400	N	20	Divergent
		800	N	20	Divergent
1000	1.0×10^{-4}	100	N	20	Divergent
		400	N	20	Divergent
		800	N	20	Divergent

Convergence led to values of

Transmissivity = 473.0 m^2/day Storativity = 1.09×10^{-3}

Leakage factor = 214.0 m Root mean square error = 9.60 mm

Appendix D11

Table of values of W(u,beta)

u	Beta						
	0.001	0.002	0.005	0.01	0.02	0.05	0.1
1.00E-06	12	11.4	10.6	9.93	9.25	8.34	7.65
2.00E-06	11.5	11	10.2	9.57	8.89	7.99	7.3
4.00E-06	11.1	10.6	9.84	9.2	8.54	7.64	6.95
6.00E-06	10.8	10.3	9.61	8.99	8.33	7.44	6.75
8.00E-06	10.5	10.1	9.45	8.84	8.18	7.29	6.61
0.00001	10.4	10	9.32	8.71	8.07	7.18	6.49
0.00002	9.82	9.51	8.9	8.33	7.7	6.82	6.15
0.00004	9.24	8.99	8.46	7.93	7.33	6.47	5.8
0.00006	8.88	8.67	8.19	7.69	7.11	6.26	5.59
0.00008	8.63	8.43	8	7.52	6.95	6.11	5.44
0.0001	8.43	8.25	7.84	7.38	6.82	5.99	5.33
0.0002	7.79	7.66	7.33	6.93	6.42	5.62	4.97
0.0004	7.14	7.04	6.78	6.45	6	5.25	4.62
0.0006	6.75	6.67	6.45	6.16	5.74	5.02	4.4
0.0008	6.48	6.4	6.21	5.94	5.55	4.86	4.25
0.001	6.26	6.2	6.02	5.77	5.4	4.73	4.13
0.002	5.59	5.54	5.41	5.22	4.91	4.32	3.76
0.004	4.91	4.88	4.78	4.64	4.4	3.89	3.38
0.006	4.52	4.49	4.41	4.29	4.08	3.62	3.14
0.008	4.23	4.21	4.14	4.04	3.85	3.43	2.98
0.01	4.02	4	3.93	3.84	3.67	3.28	2.84
0.02	3.34	3.33	3.28	3.21	3.09	2.78	2.42
0.04	2.67	2.66	2.63	2.58	2.5	2.27	1.98
0.06	2.29	2.28	2.26	2.22	2.15	1.96	1.72
0.08	2.02	2.01	1.99	1.96	1.9	1.74	1.53
0.1	1.82	1.81	1.79	1.77	1.72	1.58	1.39
0.2	1.22	1.22	1.21	1.19	1.16	1.07	0.95
0.4	0.701	0.699	0.694	0.685	0.668	0.622	0.554
0.6	0.453	0.452	0.449	0.444	0.433	0.404	0.361
0.8	0.31	0.309	0.307	0.304	0.297	0.277	0.248
1	0.219	0.218	0.217	0.214	0.21	0.196	0.176
2	0.0488	4.87E-02	4.84E-02	4.79E-02	4.68E-02	4.39E-02	3.95E-02
4	0.00377	3.76E-03	3.74E-03	3.70E-03	3.62E-03	3.40E-03	3.07E-03
6	3.59E-04	3.59E-04	3.56E-04	3.53E-04	3.45E-04	3.25E-04	2.93E-04
8	3.76E-05	3.75E-05	3.73E-05	3.69E-05	3.62E-05	3.40E-05	3.07E-05

Appendix D11 (continued)

Table of values of W(u,beta)

u	Beta						
	0.2	0.5	1	2	5	10	20
1.00E-06	6.96	6.05	5.36	4.67	3.78	3.11	2.47
2.00E-06	6.61	5.7	5.01	4.33	3.44	2.79	2.16
4.00E-06	6.27	5.36	4.67	3.99	3.11	2.47	1.86
6.00E-06	6.06	5.16	4.47	3.8	2.92	2.28	1.69
8.00E-06	5.92	5.01	4.33	3.66	2.79	2.16	1.57
0.00001	5.81	4.9	4.22	3.55	2.68	2.06	1.48
0.00002	5.46	4.56	3.88	3.22	2.37	1.76	1.22
0.00004	5.12	4.22	3.55	2.89	2.06	1.48	0.973
0.00006	4.91	4.02	3.35	2.7	1.88	1.32	0.841
0.00008	4.77	3.88	3.21	2.57	1.76	1.22	0.753
0.0001	4.66	3.77	3.11	2.47	1.67	1.14	0.688
0.0002	4.31	3.43	2.78	2.15	1.39	0.899	0.504
0.0004	3.96	3.1	2.46	1.85	1.14	0.688	0.351
0.0006	3.76	2.91	2.28	1.68	0.994	0.577	0.277
0.0008	3.62	2.77	2.15	1.57	0.898	0.504	0.23
0.001	3.5	2.67	2.05	1.48	0.827	0.451	0.198
0.002	3.15	2.34	1.75	1.21	0.624	0.308	0.116
0.004	2.8	2.03	1.47	0.966	0.45	0.197	6.19E-02
0.006	2.6	1.84	1.31	0.833	0.362	0.146	4.04E-02
0.008	2.45	1.72	1.2	0.744	0.306	0.116	2.90E-02
0.01	2.33	1.62	1.11	0.678	0.267	9.55E-02	2.21E-02
0.02	1.97	1.32	0.868	0.491	0.165	4.87E-02	2.21E-02
0.04	1.61	1.04	0.647	0.336	9.31E-02	2.16E-02	8.31E-03
0.06	1.39	0.884	0.53	0.259	6.30E-02	1.24E-02	2.53E-03
0.08	1.24	0.776	0.453	0.212	4.64E-02	7.97E-03	1.12E-03
0.1	1.12	0.695	0.397	0.179	3.59E-02	5.52E-03	5.87E-04
0.2	0.767	0.46	0.245	9.71E-02	1.43E-02	1.49E-03	3.40E-04
0.4	0.448	0.262	0.13	4.41E-02	4.48E-03	2.83E-04	4.93E-05
0.6	0.293	0.169	7.99E-02	2.47E-02	1.95E-03	8.73E-05	4.24E-06
0.8	0.201	0.115	5.29E-02	1.52E-02	9.86E-04	3.40E-05	
1	0.143	8.12E-02	3.65E-02	9.93E-03	5.47E-04	1.51E-05	
2	3.22E-02	1.80E-02	7.60E-03	1.73E-03	5.51E-05		
4	2.50E-03	1.39E-03	5.58E-04	1.08E-04	1.89E-06		
6	2.39E-04	1.33E-04	5.19E-05	9.26E-06			
8	2.51E-05	1.39E-05	5.36E-06				

Appendix D12

Table showing the values of the complementary error function

x	erfc(x)	
	Table	Programme
0.00E+00	1	1
2.00E-01	0.7773	0.7773
4.00E-01	0.5716	0.5716
6.00E-01	0.3961	0.3961
8.00E-01	0.2579	0.2579
1.00E+00	0.1573	0.1573
1.20E+00	0.0897	0.0897
1.40E+00	0.0477	0.0477
1.60E+00	0.0237	0.0237
1.80E+00	0.0109	0.0109
2.00E+00	0.0047	0.0047
2.20E+00	0.0019	0.0019
2.40E+00	0.0007	0.0007
2.60E+00	0.0002	0.0002
2.80E+00	0.0001	0.0001
3.00E+00	0	0
3.20E+00	0	0
3.40E+00	0	0
3.60E+00	0	0
3.80E+00	0	0
4.00E+00	0	0

Appendix D13

Table comparing the values of W(u,beta) from tables and the computer programme

u	beta	W (u,beta)		
		Table	Programme	Error (%)
1.00E-06	1.00E-03	1.20E+01	11.98451	0.13
1.00E-06	1.00E-02	9.93E+00	9.926066	0.04
1.00E-06	1.00E-01	7.65E+00	7.649844	0.00
1.00E-06	1.00E+00	5.36E+00	5.357667	0.04
1.00E-06	1.00E+01	3.11E+00	3.111035	0.03
1.00E-05	1.00E-03	1.04E+01	10.37415	0.25
1.00E-05	1.00E-02	8.71E+00	8.71438	0.05
1.00E-05	1.00E-01	6.49E+00	6.494551	0.07
1.00E-05	1.00E+00	4.22E+00	4.221268	0.03
1.00E-05	1.00E+01	2.06E+00	2.059059	0.05
1.00E-04	1.00E-03	8.43E+00	8.426002	0.05
1.00E-04	1.00E-02	7.38E+00	7.38047	0.01
1.00E-04	1.00E-01	5.33E+00	5.329801	0.00
1.00E-04	1.00E+00	3.11E+00	3.10829	0.05
1.00E-04	1.00E+01	1.14E+00	1.135931	0.36
1.00E-03	1.00E-03	6.26E+00	6.261006	0.02
1.00E-03	1.00E-02	5.77E+00	5.772794	0.05
1.00E-03	1.00E-01	4.13E+00	4.133827	0.09
1.00E-03	1.00E+00	2.05E+00	2.050689	0.03
1.00E-03	1.00E+01	4.51E-01	0.4512953	0.07
1.00E-02	1.00E-03	4.02E+00	4.012833	0.18
1.00E-02	1.00E-02	3.84E+00	3.837543	0.06
1.00E-02	1.00E-01	2.84E+00	2.844319	0.15
1.00E-02	1.00E+00	1.11E+00	1.112189	0.20
1.00E-02	1.00E+01	9.55E-02	0.09554196	0.04
1.00E-01	1.00E-03	1.82E+00	1.813201	0.37
1.00E-01	1.00E-02	1.77E+00	1.766322	0.21
1.00E-01	1.00E-01	1.39E+00	1.389324	0.05
1.00E-01	1.00E+00	3.97E-01	0.3970066	0.00
1.00E-01	1.00E+01	5.52E-03	0.005528968	0.16
1.00E+00	1.00E-03	2.19E-01	0.2171103	0.86
1.00E+00	1.00E-02	2.14E-01	0.2131464	0.40
1.00E+00	1.00E-01	1.76E-01	0.1758423	0.09
1.00E+00	1.00E+00	3.65E-02	0.0364678	0.09
1.00E+00	1.00E+01	1.51E-05	1.50113E-05	0.59

Appendix D14

HANTIN.DAT

HANPUTS Input File

```
        21         40
   1.0E-10        1.0
      20.0 5.556E-03
 2.894E-03   5.0E-04
   1.0E-08   5.0E-03
  1.00E+02  9.44E-02
  2.00E+02  1.25E-01
  3.00E+02  1.61E-01
  4.00E+02  1.76E-01
  5.00E+02  1.76E-01
  6.00E+02  1.91E-01
  8.00E+02  2.11E-01
  1.00E+03  2.17E-01
  1.40E+03  2.36E-01
  1.80E+03  2.60E-01
  3.60E+03  2.83E-01
  5.40E+03  3.19E-01
  7.20E+03  3.33E-01
  9.00E+03  3.33E-01
  1.08E+04  3.41E-01
  1.26E+04  3.62E-01
  1.44E+04  3.65E-01
  1.62E+04  3.49E-01
  1.80E+04  3.70E-01
  1.98E+04  3.80E-01
  2.16E+04  3.68E-01
```

Appendix D15

HANTOUT.DAT

HANPUTS Output File

```
*****************************
*                           *
*     HANPUTS - HANTUSH     *
*      CURVE MATCHING       *
*            BY             *
*  GROUNDWATER ENGINEERING  *
*          DURHAM           *
*                           *
*****************************


NUMBER OF OBSERVATION POINTS    =   21
FLOWRATE (CUB M/SEC)            =   .5556000E-02
DISTANCE FROM PUMPED WELL (M)   =   .2000000E+02

    --  AQUIFER PROPERTIES  --


TRANSMISSIVITY GUESS (MSQ/SEC)  =   .2894000E-02
STORATIVITY GUESS               =   .5000000E-03
```

-- AQUITARD PROPERTIES --

K(AQUITARD)/THICKNESS (1/S)	=	.1000000E-07
AQUITARD STORATIVITY GUESS	=	.5000000E-02
BETA (DIMENSIONLESS)	=	.2939143E-01
CONVERGENCE FACTOR	=	.1000000E-09
RELAXATION FACTOR	=	.1000000E+01

TIME	MEASURED HEAD
.1000000E+03	.9440000E-01
.2000000E+03	.1250000E+00
.3000000E+03	.1610000E+00
.4000000E+03	.1760000E+00
.5000000E+03	.1760000E+00
.6000000E+03	.1910000E+00
.8000000E+03	.2110000E+00
.1000000E+04	.2170000E+00

.1400000E+04	.2360000E+00
.1800000E+04	.2600000E+00
.3600000E+04	.2830000E+00
.5400000E+04	.3190000E+00
.7200000E+04	.3330000E+00
.9000000E+04	.3330000E+00
.1080000E+05	.3410000E+00
.1260000E+05	.3620000E+00
.1440000E+05	.3650000E+00
.1620000E+05	.3490000E+00
.1800000E+05	.3700000E+00
.1980000E+05	.3800000E+00
.2160000E+05	.3680000E+00

IT NO	ERROR	TRANS.	STORAGE	BETA
1	.3225813E+00	.3790718E-02	.7474112E-03	.2198489E-01
2	.1851199E+00	.5511262E-02	.9430498E-03	.1816889E-01
3	.5384605E-01	.6573894E-02	.9890253E-03	.1661298E-01
4	.1019597E-01	.6800507E-02	.9813937E-03	.1642541E-01
5	.6696113E-02	.6811575E-02	.9803036E-03	.1635697E-01
6	.6692371E-02	.6810784E-02	.9803783E-03	.1637197E-01
7	.6692371E-02	.6811031E-02	.9803545E-03	.1636743E-01
8	.6692371E-02	.6810957E-02	.9803616E-03	.1636880E-01

TIME(S)	HEAD OBSERVED(M)	HEAD CALCULATED(M)	LOG TIME	LOG HEAD OBSERVED	LOG HEAD CALCULATED

.1000000E+03	.9440000E-01	.9286117E-01	.2000000E+01	-.1025028E+01	-.1032166E+01
.2000000E+03	.1250000E+00	.1308160E+00	.2301030E+01	-.9030900E+00	-.8833391E+00
.3000000E+03	.1610000E+00	.1537014E+00	.2477121E+01	-.7931741E+00	-.8133221E+00
.4000000E+03	.1760000E+00	.1700404E+00	.2602060E+01	-.7544873E+00	-.7694478E+00
.5000000E+03	.1760000E+00	.1827134E+00	.2698970E+01	-.7544873E+00	-.7382297E+00
.6000000E+03	.1910000E+00	.1930435E+00	.2778151E+01	-.7189666E+00	-.7143449E+00
.8000000E+03	.2110000E+00	.2092605E+00	.2903090E+01	-.6757175E+00	-.6793127E+00
.1000000E+04	.2170000E+00	.2217415E+00	.3000000E+01	-.6635403E+00	-.6541530E+00
.1400000E+04	.2360000E+00	.2403495E+00	.3146128E+01	-.6270880E+00	-.6191568E+00
.1800000E+04	.2600000E+00	.2540488E+00	.3255273E+01	-.5850267E+00	-.5950829E+00
.3600000E+04	.2830000E+00	.2907565E+00	.3556303E+01	-.5482136E+00	-.5364705E+00
.5400000E+04	.3190000E+00	.3113883E+00	.3732394E+01	-.4962093E+00	-.5066978E+00
.7200000E+04	.3330000E+00	.3256144E+00	.3857332E+01	-.4775558E+00	-.4872964E+00
.9000000E+04	.3330000E+00	.3364053E+00	.3954243E+01	-.4775558E+00	-.4731372E+00
.1080000E+05	.3410000E+00	.3450620E+00	.4033424E+01	-.4672456E+00	-.4621029E+00
.1260000E+05	.3620000E+00	.3522685E+00	.4100371E+01	-.4412914E+00	-.4531262E+00
.1440000E+05	.3650000E+00	.3584279E+00	.4158362E+01	-.4377071E+00	-.4455981E+00
.1620000E+05	.3490000E+00	.3637973E+00	.4209515E+01	-.4571746E+00	-.4391406E+00
.1800000E+05	.3700000E+00	.3685501E+00	.4255273E+01	-.4317983E+00	-.4335034E+00
.1980000E+05	.3800000E+00	.3728092E+00	.4296665E+01	-.4202164E+00	-.4285134E+00
.2160000E+05	.3680000E+00	.3766643E+00	.4334454E+01	-.4341522E+00	-.4240456E+00

BEST FIT VALUES

==========

THE VALUE OF TRANSMISSIVITY (M SQ/DAY)	=	.5884667E+03
THE VALUE OF STORATIVITY	=	.9803616E-03
THE VALUE OF BETA	=	.1636880E-01
THE AVERAGE ERROR BETWEEN CALCULATED AND OBSERVED VALUES OF DRAWDOWN (M)	=	.6692371E-02

Appendix D16

Convergence properties of the HANPUTS programme

T guess m^2/day	S guess	Beta guess	Converge (Y/N) ?	No. of iterations	Comments
50	5.0×10^{-2}	2.0×10^{-3}	N	31	Diverged
		2.0×10^{-2}	N	21	Diverged
		1.0×10^{-1}	N	23	Diverged
50	5.0×10^{-3}	2.0×10^{-3}	Y	12	Converged
		2.0×10^{-2}	Y	26	Converged
		1.0×10^{-1}	Y	13	Converged
50	5.0×10^{-4}	2.0×10^{-3}	Y	26	Converged
		2.0×10^{-2}	Y	13	Converged
		1.0×10^{-1}	Y	9	Converged
250	5.0×10^{-2}	2.0×10^{-3}	N	27	Diverged
		2.0×10^{-2}	N	27	Diverged
		1.0×10^{-1}	N	27	Diverged
250	5.0×10^{-3}	2.0×10^{-3}	Y	19	Converged
		2.0×10^{-2}	Y	6	Converged
		1.0×10^{-1}	Y	12	Converged
250	5.0×10^{-4}	2.0×10^{-3}	Y	21	Converged
		2.0×10^{-2}	Y	6	Converged
		1.0×10^{-1}	Y	5	Converged
750	5.0×10^{-2}	2.0×10^{-3}	N	24	Diverged
		2.0×10^{-2}	N	24	Diverged
		1.0×10^{-1}	N	24	Diverged
750	5.0×10^{-3}	2.0×10^{-3}	Y	9	Converged
		2.0×10^{-2}	Y	6	Converged
		1.0×10^{-1}	N	24	Diverged
750	5.0×10^{-4}	2.0×10^{-3}	Y	17	Converged
		2.0×10^{-2}	Y	5	Converged
		1.0×10^{-1}	N	24	Diverged
1000	5.0×10^{-2}	2.0×10^{-3}	N	24	Diverged
		2.0×10^{-2}	N	24	Diverged
		1.0×10^{-1}	N	24	Diverged
1000	5.0×10^{-3}	2.0×10^{-3}	N	8	Converged
		2.0×10^{-2}	N	24	Diverged
		1.0×10^{-1}	N	24	Diverged
1000	5.0×10^{-4}	2.0×10^{-3}	N	24	Diverged
		2.0×10^{-2}	N	5	Converged
		1.0×10^{-1}	N	24	Diverged

Convergence led to values of

Transmissivity = 588.5 m^2/day Beta = 1.64×10^{-2}

Storativity = 9.80×10^{-4} Root mean square error = 6.7 mm

Appendix E

E 1: Comparison of Hermitian interpolation and the Walton well function

E 2: Comparison of Hermitian interpolation and the Hantush well function

u	r/L	W(u,r/L)			dW(u,r/L)/du			dW(u,r/L)/d(r/L)		
		Prog	Herm	% Error	Prog	Herm	% Error	Prog	Herm	% Error
2.25E-06	5.00E-03	10.8114	10.8114	0.00	-28017.08	-27909.01	0.39	-375.1042	-375.1044	0.00
2.25E-06	5.00E-02	6.2285	6.2285	0.00	0	0	0.00	-39.8213	-39.8213	0.00
2.25E-06	5.00E-01	1.8488	1.8488	0.00	0	0	0.00	-3.3131	-3.3131	0.00
2.25E-06	5.00E+00	0.0073	0.0073	0.00	0	0	0.00	-0.0081	-0.0081	0.00
2.25E-05	5.00E-03	9.8654	9.8654	0.00	-33651.67	-33653.21	0.00	-96.9899	-96.99	0.00
2.25E-05	5.00E-02	6.2285	6.2285	0.00	0	0	0.00	-39.8213	-39.8213	0.00
2.25E-05	5.00E-01	1.8488	1.8488	0.00	0	0	0.00	-3.3131	-3.3131	0.00
2.25E-05	5.00E+00	0.0073	0.0073	0.00	0	0	0.00	-0.0081	-0.0081	0.00
2.25E-04	5.00E-03	7.795	7.795	0.00	-4321.648	-4321.652	0.00	-10.9367	-10.9367	0.00
2.25E-04	5.00E-02	6.2112	6.2112	0.00	-277.881	-277.8251	0.02	-37.3332	-37.3332	0.00
2.25E-04	5.00E-01	1.8488	1.8488	0.00	0	0	0.00	-3.3131	-3.3131	0.00
2.25E-04	5.00E+00	0.0073	0.0073	0.00	0	0	0.00	-0.0081	-0.0081	0.00
2.25E-03	5.00E-03	5.5192	5.5192	0.00	-442.2208	-442.2213	0.00	-1.0933	-1.0933	0.00
2.25E-03	5.00E-02	5.2663	5.2663	0.00	-335.8542	-335.8619	0.00	-9.5451	-9.5451	0.00
2.25E-03	5.00E-01	1.8488	1.8488	0.00	0	0	0.00	-3.3131	-3.3131	0.00
2.25E-03	5.00E+00	0.0073	0.0073	0.00	0	0	0.00	-0.0081	-0.0081	0.00
2.25E-02	5.00E-03	3.2394	3.2023	1.15	-43.4556	-43.3015	0.35	0	0	0.00
2.25E-02	5.00E-02	3.2145	3.2145	0.00	-42.2655	-42.2653	0.00	-0.9908	-0.9908	0.00
2.25E-02	5.00E-01	1.8318	1.8318	0.00	-2.7047	-2.7042	0.02	-3.0685	-3.0685	0.00
2.25E-02	5.00E+00	0.0073	0.0073	0.00	0	0	0.00	-0.0081	-0.0081	0.00
2.25E-01	5.00E-03	1.1274	1.1154	1.06	-3.549	-3.5274	0.61	0	0	0.00
2.25E-01	5.00E-02	1.1259	1.1259	0.00	-3.5392	-3.5392	0.00	-0.0604	-0.0604	0.00
2.25E-01	5.00E-01	0.9883	0.9883	0.00	-2.6882	-2.6882	0.00	-0.5107	-0.5107	0.00
2.25E-01	5.00E+00	0.0073	0.0073	0.00	0	0	0.00	-0.0081	-0.0081	0.00
2.25E+00	5.00E-03	0.0348	0.0348	0.00	-0.0469	-0.0468	0.21	0	0	0.00
2.25E+00	5.00E-02	0.0348	0.0348	0.00	-0.0468	-0.0468	0.00	-0.0003	-0.0003	0.00
2.25E+00	5.00E-01	0.034	0.034	0.00	-0.0456	-0.0456	0.00	-0.003	-0.003	0.00
2.25E+00	5.00E+00	0.0044	0.0044	0.00	-0.0029	-0.0029	0.00	-0.0034	-0.0034	0.00

Appendix E1: Comparison of Hermitian interpolation and the Walton well function

u	Beta	W			dw/du			dw/dbeta		
		Prog	Herm	% Error	Prog	Herm	% Error	Prog	Herm	% Error
4.25E-06	4.50E-03	9.9012	9.9011	0.00	-132475.11	-132464.51	0.01	-194.185	-194.1763	0.00
4.25E-06	4.50E-02	7.7147	7.7147	0.00	-119053.44	-119053	0.00	-21.9143	-21.9126	0.01
4.25E-06	4.50E-01	5.4311	5.4311	0.00	-116923.67	-116924.29	0.00	-2.2029	-2.2027	0.01
4.25E-06	4.50E+00	3.1821	3.182	0.00	-111722.36	-111725.37	0.00	-0.211	-0.211	0.00
4.25E-05	4.50E-03	8.4957	8.4957	0.00	-15787.45	-15786.673	0.00	-146.0876	-146.0846	0.00
4.25E-05	4.50E-02	6.5375	6.5375	0.00	-12211.923	-12211.501	0.00	-21.2566	-21.2551	0.01
4.25E-05	4.50E-01	4.2916	4.2916	0.00	-11580.007	-11580.134	0.00	-2.1693	-2.1692	0.00
4.25E-05	4.50E+00	2.1244	2.1243	0.00	-10332.533	-10332.955	0.00	-0.195	-0.195	0.00
4.25E-04	4.50E-03	6.7733	6.7733	0.00	-1938.9109	-1938.9407	0.00	-77.636	-77.6347	0.00
4.25E-04	4.50E-02	5.3045	5.3045	0.00	-1315.5411	-1315.4897	0.00	-19.256	-19.255	0.01
4.25E-04	4.50E-01	3.1695	3.1695	0.00	-1131.8082	-1131.8002	0.00	-2.0814	-2.0813	0.00
4.25E-04	4.50E+00	1.1893	1.1892	0.01	-858.8114	-858.8347	0.00	-0.1617	-0.1617	0.00
4.25E-03	4.50E-03	4.7432	4.7432	0.00	-217.9126	-217.9149	0.00	-30.0464	-30.0468	0.00
4.25E-03	4.50E-02	3.9156	3.9156	0.00	-154.9711	-154.9685	0.00	-14.1852	-14.185	0.00
4.25E-03	4.50E-01	2.086	2.0859	0.00	-107.6132	-107.6144	0.00	-1.8608	-1.8606	0.01
4.25E-03	4.50E+00	0.4842	0.4842	0.00	-56.2812	-56.2815	0.00	-0.1051	-0.1051	0.00
4.25E-02	4.50E-03	2.5777	2.5777	0.00	-21.9775	-21.9779	0.00	-8.9922	-8.9926	0.00
4.25E-02	4.50E-02	2.2568	2.2568	0.00	-18.0822	-18.0823	0.00	-6.7812	-6.7813	0.00
4.25E-02	4.50E-01	1.0812	1.0812	0.00	-9.63	-9.6299	0.00	-1.3481	-1.348	0.01
4.25E-02	4.50E+00	0.1056	0.1056	0.00	-2.1827	-2.1824	0.01	-0.0395	-0.0394	0.25
4.25E-01	4.50E-03	0.6523	0.6523	0.00	-1.5172	-1.5172	0.00	-1.4877	-1.4877	0.00
4.25E-01	4.50E-02	0.5935	0.5935	0.00	-1.3637	-1.3637	0.00	-1.3905	-1.3905	0.00
4.25E-01	4.50E-01	0.2679	0.2679	0.00	-0.6239	-0.6239	0.00	-0.4468	-0.4468	0.00
4.25E-01	4.50E+00	0.0056	0.0056	0.00	-0.0243	-0.0243	0.00	-0.0038	-0.0038	0.00
4.25E+00	4.50E-03	0.0027	0.0027	0.00	-0.0033	-0.0033	0.00	-0.0047	-0.0047	0.00
4.25E+00	4.50E-02	0.0025	0.0025	0.00	-0.003	-0.003	0.00	-0.0047	-0.0047	0.00
4.25E+00	4.50E-01	0.0011	0.0011	0.00	-0.0014	-0.0014	0.00	-0.0022	-0.0022	0.00
4.25E+00	4.50E+00	0	0	0.00	0	0	0.00	0	0	0.00

Appendix E2: Comparison of Hermitian interplation and the Hantush well function

Appendix F

F 1: Confined pump test data

F 2: Leaky pump test data

Appendix F1
Confined pump test data

Pumping test 'Oude Korendijk'				Todd data	
Radius = 30 m		Radius = 90 m		Radius = 60 m	
Time (s)	Drawdown (m)	Time (s)	Drawdown (m)	Time (s)	Drawdown (m)
6.00E+00	0.04	9.00E+01	0.015	6.00E+01	0.2
1.50E+01	0.08	1.20E+02	0.021	9.00E+01	0.27
3.00E+01	0.13	1.30E+02	0.023	1.20E+02	0.3
4.20E+01	0.18	1.60E+02	0.044	1.50E+02	0.34
6.00E+01	0.23	1.80E+02	0.054	1.80E+02	0.37
8.40E+01	0.28	2.10E+02	0.075	2.40E+02	0.41
1.14E+02	0.33	2.40E+02	0.09	3.00E+02	0.45
1.40E+02	0.36	2.60E+02	0.104	3.60E+02	0.48
1.68E+02	0.39	3.30E+02	0.133	4.80E+02	0.53
2.02E+02	0.42	3.60E+02	0.153	6.00E+02	0.57
2.40E+02	0.45	4.50E+02	0.178	7.20E+02	0.6
3.21E+02	0.5	5.40E+02	0.206	8.40E+02	0.63
4.98E+02	0.57	7.80E+02	0.25	1.08E+03	0.67
5.22E+02	0.58	9.00E+02	0.275	1.44E+03	0.72
6.00E+02	0.6	1.08E+03	0.305	1.80E+03	0.76
7.86E+02	0.64	1.50E+03	0.348	2.40E+03	0.81
1.08E+03	0.68	1.80E+03	0.364	3.00E+03	0.85
1.62E+03	0.742	2.40E+03	0.404	3.60E+03	0.9
1.98E+03	0.753	3.18E+03	0.429	4.80E+03	0.93
2.46E+03	0.779	3.60E+03	0.444	6.00E+03	0.96
2.88E+03	0.793	4.50E+03	0.467	7.20E+03	1
3.54E+03	0.819	5.40E+03	0.494	9.00E+03	1.04
5.70E+03	0.873	6.30E+03	0.507	1.08E+04	1.07
8.34E+03	0.915	7.20E+03	0.528	1.26E+04	1.1
1.09E+04	0.935	9.00E+03	0.55	1.44E+04	1.12
1.47E+04	0.966	1.08E+04	0.569		
1.80E+04	0.99	1.49E+04	0.593		
2.16E+04	1.007	1.81E+04	0.614		
2.88E+04	1.05	2.18E+04	0.636		
3.60E+04	1.053	2.53E+04	0.657		
4.37E+04	1.072	3.25E+04	0.679		

Radius = 30m		Radius = 60m		Radius = 90m		Radius = 120m	
Time (s)	Drawdown (m)	Time (s)	Drawdown (m)	Time (s)	Drawdown (m)	Time (s)	Drawdown (m)
1.32E+03	0.138	1.62E+03	0.081	2.10E+03	0.069	2.16E+03	0.057
1.56E+03	0.141	2.04E+03	0.089	2.64E+03	0.077	2.70E+03	0.063
1.98E+03	0.15	2.58E+03	0.094	3.24E+03	0.083	3.30E+03	0.068
2.52E+03	0.156	3.18E+03	0.101	4.04E+03	0.091	4.32E+03	0.075
3.12E+03	0.163	4.08E+03	0.109	5.82E+03	0.1	5.88E+03	0.086
3.96E+03	0.171	5.76E+03	0.12	7.74E+03	0.109	7.80E+03	0.092
5.70E+03	0.18	7.62E+03	0.127	1.08E+04	0.12	1.08E+04	0.105
7.50E+03	0.19	1.08E+04	0.137	1.44E+04	0.129	1.44E+04	0.113
1.08E+04	0.201	1.44E+04	0.148	1.80E+04	0.136	1.80E+04	0.122
1.44E+04	0.21	1.80E+04	0.155	2.16E+04	0.141	2.16E+04	0.125
1.80E+04	0.217	2.16E+04	0.158	2.52E+04	0.142	2.52E+04	0.127
2.16E+04	0.22	2.52E+04	0.16	2.88E+04	0.143	2.88E+04	0.129
2.52E+04	0.224	2.88E+04	0.164				
2.88E+04	0.228						

Appendix F2
Leaky pump test data